



Universiteit  
Leiden  
The Netherlands

## **T and NK cell immunity after hematopoietic stem cell transplantation**

Lugthart, G.

### **Citation**

Lugthart, G. (2018, March 27). *T and NK cell immunity after hematopoietic stem cell transplantation*. Retrieved from <https://hdl.handle.net/1887/61077>

Version: Not Applicable (or Unknown)

License: [Licence agreement concerning inclusion of doctoral thesis in the Institutional Repository of the University of Leiden](#)

Downloaded from: <https://hdl.handle.net/1887/61077>

**Note:** To cite this publication please use the final published version (if applicable).

Cover Page



Universiteit Leiden



The handle <http://hdl.handle.net/1887/61077> holds various files of this Leiden University dissertation.

**Author:** Lugthart, G.

**Title:** T and NK cell immunity after hematopoietic stem cell transplantation

**Issue Date:** 2018-03-27

**T and NK cell Immunity  
after  
Hematopoietic Stem Cell Transplantation**

**Afweer door T- en NK cellen na  
Hematopoïetische Stamcel Transplantatie**

G. Lugthart

T and NK cell Immunity after Hematopoietic Stem Cell Transplantation.

© 2018 G. Lugthart, Leiden, The Netherlands

ISBN: 978-94-6361-070-4

No part of this thesis may be reproduced, stored in a retrieval system or transmitted in any form or by any means without permission from the author or, when appropriate, from the publishers of the published chapters.

The research described in this thesis was performed at the Laboratory of Pediatric Immunology at the Leiden University Medical Center Willem-Alexander Children's Hospital, Leiden, The Netherlands (Chapters 2, 4, 5, 6 & 7) and the Laboratory of Molecular and Cellular Immunology at the University College London Great Ormond Street Hospital Institute of Child Health, London, UK (Chapter 3).

The work described in this thesis was partially supported by a grant from the Dutch Cancer Society (grant UL-2011-5133). Gertjan Lugthart received a Leiden University Medical Center MD/PhD fellowship to perform this work. The printing of this thesis was financially supported by the LUMC department of pediatrics, ITK diagnostics and Greiner Bio-One.

Cover design: Atze de Vries

Lay-out: Gertjan Lugthart

Printing: Optima Grafische Communicatie, Rotterdam

**T and NK cell Immunity  
after  
Hematopoietic Stem Cell Transplantation**

**Afweer door T- en NK cellen na  
Hematopoïetische Stamcel Transplantatie**

**Proefschrift**

ter verkrijging van de graad van  
Doctor aan de Universiteit Leiden  
op gezag van Rector Magnificus prof. mr. C.J.J.M. Stolker,  
volgens het besluit van het College voor Promoties  
te verdedigen op dinsdag 27 maart 2018 klokke 16:15 uur

door

**Gerrit Lugthart**  
geboren te Gorinchem  
in 1987



Promotor: Prof. dr. A.C. Lankester

Co-promotores: Dr. M.W. Schilham  
Dr. M.J.D. van Tol

Promotiecommissie: Prof. dr. F.Koning  
Prof. dr. J.H.F. Falkenburg  
Prof. dr. R.A.W. van Lier, University of Amsterdam  
Dr. J.N. Samsom, Erasmus University Rotterdam





# Table of contents

Chapter 1	General introduction	9
Chapter 2	Early CMV reactivation leaves a specific and dynamic imprint on the reconstituting T cell compartment long term post hematopoietic stem cell transplantation	31
Chapter 3	Simultaneous generation of multivirus-specific and regulatory T cells for adoptive immunotherapy	51
Chapter 4	The effect of cidofovir on adenovirus plasma DNA levels in stem cell transplantation recipients without T cell reconstitution	73
Chapter 5	CD56 <sup>dim</sup> CD16 <sup>-</sup> NK cell phenotype can be induced by cryopreservation	91
Chapter 6	Expansion of cytotoxic CD56 <sup>bright</sup> NK cells during T cell deficiency after allogeneic hematopoietic stem cell transplantation	97
Chapter 7	Human lymphoid tissues harbor a distinct CD69 <sup>+</sup> CXCR6 <sup>+</sup> natural killer cell population	119
Chapter 8	Summary	139
Chapter 9	General discussion and future perspectives	143
	References	157
	Dutch summary / Nederlandse samenvatting	173
	List of publications	181
	Curriculum vitae	185
	Acknowledgements / Dankwoord	189



# **Chapter 1**

## **General introduction**



# 1 Allogeneic hematopoietic stem cell transplantation

Hematopoietic stem cells constitute a life-time source for red blood cells and platelets as well as for white blood cells that form the immune system. The allogeneic transplantation of these stem cells provides a therapy for severe hematological, immunological and metabolic disorders by replacing the patients (defect) hematopoietic system with that of a healthy donor.<sup>1</sup> Furthermore, hematopoietic stem cell transplantation (HSCT) is applied as rescue therapy in patients with hematological malignancies, to restore the hematopoietic system after intensive chemo- and radiation therapy which not only kills leukemic cells but also kills healthy hematopoietic stem cells.<sup>1</sup>

1

## 1.1 History

In 1968, both in Minneapolis and Leiden, the first successful allogeneic HSCT were performed with HLA-identical sibling donors in children suffering from severe combined immune deficiency (SCID).<sup>2-4</sup> In the last 50 years, the worldwide number of allogeneic HSCT that is performed annually has grown exponentially to almost 16.000 in 2014 (Figure 1.1).<sup>5</sup> After the first transplantation for SCID, HSCT was also successfully used to treat severe aplastic anemia (SAA) and as rescue therapy for hematological malignancies.<sup>4;6;7</sup> The first decades, HSCT was marked by a high treatment related morbidity and mortality.<sup>1</sup> When outcomes of HSCT improved as result of advances in transplantation technology, supportive care and improved HLA typing, HSCT became an acceptable treatment option for severe hemoglobinopathies as well as severe metabolic disorders.<sup>8</sup> In the early years, the applicability of HSCT was limited to the use of HLA identical sibling donors (identical related donor, IRD). The first successful HLA matched unrelated donor (MUD) transplantation was performed in 1979, facilitating allogeneic HSCT for patients with an HSCT indication for whom no IRD was available.<sup>9</sup> In the next decade, haplo-identical donors and cord blood (CB) transplantations were introduced as alternatives for IRD and MUD transplantations.<sup>10-12</sup> Whereas bone marrow (BM) was the main stem cell source in the first 25 years of HSCT, the use of stem cells that are mobilized into peripheral blood (PBSC) has grown extensively since the introduction in 1993.<sup>5;13</sup>

Over the years, scientific developments have greatly improved the outcome after HSCT (Figure 1.1). The morbidity and mortality after MUD transplantations are now comparable to the IRD setting, while the outcome of HSCT in patients who received an alternative donor graft (CB or haplo-identical) is steadily improving and approaching the outcome in MUD transplantations. This is mainly due to the increasing understanding of transplant immunology, technical developments in HLA-typing, lower toxicity of conditioning regimens, ongoing improvements in the procedures to reduce alloreactivity and infectious complications and, more recently, also personalized medicine, such as therapeutic drug monitoring and personalized conditioning.

The successful outcome after HSCT depends on the selection of the best donor and graft source and the well-considered and targeted application of strategies to reduce the risk of graft-versus host disease without compromising immune reconstitution. This balance will be further discussed in the next sections.

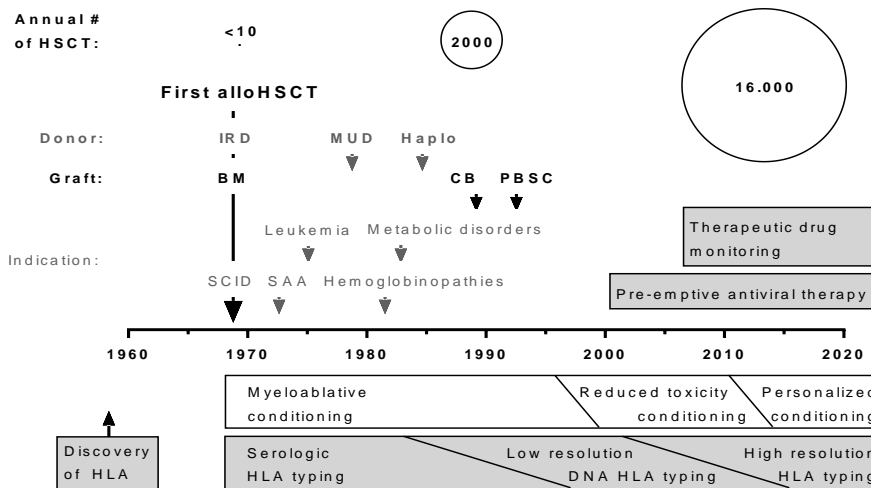


Figure 1.1 Milestones and major improvements in the history of allogeneic HSCT.

## 1.2 Alloreactivity

The largest challenge for the successful application of allogeneic HSCT is the prevention and management of alloreactivity. Alloreactivity is caused by T cells recognizing histo-incompatible cells. The chance of alloreactivity is increased when HLA-disparity is present between donor and recipient, but alloreactivity can also be directed to minor histocompatibility antigens.<sup>14-16</sup>

**Host-versus-graft reactions** are caused by recipient T cells and lead to the killing of donor (stem) cells leading to failure of engraftment or graft rejection, which is associated with high mortality due to secondary infections.<sup>17</sup>

**Graft-versus-host reactions** are caused by donor T cells and are directed to both hematopoietic and non-hematopoietic tissues of the recipient. Graft-versus-host reactions directed to hematopoietic cells of the recipient can be beneficial as the killing of recipient cells in the bone marrow creates space for the donor stem cells. Also, leukemic cells that survived the conditioning therapy can be killed by donor T cells in a so-called **graft-versus-leukemia (GvL)** reaction.<sup>15</sup> However, graft-versus-host reactions also cause **graft-versus-host disease (GvHD)**. The pathophysiology of GvHD can be described in three steps: first, the conditioning therapy causes tissue damage and inflammation, leading to activation of antigen presenting cells (APC) of the host. Second, donor-derived cells interact with these host APC to get activated and expand. Thirdly, donor T cells cause further tissue damage and a general inflammatory condition, which initiates a vicious circle.<sup>16</sup> GvHD can be both acute and chronic, and tissues mainly affected are skin, intestine and liver. Symptoms can vary from a skin rash to desquamation, and from nausea to massive bloody diarrhea and ileus. In case of (suspected) GvHD, treatment is installed using immunosuppressive medication, starting with high dose steroids. As second line treatment, other immunosuppressive drugs and biologicals (e.g. MMF and Infliximab) are used.<sup>16</sup> In an experimental setting, extracorporeal photopheresis and the infusion of mesenchymal stromal cells

are applied. Steroid refractory GvHD is associated with a high mortality, both directly and because of immunosuppression and secondary infections.<sup>16</sup>

### 1.3 HLA-matching, donor type and graft source

The first step in the prevention of alloreactivity is the search for an optimal, HLA-matched donor (Figure 1.2). The human HLA system is highly complex and polymorphic. It consists of 12 genes on the short arm of chromosome 6 that encode for HLA class I antigens (HLA-A, -B and -C) and HLA class II antigens (DR, DQ, DP). Currently, over 2500 HLA-alleles have been identified, resulting in an immense possibility of unique combinations. At first, HLA typing was based on serologic (antigenic) testing (*e.g.* HLA-A2) or low resolution molecular (DNA) typing (*e.g.* A\*02). Because each serotype contains different alleles, a donor matched at the serotype level can still be mismatched at the allele level. Therefore, high resolution molecular typing at the allele level is nowadays used to match unrelated donors (*e.g.* A\*0201). The 5 or 6 most important HLA genes (A/B/C/DRB1/DQB1/(DPB1)) are routinely tested in the matching procedure before HSCT. Because genes encoding these major HLA alleles are present on both chromosomes, a full HLA match is 10/10 or 12/12.<sup>14;18</sup>

An **HLA identical related donor** (IRD) is the donor of first choice. Due to Mendelian inheritance, the chance that two siblings are HLA identical is 25%. An IRD is available in 13-50% of patients, which is dependent on the number of siblings.<sup>19;20</sup>

If no IRD is available, the search is extended, looking for a **matched unrelated donor** (MUD) in the Bone Marrow Donors Worldwide database.<sup>21</sup> MUD donors are available for 30-70% of HSCT recipients.<sup>19;20</sup> The chance a MUD is available is largely dependent of the ethnic background of the recipient. Caucasians have a better chance of finding a MUD than people with an ethnic minority background<sup>20;22</sup>. If no fully matched MUD donor is available, the best matched unrelated donor (*e.g.* 9/10 or 8/10 match) can be used, at the cost of an increased risk of alloreactivity.

Alternatives for MUD and IRD transplantation are haplo-identical donors or cord blood (CB) transplantation.<sup>23</sup> In contrast to IRD and MUD donors, both cord blood units and haplo-identical donors are almost always directly available. Although for different reasons, both haplo-identical and cord blood transplantations are associated with a delayed immune reconstitution and increased risk for infectious complications in comparison to IRD and MUD transplantations.<sup>1;4</sup>

**Haplo-identical donors** are family members (*e.g.* parents or children) that share one haplotype with the recipient, resulting in a 5/10 HLA match.<sup>23</sup> Due to the high level of HLA-disparity, haplo-identical transplantations require additional strategies to reduce the risk of graft rejection and GvHD, which may also cause a delayed immune reconstitution, and consequently increase the risk of infectious complications. However, the outcome of haplo-identical transplantation has greatly improved over time as a result of ongoing improvements in the procedures applied to reduce alloreactivity and infectious complications, which will be discussed later.<sup>23</sup>

**Cord blood** is a residual product that naturally contains a high concentration of hematopoietic stem cells which is cryopreserved and stored in cord blood banks.<sup>24;25</sup> Cord blood grafts are rapidly available, have a high regenerative capacity and are relatively tolerant, allowing for larger HLA mismatches.<sup>25</sup> However, the rate of immune reconstitution after CB transplantation is

highly dependent on the total number of stem cells that is present in a cord blood graft, carrying the risk of delayed immune reconstitution and infectious complications.<sup>24,25</sup> To improve immune reconstitution, double cord blood units can be given. Due to the advances in HLA-matching technologies and increasing numbers of available CB units, the matching of CB transplantations has improved.<sup>25</sup> Together with advances in the procedures to reduce alloreactivity, this has led to strong improvements in immune reconstitution and the outcome of CB transplantations.<sup>24,25</sup>

The neonatal period is the only moment that hematopoietic stem cells circulate in the blood at high concentrations. For adult donors, hematopoietic stem cells can be harvested from **bone marrow** (BM) or **peripheral blood** (PBSC) after mobilization with granulocyte colony-stimulating factor (G-CSF) mobilization.<sup>24-26</sup> The advantage of PBSC donation is that no general anesthesia is needed for the donor. Because PBSC grafts contain 10 times more lymphocytes than BM grafts, the immune reconstitution after PBSC transplantation is often faster than after BM transplantation. However, PBSC grafts are associated with an increased risk of chronic GvHD.<sup>26</sup> For pediatric donors, BM donation is preferred to limit the exposure of healthy children to G-CSF.

#### 1.4 Conditioning therapy

The HSCT starts with the preparation of the recipient during conditioning therapy (Figure 1.2). The conditioning therapy is given in the weeks before HSCT. It aims to eradicate the recipient's hematopoietic stem cells and **makes space in the stem cell niche** of the bone marrow (myeloablation). The stem cell niche in bone marrow is required to support the infused donor stem cells from the graft to proliferate and differentiate. Secondly, the conditioning therapy **eradicates residual malignant cells** to improve the chance of leukemia free survival. Thirdly, the conditioning therapy **eliminates the recipient's immune system** to prevent the rejection of the graft by the recipient's T cells (immunoablation).<sup>1,27</sup> Many different conditioning regimens have been developed and can be divided in myeloablative or non-myeloablative regimens. In general, myeloablative regimens consist of an alkylating agent (*e.g.* Busulfan, Melphalan, Treosulfan) or Total Body Irradiation (TBI), in combination with an immunoablative agent (*e.g.* Fludarabine).<sup>27</sup> Non-myeloablative or reduced intensity conditioning regimens consist of a low dose of an alkylating agent or TBI, in combination with an immunoablative agent. Non-myeloablative regimens are mainly applied in older patients and patients with a poor clinical condition to reduce organ toxicity.<sup>1,27</sup>

In the last decades, the conditioning therapy has greatly improved, resulting in less toxic, more effective conditioning regimens. For example, TBI is frequently replaced by Busulfan and, more recently, Treosulfan. Also, Cyclophosphamide is increasingly being replaced by Fludarabine in most (pediatric) HSCT regimens.<sup>27</sup> In addition, therapeutic drug monitoring and personalized dosing regimens contributed to a reduction of toxicity.<sup>28</sup>



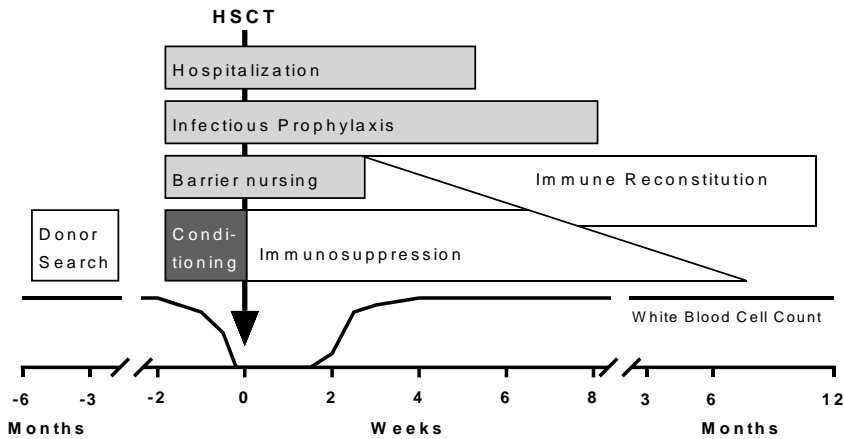


Figure 1.2. Overview of the allogeneic HSCT procedure.

### 1.5 Prevention of graft-versus-host disease

The risk of GvHD is the product of the level of HLA-matching, donor type and graft source, and is strongly dependent on T cells co-transplanted with the graft. Based on these input parameters, the best combination of strategies to prevent alloreactivity is chosen. Interventions to reduce the risk of graft-versus-host disease, which will be discussed in this paragraph, include graft manipulation, serotherapy and post-transplant immunosuppression.

Too strong suppression of alloreactivity, however, may lead to reduction of graft-versus-leukemia reactions as well as delayed immune reconstitution, increasing the risk of infectious complications. Therefore, interventions to reduce the risk of GvHD have to be applied well-considered and targeted (Figure 1.3).

Besides hematopoietic stem cells, the stem cell graft also contains lymphocytes. Co-transplanted T cells can have both positive (*e.g.* faster immune reconstitution) and negative effects (*e.g.* risk of GvHD). **Graft manipulation** can be used to reduce the number of T cells that are present in the graft. Both the selection of hematopoietic stem cells (positive selection) and depletion of T cells (negative selection) are applied for this purpose. This reduces the risk of GvHD, but is associated with delayed T cell reconstitution. Graft manipulation is mainly used for mismatched unrelated and haplo-identical donor transplantations.<sup>23;24</sup>

**Serotherapy** is the treatment with lymphocyte depleting antibodies usually administered to the patient in the week before the HSCT, with the aim to reduce the risk of graft rejection and GvHD. Only IRD transplant recipients do not routinely receive serotherapy. Serotherapy is a special form of immuno-ablative conditioning therapy. Due to the long half-time of the antibodies, they are still present during the HSCT procedure and in the weeks thereafter. Consequently, not only the recipients T cells are killed (preventing graft rejection), but also donor T cells that are present in the graft and donor T cells that reconstitute from the graft in the early period after engraftment are killed. Serotherapy plays an important role in the prevention of GvHD, but overdosing of serotherapy has a negative impact on immune reconstitution.<sup>29;30</sup> Different serotherapy agents are

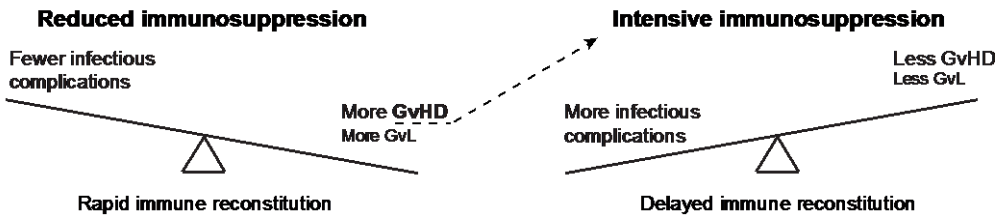


**Figure 1.3. Balance between the risk of GvHD and infectious complications after HSCT.**

The risk of GvHD and infections are related to interventions to prevent alloreactivity, such as T cell depletion of the graft, serotherapy before HSCT and immunosuppressive drugs after HSCT. Abbreviations: GvHD: Graft versus host disease, GvL: graft versus leukemia reaction.

used in the HSCT setting. Anti-thymocyte globulin (ATG) is a polyclonal antibody preparate, produced in rabbits or horses after immunization with human thymocytes or human T cell lines. ATG recognizes a wide range of antigens present on lymphocytes, but also other tissues like endothelial cells. Alemtuzumab (Campath®) is a humanized monoclonal antibody recognizing CD52, an antigen present on all lymphocytes. The half-life of ATG and Alemtuzumab is 4-14 days and 15-21 days, respectively.<sup>31;32</sup> Consequently, immune reconstitution is slower in Alemtuzumab treated patients.<sup>33</sup>

In the recent years, retrospective pharmacokinetics/pharmacodynamics studies have generated knowledge to enable the personalized dosing of serotherapy based on body weight and the number of lymphocytes present at the start of condition.<sup>30</sup> In the near future, personalized dosing of serotherapy may prevent overdosing of serotherapy, resulting in faster T cell reconstitution without an increased risk of GvHD.<sup>30</sup>

**Post-transplant immunosuppressive drugs** are used routinely to prevent GvHD. These drugs prevent the activation of proliferation of activated (alloreactive) T cells.<sup>16</sup> Often, the calcineurin inhibitor Cyclosporin A is used either alone or in combination with a short course of Methotrexate. Depending on the HLA-matching, donor type and graft source, also Mycophenolate Mofetil, Tacrolimus, Sirolimus and prednisone are sometimes used for the prophylaxis of GvHD.<sup>16</sup> The duration of post-transplant immunosuppression depends on the indication for the HSCT. In patients with hematological malignancies, immunosuppressive drugs are often tapered after 6-8 weeks if GvHD does not occur, to stimulate the graft-versus leukemia reactions.<sup>34</sup> For patients with non-malignant HSCT indications, for whom alloreactivity is not beneficial and should be avoided, immunosuppressive drugs are generally tapered after 3-6 months (Figure 1.2 and 1.3).<sup>16</sup>

Besides the major determinants HLA-matching, donor type and graft source, also genetic factors (e.g. polymorphisms of cytokines and/or -receptors), conditioning-induced tissue-damage and the composition of the intestinal microbiome are associated with the development of GvHD. Therefore, **reduced-toxicity conditioning** and the use of **intestinal decontamination** to eliminate the microbiome can also reduce the risk of GvHD.<sup>16;35;36</sup>

## 2. Viral complications after HSCT

T cell immunity is pivotal to provide protection against and achieve sustained control of viral infections.<sup>37-39</sup> In immunocompetent individuals, herpesvirus infections generally cause mild symptoms after which latency is established and reactivations can occur sporadically throughout life.<sup>40</sup> During the T cell deficient period after HSCT, patients are at risk for the reactivation of latent herpesvirus infections as well as a protracted and severe course of respiratory virus infections. From the group of herpesviruses, cytomegalovirus (CMV) and Epstein-Barr virus (EBV) reactivations have the largest clinical impact, whereas human adenovirus (HAdV) is responsible for the most severe respiratory and gastro-intestinal complications in pediatric HSCT recipients.<sup>41-44</sup>

Viral complications occur mainly in HSCT recipients at risk for a delayed immune reconstitution, such as patients who received (a high dose of) serotherapy (Figure 1.4, patient 2 and 3).

Three groups of patients have an increased risk of severely delayed T cell reconstitution leading to disseminated and life-threatening virus infections<sup>41-44</sup> (Figure 1.4, patient 3):

1. haplo-identical transplantation with T cell depletion of the graft,
2. cord blood transplantations with high dose serotherapy and a delayed immune reconstitution, *and*
3. severe immunosuppression due to graft-versus host disease.

The prevention of viral reactivation and infection would be the best way to reduce morbidity and mortality caused by these viruses. The prophylactic use of antiviral medication is restricted by the limited effectiveness and considerable toxicity of antiviral drugs. For CMV, EBV and HAdV, no effective prophylactic drugs are available. Once these viruses become symptomatic, they are very often disseminated and treatment started at that moment will be too late. For this reason, these viruses are routinely monitored in high risk patients.<sup>45</sup> Monitoring is performed on weekly plasma samples in which viral load is determined by polymerase chain reaction (PCR) technology. Once the viral load reaches a certain threshold (most often 1000 DNA copies/ml of blood) at two consecutive time points, pre-emptive treatment is installed.<sup>45</sup>

### 2.1 Cytomegalovirus and Epstein Barr virus

For both CMV and EBV, primary infection in young children causes mild flu-like symptoms, whereas primary infection in adolescents and adults can cause infectious mononucleosis (M. Pfeiffer, EBV) or infectious mononucleosis-like disease (CMV).<sup>40</sup> In the adult population, 60% and 90% of individuals is seropositive for CMV and EBV, respectively. As a consequence, most HSCT recipients are at risk for reactivation. Seropositive patients, who receive a graft from a seronegative donor, are at risk for severe infections as no virus-specific memory T cells are co-infused with the graft.<sup>42;43;46</sup> The selection of donors-recipient combinations based on CMV serostatus is applied, but this is only possible when two or more donors with a comparable HLA match are available.<sup>46</sup>

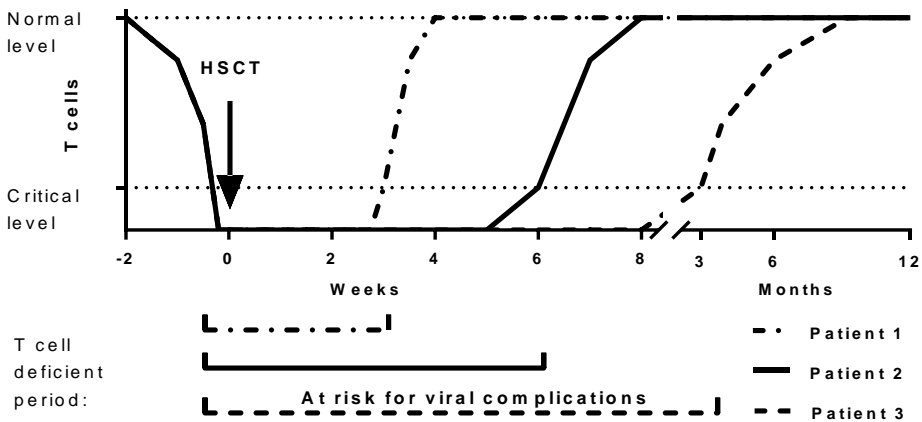


**Figure 1.4 Relation between T cell reconstitution and the risk off viral complications.**  
 Patient 1: IRD transplantation, no serotherapy. Patient 2: MUD transplantation with serotherapy. Patient 3: Cord blood transplantation with serotherapy or haplo-identical transplantation with T cell depletion and serotherapy.

CMV reactivation after HSCT can lead to disseminated infections causing interstitial pneumonitis, colitis and hepatitis.<sup>43</sup> EBV reactivation in immunocompromised patients can lead to post-transplant lymphoproliferative disease (PTLD), a life-threatening neoplastic condition caused by the uncontrolled proliferation of EBV-infected B cells.<sup>42</sup>

For CMV, pre-emptive treatment consists of intravenous ganciclovir or foscarnet. Since the introduction of pre-emptive CMV treatment, two decades ago, morbidity and mortality have dropped significantly. However, both drugs have a considerable toxicity profile. Ganciclovir causes myelosuppression, which is undesirable after HSCT, and foscarnet is associated with severe nephrotoxicity.<sup>47</sup>

For EBV, rituximab, a monoclonal antibody against CD20, is used as pre-emptive treatment. Rituximab depletes B cells, thereby removing the major pool of cells the virus is dependent on for its replication. The use of rituximab has led to a strong reduction of EBV-PTLD, but is obviously associated with a delayed B cell reconstitution.<sup>39;42</sup>

**2.2 Other herpesviruses**

Herpes Simplex Virus (HSV) and Varicella Zoster Virus (VZV) reactivations after HSCT can have a prolonged course but are often limited to oral mucosa and skin. Dissemination of disease, causing pneumonia or meningitis sporadically occurs.<sup>48</sup> For HSV and VZV, prophylactic acyclovir treatment is applied successfully.<sup>48</sup> Human herpesvirus 6 (HHV6) causes the sixth disease (exanthema subitum) upon primary infection. Reactivations generally occur in the first month after HSCT and cause fever and skin rash, which is generally self-limiting but may be mistaken for GvHD.<sup>49</sup>

### 2.3 Human Adenovirus

Although HAdV infection does not lead to a state of latency, the virus can remain detectable for a substantial period of time after primary infection. This may be the reason that HAdV infections or reactivations are mainly seen in pediatric HSCT recipients. Currently, more than 50 serotypes have been described. In healthy individuals, HAdV infections cause self-limiting infections such as conjunctivitis, upper respiratory tract-, urinary tract- or gastrointestinal infections.<sup>50</sup> After HSCT, HAdV reactivations or primary infections can progress to viremia and disseminated disease. In the absence of T cell surveillance, the mortality of HAdV viremia is high because of progression to HAdV related multi-organ failure.<sup>41;51</sup>

Ribavirin and cidofovir have been explored for the pre-emptive treatment of HAdV infections. However, HAdV remains a major clinical problem despite pre-emptive treatment. Ribavirin was shown to be ineffective in patients without lymphocyte reconstitution.<sup>52</sup> Cidofovir is commonly used as pre-emptive treatment for HAdV but is associated with severe nephrotoxicity.<sup>53-56</sup> Also, the clinical effect is often disappointing, with HAdV clearance ranging from 24-98% of patients.<sup>54-59</sup> Recently, promising data have been published for brincidofovir, the orally bioavailable lipid conjugate of cidofovir. This drug has a reduced toxicity profile, while higher intracellular concentrations are reached. The majority of HSCT recipients with HAdV infections had a reduction of HAdV load during brincidofovir treatment.<sup>60;61</sup>

### 3. Immune reconstitution after HSCT

As discussed in the previous sections, immuno-ablation, leading to white blood cell aplasia, is applied in order to create a permissive environment for the stem cell graft and prevent alloreactivity. However, this induced immunodeficiency is associated with an increased risk for opportunistic infections (Figure 1.3). During white blood cell aplasia, patients are at risk for severe bacterial, viral and fungal infections. A disseminated course of viral and fungal infections may occur during lymphopenia. Therefore, the rapid reconstitution of the immune system is of great importance to reduce transplant related morbidity and mortality.

In this section, the typical pattern of immune reconstitution will be described, as well as the main factors influencing immune reconstitution and interventions explored to improve immune reconstitution. In view of the other chapters in this thesis, the focus of this section will be on T cells and NK cells.

Generally, the cells of the innate immune system (Monocytes, Neutrophils and NK cells) recover within a month after HSCT. T cell reconstitution often occurs in the second month whereas B cells are the last lymphocyte subset that reconstitutes after HSCT (Figure 1.5).<sup>33;62</sup> As already discussed in the first section of this chapter, many HSCT related parameters have an impact on immune reconstitution. Especially T cell reconstitution is strongly affected by T cell depletion of the graft and serotherapy (Figure 1.4).

#### 3.1 Recovery of innate immunity

The first line of immunity is represented by the epithelial and mucosal barriers that prevent tissues against invasion of microbes. This barrier is often disrupted by the pretransplant chemotherapy and irradiation and usually recovers within weeks, although this can be delayed by GvHD.<sup>63</sup> Most complement factors are produced by liver cells and are generally not deficient after HSCT.<sup>64;65</sup> Neutrophils and monocytes are the first cells that recover from the donor derived stem cells. Neutrophil recovery is used as a marker for engraftment, defined by the moment neutrophils reach  $0.5 \times 10^9$  cells / ml of blood.

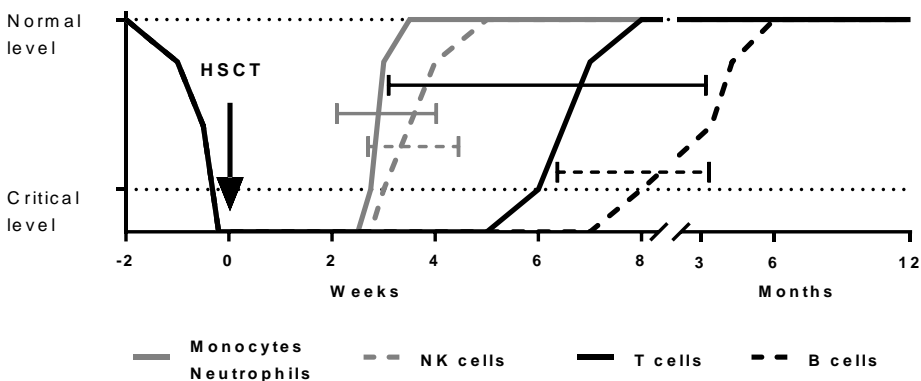
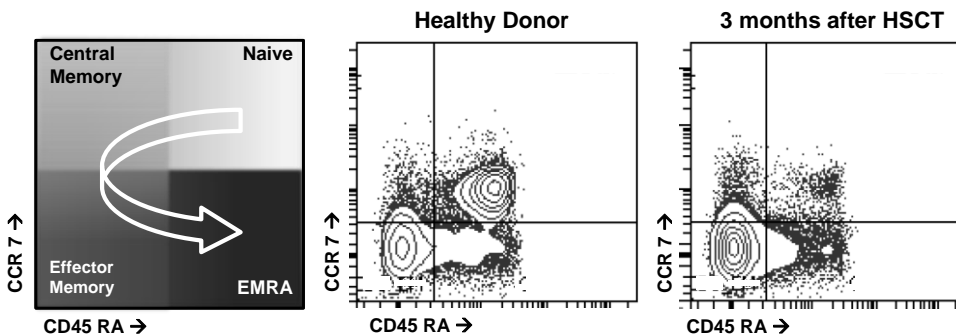


Figure 1.5. Typical reconstitution of innate (gray) and adaptive (black) immune cell subsets after HSCT.

Engraftment generally occurs within 2-4 weeks after HSCT (Figure 1.5).<sup>33,62</sup> Rapid engraftment is observed in patients who received a PBSC graft and delayed engraftment may occur in patients who received a cord blood graft or a graft from a haplo-identical donor. Dendritic cells in blood reconstitute from donor stem cells within weeks after HSCT. However, the replacement of the recipients tissue-residing antigen presenting cells may take several months.<sup>66,67</sup> Natural killer (NK) cells are the first lymphocytes that reappear in the circulation after HSCT (Figure 1.5). The reconstitution of NK cells will be discussed separately in the last section of this chapter.

### 3.2. T lymphocytes

T cells are the key players of the adaptive immune system and provide life-long pathogen specific protection. As a result of T cell receptor rearrangement, each T cell clone recognizes only one specific epitope. T cells develop and are educated in the thymus. In the thymus, T cells that do not recognize self-MHC and T cells that have a too strong affinity to self-MHC are removed to end up with useful T cells that can interact with other cells, but which are generally not auto-reactive (central tolerance).<sup>68</sup> However, T cells are only educated to be tolerant for self-MHC, leaving the possibility of occurrence of alloreactivity after HSCT. The human T cell compartment consists of  $CD4^+$  T helper cells and  $CD8^+$  cytotoxic T cells.  $CD4^+$  T cells orchestrate immune responses via the secretion of cytokines and interaction with other immune cells. Distinct subpopulations of  $CD4^+$  T cells have specific cytokine profiles to direct (*e.g.* Th1, Th2 and Th17) or regulate (regulatory T cells, Treg) the immune response.<sup>69</sup>  $CD8^+$  T cells are cytotoxic and destroy virus-infected and tumor-transformed cells. Once naïve T cells have encountered their specific antigen, T cells are activated, proliferate and differentiate into effector and memory cells. The differentiation of human T cells can be discerned based on the expression of cell surface markers (*e.g.* CD45RA and CCR7, Figure 1.6). Naïve ( $CD45RA^+ CCR7^+$ ) cells differentiate upon antigen exposure into central memory (CM,  $CD45RA^- CCR7^+$ ) and effector memory (EM,  $CD45RA^- CCR7^-$ ) cells and eventually regain CD45RA when differentiating into end-stage effector (EMRA,  $CCR7^- CD45RA^+$ ) cells.<sup>70</sup> Whereas the expression of co-stimulatory molecules and chemokine receptors varies between the differentiation stages, ex-vivo cytolytic capacity increases during differentiation and telomere length shortens.<sup>70</sup>



**Figure 1.6. T cell differentiation stages.**

T cell differentiation can be discerned based on the expression of CCR7 and CD45RA in healthy individuals and early after HSCT.  $CD8^+$  T cell differentiation is depicted.

### 3.2.1 T cell reconstitution after HSCT

The recovery of normal numbers of T lymphocytes after HSCT takes months, but the complete and balanced reconstitution of the adaptive immune system ranging from naïve cells to effector- and memory cells takes many years.<sup>62;71</sup>

In the first months after HSCT, the repopulation of the T cell compartment is facilitated by cytokine- and antigen-driven homeostatic peripheral expansion of T cells that were transplanted with the graft. Both memory cells and naïve cells that were transplanted with the graft will differentiate and expand rapidly when they encounter the antigen of their specificity. As a result, the first stage of T cell reconstitution is strongly skewed towards memory cells (Figure 1.6).<sup>33;62</sup> This expansion of memory cells is more rapid for CD8<sup>+</sup> T cells than for CD4<sup>+</sup> T cells. The early reconstitution of T cells is strongly affected by T cells depletion of the graft, as well as the use of serotherapy (Figure 1.3). Also, cord-blood grafts are associated with a delayed T cell reconstitution.<sup>33;62</sup>

The thymus-dependent generation of naïve T cells, essential for building a balanced immune system with a broad specificity against neo- and recall antigens is delayed for many months to years.<sup>71</sup> T cells that develop from donor stem cells will undergo selection in the thymus of the recipient and should be tolerant for the recipient's tissues. In children, the reconstitution of naïve T cells is better than in adults, which is related to the involution of the thymus during life. Damage to the thymus caused by the conditioning regimen or GvHD has a negative impact on the reconstitution of naïve T cells.<sup>62;71</sup>

### 3.2.2 Strategies to improve T cell reconstitution

Reconstitution of CD4<sup>+</sup> and CD8<sup>+</sup> T cell immunity is pivotal to provide protection against and achieve sustained control of viral reactivations as well as anti-leukemic reactions.<sup>15;37-39</sup> However, T cells are also responsible for GvHD, which is mainly caused by (naïve) T cells transplanted with the graft.<sup>16</sup> The improvement of T cell reconstitution is therefore a delicate issue. The easiest way to improve T cell reconstitution is the omission of serotherapy from the conditioning regimen, as is applied in the IRD transplant setting. However, this is not possible in other transplant settings due to the risk of GvHD. However, personalized dosing of serotherapy can be applied to prevent overdosing and results in faster T cell reconstitution without increasing the risk of GvHD.<sup>30</sup> Also, the early tapering of CsA immunosuppression and omission of methotrexate from GvHD prophylaxis has been used to improve T cell reconstitution and to enable GvL reactions.<sup>34</sup>

Alternatively, donor lymphocytes can be infused in the period after the HSCT. Donor lymphocyte infusions (DLI) contain both virus-specific memory T cells as well as naïve T cells that can generate de novo graft-versus-leukemia reactions.<sup>72;73</sup> Even when given months after HSCT, under non-inflammatory conditions, unselected DLI are still associated with the development of GvHD.<sup>72;73</sup> The use of unselected DLI in the early, inflammatory phase after HSCT to treat viral infections bears a large risk of GvHD development. Therefore, adoptive transfer of virus specific T cells from the donor to restore anti-viral immunity after HSCT has been explored. By the *ex vivo* selection of virus-specific cells, co-transfer of alloreactive cells can be limited, thus reducing



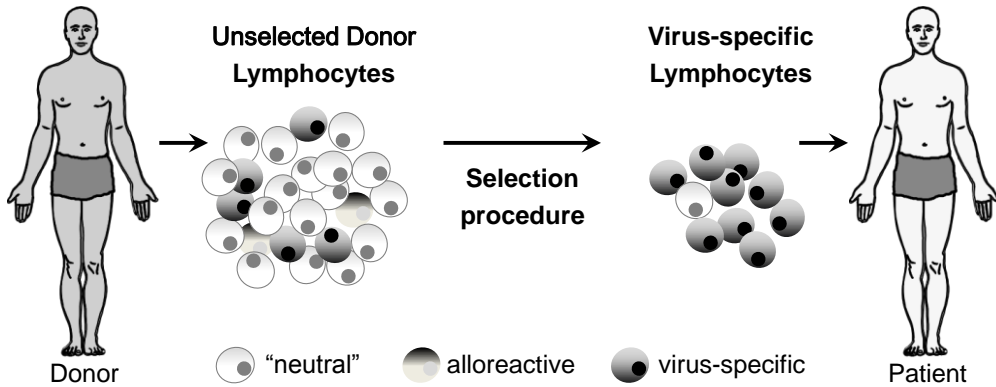


Figure 1.7. Selection of virus-specific T cells for adoptive immunotherapy.

the risk of GvHD development (Figure 1.7). The first approach used for the generation of virus-specific T cell products is the repetitive stimulation of donor lymphocytes with APCs transfected with viral vectors encoding for viral peptides (CMV, HAAdV) or EBV-transformed B cells. This strategy yields large numbers of virus-specific (mainly CD8<sup>+</sup>) T cells which have been safely used in clinical trials.<sup>74-76</sup> However, due to the high workload and long culture period, this approach is unfeasible for broad application. The second approach aims to select virus-specific cells directly *ex vivo*. Tetramer based magnetic isolation uses MHC class I tetramers loaded with viral peptides, which bind virus-specific cells via their T cell receptor. The virus-specific cells are then labelled with magnetic beads, and isolated via a magnetic column. This method is rapid and has been used for the selection of CMV-specific CD8<sup>+</sup> T-lymphocytes.<sup>77</sup> However, MHC class I tetramers are limited to certain HLA class I alleles and do not select CD4<sup>+</sup> virus-specific T-cells.

Thirdly, the interferon- $\gamma$  (IFN- $\gamma$ ) capture assay has been developed. In this approach, PBMC are stimulated with viral peptide pools for a couple of hours. Virus-specific T cells become activated and produce IFN- $\gamma$ . The IFN- $\gamma$  secreting virus-specific cells are then labelled with magnetic beads and isolated via a magnetic column. This method enables the rapid enrichment of both CD4<sup>+</sup> and CD8<sup>+</sup> virus-specific cells. However, only a subset of virus-specific T cells secrete IFN- $\gamma$  upon activation.<sup>78,79</sup> This method has been successfully used in the clinical setting to select T-cells specific for CMV, EBV and HAAdV.<sup>80-82</sup>

Both tetramer-based and IFN- $\gamma$  capture based techniques yield low numbers of virus-specific cells, which will proliferate *in vivo* upon antigenic stimulation after infusion in a patient with a viral reactivation. Transfused virus-specific T cells are detectable and provide protection for years after infusion. However, the production of virus-specific T cell products remains very labor-intensive and is only available in a small number of transplant centers. To address this problem, third party biobanks have been started in the United States and United Kingdom, in which virus-specific T cells from donors with common HLA-types are produced and cryopreserved, available for “of the shelf” use in HSCT recipients with a viral reactivation.<sup>83</sup>

### 3.3. Natural Killer cells

NK cells play a role in the innate immune defense through the direct lysis of virus-infected and malignant cells. Furthermore, they secrete cytokines and chemokines that initiate, enhance and regulate immune responses.<sup>84-87</sup> NK cells are a member of the large family of innate lymphoid cells (ILC). However, unlike the other ILC, NK cells are cytolytic and express perforin. They are classified in ILC group 1 based on their production of the inflammatory cytokines IFN- $\gamma$  and TNF- $\alpha$ . They can be distinguished from other ILC by the expression of the transcription factor Eomesodermin (EOMES) and the cytolytic protein perforin.<sup>88;89</sup> In the last decade, the development of human NK cells from hematopoietic stem cells has been studied extensively. The first CD34+ stages of human NK cell development (stage 1 and 2) are observed in both bone marrow and secondary lymphoid tissues.<sup>90;91</sup> Subsequently, stage 3 NK cell development mainly occurs in secondary lymphoid tissues.<sup>91-93</sup> At this stage, NK cells acquire the expression of CD56 and express high levels of CD117 (c-kit) and CD127 (IL7R $\alpha$ ), showing close homology to type 3 ILCs.<sup>88;91;94</sup> Two distinct EOMES<sup>+</sup>perforin<sup>+</sup> NK cell populations are present in human peripheral blood: the minor CD56<sup>bright</sup>CD16<sup>+/-</sup> (CD56<sup>bright</sup>, stage 4) subset which constitutes 5-15% of NK cells, and the major CD56<sup>dim</sup>CD16<sup>+</sup> (CD56<sup>dim</sup>, stage 5) subset (Figure 1.8).<sup>87;95</sup> CD56<sup>bright</sup> NK cells are generally considered to be the precursors of CD56<sup>dim</sup> NK cells.<sup>91;96</sup> For example, CD56<sup>bright</sup> NK cells have longer telomeres and express low levels of stem cell factor receptor c-kit (CD117).<sup>97;98</sup> The expression of the inhibitory receptor NKG2A, expressed by all CD56<sup>bright</sup> NK cells, is lost during the differentiation of CD56<sup>dim</sup> NK cells, which ultimately acquire killer-immunoglobulin-receptors (KIRs) and the terminal differentiation marker CD57 (Figure 1.8).<sup>99</sup> Both subsets have their own functional profile; CD56<sup>bright</sup> NK cells are mainly cytokine producers. Although they constitutively express perforin, they do not express granzyme B and require pre-activation to exert cytotoxicity (Figure 1.8). In contrast, CD56<sup>dim</sup> NK cells constitutively express perforin and granzyme B and efficiently lyse target cells without prior stimulation.<sup>87;95;100;101</sup> However, both subsets can be cytotoxic and produce cytokines, after the appropriate *in vitro* stimulation.<sup>100-105</sup> Although the CD56<sup>dim</sup> NK cells predominate in blood, the CD56<sup>bright</sup> NK represent the majority of NK cells in both lymphoid and non-lymphoid tissues.<sup>106-108</sup>

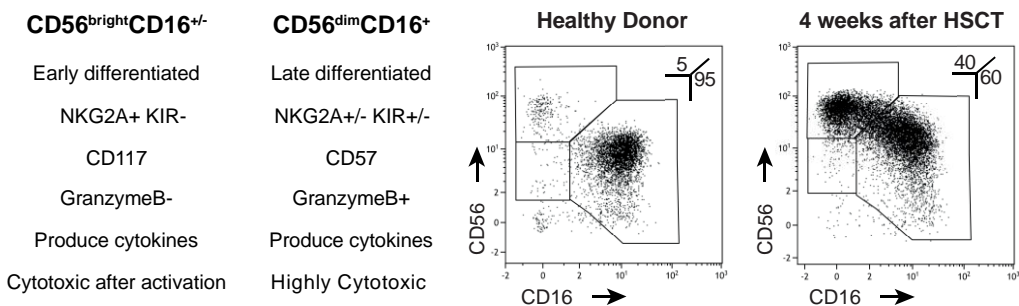


**Figure 1.8. Circulating human NK cell subsets.**

Hallmarks of CD56<sup>bright</sup>CD16<sup>+/-</sup> and CD56<sup>dim</sup>CD16<sup>+</sup> NK cell subsets and their typical distribution in blood of healthy individuals and patients early after HSCT.

### 3.3.1 NK cell cytotoxicity, activation and tolerance

Unlike T cells, NK cells do not require prior activation to exert their killing function and are not restricted to MHC-class I presentation of viral antigens; rather, they recognize “missing self” (the down regulation of MHC molecules) and “induced or altered self” (the expression of stress-induced or virus-encoded ligands) on virus-infected or malignant cells.<sup>87;109</sup> The overall responsiveness of NK cells can be increased by monokines (*e.g.* IL2/IL12/IL15/IL18) produced by other immune cells like dendritic cells and monocytes (Figure 1.9).<sup>87;110</sup> The killing activity of NK cells is regulated by a balance of inhibitory and activating signals. In the presence of MHC class I molecules on a target-cell, inhibitory NK-cell receptors are triggered. This leads to the delivery of inhibitory signals via the intracellular immunoreceptor tyrosine-based inhibitory motif (ITIM) domain, preventing NK cell activation and lysis of the target-cell. When MHC class I molecules are downregulated, as in the case of tumor cells or virus- infected cells, no inhibitory signal is delivered. Instead, positive signals through activating receptors with an intracellular immunoreceptor tyrosine-based inhibitory motif (ITAM) dominate, which induces NK cell activation and lysis of target cells.<sup>87;109;111</sup>

Activating signals to the NK cell can be induced by the activating receptor NKG2D when it binds MHC class I-like ligands that are induced by virus infection and malignant transformation, but also by activating KIRs and the heterodimeric CD94-NKG2C receptors that recognize MHC-class I ligands, and by a number of other activating receptors (*e.g.* NKp30, NKp44, NKp46) for which the cellular ligands have yet to be identified.<sup>87;109</sup>

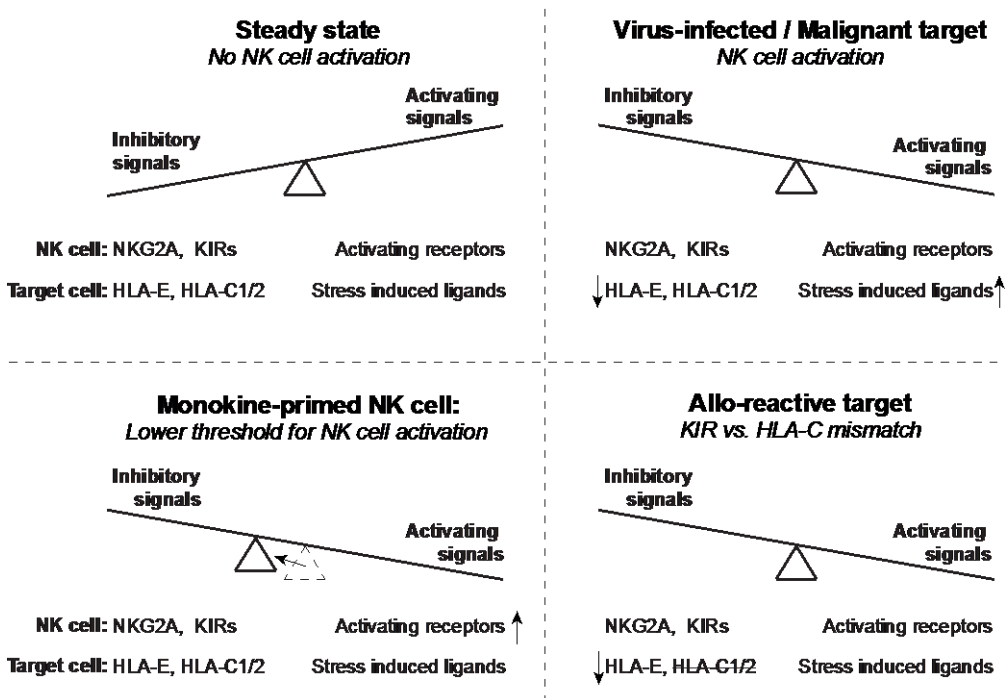


Figure 1.9. Principles of NK cell activation and tolerance.

Inhibitory NK cell receptors that recognize MHC-class I molecules include inhibitory killer immunoglobulin-like receptors (KIR) recognizing HLA-C molecules, and the inhibitory CD94-NKG2A heterodimeric receptors recognizing the non-classical HLA-E molecule. To prevent, the killing of healthy cells in the body (auto-reactivity), NK cells need to express at least one inhibitory receptor for MHC class I to be “licensed to kill”: NK cells lacking an inhibitory receptor for self MHC are hyporesponsive.<sup>102;111;112</sup> The KIR expression repertoire, encoded on chromosome 19 is polymorphic amongst individuals. Two main groups of KIRs are recognized, the A and B haplotype. KIR A haplotypes recognize (and are inhibited by) HLA-C1 and the ligand for KIR B haplotypes is HLA-C2.<sup>113</sup> As KIRs and HLA-C are inherited independently, individuals can have NK cells expressing KIRs for which no ligand is available. These “uneducated” NK cells will become hyporesponsive.<sup>102;112</sup> In conclusion, the cytotoxicity of NK cells is the result of the balance between a) resting vs. activation/priming as mediated by monokines produced by other immune cells and b) inhibitory vs. activating signals by target cell-interaction (Figure 1.9).

### 3.3.2 Role of NK cells in immune responses

NK cells play a role in the control of viral load early during infection. NK cells contribute to the first line of immune defense through the lysis of virus-infected cells. Furthermore, NK cells play an important role in the initiation, enhancement and regulation of immune responses, directly through the secretion of cytokines and chemokines as well as indirectly via their interaction with other innate immune cells.<sup>84-87;114-116</sup> The best illustrations of the clinical relevance of NK cells are rare patients with isolated NK cell deficiencies, who are susceptible to herpesvirus infections.<sup>117;118</sup> CMV infection is associated with an increase in late differentiated NKG2A<sup>-</sup> KIR<sup>+</sup> NKG2C<sup>+</sup> CD56<sup>dim</sup> NK cells.<sup>119</sup> In healthy individuals with primary EBV infections, an expansion of CD56<sup>bright</sup> and early differentiated NKG2A<sup>+</sup> KIR<sup>-</sup> CD56<sup>dim</sup> NK cells has been described.<sup>120;121</sup>

Secondly, NK cells can function as anti-tumor effector cells via the elimination of malignancies with reduced MHC-class I expression that evade CD8<sup>+</sup> T cell-mediated control and of tumors with increased expression of activating NK cell receptor ligands.<sup>87</sup>

Thirdly, NK cell alloreactivity, based on the mismatch of KIR and KIR-ligands has been exploited in the setting of haplo-identical HSCT.<sup>122-124</sup> For example, when NK cells from a KIR A haplotype donor (tolerant for HLA-C1) are transplanted into a HLA C1 negative patient, no inhibitory signal is provided by the recipients hematopoietic cells, resulting in NK cell alloreactivity against HLA-C1 negative leukemic cells (Figure 1.8). Seminal studies have shown that the patients receiving a haplo-identical HSCT with NK cell alloreactivity in the graft vs. host direction have a reduced relapse rate and better overall survival.<sup>122</sup> In line with this, *in vitro* (monokine) activated donor derived NK cells have been exploited for the use as adoptive immunotherapy, especially in the haplo-identical HSCT setting, but also in the setting of primary malignancies susceptible for NK cell mediated cytotoxicity.<sup>123;124</sup>

### 3.3.3 NK cell reconstitution after HSCT

NK cells are the first lymphocytes that reconstitute after HSCT, reaching normal numbers within 3-4 week after HSCT.<sup>33;125</sup> Typically, the phenotype of NK cells after HSCT is skewed towards the (NKG2A<sup>+</sup>) CD56<sup>bright</sup> NK cell phenotype (Figure 1.7). Because of the short life-time of NK cells and the phenotypic difference between the NK cells appearing early after HSCT and healthy donor NK cells, these NK cells are considered to reconstitute from stem cells in the graft. Various studies reported the existence of phenotypic and functional intermediate stages in the progression from CD56<sup>bright</sup> to CD56<sup>dim</sup> NK cells after HSCT. These studies mainly focused on CD16, CD27 or CD117, for which CD56<sup>bright</sup> NK cells have a bimodal expression profile.<sup>100;126-128</sup> The phenotype of CD56<sup>dim</sup> NK cells recovering after HSCT also differs from healthy donor CD56<sup>dim</sup> NK cells. The first CD56<sup>dim</sup> NK cells are mainly NKG2A<sup>+</sup> and KIR<sup>-</sup>. CD56<sup>dim</sup> NK cells lose the expression of NKG2A and gain the expression of KIRs during the first year after HSCT, recapitulating NK cell differentiation.<sup>99</sup> In patients with CMV reactivation after HSCT, a specific expansion of NKG2A<sup>-</sup>KIR<sup>+</sup>NKG2C<sup>+</sup> CD56<sup>dim</sup> NK cells has been described.<sup>129</sup>

Contradicting data exist on the functional capacity of NK cells after HSCT. Various reports have described a normal cytotoxicity early after HSCT but a delayed recovery of IFN- $\gamma$  production upon target cell recognition.<sup>130-132</sup> Other studies reported a reduced cytotoxicity of NK cells in the first months after HSCT.<sup>133-135</sup> A third group of studies showed that post-transplant NK cells display a reduced cytotoxicity against AML blasts expressing the NKG2A-ligand HLA-E, but have a normal killing of other target cells like K562 and EBV-LCL.<sup>135-138</sup> The relative hypofunction of NK cells after HSCT may be explained by induced tolerance because of the absence of self-KIRs for donor NK cells in the host. Another possible explanation for the reduced functionality of NK cells is the inhibition via NKG2A as most (CD56<sup>bright</sup> and CD56<sup>dim</sup>) NK cells that reconstitute are NKG2A<sup>+</sup> after HSCT.



## 4 Objectives and outline of this thesis

Immune reconstitution is a major predictor of the outcome of viral complications after HSCT. A better understanding of immune reconstitution after HSCT and the interplay between different players of the immune system may provide tools to improve this immune reconstitution.

The **first part** (Chapter 2-4) of this thesis focusses on the relation between viral reactivations and T cell reconstitution. The importance of early T cell reconstitution to prevent and clear viral reactivations has been well established. However, the long term impact of viral reactivations on the composition of the immune system is largely unknown. In **Chapter 2**, we studied the impact of early CMV, EBV and HAdV infections on the composition and balance of the T cell compartment long term after HSCT. **Chapter 3** describes the development of a clinical grade method to select virus specific T cells for the restoration of T cell immunity for CMV, EBV and HAdV in one single procedure. For this, alternatives for the IFN- $\gamma$  capture assay to select virus-specific T cells were explored, using the upregulation of various activation markers on virus-specific T cells upon peptide pool stimulation. **Chapter 4** addresses the effectiveness of pre-emptive Cidofovir therapy for HAdV infections after HSCT. To correct for the confounding effect of reconstitution of T cell immunity on the reduction of HAdV viral load during cidofovir treatment, we focused on patients lacking T cell reconstitution. We discovered that the reduction of HAdV load in the absence of T cells was always associated with an expansion of (CD56<sup>bright</sup>) NK cells.

The **second part** (Chapter 5-7) of this thesis is focused on NK cells. In steady state conditions, the role of NK cells in anti-microbial immunity may be overshadowed by the presence of T cells. As NK cell reconstitution often precedes the recovery of T cells after HSCT, this creates a window of opportunity to study NK cells in the absence of T cells. **Chapter 5** addresses one of the restrictions of working with cryopreserved material. Whereas T cells are relatively resistant to cryopreservation, NK cells may display phenotypic changes which have to be accounted for when working with biobanked material. **Chapter 6**, describes the quantitative as well as phenotypic and functional reconstitution of CD56<sup>bright</sup> NK cells in patients with a rapid and a delayed T cell reconstitution to unveil changes in the NK cell compartment during transient T cell deficiency after HSCT. In **Chapter 7**, we studied the phenotype and homing potential of CD56<sup>bright</sup> NK cells in blood and lymphoid organs, which is the primary location for interactions between NK cells and other immune cells. We discovered a major tissue-resident NK cell population, which was further characterized. Also, the reconstitution of the different NK cell subsets in bone marrow after HSCT was studied.

The findings and implications of the work reported in this thesis are summarized in **Chapter 8** and discussed in **Chapter 9**.





# Chapter 2

## Early CMV reactivation leaves a specific and dynamic imprint on the reconstituting T cell compartment long term post hematopoietic stem cell transplantation

Published in:  
Biology of Blood and Marrow Transplantation  
2014; 20: 655-661

Gertjan Lugthart  
Monique M. van Ostaijen-ten Dam  
Cornelia M. Jol - van der Zijde  
Tessa C. van Holten  
Michel G.D. Kester  
Mirjam H.M. Heemskerk  
Robbert G.M. Bredius  
Maarten J.D. van Tol *and*  
Arjan C. Lankester

## Abstract

Human Cytomegalovirus (CMV) reactivation frequently occurs during the early phase of immune recovery after allogeneic hematopoietic stem cell transplantation (HSCT). Whereas the recovery of virus-specific immunity in the early phase after HSCT is extensively studied, the impact of CMV on the reconstitution and composition of the T cell compartment long term post HSCT is unknown. We analyzed T cell reconstitution one to two year after HSCT in 131 pediatric patients. One year post HSCT, patients with early CMV reactivation (n=46) had three-fold higher CD8<sup>+</sup> T cell numbers (median 1323 vs. 424 cells/ $\mu$ l,  $p<0.0001$ ) compared to patients without CMV reactivation (n=85). This effect, caused by a major expansion of CD8<sup>+</sup> effector memory (EM) and end-stage effector (EMRA) T cells, was independent of pre-transplant donor and recipient CMV serostatus and not seen after Epstein-Barr virus or Adenovirus reactivations. At one and two year post HSCT, the absolute numbers of CD8<sup>+</sup> naive and central memory (CM) T cells as well as CD4<sup>+</sup> naïve, CM, EM and EMRA T cells did not differ between patients with and without CMV reactivation. In the second year post HSCT, a significant contraction of the initially expanded CD8<sup>+</sup> EM and EMRA T cell compartments was observed in patients with early CMV reactivation. In conclusion, CMV reactivation early after pediatric HSCT leaves a specific and dynamic imprint on the size and composition of CD8<sup>+</sup> T cell compartment without compromising the reconstitution of CD8<sup>+</sup> and CD4<sup>+</sup> naive and central memory T cells pivotal in the response to neo- and recall antigens.

## Introduction

In immunocompetent individuals, CMV infection generally causes mild symptoms after which latency is established and asymptomatic reactivations can occur sporadically throughout life.<sup>139</sup> In contrast, CMV reactivation occurs frequently during the transient period of immune deficiency after allogeneic hematopoietic stem cell transplantation (HSCT) in case of a CMV seropositive donor and / or recipient. This donor- or recipient derived CMV infection or reactivation, hereafter called reactivation, can lead to disseminated infections causing interstitial pneumonitis, colitis and hepatitis which are, despite the pre-emptive use of antiviral medication, a major cause of morbidity and mortality.<sup>46;140</sup> Reconstitution of CD4<sup>+</sup> and CD8<sup>+</sup> T cell immunity is pivotal to provide protection against and achieve sustained control of CMV reactivations.<sup>37;141;142</sup> In the first months after HSCT, the repopulation of the T cell compartment is facilitated by cytokine- and antigen-driven homeostatic peripheral expansion of T cells that were transplanted with the graft.<sup>143;144</sup> The thymic-dependent T cell reconstitution of naive and central memory cells, essential for a balanced immune system with a broad specificity against neo- and recall antigens is delayed for many months to years.<sup>143</sup>

The differentiation stages of human T cells can be discerned based on the expression of cell surface markers CD45RA and CCR7. Naive (CD45RA<sup>+</sup> CCR7<sup>+</sup>) cells differentiate upon antigen exposure into central memory (CM, CD45RA<sup>-</sup> CCR7<sup>+</sup>) and effector memory (EM, CD45RA<sup>-</sup> CCR7<sup>-</sup>) cells and eventually regain CD45RA when differentiating into end-stage effector (EMRA, CCR7<sup>-</sup> CD45RA<sup>+</sup>) cells.<sup>70</sup> Whereas the expression of co-stimulatory molecules and chemokine receptors varies between the differentiation stages, ex-vivo cytolytic capacity increases during differentiation and telomere length shortens.<sup>70;145</sup> With increasing age, a continuous accumulation of CMV-specific CD8<sup>+</sup> T cells, also called “memory inflation”, has been described in healthy CMV seropositive individuals. These cells mainly represent EM and EMRA T cells.<sup>146-148</sup> A durable expansion of these late differentiated T cells has also been observed in infants with congenital and post-natal CMV infections<sup>149-152</sup> and after primary CMV infection or reactivation in patients continuously receiving immunosuppressive medication after solid organ transplantation (SOT).<sup>147;153;154</sup>

In the recent years, the interaction between viral reactivations and early immune reconstitution after HSCT has been studied extensively.<sup>37;141;142;155;156</sup> However, apart from an early report in 1985, the influence of viral reactivations occurring during the early phase of immune reconstitution on the composition of the T cell compartment in steady state conditions after HSCT is largely unknown.<sup>157</sup> In this study, we report the impact of early CMV reactivations on the reconstitution and composition of the T cell compartment one and two year after HSCT in a large cohort of pediatric HSCT recipients.

## Methods

### Ethics Statement

All transplantations were performed according to European society for Blood and Marrow Transplantation guidelines. Blood samples were routinely obtained and analyzed after approval by the institutional review board (protocol P01.028). Informed consent was provided by the patient and/or a parent or guardian.

### Patients and blood sampling

Between 1-1-2002 and 31-12-2011, 227 children received a Bone Marrow or Peripheral Blood Stem Cell transplantation following myeloablative conditioning for malignant and non-malignant hematological disorders in the Leiden University Medical Center (LUMC). A total of 59 patients died in the first year and 11 were lost to follow up (Figure 2.S1). Of the 157 remaining patients, 26 were excluded, resulting in a cohort of 131 patients. Exclusion criteria were relapse of malignant disease (n=8) or autologous reinfusion (n=1) in the first year after HSCT, systemic immunosuppressive drugs at one year post HSCT (n=15), or clinically relevant CMV infection after day +250 (n=2). Patients who received two transplantations (n=14) were analyzed only after their second transplantation. Peripheral blood samples were obtained for routine analysis at different time points after HSCT and the sample drawn closest to one year (median 363 days, range 302-478 days) post HSCT was analyzed in this study. In 76 patients, this sample could be compared with a sample obtained two year (median 729, range 498-849 days) post HSCT and at least 180 days after the first sample.

### Monitoring and treatment of viral reactivations

After HSCT, plasma was routinely screened for Epstein Barr Virus (EBV), CMV and Human Adenovirus (HAdV) DNA by real time quantitative (RQ) PCR.<sup>158-160</sup> The limit of detection in these assays was 50 (1.7 log) viral DNA copies/ml. Reactivation of CMV, EBV and HAdV was defined as detection of viral DNA in plasma at least once, whereas pre-emptive treatment with respectively Ganciclovir, Rituximab or Cidofovir was initiated upon detection of 1000 (3 log) or more viral DNA copies/ml at two or more consecutive time points.<sup>161-163</sup>

### Flow cytometric analysis

To determine the size of individual lymphocyte populations and subsets, peripheral blood mononuclear cells (PBMC) were analyzed by flow cytometry. PBMC were separated using ficoll-isopaque density gradient centrifugation (LUMC Pharmacy, Leiden, NL). PBMC were stained with CD45, CD14, CD33, CD235a, CD3, CD19, CD56, CD4, CD8 and TCR- $\gamma\delta$  antibodies, listed in Table 2.S1. Four-color flow cytometry was performed on a BD FACS Calibur II flow cytometer (Becton Dickinson Biosciences (BD), Franklin Lakes, NJ, US) and data were analyzed using BD Cellquest software. Lymphocytes were defined as CD45<sup>+</sup> CD33/CD235a/CD14<sup>-</sup> cells within the forward / sideward scatter lymphocyte gate and absolute cell numbers per  $\mu$ l of peripheral blood were calculated. In a representative subcohort of 53 consecutive patients who

All patients	no CMV reactivation		CMV reactivation		p - value	
	85	46	Univariate	Multivariate	Univariate	Multivariate
Age of recipient	7.9 (0.4 - 18)	13 (0.5 - 19)	0.001 (c)	0.016 (d)		
Sex of recipient	56 (66%)	32 (70%)	0.70 (a)			
CMV serostatus of recipient	26 (31%)	38 (83%)	<0.0001 (a)			
Age of donor	24 (2.0 - 52)	28 (1.0 - 57)	0.58 (c)			
Sex of donor	43 (51%)	23 (50%)	1.0 (a)			
CMV serostatus of donor	26 (31%)	36 (78%)	<0.0001 (a)			
Indication for HSCT	27 (32%)	21 (46%)	0.13 (a)			
	58 (68%)	25 (54%)				
Donor type	35 (41%)	17 (37%)	0.72 (b)			
	9 (11%)	7 (15%)				
	41 (48%)	22 (48%)				
Graft source	71 (84%)	36 (78%)	0.48 (a)			
	14 (17%)	10 (22%)				
Conditioning regimen	37 (44%)	18 (39%)	0.71 (a)			
	48 (57%)	28 (61%)				
Serotherapy	23 (27%)	10 (22%)	0.49 (b)			
	53 (63%)	28 (61%)				
	9 (11%)	8 (17%)				
T cell depletion	9 (11%)	8 (17%)	0.29 (a)			
Donor Lymphocyte Infusion	5 (6%)	2 (4%)	1.0 (a)			
Stem Cell Boost	2 (2%)	1 (2%)	1.0 (a)			
Acute GVHD ≥ grade 2	13 (15%)	5 (11%)	0.60 (a)			
Peak CMV load	N.A.	3.8 (2.3 - 6.0)	N.A.			
Duration CMV reactivation	N.A.	36 (1 - 185)	N.A.			
Start CMV reactivation	N.A.	26 (5 - 62)	N.A.			
End CMV reactivation	N.A.	80 (13 - 211)	N.A.			
Ganciclovir therapy for CMV	N.A.	33 (72%)	N.A.			
EBV reactivation	50 (59%)	22 (48%)	0.20 (a)			
Rituximab therapy for EBV	11 (13%)	7 (15%)	0.79 (a)			
HAdV reactivation	20 (24%)	15 (33%)	0.30 (a)			
Cidofovir therapy for HAdV	7 (8%)	2 (4%)	0.49 (a)			

**Table 2.1. Characteristics of patients with and without early cytomegalovirus reactivation.**

Categorical data are displayed as: number (percentage). Numerical data are displayed as: median (range). p-values: (a) Fisher's Exact test, (b) Pearson Chi Square test, (c) Mann-Whitney U test, (d) logistic regression analysis. N.A.: Not Applicable, HSCT: Hematopoietic Stem Cell Transplantation, CMV: Cytomegalovirus, EBV: Epstein-Barr-virus, HAdV: Human Adenovirus, GVHD: Graft-versus-Host-Disease. Applied T cell depletion methods: erythrocyte rosetting (n=2), alemtuzumab in the bag (n=4) and CliniMACS CD34 enrichment (n=11). transplantation between 2008 and 2011, T cell differentiation was also analyzed based on CD45RA and CCR7 expression.

underwent transplantation between 2008 and 2011, T cell differentiation was also analyzed based on CD45RA and CCR7 expression.

### Statistical analysis

Statistical analysis was performed using SPSS Statistics 20 (IBM SPSS Inc, Chicago, IL, US). GraphPad Prism software (version 6.00; GraphPad Software, San Diego, CA, US) was used to construct figures. Because cell numbers did not follow Gaussian distribution, Mann-Whitney U test (2 groups), Kruskal-Wallis test (> 2 groups) and Wilcoxon Matched-pairs signed ranks test (paired analysis) were used for the univariate analysis of numerical parameters. Pearson's correlation test was performed on log-transformed data for analysis of univariate correlations. Fisher exact test (2 groups) and Pearson's Chi-square test (> 2 groups) were used for univariate analysis of categorical parameters. Logistic regression analysis and linear regression analysis on log-transformed data were performed for multivariate analysis of parameters with  $p$ -values  $\leq 0.10$  in univariate analysis.

## Results

### Incidence of CMV reactivations and description of patients

In the study cohort of 131 pediatric stem cell transplantation recipients who were available for follow up one year post HSCT, 46 patients (35%) experienced a CMV reactivation in the first 100 days post HSCT. The median duration of CMV viremia was 36 (range 1 – 185) days, starting 5 – 62 (median 26) days after HSCT. The criteria for pre-emptive Ganciclovir treatment were met in 33 of 46 patients (Table 2.1). At the time of transplantation, patients with CMV reactivation after HSCT were more often CMV seropositive (83 vs. 31 %,  $p < 0.0001$ ) and were older (median 13.0 vs. 7.9 year,  $p = 0.001$ ) than patients without CMV reactivation. Also, patients receiving a graft from a CMV seropositive donor more often experienced a CMV reactivation (78 vs. 31 %,  $p < 0.0001$ ). As shown in Table 2.1, no significant differences were observed in other HSCT related parameters. In a logistic regression analysis of parameters with  $p$ -values  $< 0.10$  in univariate analysis, pre-transplant CMV serostatus of recipient and donor as well as patient age differed significantly between children with and without CMV reactivation post HSCT ( $p < 0.0001$ ,  $p < 0.0001$  and  $p = 0.017$ , respectively).

### Patients with early CMV reactivation had higher CD8<sup>+</sup> T cell numbers one year post HSCT

Compared with 85 patients without CMV reactivation, 46 patients with early CMV reactivation had significantly higher lymphocyte numbers one year after HSCT. This could be attributed to an increase of CD3<sup>+</sup> T cells (median 2083 vs. 1257 cells/ $\mu$ l,  $p < 0.0001$ ) whereas NK- and B cell numbers were three-fold higher (median 1323 vs. 424 cells/ $\mu$ l,  $p < 0.0001$ ) in patients with CMV

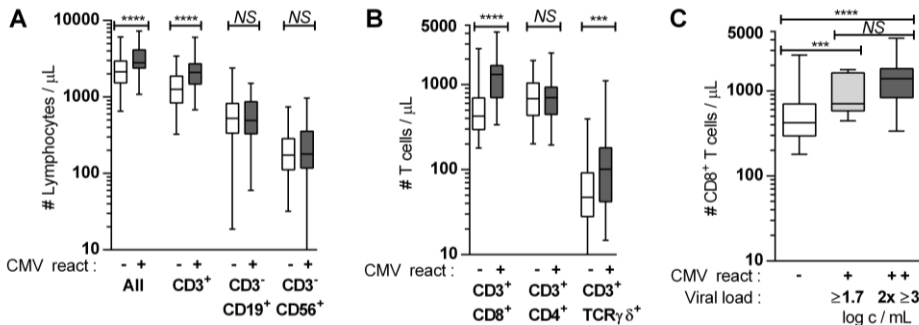


**Figure 2.1. Impact of early CMV reactivation on lymphocyte numbers and -subsets one year post HSCT.**

**(A)** Absolute numbers of lymphocytes, CD3<sup>+</sup> T cells, CD3<sup>-</sup>CD19<sup>+</sup> B-cells and CD3<sup>-</sup>CD56<sup>+</sup> NK cells and **(B)** CD8<sup>+</sup> T cells, CD4<sup>+</sup> T cells and T cell receptor  $\gamma\delta$ <sup>+</sup> T cells from 85 patients without CMV reactivation (white bars, CMV DNA load always < 1.7 log copies/ml (c / ml)) and 46 patients with CMV reactivation (gray bars, CMV DNA load  $\geq 1x >1.7$  log). **(C)** Absolute numbers of CD8<sup>+</sup> T cells of 85 patients without detectable CMV reactivation (white bars), 13 patients with detectable CMV DNA in plasma but not  $\geq 3$  log c / ml at two consecutive time points (light gray bars) and 33 patients with a CMV load  $\geq 3$  log c / ml at two or more consecutive time points (dark gray bars). Shown are cells/ $\mu\text{L}$  of peripheral blood one year post HSCT. Bars: median, interquartile range and overall range. p-values: Mann-Whitney test, NS:  $p > 0.05$ , \*\*\*,  $p < 0.001$ , \*\*\*\*,  $p < 0.0001$

reactivation (Figure 2.1B). Patients with a low level CMV reactivation ( $n=13$ ), i.e. CMV plasma DNA load above the limit of detection, but not at two consecutive time points above 3.0 log copies/ml, already had significantly higher CD8<sup>+</sup> T cell numbers one year post HSCT than patients without CMV reactivation (median 709 vs. 424 cells/ $\mu\text{L}$ ,  $p=0.0001$ , Figure 2.1C). The highest measured plasma CMV DNA load and the time between CMV clearance and analysis at one year post HSCT did not influence the number of CD8<sup>+</sup> T cells at one year post HSCT (Figure 2.S2). Also, the impact of early CMV reactivation on the CD8<sup>+</sup> T cell compartment did not differ between patients who received a stem cell graft from an HLA-identical related donor, matched unrelated donor or haplo-identical donor (data not shown).

CD4<sup>+</sup> T cell numbers were comparable in patients with and without CMV reactivation (median 702 vs. 684 cells/ $\mu\text{L}$ ,  $p=0.79$ , Figure 2.1B). Although  $\gamma\delta$  T cells only represented a small proportion (median 4 %) of all T cells,  $\gamma\delta$  T cell levels were twofold higher in patients with an early CMV reactivation (median 104 vs. 47 cells/ $\mu\text{L}$ ,  $p=0.0005$ , Figure 2.1B).

### The expansion of the CD8<sup>+</sup> T cell subset was independent of pre-transplant CMV serostatus and not seen after EBV and HAAdV reactivation

In univariate analysis, CD8<sup>+</sup> T cell numbers - but not CD4<sup>+</sup> T cell numbers (data not shown) - were significantly influenced by CMV reactivation after HSCT (median 1323 vs. 424 cells/ $\mu\text{L}$ ,  $p < 0.0001$ ) as well as by pre-transplant CMV serostatus of donor (median 780 vs. 460 cells/ $\mu\text{L}$ ,  $p < 0.0001$ ) and recipient (median 880 vs. 440 cells/ $\mu\text{L}$ ,  $p < 0.0001$ , Figure 2.S3). However, in multivariate regression analysis, pre-transplant serostatus of the donor ( $p=0.22$ ) and recipient ( $p=0.14$ ) did not influence CD8<sup>+</sup> T cell numbers independently. This is illustrated in Figure 2.2A,

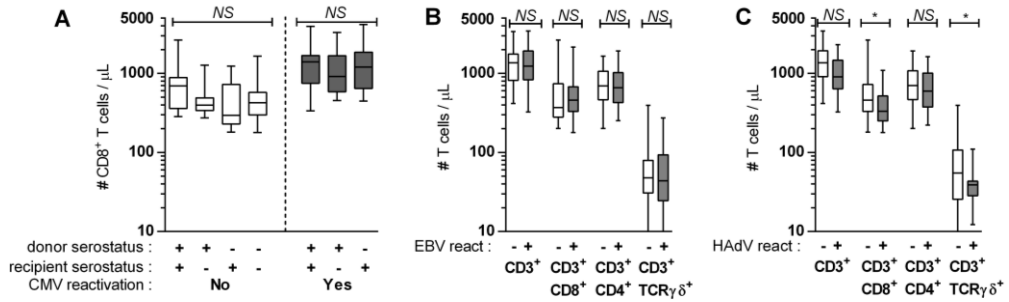


**Figure 2.2. Influence of pre-transplant CMV serostatus and early EBV and HAdV reactivation.**

**(A)** Influence of donor and recipient pre-transplant CMV serostatus on CD8<sup>+</sup> T cell numbers in patients without CMV reactivation (white bars, + / +: n=14, + / -: n=12, - / +: n=13 and - / -: n=46) and patients with CMV reactivation (gray bars, + / +: n=28, + / -: n=8 and - / +, n=10). **(B & C)** Absolute numbers of CD3<sup>+</sup>, CD4<sup>+</sup>, CD8<sup>+</sup> and T cell receptor  $\gamma\delta$ <sup>+</sup> T cell in 85 patients without CMV reactivation. **(B)** 35 patients without vs. 50 patients with early Epstein-Barr virus (EBV) reactivation and **(C)** 65 patients without vs. 20 patients with early Human Adenovirus (HAdV) reactivation. White bars (-): plasma DNA load always < 1.7 log. Gray bars (+): plasma DNA load at least once > 1.7 log. Shown are cells/ $\mu$ l of peripheral blood one year post HSCT. Bars: median, interquartile range and overall range, *p*-values: Kruskal-Wallis test (A) or Mann-Whitney test (B & C). NS: *p* > 0.05, \*: *p* < 0.05.

showing the size of the CD8<sup>+</sup> T cell compartment for patients with- and without early CMV reactivation distributed over the different pre-transplant donor-recipient serostatus combinations. Epstein-Barr Virus (EBV) or Human Adenovirus (HAdV) reactivations as well as other HSCT related variables including T cell depletion of the graft, serotherapy and age of donor and recipient did not significantly influence CD8<sup>+</sup> T cell numbers one year post HSCT (Figure 2.S3). Considering the high impact of CMV reactivation on the CD8<sup>+</sup> T cell compartment, we separately analyzed the effect of early EBV and HAdV reactivations in the 85 patients without CMV reactivation. One year post HSCT, T-, B- and NK cell numbers did not differ between patients with and without EBV or HAdV reactivations (Figure 2.S4). Also, the size of CD8, CD4 and  $\gamma\delta$  T cell subsets did not differ between patients with (n=50) and without (n=35) EBV reactivation (Figure 2.2B). Patients with HAdV reactivations (n=20) had lower numbers of CD8<sup>+</sup> T cells and  $\gamma\delta$  T cells than patients (n=65) without HAdV reactivation (Figure 2.2C). However, patients with and without HAdV reactivations were not fully comparable (Table 2.S2). After multivariate correction for alemtuzumab serotherapy and T cell depletion of the graft, the impact of early HAdV reactivation on CD8<sup>+</sup> T cell numbers one year post HSCT was not statistically significant (*p*=0.11).

### The increase of CD8<sup>+</sup> T cells after CMV reactivation was caused by an expansion of EM and EMRA cells

In a sub-cohort of 53 consecutive patients transplanted between 2008 and 2011, we further determined the differentiation stages of CD4<sup>+</sup> and CD8<sup>+</sup> T cells. Patients in this sub-cohort did not differ significantly from the whole cohort with respect to the parameters listed in Table 2.1 (data not shown). In both T cell subsets, but most pronounced in the CD8<sup>+</sup> T cell subset, the proportion



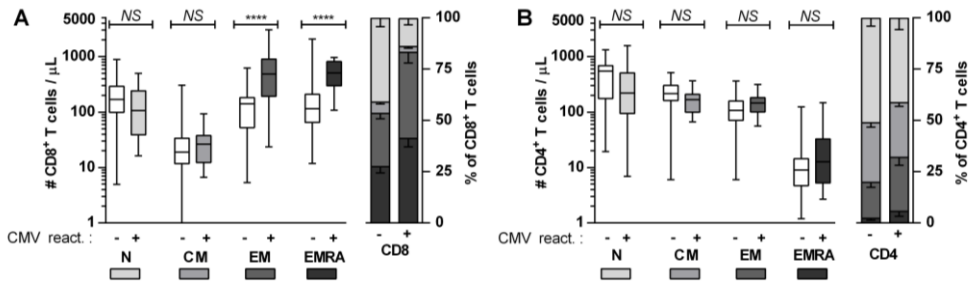


**Figure 2.3. Early CMV reactivation and T cell differentiation one year post HSCT.**

Absolute numbers (left panels) and relative contribution (right panels) of T cell differentiation stages to the (A) CD8<sup>+</sup> and (B) CD4<sup>+</sup> T cell subsets in a subcohort of 35 patients without (-) and 18 patients with (+) CMV reactivation. N: naïve (very light gray, CD45RA<sup>+</sup> CCR7<sup>+</sup>), CM: central memory (light gray, CD45RA<sup>-</sup> CCR7<sup>+</sup>), EM: effector memory (gray, CD45RA<sup>-</sup> CCR7<sup>-</sup>), EMRA: EMRA (dark gray, CD45RA<sup>+</sup> CCR7<sup>-</sup>). Absolute numbers: shown are cells/ $\mu$ L of peripheral blood one year post HSCT. Bars: median, interquartile range and overall range. *p*-values: Mann-Whitney test. NS: *p* > 0.05, \*\*\*\*: *p* < 0.0001. Relative contribution: bars show mean percentage of the CD8<sup>+</sup> or CD4<sup>+</sup> T cell subset with Standard Error of the Mean.

of effector memory and end-stage effector T cells was enlarged in patients with (n=18) compared to patients without (n=35) early CMV reactivation. Together, the cells of the EM and EMRA phenotype constituted a median of 88% of the CD8<sup>+</sup> T cell subset in patients with early CMV reactivation compared to 55% in patients without CMV reactivation (*p* < 0.0001, Figure 2.3A).

Next, we calculated absolute cell numbers for the T cell differentiation stages. The altered memory differentiation in the CD8<sup>+</sup> T cell subset in patients with early CMV reactivation was caused by a major expansion of CD8<sup>+</sup> EM and EMRA T cells (median 485 vs. 141, *p* < 0.0001 and 509 vs. 114 cells/ $\mu$ L, *p* < 0.0001, Figure 2.3 A). The size of the CD8<sup>+</sup> naïve and CM T cell compartment were not significantly affected by early CMV reactivation. The increased contribution of CD4<sup>+</sup> memory T cells in patients with early CMV reactivation was caused by a non-significant increase of CD4<sup>+</sup> and EMRA T cells and a non-significant reduction of CD4<sup>+</sup> naïve and CM T cell numbers (Figure 2.3B).

### Dynamics of CD8<sup>+</sup> T cell expansion in patients with early CMV reactivation after HSCT

Within the 46 patients with an early CMV reactivation, we categorized patients based on the size of the primary CD8<sup>+</sup> T cell recovery at the moment of CMV clearance. In patients with CD8<sup>+</sup> T cell numbers < 500 cells/ $\mu$ L at the moment of CMV clearance (n=21), the CD8<sup>+</sup> T cell number gradually increased after the clearance of CMV (Figure 2.4A). In contrast, in patients with CD8<sup>+</sup> T cell numbers > 500 cells/ $\mu$ L at the moment of CMV clearance (n=25), this subset did not further expand (Figure 2.4A). Whereas at one year post HSCT, the CD8<sup>+</sup> T cell number was not influenced by T cell depletion of the graft (Figure 2.S3), all patients (n=8) who received a T cell depleted graft had CD8<sup>+</sup> T cell numbers < 500 cells/ $\mu$ L at the moment of CMV clearance (*p* = 0.001,

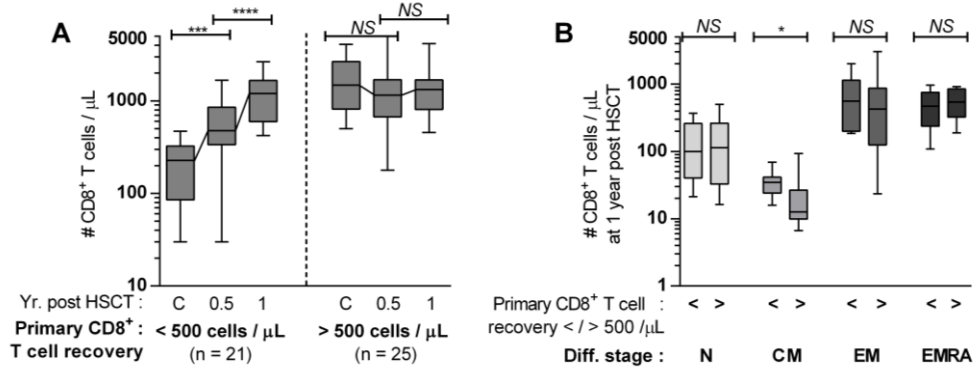


**Figure 2.4. Dynamics of CD8<sup>+</sup> T cell expansion in patients with early CMV reactivation.**

**(A)** Dynamics of CD8<sup>+</sup> T cell reconstitution after CMV clearance in 21 patients with a primary CD8<sup>+</sup> T cell recovery < 500 cells/μL and 25 patients with a primary recovery > 500 cells/μL. Shown are cells/μL of peripheral blood at the moment of CMV clearance (C), 0.5 year and 1 year after HSCT. Bars: median, interquartile range and overall range. Lines connect median values. *p*-values: Wilcoxon Matched-pairs signed ranks test. NS: *p* > 0.05, \*\*\*: *p* < 0.001, \*\*\*\*: *p* < 0.0001.

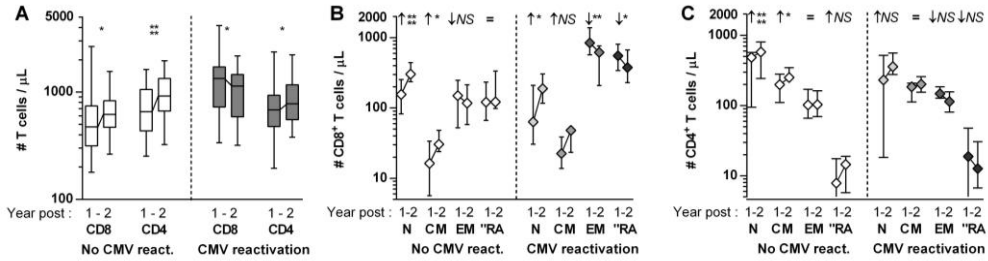
**(B)** Absolute numbers of T cell differentiation stages one year after HSCT in 9 patients with a primary CD8<sup>+</sup> T cell recovery < 500 cells/μL and 9 patients with a primary recovery > 500 cells/μL. N: naive (very light gray, CD45RA<sup>+</sup> CCR7<sup>+</sup>), CM: central memory (light gray, CD45RA<sup>+</sup> CCR7<sup>+</sup>), EM: effector memory (gray, CD45RA<sup>+</sup> CCR7<sup>+</sup>), EMRA (dark gray, CD45RA<sup>+</sup> CCR7<sup>+</sup>). Shown are cells/μL of peripheral blood one year post HSCT. Bars: median, interquartile range and overall range. *p*-values: Mann-Whitney test. NS: *p* > 0.05, \*: *p* < 0.05.

Table 2.S3). Although the dynamics of the CD8<sup>+</sup> T cell expansion differed, the size and composition of the CD8<sup>+</sup> T cell compartment at one year post HSCT were comparable between patients with high or low CD8<sup>+</sup> T cell numbers at the time of CMV clearance (Figure 2.4B).

### Ongoing reconstitution of naive and CM cells in parallel with contraction of EM and EMRA CD8<sup>+</sup> T cells in the second year post HSCT

Finally, we investigated the influence of early CMV reactivations on the T cell reconstitution in the second year after HSCT. The number of CD8<sup>+</sup> T cells decreased in patients with early CMV reactivation (*n*=34, median 1340 to 1141 cells/μL, *p*=0.010) whereas an increase in CD8<sup>+</sup> T cell numbers was seen in patients without CMV reactivation (*n*=42, median 473 to 619 cells/μL, *p*=0.043, Figure 2.5A). Still, the CD8<sup>+</sup> T cell number at two years post HSCT remained significantly higher in patients with early CMV reactivation (*p*=0.0002). In both groups, CD4<sup>+</sup> T cell numbers increased in the second year after HSCT.

More profound changes were observed in the separate T cell differentiation compartments in a sub-cohort of 31 HSCT recipients transplanted between 2008 and 2010. In patients with early CMV reactivation (*n*=12), a contraction of late differentiated CD8<sup>+</sup> EM (median 825 to 618, *p*=0.0068) and EMRA T cells (555 to 378 cells/μL, *p*=0.0342) was observed. This was accompanied by a further reconstitution of CD8<sup>+</sup> naive and CM T cells (Figure 2.5B). In patients without CMV reactivation (*n*=19), CD8<sup>+</sup> naive and CM cell numbers increased, while the size of



**Figure 2.5. Dynamics of T cell reconstitution one and two year after HSCT.**

**(A)** Paired analysis of absolute numbers of CD8<sup>+</sup> and CD4<sup>+</sup> T cells in 42 patients without and 34 patients with early CMV reactivation at one and two year post HSCT. Shown are cells/μl of peripheral blood one and two year post HSCT.

**(B & C)** Paired analysis of absolute numbers of (B) CD8<sup>+</sup> and (C) CD4<sup>+</sup> N, CM, EM and EMRA T cells in 19 patients without (-) and 12 patients with (+) CMV reactivation at one and two year post HSCT. N: naive (very light gray, CD45RA<sup>+</sup> CCR7<sup>+</sup>), CM: central memory (light gray, CD45RA<sup>-</sup> CCR7<sup>+</sup>), EM: effector memory (gray, CD45RA<sup>-</sup> CCR7<sup>-</sup>), EMRA (dark gray, CD45RA<sup>+</sup> CCR7<sup>-</sup>). Shown are cells/μl of peripheral blood one and two year post HSCT. Bars (A): median, interquartile range and overall range. Diamonds (B & C): Median and interquartile range. Lines connect median values one and two year post HSCT. Arrows (↑ / ↓): increase / reduction. *p*-values: Wilcoxon Matched-pairs signed ranks test. = : *p* > 0.10, NS: 0.05 < *p* < 0.10, \*: *p* < 0.05, \*\*: *p* < 0.01, \*\*\*\*: *p* < 0.001.

the CD8<sup>+</sup> EM and EMRA compartments remained stable over time. The increase of CD4<sup>+</sup> T cell numbers was caused by an expansion of naive and CM cells both in patients with and without early CMV reactivation (Figure 2.5C).

## Discussion

Here, we provide evidence that early and transient CMV reactivation leaves a long-lasting, dynamic and specific signature on the composition of the T cell compartment in pediatric HSCT recipients. One year post transplant, patients that had encountered (and cleared) early CMV reactivation showed a marked relative as well as absolute expansion of the CD8<sup>+</sup> EM and EMRA T cell populations. This typical pattern was not seen in patients with early EBV or HAdV reactivation and early CMV reactivation did not compromise the reconstitution of the naive and CM compartments. Furthermore, the CMV signature on T cell reconstitution was subjected to dynamic changes in the year thereafter. This throws a new light on the early findings by Würsch *et al.* in 1985, describing the impact of early CMV infection on the developing T cell immunity in adult HSCT recipients.<sup>157</sup>

One year post HSCT, none of the patients included in this study had active CMV infection. Also, pre-transplant CMV seropositivity of donor or recipient without detectable CMV viremia post HSCT did not trigger the expansion of CD8<sup>+</sup> T cells. Therefore, we hypothesize that CMV reactivation and -viremia in the immunocompromized period early post HSCT leads to infection

of large numbers of cells, which remain infected latently and can lead to subclinical reactivations, providing antigenic stimulus for the ongoing expansion and differentiation of CMV-specific T cells in a pro-inflammatory environment.<sup>143;144;164;165</sup> This proceeds after discontinuation of immunosuppressive medication post HSCT and is most evidently observed in patients with a relatively small number of CD8<sup>+</sup> T cells at the moment of CMV clearance. However, the relative contribution of peripherally expanded memory cells which have been transplanted with the graft and differentiated, newly educated naive T cells to the pool of CD8<sup>+</sup> EM and EMRA T cells is not known.<sup>143;144</sup> Although our observations do not allow for a definitive conclusion about the specificity of the expanded CD8<sup>+</sup> T cells, the differentiation of virus-specific T cells has been studied extensively. CMV specific CD8<sup>+</sup> T cells are mainly of the late differentiated EM and EMRA phenotypes and especially the EMRA phenotype is more often seen in the context of CMV compared to other viruses.<sup>146;147;166</sup> Of note, T cell exhaustion, characterized by the upregulation of inhibitory receptors like PD-1 and the progressive loss of cytokine production, proliferative capacity and cytolytic function,<sup>167</sup> has not been found applicable for CMV-specific T cells.<sup>168-170</sup>

CD4<sup>+</sup> T cells are essential for the maintenance of CMV-specific CD8<sup>+</sup> T cell responses and can also acquire direct cytolytic capacity.<sup>171-173</sup> Indeed, one and two year post HSCT, a minor but stable expansion of CD4<sup>+</sup> T cells of the late EMRA phenotype was found in patients with early CMV reactivation. More profound changes were present in the  $\gamma\delta$ -T cell subset. Their role in CMV clearance has been well established and these cells can compose up to 30% of T cells at the time of CMV clearance.<sup>174;175</sup>

We show that, although their relative contribution to the respective T cell subsets was decreased, the numerical reconstitution of naive and central memory cells in both the CD8<sup>+</sup> and the CD4<sup>+</sup> T cell subset was not negatively affected by early CMV reactivation. This indicates that thymic output and the generation of a central memory compartment are not disturbed. The reconstitution of early differentiated T cells is essential for a healthy and balanced adaptive immune system with the capacity to produce cellular immune responses against neo- and recall antigens.<sup>143</sup> However, in contrast to for example recall vaccination responses, the evaluation of T cell responses against neo antigens it is very difficult. Still, this hypothesis is supported by the observation that the memory compartment is flexible and expansion of CMV-specific memory cells does not result in lower numbers of EBV- and influenza specific T cells after solid organ transplantation.<sup>166</sup> Furthermore, the accumulation of late differentiated CMV-specific memory cells has not been observed in lymph nodes, leaving immunologic space for the generation of new immune responses.<sup>176</sup>

CMV reactivation in adult solid organ transplant (SOT) recipients receiving life-long immunosuppressive medication has been correlated to an accelerated and ongoing accumulation of late differentiated T cells with a stable (relative) contribution of CMV specific T cells.<sup>154;165;177</sup> Although the number of CD8<sup>+</sup> T cells expanded after CMV clearance in pediatric HSCT recipients with a small primary CD8<sup>+</sup> T cell response, a stable condition was reached early in children with high CD8<sup>+</sup> T cell numbers at the moment of CMV clearance. Also, we did not observe a further expansion of memory cells in the second year after HSCT but even noticed a reduction of the CD8<sup>+</sup> EM and EMRA compartment in children with early CMV reactivations.

The SOT setting differs fundamentally from HSCT as in HSCT recipients, CMV reactivations occur in a newly reconstituting immune system. Furthermore, SOT recipients receive life-long immunosuppressive medication, while in our cohort immunosuppression was tapered 3 to 6 months after transplantation.

We compared our results to reported findings in a more physiological setting of CMV infection in healthy Gambian infants as well. One year post infection, the proportion of late differentiated CD8<sup>+</sup> T cells was much smaller (mean 17%) in CMV infected infants than in our cohort but, similarly to our data after HSCT, the relative contribution of these cells to the CD8<sup>+</sup> T cell compartment decreased slightly in the second year after infection.<sup>151;152</sup> Although no absolute cell numbers were assessed in these studies, the difference might be explained by a large contribution of naive T cells in infants compared to pediatric HSCT recipients as well as the severity of the CMV infection after HSCT as discussed above.

Although we analyzed T cell reconstitution in a large cohort of HSCT recipients, the size and diversity of the subcohort of patients with an hematological malignancy did not allow for a reliable evaluation of the impact of early CMV reactivation on the relapse risk.<sup>178</sup> Also, extended follow up is required to evaluate the impact of early CMV reactivation on long term clinical outcome. One year after HSCT, the phenotype of the CD8<sup>+</sup> T cell subset of pediatric HSCT recipients with early CMV reactivation closely resembled that of the CD8<sup>+</sup> T cells of elderly CMV seropositive individuals.<sup>148</sup> However, the expansion of naive and CM cells together with a dynamic contraction of the CD8<sup>+</sup> late differentiated memory T cell compartment in the second year after HSCT imply that an ongoing process of immune-regulation and further reconstitution is operative in modeling the cellular immune system after discontinuation of immunosuppressive medication. Altogether, CMV reactivation early after HSCT leads to a dynamic expansion of late differentiated CD8<sup>+</sup> T cells on top of a normal reconstitution of the naive and central memory compartment.

## Acknowledgements

The authors would like to thank prof. dr. R.M. van Lier for critical reading of the manuscript and prof. dr. H. Putter for expert statistical advice.

## Funding and Disclosures

GL was supported by a Leiden University Medical Center MD/PhD fellowship. All authors declare that no potential financial conflicts of interest exist.

## Supplemental data

Type	Antibody	Fluorochrome	Clone	Supplier
<b>A) Lymphocyte subsets</b>				
<i>Lymphocyte gate</i>	<b>CD45</b>	FITC	2D1	BD
	<b>CD14</b>	PE	MOP9	BD
	<b>CD33</b>	PE	P67.6	BD
	<b>CD235a</b>	PE	11E4B-7-6	BC
<i>Lymphocyte subset</i>	<b>CD3</b>	PerCP-Cy5.5	SK7	BD
	<b>CD19</b>	APC	J4.119	BC
	<b>CD56</b>	APC	N901	BC
<i>T-cell subset</i>	<b>CD4</b>	PE	SK3	BD
	<b>CD8</b>	APC	B9.11	BC
	<b>TCR-<math>\gamma\delta</math></b>	FITC	11F2	BD
<b>B) T-cell differentiation</b>				
<i>T-cell subset</i>	<b>CD3</b>	PerCP-Cy5.5	SK7	BD
	<b>CD8</b>	APC	B9.11	BC
	<b>CD4</b>	APC	13B8.2	BC
<i>T-cell differentiation</i>	<b>CD45RA</b>	PE	2H4	BC
	<b>CCR7</b>	FITC	150503	R&D

**Table 2.S1. Antibodies used for flow cytometry.**

Staining was performed for 30 minutes at 4°C in FACS buffer: Phosphate Buffered Saline (Braun, Melsungen, GE) + 10 mg / ml Bovine Serum Albumin (Sigma-Aldrich, St. Louis, MO, US) + 3 mM Ethylenediaminetetraacetic Acid (Merck Darmstadt, GE). FITC: Fluorescein isothiocyanate, PE: phycoerythrin, PERCP: Peridinin chlorophyll, Cy: Cyanine, APC: Allophycocyanin. BD: Becton Dickinson Biosciences, Franklin Lakes, NJ, US, BC: Beckman Coulter, Brea, CA, US, R&D: R&D systems, Minneapolis, MN, US.

All patients		no HAdV reactivation	HAdV reactivation		p - value	
		65	20			
Age of recipient	<i>Year</i>	7.9	(0.4 - 17)	7.9	(2.1 - 18)	0.79 (c)
Sex of recipient	<i>Male</i>	45	(69 %)	11	(55 %)	0.28 (a)
CMV serostatus of recipient	<i>Positive (anti-CMV IgG)</i>	23	(35 %)	3	(15 %)	0.10 (a)
Age of donor	<i>Year</i>	24	(2.0 - 52)	29	(3.4 - 52)	0.095 (c)
Sex of donor	<i>Male</i>	32	(49 %)	11	(55 %)	0.80 (a)
CMV serostatus of donor	<i>Positive (anti-CMV IgG)</i>	22	(34 %)	4	(20 %)	0.28 (a)
Indication for HSCT	<i>Non-malign hematology</i>	18	(28 %)	9	(45 %)	0.17 (a)
	<i>Malign hematology</i>	47	(72 %)	11	(55 %)	
Donor type	<i>Identical Related</i>	30	(46 %)	5	(25 %)	0.033 (b)
	<i>Haplo-identical</i>	4	(6 %)	5	(25 %)	
	<i>Matched Unrelated</i>	31	(48 %)	10	(50 %)	
Graft source	<i>Bone Marrow</i>	59	(86 %)	15	(75 %)	0.30 (a)
	<i>Peripheral Blood Stem Cells</i>	9	(14 %)	5	(25 %)	
Conditioning regimen	<i>Total Body Irradiation based</i>	29	(45 %)	8	(40 %)	0.80 (a)
	<i>Chemotherapy based</i>	36	(55 %)	12	(60 %)	
Serotherapy	<i>None</i>	22	(34 %)	1	(5 %)	0.006 (b)
	<i>Anti-Thymocyte Globulin</i>	39	(60 %)	14	(70 %)	
	<i>Alemtuzumab</i>	4	(6 %)	5	(25 %)	
T-cell depletion	<i>Yes</i>	4	(6 %)	5	(25 %)	0.03 (a)
Donor Lymphocyte Infusion	<i>Yes</i>	3	(5 %)	2	(10 %)	0.59 (a)
Stem Cell Boost	<i>Yes</i>	0	(0 %)	2	(10 %)	0.053 (a)
Acute GVHD $\geq$ grade 2	<i>Yes</i>	10	(15 %)	3	(15 %)	1.0 (a)
EBV reactivation	<i>EBV DNA load <math>\geq</math> 2.3 log</i>	37	(57 %)	14	(70 %)	0.43 (a)
Rituximab therapy for EBV	<i>DNA load <math>\geq</math> twice <math>\geq</math> 3.0 log</i>	5	(8 %)	6	(30 %)	0.018 (a)
Cidofovir therapy for HAdV	<i>DNA load <math>\geq</math> twice <math>\geq</math> 3.0 log</i>			7	(35 %)	NA

**Table 2.S2. Characteristics of patients with and without early Adenovirus (HAdV) reactivation (CMV reactivation excluded)**

Categorical data are displayed as: number (percentage). Numerical data are displayed as: median (range). p - values: (a) Fisher's Exact test, (b) Pearson Chi Square test, (c) Mann-Whitney U test. N.A.: Not Applicable, HSCT: Hematopoietic Stem Cell Transplantation, CMV: Cytomegalovirus, EBV: Epstein-Barr virus, HAdV: Adenovirus, GVHD: Graft-versus-Host-Disease

All patients		<500 CD8 <sup>+</sup> T cells / $\mu$ L		>500 CD8 <sup>+</sup> T cells / $\mu$ L		<i>p</i> - value	
		21		25		Univariate	Multivariate
Age of recipient	<i>Year</i>	11	(2.7 - 16)	13	(0.5 - 19)	0.12	(c)
Sex of recipient	<i>Male</i>	13	(61 %)	19	(76 %)	0.30	(a)
CMV serostatus of recipient	<i>Positive (anti-CMV IgG)</i>	17	(81 %)	21	(84 %)	0.78	(a)
Age of donor	<i>Year</i>	34	(2.0 - 57)	23	(1.0 - 43)	0.027	(c)
Sex of donor	<i>Male</i>	9	(43 %)	14	(56 %)	0.38	(a)
CMV serostatus of donor	<i>Positive (anti-CMV IgG)</i>	19	(91 %)	17	(68 %)	0.07	(a)
Indication for HSCT	<i>Non-malign hematology</i>	10	(47 %)	11	(44 %)	0.81	(a)
	<i>Malign hematology</i>	11	(53 %)	14	(56 %)		
Donor type	<i>Identical Related</i>	6	(52 %)	11	(44 %)	0.07	(b)
	<i>Haplo-identical</i>	6	(29 %)	1	(4 %)		
	<i>Matched Unrelated</i>	9	(29 %)	13	(52 %)		0.84 (d)
Graft source	<i>Bone Marrow</i>	15	(71 %)	24	(84 %)	0.30	(a)
	<i>Peripheral Blood Stem Cells</i>	6	(29 %)	4	(16 %)		
Conditioning regimen	<i>Total Body Irradiation based</i>	10	(48 %)	8	(32 %)	0.28	(a)
	<i>Chemotherapy based</i>	11	(52 %)	17	(68 %)		
Serotherapy	<i>None</i>	2	(10 %)	8	(32 %)	0.15	(b)
	<i>Anti-Thymocyte Globulin</i>	14	(67 %)	14	(56 %)		
	<i>Alemtuzumab</i>	5	(24 %)	3	(12 %)		
T cell depletion	<i>Yes</i>	8	(38 %)	0	(0 %)	0.001	(a)
Donor Lymphocyte Infusion	<i>Yes</i>	0	(0 %)	2	(8 %)	0.19	(a)
Stem Cell Boost	<i>Yes</i>	1	(5 %)	0	(0 %)	0.27	(a)
Acute GVHD $\geq$ grade 2	<i>Yes</i>	1	(5 %)	4	(16 %)	0.23	(a)
Peak CMV load	<i>Log copies / mL</i>	3.9	(2.3 - 6.0)	3.7	(2.3 - 5.9)	0.88	(c)
Duration CMV reactivation	<i>Day</i>	35	(1 - 134)	36	(2 - 185)	0.37	(c)
Start CMV reactivation	<i>First day PCR <math>\geq</math> 1.7 log</i>	19	(6 - 46)	26	(5 - 62)	0.88	(c)
End CMV reactivation	<i>Last day PCR <math>\geq</math> 1.7 log</i>	73	(13 - 146)	83	(27 - 211)	0.15	(c)
Ganciclovir therapy for CMV	<i>DNA load <math>\geq</math> twice <math>\geq</math> 3 log</i>	6	(29 %)	7	(28 %)	0.97	(a)
EBV reactivation	<i>EBV DNA load <math>\geq</math> 1.7 log</i>	10	(48 %)	12	(48 %)	0.98	(a)
Rituximab therapy for EBV	<i>DNA load <math>\geq</math> twice <math>\geq</math> 3 log</i>	3	(14 %)	4	(16 %)	0.87	(a)
HAdV reactivation	<i>HAdV DNA load <math>\geq</math> 1.7 log</i>	6	(29 %)	9	(36 %)	0.60	(a)
Cidofovir therapy for HAdV	<i>DNA load <math>\geq</math> twice <math>\geq</math> 3 log</i>	1	(5 %)	1	(4 %)	0.90	(a)

**Table 2.S3. Characteristics of patients with a primary CD8<sup>+</sup> T cell recovery < 500 or > 500 cells /  $\mu$ l at the time of CMV clearance**

Categorical data are displayed as: number (percentage). Numerical data are displayed as: median (range). *p* - values: (a) Fisher's Exact test, (b) Pearson Chi Square test, (c) Mann-Whitney U test, (d) logistic regression analysis. N.A.: Not Applicable, HSCT: Hematopoietic Stem Cell Transplantation, CMV: Cytomegalovirus, EBV: Epstein-Barr virus, HAdV: Adenovirus, GVHD: Graft-versus-Host-Disease. Type of T cell depletion: alemtuzumab in the bag (n=3) and CliniMACS CD34 enrichment (n=5).



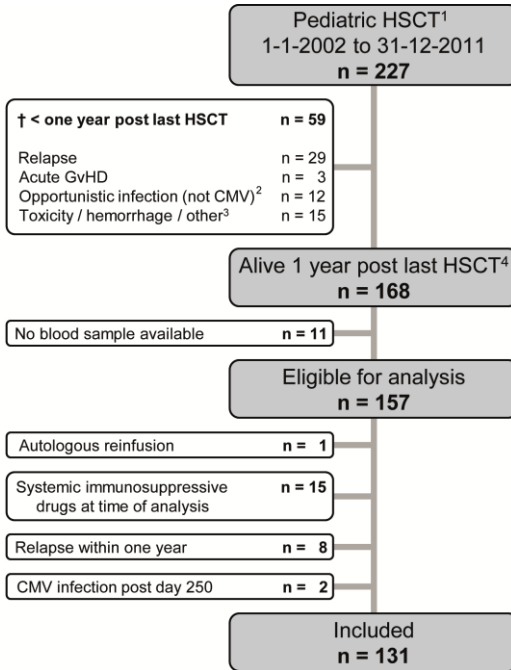


**Figure 2.S1. Flow chart of patient inclusion.**

<sup>1</sup>Bone Marrow or Peripheral Blood Stem Cell transplantation following myeloablative conditioning for malignant and non-malignant hematological disorders.

<sup>2</sup>Death from human adenovirus, respiratory syncytial virus, aspergillus or candida infection or bacterial sepsis.

<sup>3</sup>Death from transplant toxicity, veno occlusive disease, respiratory failure, hemorrhage, hyperhemolysis syndrome or post-transplant lymphoproliferative disease.

<sup>4</sup>Patients who received >1 HSCT were only included after the last HSCT. Abbreviations: GvHD: graft-versus-host disease, CMV: cytomegalovirus.

2

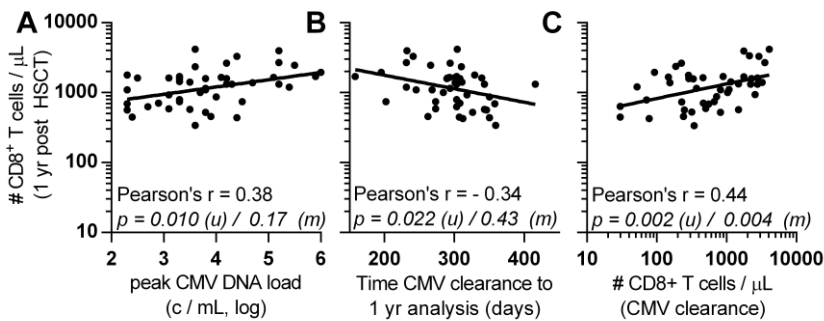


**Figure 2.S2. Factors influencing CD8<sup>+</sup> T cell numbers one year post HSCT in 46 patients with early CMV reactivation.**

Correlation between CD8<sup>+</sup> T cell numbers one year post HSCT and (A) highest measured plasma CMV DNA load, (B) time between CMV clearance and analysis 1 year post HSCT and (C) CD8<sup>+</sup> T cell numbers at time of CMV clearance. Shown are cells/μL of peripheral blood. Pearson's r: Pearson's correlation coefficient, univariate p-values (u): Pearson's correlation test, multivariate p-values (m): linear regression analysis.

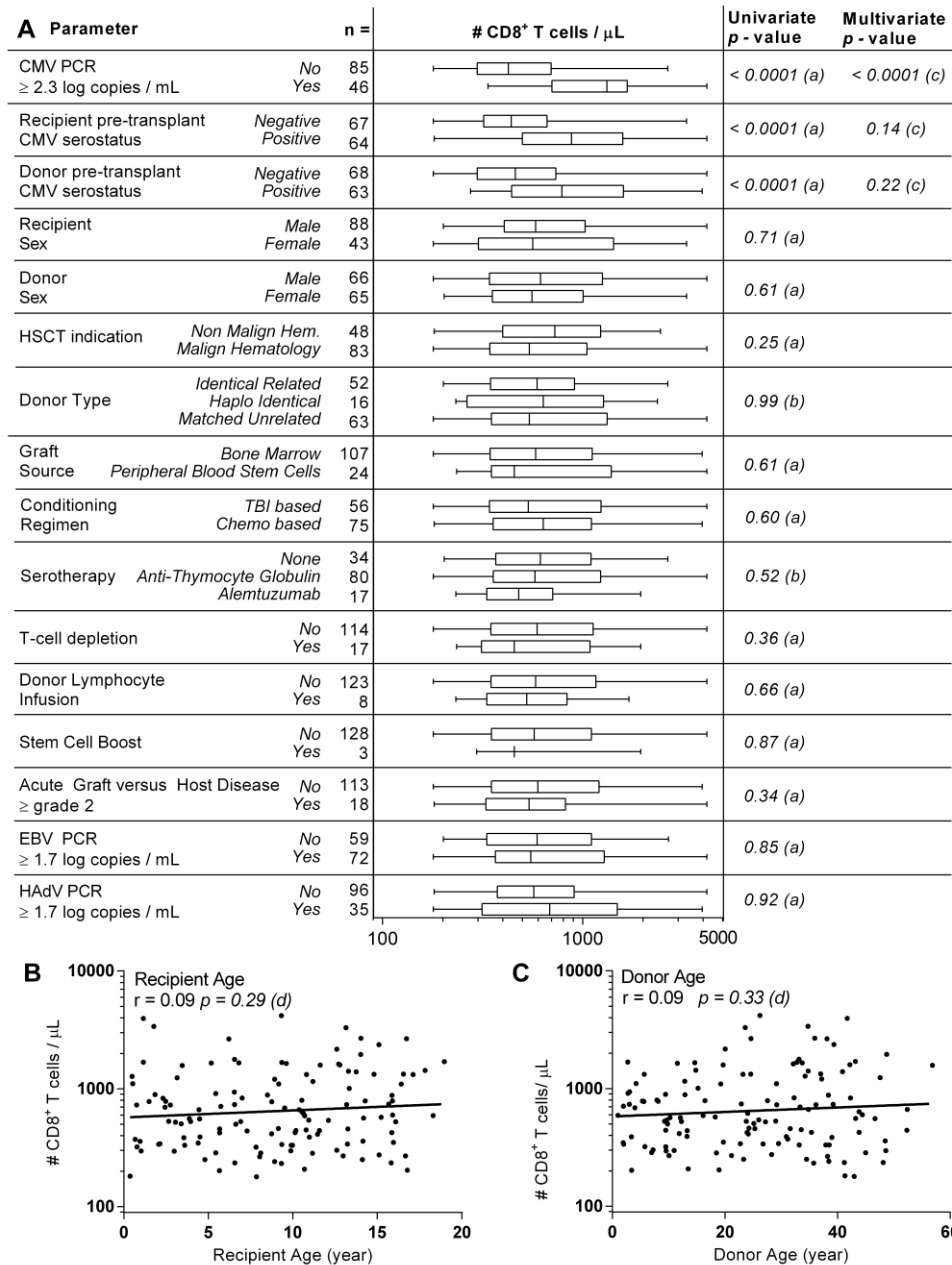


**Figure 2.S3. Influence of HSCT related parameters on CD8<sup>+</sup> T cell numbers one year post HSCT in all 131 patients.**

Influence of **(A)** HSCT parameters, **(B)** recipient age and **(C)** donor age on CD8<sup>+</sup> T cell numbers one year post HSCT in all 131 patients. CMV: Cytomegalovirus, EBV: Epstein-Barr virus, HAAdV: Human Adenovirus.

Shown are cells/ $\mu$ l of peripheral blood one year post HSCT. Bars: median, interquartile range and overall range. p-values: a: Mann-Whitney test, b: Kruskal-Wallis test, c: linear regression analysis, d: Pearson's correlation test. r: Pearson's correlation coefficient.

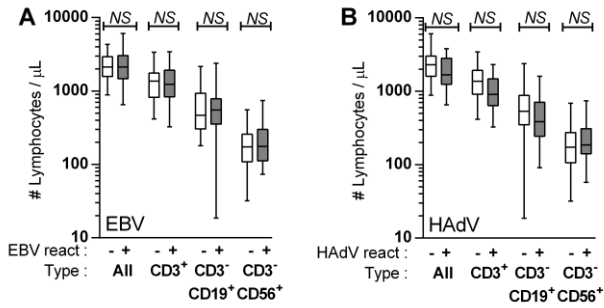


**Figure 2.S4. Influence of EBV and HAdV reactivations.**

Absolute numbers of lymphocytes, CD3<sup>+</sup> T cells, CD3<sup>-</sup>CD19<sup>+</sup> B-cells and CD3<sup>-</sup>CD56<sup>+</sup> NK cells in 85 patients without CMV reactivation. **(A)** 35 patients without vs. 50 patients with early Epstein-Barr virus (EBV) reactivation and **(B)** 65 patients without vs. 20 patients with early Human Adenovirus (HAdV) reactivation. White bars (-): plasma DNA load always < 1.7 log. Gray bars (+): plasma DNA load at least once > 1.7 log. Shown are cells/ $\mu$ l of peripheral blood one year post HSCT. Bars: median, interquartile range and overall range, *p*-values: Mann-Whitney test. NS: *p* > 0.05.



# Chapter 3

## Simultaneous generation of multivirus-specific and regulatory T cells for adoptive immunotherapy

Published in:  
Journal of Immunotherapy  
2012; 35: 42-53

Gertjan Lugthart  
Sarah J. Albon  
Ida Ricciardelli  
Michel G.D. Kester  
Pauline Meij  
Arjan C. Lankester *and*  
Persis J. Amrolia

## Abstract

Previous studies have established that adoptive immunotherapy with donor-derived virus specific T-cells can prevent/treat viral complications post stem cell transplant and regulatory T-cells show promise as inhibitors of graft-versus-host disease. Based on flow cytometric analysis of upregulation of activation markers following stimulation with viral peptide pools, we have developed a rapid and clinically applicable protocol for the simultaneous selection of virus-specific T-cells (following stimulation with peptide pools for the immunodominant antigens of cytomegalovirus, Epstein-Barr virus and adenovirus) and regulatory T-cells using CD25 immunomagnetic selection.

Using tetramer staining, we detected enrichment of CD8<sup>+</sup> T-cells recognizing peptide epitopes from cytomegalovirus and Epstein-Barr virus antigens following CD25 selection in 6 of 7 donors. Enzyme-linked immunospot assays demonstrated the simultaneous presence of bi- or tri-virus specific cells in all evaluated donors, with a median 29-fold (6-168), 40-fold (1-247) and 16-fold (1-219) enrichment of cells secreting interferon- $\gamma$  in response to cytomegalovirus pp65, adenovirus hexon and Epstein-Barr virus lymphoblastoid cells compared to unmanipulated PBMC from the same donors. Furthermore, the CD25 enriched cells lost alloreactivity in <sup>3</sup>H-thymidine proliferation assays and showed highly effective (median 98%) suppression of alloreactivity in all evaluated donors.

In summary, we have developed a rapid, simple GMP compliant methodology for the simultaneous selection of T-cells with multiple viral-specificities and regulatory T-cells. Adoptive transfer of T-cells generated using this strategy may enable restoration of cellular immunity to viruses post allogeneic stem cell transplant with a low risk of graft-versus-host disease. Because of the speed and simplicity of this methodology, this approach may significantly broaden the applicability of adoptive immunotherapy.

## Introduction

Adoptive transfer of virus specific cytotoxic T-cells (CTL) generated by repetitive antigenic stimulation of donor T-cells, is a safe and effective method of restoring anti-viral immunity after stem cell transplant (SCT).<sup>74-76;80;179-181</sup> However, the use of specialized antigen presenting cells (APC), viral vectors, high workload and long culture period make this approach unfeasible for broad application. What is needed is a rapid, simple method for the generation of multi-virus specific cells. Currently two clinically applicable technologies are available to do this, but both have significant limitations. Multimer based magnetic isolation, which has been used for the selection of CMV-specific CD8<sup>+</sup> T-lymphocytes,<sup>77</sup> is rapid but is limited to certain HLA restrictions, does not select CD4<sup>+</sup> virus-specific T-cells and the production of tetramers under Good Manufacturing Practice (GMP) conditions is highly challenging. Interferon- $\gamma$  (IFN- $\gamma$ ) capture enables the rapid enrichment of both CD4<sup>+</sup> and CD8<sup>+</sup> virus-specific cells but only a subset of virus-specific T-cells secrete IFN- $\gamma$  upon activation.<sup>78;79</sup> This method has been successfully used in the clinical setting to select T-cells specific for Cytomegalovirus (CMV), human adenovirus (HAdV) or Epstein-Barr Virus (EBV) singly.<sup>80-82</sup> A number of groups studied IFN- $\gamma$  capture for the enrichment of multi-virus specific cells, but still employed viral vectors or nucleofection of specialized APC<sup>182;183</sup>, precluding broader implementation of this strategy. An alternative to this is the use of recombinant viral peptide pools, which can be generated under GMP conditions and used without the need for professional APC. This approach has been used clinically for both HAdV<sup>184</sup> and EBV.<sup>81</sup> Since the immunodominant antigens from CMV (pp65), HAdV (hexon) and EBV (EBNA1,3 and LMP2) have been characterized,<sup>184-187</sup> it is now possible to stimulate T-cells with overlapping peptide pools from all these antigens simultaneously.

Given the limitations above, new methods for the selection of virus-specific T-lymphocytes are needed. The selection of T-cells upregulating cell-surface activation markers in response to stimulation with viral epitopes is a promising alternative. Activated T-cells express a variety of candidate surface markers including the IL-2 receptor  $\alpha$  chain (CD25), the early activation marker CD69, the transferrin receptor (CD71) and tumor necrosis factor receptor superfamily member 9 (CD137). There is no data on the relative upregulation of these markers following stimulation with viral antigens. In this study, we compared the upregulation of cell surface markers and IFN- $\gamma$  secretion upon stimulation with viral peptide pools. We have identified CD25 as the optimal marker for selection of virally-activated T-cells and have developed a clinically applicable CD25-based protocol for the enrichment of CMV, EBV and HAdV specific T-lymphocytes from a single culture. Selection of CD25<sup>+</sup> CTL should not only enrich for virus-specific CTL, but also deplete alloreactive T-cells, which will not be activated and therefore do not upregulate CD25. Further, since CD25 is also highly expressed on natural regulatory T-cells (Tregs), we rationalized that if these were also enriched by CD25-selection, adoptive transfer of T-cells generated using this strategy may enable both restoration of cellular immunity to viruses and prevention of GVHD post allogeneic SCT.

## Materials and Methods

### Viral antigens

The EBV peptide pool used was that described by Moosmann *et al.*<sup>81</sup> from JPT Peptide Technologies, (Berlin, Germany), consisting of 19 HLA class I restricted epitopes and 4 HLA class II restricted epitopes from 5 latent antigens (LMP2, EBNA1, EBNA3A, EBNA3B, EBNA3C), 4 immediate early/early antigens (BZLF1, BRLF1, BMLF1, BHRF1) and 2 late/structural antigens (BLLF1, BNRF1). The EBV epitopes were selected on the basis of being the immunodominant epitopes restricted by common HLA Class I and II alleles as shown by ELISPOT/tetramer analyses of peripheral blood from seropositive individuals and because they represent the main specificities that grow out in EBV CTL cultures. For CMV and HAdV, PepTivator peptide pools (Miltenyi Biotec, Bergisch Gladbach, Germany) for the immunodominant CMV-pp65 and HAdV5-Hexon were used, consisting of 15-mer peptides with 11-amino acid overlap covering the complete sequence of the CMV-pp65 and HAdV5-hexon protein. A list of peptides used is shown in Table 3.S1.

### Donor cells and generation of EBV-transformed lymphoblastoid cell lines

For the comparison of different activation markers and IFN- $\gamma$  capture, blood samples were drawn from 5 healthy CMV seropositive and EBV seropositive donors after informed consent. Peripheral blood mononuclear cells (PBMC) were separated using ficoll-paque density gradient centrifugation (Ficoll Paque Plus, GE Healthcare, Waukesha, WI, USA), washed twice and resuspended in serum free AIM-V cell culture media (Invitrogen/Gibco, San Diego, CA, USA) and a viability count was performed.

For the clinical grade CD25 enrichment, 7 single donor buffy coats (BC, National Blood Service, Colindale, UK) from CMV seropositive donors were used. Donors were tissue-typed for HLA Class I and II at medium resolution using Luminex technology. EBV-transformed lymphoblastoid cell lines (LCL) were generated by culturing PBMC with EBV containing supernatant of B95-8 cells as described.<sup>188</sup> LCL were maintained in RPMI 1640 (Gibco/Invitrogen) with 10% fetal calf serum (FCS, Sigma-Aldrich, St Louis, MO, USA).  $1.2 \times 10^8$  PBMC were frozen in freezing medium (AIM-V medium with 10% Dimethyl Sulfoxide (DMSO, Sigma-Aldrich, Saint Louis, USA) and 10% Human Serum Albumin (HSA, Bio Products Laboratory, Herts, UK) and stored in liquid nitrogen for subsequent experiments, while the remainder was used for the CD25 enrichment.

### Flow cytometric comparison of different activation markers

The kinetics of IFN- $\gamma$  secretion and upregulation of CD25, CD69, CD71 and CD137 on T-cells were compared flow cytometrically at serial time points after stimulation with viral peptides.  $2 \times 10^6$ /ml/well PBMC from 5 healthy CMV seropositive donors were cultured in serum free AIM-V medium in a 24-well cell culture plate (Greiner Bio-One, Kremsmünster, Austria), and stimulated with 1  $\mu$ g/peptide/ml CMV-pp65 PepTivator mix or HAdV5-Hexon PepTivator mix. PHA (5  $\mu$ g/ml) and medium were used as positive and negative controls. Cells were cultured at 37°C, and



at 0h, 6h, 24h, 72h and 120h after stimulation, were washed and resuspended in PBS. Half the cells were used for cell-surface staining with the following mAbs: anti-CD4 FITC, PE-labeled anti-CD25, anti-CD69, anti-CD71, anti-CD137 and anti-IgG and anti-CD3 APC-Cy7 (BD Biosciences, Franklin Lakes, NJ, USA). The remainder of the cells was assayed for IFN- $\gamma$  secretion using the cytokine capture system (Miltenyi), as per manufacturer's instructions. ToPro3 was added to exclude dead cells and flow cytometric analysis was performed using the BD FACSAarray flow cytometer (BD Biosciences) and FlowJo analysis software (Tree Star Inc, Ashland, OR, USA). The percentage of surface marker upregulation and IFN- $\gamma$  secretion was calculated as percentage of CD3<sup>+</sup>, CD3<sup>+</sup>CD4<sup>+</sup> and CD3<sup>+</sup>CD8<sup>+</sup> cells after subtraction of IgG isotype control and unstimulated control.

### Clinical grade enrichment of tri-virus specific cells

Normal donor PBMC from 7 buffy coats (see Table 3.1 for HLA typing and EBV/CMV serology) were stimulated with CMV, EBV and HAdV peptides, cultured for 3 days and CD25<sup>+</sup> cells enriched on the CliniMACS plus system (Miltenyi). At day 0, a median  $4 \times 10^8$  PBMC were resuspended in 10 ml serum free AIM-V medium with 1  $\mu$ g/peptide/ml CMV pp65 PepTivator mix, HAdV5 Hexon PepTivator mix and EBV peptide mix. After 1h incubation at 37°C / 5% CO<sub>2</sub> under continuous rotation, cells were diluted to  $2 \times 10^6$ /ml and cultured in T175 flasks. At day 3, cells were harvested and resuspended in CliniMACS buffer (PBS with 2mM EDTA + 0.5% HSA) and stained with 0.1 ml CD25 reagent (Miltenyi) per  $10^8$  cells for 30' at room temperature according to the manufacturer's protocol. Cells were washed, resuspended in 100ml CliniMACS buffer and enrichment performed under Good Manufacturing Practise (GMP) conditions on the CliniMACS PLUS instrument using Enrichment Program 3.2 and a TS600 research tubing set (Miltenyi). Enriched cells were washed, resuspended at  $2 \times 10^6$ /ml and sampled for flow cytometry. The remaining cells were rested for 3 days in 24-well plates with 40 IU/ml IL-2 (Genscript inc., Piscataway, NJ, USA) and irradiated (30Gy) autologous feeder cells at a ratio of 1:1 before assessment of anti-viral responses using tetramer staining, ELISPOT, cytotoxicity and proliferation assays and regulatory capacity in suppression assays.

### Phenotyping and tetramer staining of CD25 enriched cells

The following mAbs were used to determine the phenotype of selected cells: FITC-labeled anti-CD4, PE-labeled anti-CD25, anti-CD45RA, anti-CD16, anti-CD56, anti-FoxP3 and anti-IgG, PerCP-labeled anti-CD8, APC-labeled anti-CD127 and anti-IgG, APC-Cy7-labeled anti-CD3 and PE-Cy5-labeled anti-CD25 and anti-IgG. All antibodies were purchased from BD Biosciences, except for the anti-CD127 (Miltenyi Biotec) and CD16 (eBioscience, San Diego, CA, USA) antibodies. For the intracellular staining of FoxP3, the FoxP3 staining set (eBioscience) was used, according to the manufacturer's protocol. Briefly, cells were stained with mAbs for cell surface staining, washed in FACS buffer and fixed in Fixation/Permeabilisation buffer. The following day, cells were washed thoroughly with permeabilisation buffer, blocked with 2% normal rat serum in permeabilisation buffer and stained with FoxP3 mAb or IgG isotype control.

	HLA restriction					Serology		EBV peptide pool match		
	A-allele	B-allele	DRB1-allele			CM V	EBV	HLA-alleles	EBV-antigens	
<b>BC1</b>	0301	0702	4001	0101	1501	+	+	4	5	
<b>BC2</b>	0101	2402	0801	1501	0401	1101	+	+	3	6
<b>BC3</b>	0201	3301	1402	4402	0701	1501	+	+	3	6
<b>BC4</b>	0201	1101	0702	3701	0101	1501	+	+	4	7
<b>BC5</b>	0101	0201	0801	1501	0407	1301	+	+	4	8
<b>BC6</b>	0201		1801	4402	1104	1301	+	+	4	8
<b>BC7</b>	0301	1101	1518	5701	0701	1301	+	+	3	4

**Table 3. 1. Donor HLA restriction, serology and of EBV antigens.**

HLA restriction, CMV and EBV serology of 7 buffy coats used for CD25 selection. For each donor, the number of HLA-alleles shared with the HLA-alleles of the EBV peptide pool and maximum number of EBV antigens that could be recognized is depicted.

The following PE-labeled major histocompatibility complex (MHC) tetramers were produced as described previously<sup>189</sup> and used to detect viral-specific CD8+ T-cells: CMV- pp65 specific HLA-A\*0101- YSEHPTFTSQY (pp65-A1-YSE), HLA-A\*0201-NLVPMVATV (pp65-A2-NLV), HLA-A\*0301-VLCPKNMIK (pp65-A3-VLC), HLA-A\*2401 QYD (pp65-A24-QYD), HLA-B\*0702-TPRYTGGGAM (pp65-B7-TPR) and HLA-B\*0702-RPHERNGFTV (pp65-B7-RPH); EBV- BMLF-1-specific HLA-A\*0201-GLCTLVAML (BMLF1-A2-GLC), LMP-2-specific HLA-A\*0201-CLGGLTMV (LMP2-A2-CLG), EBNA-3A-specific HLA-A\*0301-RLRAEAQVK (EBNA3A-A3-RLR) and HLA-B\*0702-RPPIFIRRL (EBNA3A-B7-RPP), and BZLF-1-specific HLA-B\*0801-RAKFKQLL (BZLF1-B8-RAK): all of these tetramers utilise peptides present in the peptide mix used in the manufacturing protocol for CD25-enriched CTL Adenovirus -hexon-specific HLA-A\*2404-TYFSLNKF (Hx-A24-TYF), HLA-A\*0101-TDLGQNLLY (hx-A1-TDL), and HLA B\*0702-KPYSGTAYNSL (Hx-B7-KPY). Cells were stained with tetramers appropriate to the donors' HLA restriction.  $3 \times 10^5$  unmanipulated PBMC or CD25-enriched T-cells were stained per tube with PE-labeled tetramer for 15 minutes at room temperature and co-stained for cell surface markers with PerCP-labeled anti-CD8 and APC-Cy7-labeled anti-CD3 mAbs. PBMC from donors with known positive populations served as positive controls and PBMC from normal donors negative for the restricting HLA-type were used as additional negative controls. 4',6-diamidino-2-phenylindole (DAPI) staining was used to exclude dead cells and at least 20,000 events in the CD3+/CD8+ lymphocyte gate were analyzed. The percentage of tetramer+ cells in the CD3+/CD8+ lymphocyte gate was expressed as a proportion of the CD8+ cells with the unstained and HLA-mismatched control subtracted. For a population to be considered positive, a distinct population of > 25 CD3+CD8+ tetramer+ events with the staining characteristics of the positive control population had to be acquired. Flow cytometric analysis was performed using the BD LSRII flow cytometer (BD Biosciences) and FlowJo analysis software.

### Enzyme-linked Immunospot Assay

Enzyme-linked immunospot assay (ELISPOT) was used to determine the frequency of virus-specific interferon- $\gamma$  (IFN- $\gamma$ ) producing cells as described previously.<sup>190</sup> The following stimulators were used to monitor anti-viral responses: autologous LCLs, autologous PBMC pulsed with

CMV-pp65 or HAdV5-Hexon PepTivator mix (1 µg/peptide/ml). Serial dilutions were performed for one donor to titrate the number of effector cells per well. Based on this,  $2 \times 10^5$  unmanipulated PBMC or  $2 \times 10^4$  CD25 enriched cells were cultured with  $2 \times 10^5$  irradiated stimulators per well in 200 µl AIM-V in triplicates. After 18 hours the plates were stained with biotinylated detection mAbs and developed as described.<sup>190</sup> Plates were read using an AID EliSpot reader and counted with AID EliSpot system software (version 4.0, AutoImmun Diagnostika GmbH, Strassberg, Germany). The virus-specific cell frequency was expressed as the mean specific spot-forming cells (SFC) of triplicates after subtracting the mean frequency of spots from unstimulated responders and stimulators alone.

### Proliferation and suppression assay

The <sup>3</sup>H-thymidine incorporation assay was used to assess the proliferative capacity of the enriched cells upon stimulation. CD25 enriched cells and PBMC from the same donor were plated in triplicate in round bottom 96 well plates (NUNC) at  $2 \times 10^5$  cells per well in 200 µl AIM-V in triplicates and stimulated with  $5 \times 10^3$  autologous LCLs or  $2 \times 10^5$  autologous PBMC pulsed with CMV-pp65 or HAdV5-Hexon PepTivator mix (1 µg/peptide/ml), autologous PBMC alone or allogeneic PBMC. Medium and 5 µg/ml Phytohaemagglutinin (PHA) were used as negative and positive controls. To assess the enrichment of regulatory T-lymphocytes with the capacity to suppress alloreactivity, a suppression assay was performed.  $2 \times 10^5$  autologous PBMC and  $2 \times 10^5$  irradiated allogeneic PBMC were plated out in triplicate in a round bottom 96 well plate. As suppressor cells, CD25 enriched cells were added in serial dilutions ( $2 \times 10^5 - 5 \times 10^4$ ). After 5 days incubation at 37°C / 5% CO<sub>2</sub>, 1 µCi tritiated thymidine (<sup>3</sup>H-thymidine, GE Healthcare) was added to each well for 18-20 hours. The plates were harvested and <sup>3</sup>H-thymidine incorporation was measured with a MicroBeta TriLux (Perkin-Elmer Weiterstadt, Germany). The data are presented as average of the triplicates after subtraction of unstimulated cells and stimulators and suppressors alone.

### Cytotoxicity assay

A standard <sup>51</sup>Cr release assay was performed to determine the virus-specific cytolytic activity of the CD25 enriched cells. Autologous and allogeneic EBV-LCLs were used as targets. The target cells were labelled with 100 µCi <sup>51</sup>Cr (Amersham Pharmacia Biotech, Piscataway, NJ) for 2 hours at 37°C. <sup>51</sup>Cr-labeled LCLs were plated at  $5 \times 10^3$  cells per well, respectively, and cultured with CD25 enriched cells at different concentrations (effector to target ratios: 30:1, 5:1, and 1:1) in 96-well U-bottom plates. Target cells in complete media or lysed with 1% TritonX-100 (Sigma-Aldrich) were used to determine spontaneous and maximum release, respectively. After 6 hours of incubation at 37°C, plates were spun and 25-µl supernatant were harvested and transferred to 96-well Wallac isoplates (Perkin-Elmer, Weiterstadt, Germany) and mixed with 150-µl OptiPhase Supermix Cocktail (Perkin-Elmer). Counts were measured on a MicroBeta TriLux (Perkin-Elmer) and the percent-specific lysis was calculated as [(specific release-spontaneous release)/(maximum release-spontaneous release)] x 100.

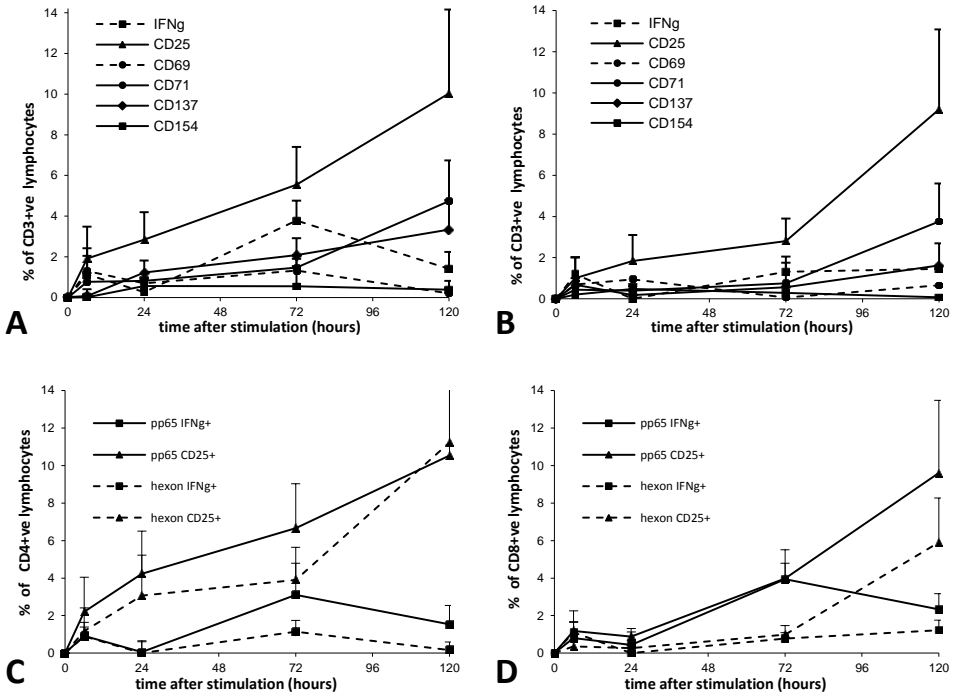


**Figure 3.1. Flow cytometric analysis of activation marker expression.**

Expression was evaluated 0, 6, 24, 72 and 120 hours after stimulation with CMV pp65 and HAdV5 hexon PepTivator mix at 1  $\mu\text{g}/\text{peptide}/\text{ml}$ . **(A-B)** percentage of interferon- $\gamma$  (IFN- $\gamma$ ) secreting and CD25, CD69, CD71 and CD137 expressing CD3<sup>+</sup> lymphocytes after stimulation with pp65 (A) and hexon (B) peptides.

**(C-D)** percentage of IFN- $\gamma$  secreting and CD25 expressing CD4<sup>+</sup> (C) and CD8<sup>+</sup> (D) lymphocytes. Uninterrupted lines represent pp65 stimulated culture while dashed lines show hexon stimulated cultures. Square dots symbolize IFN- $\gamma$  secreting cells while triangles show CD25 positive cells. Shown is the mean percentage (+SEM) of 5 healthy donors after subtraction of IgG isotype control and unstimulated control.

### Statistical analysis

The upregulation of CD25 during culture with viral peptides, enrichment of CD25 and CD45RA expressing cells and the percentage of virus specific tetramer positive cells before and after enrichment were compared using the one-tailed paired t-test. This test was also used to compare virus specific IFN- $\gamma$  secretion in the ELISPOT assays and alloreactivity and suppression in the proliferation assay. Prism statistical software (version 5.01; Graph-Pad Software, San Diego, CA, USA) was used to perform all statistical tests.

### Ethics

Ethical approval for this study was obtained through the University College London non-NHS research ethics committee and blood samples were taken with informed consent.

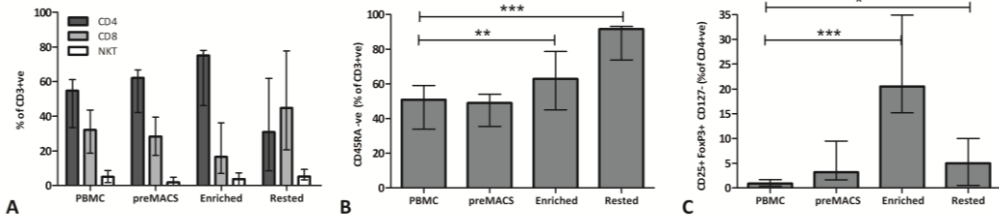


**Figure 3.2. Immunophenotype of CD3<sup>+</sup> T-lymphocytes at 4 key time points during clinical grade CD25 selection:** before procedure (PBMC), after 3 day culture (preMACS), immediately after CD25 selection (enriched) and 3 days after enrichment (rested). Shown is the median of 7 donors with error bars indicating highest and lowest value of: **(A)** percentage of CD4<sup>+</sup>, CD8<sup>+</sup> and Natural Killer T-cells (NKT, CD3<sup>+</sup>, CD16<sup>+</sup>/CD56<sup>+</sup>) within CD3<sup>+</sup> lymphocyte gate. **(B)** percentage of memory T-lymphocytes (CD45RA<sup>-ve</sup>) within CD3<sup>+</sup> lymphocyte gate. **(C)** percentage of regulatory T-cells (CD25<sup>+</sup>, FoxP3<sup>+</sup> and CD127<sup>-</sup>), within CD3<sup>+</sup> CD4<sup>+</sup> lymphocyte gate. \*  $p < 0.05$ , \*\*\*  $p < 0.001$  in paired t-test.

## Results

### Flow cytometric comparison of activation markers upregulation in response to viral antigens

To determine the optimal target for selection of viral peptide activated lymphocytes, we compared IFN- $\gamma$  secretion with the upregulation of CD25, CD69, CD71 and CD137 in PBMC from 5 healthy CMV seropositive donors. For both hexon and pp65 stimulated PBMC, IFN- $\gamma$  secretion rose by 6 hours and peaked at 72h after stimulation (pp65: mean 3.8% positive T-cells above unstimulated controls, hexon: mean 1.3%). CD25 (IL-2R $\alpha$ ) was the activation marker that was most upregulated with a mean 10.03% and 9.20% positive T-cells for pp65 and hexon stimulated PBMC at day 5 (Figure 3.1 A-B). CD69 upregulation was highest in the first 24 hour after stimulation (pp65: mean 1.30%; hexon: mean 0.95%) and the percentages of CD71<sup>+</sup> and CD137<sup>+</sup> T-cells rose progressively during culture to a peak 4.73% / 3.34% above background for pp65 and 3.76% / 1.20% for hexon stimulated PBMC after 5 days. In the unstimulated control, the basal expression of CD69 and CD137 was low (< 0.75%), whereas CD25, IFN- $\gamma$  and CD71 showed significant expression in unstimulated T-cells (mean 1.3%, 1.2% and 2.45% of CD3<sup>+</sup> lymphocytes).

Similar data on up-regulation of IFN- $\gamma$  and CD25 were obtained in separate experiments on normal donors PBMC (Figure 3.S1) following stimulation with EBV peptide mix. CD25 expression peaked at 7 days, with mean of 1.6% of CD25<sup>+</sup> T-cells above unstimulated controls, whereas, as with pp65 and hexon, peak IFN- $\gamma$  secretion was rather lower (0.5% at 72 hours).

These studies indicated that IFN- $\gamma$  is only secreted by a subpopulation of virus-specific T-cells and identified CD25 as a promising target for selection of virus-specific T-cells following stimulation with viral peptide epitopes. Comparison of the IFN- $\gamma$  secretion and upregulation of CD25 in CD4<sup>+</sup> and CD8<sup>+</sup> lymphocytes showed that after stimulation with either pp65 or hexon peptides, the majority of cells upregulating CD25 but not secreting IFN- $\gamma$  were in the CD4<sup>+</sup> compartment (Figure 3.1 C-D).

	Before enrichment		After procedure		3 Day rested
	Unmanipulated	3 Day cultured	Depleted	Enriched	Enriched
Viable Cell number (x 10 <sup>7</sup> )	40 (35-100)	27 (11-81)	12 (3.6-33.2)	2.2 (1.1-3.1)	1.7 (1.2-8.7)
T-lymphocyte (% PBMC)	63 (58-80)	79 (57-86)	82 (71-91)	71 (61-77)	84 (80-96)
NK (% of PBMC)	12 (6.6-16)	5.7 (4.7-7.2)	6.4 (4.7-9.0)	5.4 (1.5-8.3)	3.1 (0.5-5.3)
NKT (% of CD3 <sup>+</sup> )	5.1 (1.7-8.6)	1.8 (0.1-4.8)	1.4 (0.2-6.4)	3.8 (0.4-7.4)	4.3 (3.4-8.4)
Treg (% of CD4 <sup>+</sup> )	0.9 (0.35-1.7)	3.2 (1.7-9.5)	ND	21 (15-35)	5.0 (0.5-10)
CD25 <sup>+</sup> (% of CD3 <sup>+</sup> )	1.4 (0.8-4.1)	6.4 (4.1-14)	0.0 (0.0-0.8)	44 (31-60)	35 (20-82)
CD25 <sup>+</sup> (% of CD4 <sup>+</sup> )	2.9 (1.5-6.2)	7.1 (4.0-17)	0.2 (0.0-1.0)	31 (21-59)	35 (11-73)
CD25 <sup>+</sup> (% of CD8 <sup>+</sup> )	0.0 (0.0-1.6)	7.8 (5.4-15)	0.0 (0.0-0.9)	97 (83-100)	68 (30-87)

**Table 3. 2. Enrichment of tri-virus specific cells through clinical grade CD25 enrichment.**

The median and range of 7 clinical grade CD25 enrichment experiments using PBMC from CMV seropositive buffy coats after 3 day culture with viral peptide mixes for CMV, HAAdV and EBV is shown. T-lymphocyte: CD3<sup>+</sup> cells, Natural Killer (NK): CD3<sup>+</sup> CD16<sup>+</sup>/CD56<sup>+</sup>, Natural Killer T-cells (NKT) : CD3<sup>+</sup> CD16<sup>+</sup>/CD56<sup>+</sup>, Regulatory T-cells (Treg): CD4<sup>+</sup> CD25<sup>+</sup> FoxP3<sup>+</sup> CD127<sup>-</sup>. ND: Not Done.

### Clinical grade enrichment of tri-virus specific cells

Based on the expression pattern after stimulation with viral peptides, we next explored CD25 enrichment using an immunomagnetic positive selection as a potential methodology for the selection of multi-virus specific CTL. To limit non-specific activation of bystander cells, we chose to select for CD25<sup>+</sup> after 3 days of stimulation with viral peptides. CD25 selection was performed using clinical grade reagents using the CliniMACS system (Miltenyi) under GMP conditions. Seven enrichments (Table 3.2) were performed starting with a median 4.0 x 10<sup>8</sup> PBMC from CMV seropositive buffy coats. A median 1.4% of unstimulated PBMC at day 0 were CD25<sup>+</sup>: most of these were in the CD4<sup>+</sup> subset, presumably reflecting Tregs. Following 3 day culture in serum-free medium with CMV, EBV and HAAdV peptide pools, a median 6.4% of CD3<sup>+</sup> cells expressed CD25 (upregulation  $p < 0.01$ ). Following CD25 positive selection, 1.1 - 3.1 x 10<sup>7</sup> (median 2.2 x 10<sup>7</sup>, 3.3% of starting PBMC dose) cells were collected in the enriched fraction, of which a median 44% were CD25<sup>+</sup> (Table 3.2).

As shown in Table 3.2, CD25 selection was highly efficient, as no CD25<sup>+</sup> cells were detected in the depleted fraction, but the percentage of CD25<sup>+</sup> T-cells was higher in CD8<sup>+</sup> (median 97%) than in CD4<sup>+</sup> T-cells (median 31% CD25<sup>+</sup>, enrichment  $p < 0.0001$  and  $p < 0.001$  respectively). To optimize detection of functional anti-viral responses, CD25 selected T-cells were rested for 3 days following selection prior to restimulation. Immediately after selection, the majority of CD25-enriched cells were CD4<sup>+</sup>, however as shown in Figure 3.2A, CD8<sup>+</sup> T-cells expanded preferentially during the resting period. Further, we observed a significant enrichment of the CD45RA<sup>-</sup> population during this period (Figure 3.2B), consistent with preferential expansion of antigen-stimulated memory T-cells.

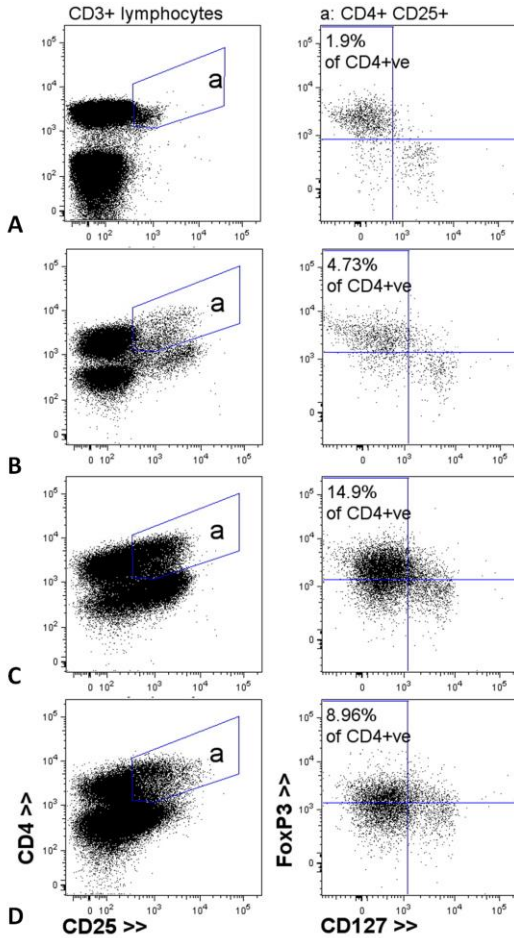


**Figure 3.3.** CD4<sup>+</sup>CD25<sup>+</sup> T-cells with a Treg phenotype (FoxP3<sup>+</sup> CD127<sup>-</sup>) are enriched during CD25 selection.

From one representative donor, FACS plots of CD3<sup>+</sup> T-lymphocytes are shown: **(A)** before procedure, **(B)** after 3 day culture, **(C)** immediately after enrichment and **(D)** 3 days after enrichment. In the left panel CD4 is plotted against CD25, whereas in the right panel FoxP3 is plotted against CD127 for CD4<sup>+</sup> CD25<sup>+</sup> cells. The percentage of cells with regulatory phenotype is shown in left upper quadrant as percentage of CD4<sup>+</sup> T-lymphocytes. Note the decrease in MFI of CD25 and FoxP3 during resting period, which may reflect transient expression in activated T-cells.

To determine whether Tregs are also enriched by CD25 based selection, we compared the frequency of CD4<sup>+</sup> FoxP3<sup>+</sup>CD127<sup>-</sup> T-cells in unmanipulated PBMC with CD25 enriched cells immediately after selection and 3 days post enrichment. As shown in Figure 3.2C, in unmanipulated PBMC, a median 0.9% of CD4<sup>+</sup> cells were CD25<sup>+</sup> FoxP3<sup>+</sup> CD127<sup>-</sup> T-cells with this regulatory phenotype were enriched immediately after CD25 selection (median 21%,  $p < 0.001$ ) but declined to a median 5% of CD4<sup>+</sup> cells after resting ( $p < 0.05$ ). Figure 3.3 shows representative FACS plots for the CD25, FoxP3 and CD127 staining in unmanipulated, cultured, CD25-selected and rested cells.

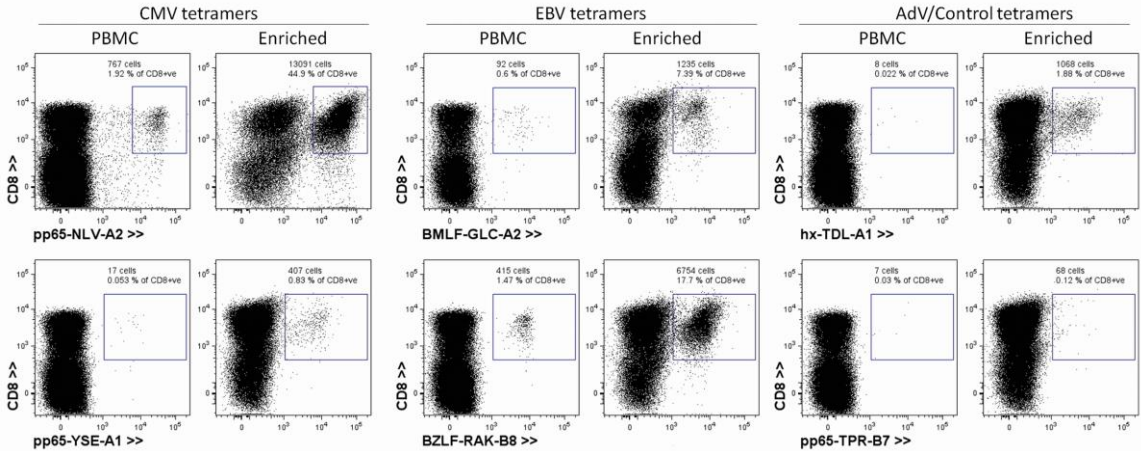


**Figure 3.4. Simultaneous enrichment of CMV, EBV and HAdV- specific CD8<sup>+</sup> T-cells detected by tetramer staining.**

Representative FACS plots (gated on live, CD3<sup>+</sup> T-cells) from donor 5 comparing unmanipulated PBMC and rested CD25 selected CTL are shown. Plotted are HLA class I tetramers for pp65-NLV-A2, pp65-YSE-A1, BMLF-GLC-A2, BZLF-RAK-B8 and hexon-TDL-A2 against CD8. pp65-TPR-B7 was used as an HLA mismatched negative control. The percentage of tetramer<sup>+</sup> cells within the CD8<sup>+</sup> gate is shown.

### Anti-viral responses of CD25-selected cytotoxic T-lymphocytes

In donors with the appropriate HLA-restriction, we analyzed the frequency of CMV, HAdV and EBV-specific CD8<sup>+</sup> T-cells in unmanipulated PBMC and the CD25 selected fraction using MHC-peptide tetramers. Immediately after enrichment, clusters of tetramer<sup>+</sup> cells were less distinctive than in unmanipulated cells, so results are presented comparing unmanipulated PBMC and CD25 selected T-cells that had been rested for 3 days (Table 3.3). In 6 out of 7 donors, populations of tetramer<sup>+</sup> CMV and EBV specific CTL could be detected in unmanipulated PBMC and 3 of the donors had tetramer<sup>+</sup> cells for more than one EBV epitope. Following CD25 selection, for CMV tetramers, a median 20-fold (4.4 – 53,  $p < 0.01$ ) fold enrichment was seen, leading to a median 45% pp65 specific CD8<sup>+</sup> cells in the enriched rested fraction. For EBV tetramers, the median enrichment was 14-fold (4.3-38,  $p < 0.01$ ) and a median 5.3% of CD8<sup>+</sup> cells in the enriched rested fraction stained with EBV tetramers. Only 1 of 5 evaluable donors had a detectable population of HAdV tetramer<sup>+</sup> cells in unmanipulated PBMC. In this donor (BC5), a population of 0.02% of unmanipulated CD8<sup>+</sup> T-lymphocytes positive for tetramer HAdV5 hx-TDL-A1 was enriched to 1.7% in the rested CD25 selected fraction. Figure 3.4 shows representative FACS plots illustrating the simultaneous presence of CD8<sup>+</sup> T-lymphocytes (from donor 5) recognizing peptides from CMV, EBV and HAdV.



Donor	Cytomegalovirus			Epstein-Barr Virus			Adenovirus		
	Epitope	U	E	Epitope	U	E	Epitope	U	E
BC 1	pp65-VLC-A3	neg	neg	EBNA3A-RPP-B7	0.37%	1.6%	hx-KPY-B7	neg	neg
	pp65-TPR-B7	18%	80%	EBNA3A-RLR-A3	neg	neg			
BC 2	pp65-YSE-A1	0.03%	1.6%	BZLF1-RAK-B8	0.31%	6.6%	hx-TDL-A1	neg	neg
	pp6- QYD-A24	neg	neg				hx-TYF-A24	neg	neg
	pp65-VYA-A24	neg	neg						
BC 3	pp65-NLV-A2	0.99%	46%	BMLF1-GLC-A2	0.05%	2.2%	NA		
				LMP2-CLG-A2	neg	neg			
BC 4	pp65-NLV-A2	neg	neg	BMLF1-GLC-A2	0.44%	5.3%	hx-KPY-B7	neg	neg
	pp65-TPR-B7	1.3%	26%	LMP2-CLG-A2	neg	neg			
				EBNA3A-RPP-B7	0.09%	1.5%			
BC 5	pp65-YSE-A1	0.05%	0.7%	EBNA3A-RLR-A3	0.16%	1.4%			
				BMLF1-GLC-A2	0.59%	8.5%	hx-TDL-A1	0.02%	1.9%
				LMP2-CLG-A2	0.05%	0.3%			
BC 6	pp65-NLV-A2	3.10%	55%	BZLF1-RAK-B8	1.4%	17%			
				BMLF1-GLC-A2	0.12%	3.0%	NA		
				LMP2-CLG-A2	0.10	5.8%			
BC7	pp65-VLC-A3	neg	neg	EBNA3A-RLR-A3	neg	neg	NA		

**Table 3. 3. Enrichment of virus specific CD8<sup>+</sup> T-lymphocytes assessed by tetramer staining.**

Shown is the percentage of living CD3<sup>+</sup> CD8<sup>+</sup> lymphocytes positive for the corresponding tetramer with unstained control subtracted. Unmanipulated PBMC (U) and CD25-enriched cells 3 days post enrichment (E) are compared. When no cluster of positive cells was detected, this donor was considered to be negative for this tetramer (neg) while NA indicates not applicable as not appropriate HLA type for tetramer analysis.

We next assessed the functional capacity of CD25 selected T-cells to secrete cytokines in response to viral antigens using IFN- $\gamma$  ELISPOT assays. Unmanipulated PBMC and rested CD25 enriched cells from 5 donors were stimulated with irradiated PBMC pulsed with CMV pp65 or HAdV hexon PepTivator mix or irradiated autologous EBV-LCL. As shown in Figure 3.5 A-C, we observed a median 29-fold (6 - 168,  $p < 0.05$ ), 40-fold (1 - 247,  $p = 0.156$ ), and 16-fold (1 - 219,  $p < 0.05$ ) increase in cells secreting IFN- $\gamma$  after stimulation with pp65 peptides, hexon peptides, or LCL respectively in CD25 selected cells compared with unmanipulated PBMC from the same donors.

Using this methodology, CD25 selected T-cells showed significant ( $> 25$  SFC/  $10^5$  cells) responses to CMV and EBV in all 5 donors and to HAdV in 3 donors. BC 1 and 4 had a low response to HAdV in both unmanipulated and enriched cells, suggesting these donors may not have had a pre-existing memory T-cell response to HAdV hexon.

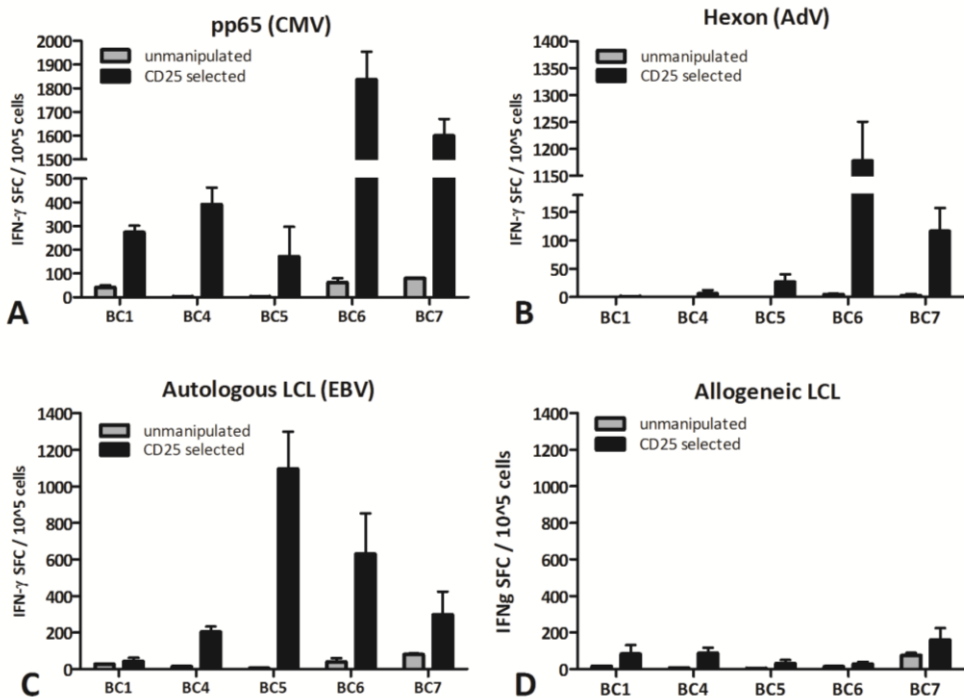


**Figure 3.5. Enrichment of the IFN- $\gamma$  secreting cells specific for all 3 viruses in the CD25 enriched fraction.** ELISPOT assays comparing IFN- $\gamma$  response of unmanipulated PBMC (grey) and CD25 selected, rested CTL (black) to (A) autologous CMV-pp65 peptide pulsed PBMC, (B) autologous HAdV5-hexon peptide pulsed PBMC and (C) autologous EBV-LCL in 5 donors. Shown is the mean number of spot forming cells (SFC) per 10<sup>5</sup> cells of triplicates after subtraction of response to autologous PBMC. Error bars represent standard error of the mean (SEM).

Given the numbers of CD25-enriched T-cells obtained, it was not possible to evaluate cytotoxic activity fully. Nonetheless, to investigate whether CD25 enriched T-cells were able to kill virally infected cells, in 2 donors we evaluated cytotoxic activity in a standard <sup>51</sup>Cr release assay against autologous and allogeneic EBV LCL. Our data show that the CD25 enriched T-cells show significant cytotoxicity against autologous EBV LCL but not allogeneic LCL (32.2% vs 11.5 % at a 30:1 ratio, Figure 3.6). Thus, our data demonstrate that CD25 enriched T cells are able to kill virally infected target cells in an MHC-restricted fashion.

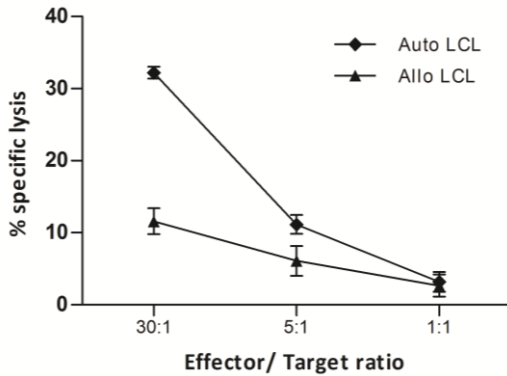


**Figure 3.6. CD25 enriched T cells show EBV-specific cytotoxic activity.**

A standard  $^{51}\text{Cr}$  release assay was performed to determine the EBV virus-specific cytolytic activity of the CD25 enriched cells. The Figure 3 shows the percentage of specific chromium release from target cells. Autologous and allogeneic LCL were labeled with  $^{51}\text{Cr}$  and incubated with CD25 cells for 6 h at the E:T ratios indicated.

### CD25 selected T-cells suppress alloreactivity

To determine the alloreactivity of CD25 enriched cells and their ability to proliferate in response to viral antigens, we next analyzed the proliferative response of CD25 selected CTL to irradiated allogeneic PBMC, autologous PBMC pulsed with CMV pp65/HAdV hexon PepTivator mixes or autologous LCL in  $^3\text{H}$ -thymidine uptake assays. As illustrated in Figure 3.7A, in all 5 donors, CD25 enriched CTL showed a very marked depletion of proliferative responses to allogeneic stimulators compared to unmanipulated PBMC from the same donors

( $p < 0.05$ ), suggesting reduced alloreactivity. However, in 4 of 5 donors, CD25 enriched CTL also showed little proliferative response to viral antigens (pp65, HAdV and autologous LCL), in contrast to unmanipulated PBMC. Consistent with our flow cytometric data, this suggested that the CD25 selected fraction also contained a significant proportion of regulatory cells, which may inhibit proliferation in response to stimulation with viral antigens as well as alloantigens *in vitro*.

To elucidate whether Tregs within the CD25 selected CTL are functional, we assessed the capacity of CD25 selected CTL to suppress alloreactive proliferative responses. For this, we added CD25 enriched cells in different concentrations to autologous PBMC stimulated with irradiated allogeneic PBMC and measured proliferation in a standard allo-MLR. As shown in Figure 3.7B, our results demonstrate that CD25 selected CTL do indeed suppress alloreactive proliferative responses in a dose-dependent manner, with a median 98% reduction in proliferation at a suppressor :effector ratio of 1:1 ( $p < 0.01$ ).

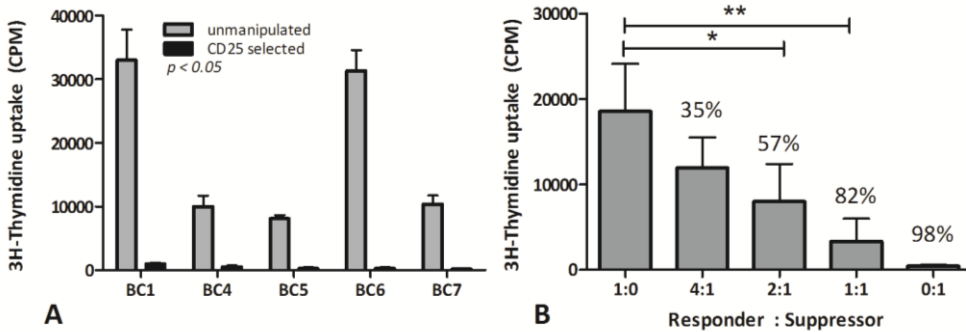


**Figure 3.7. Suppression of alloreactivity by CD25 enriched cells.**

**(A)** Proliferative response of unmanipulated PBMC (grey) and CD25 enriched CTL (black) to allogeneic PBMC stimulators in 5 donors. Bars represent mean  $^3\text{H}$ -thymidine incorporation in counts per minute (CPM) of triplicates after subtraction of stimulators and responders alone. Error bars show SEM.

**(B)** Unmanipulated (responder) PBMC were cultured for 5 days with irradiated allogeneic PBMC and serial dilutions of CD25 enriched cells from the same donor (suppressor). Bars show mean  $^3\text{H}$ -thymidine incorporation in CPM in 5 donors, error bars show SEM. Percentages reflect the mean percentage of suppression for the different responder: suppressor ratios. The assay was performed in triplicates and stimulators, responders and suppressors alone are subtracted. \*  $p < 0.05$ , \*\*  $p < 0.01$  in paired t-test.

## Discussion

The complexity of protocols needed for generation of CTL and Tregs has prevented broader application of adoptive immunotherapy beyond major academic centers. Here, we have developed a rapid (3 days), simple and clinically applicable method for the simultaneous selection of multi-virus specific CTL and Tregs for adoptive transfer.

We have shown CD25 (IL-2R $\alpha$ ) to be an excellent marker for the selection of virus activated T-cells. CD25 was upregulated upon activation with viral peptides on a larger proportion of virus-specific T-cells than IFN- $\gamma$  or other activation markers tested. In this regard, it is clear that only a subset of virus-specific Th1 cells secrete IFN- $\gamma$ ,<sup>79</sup> so that CD25 based selection may enable the selection of activated virus specific T-cells that are not secreting IFN- $\gamma$ , representing a significant HAdVantage over existing IFN- $\gamma$  methodology. CD25 enrichment results in a mixed population of both CD4 and CD8 effector T cells. However, it should be noted that we have not fully characterized the cytokine secretion profile of virus-specific CTL obtained by CD25 enrichment and this requires further study.

Our approach represents a significant HAdVance over previous methodologies for generation of multi-virus specific CTL,<sup>180:183;190</sup> in that it avoids the necessity for viral vectors and generation of specialized antigen-presenting cells such as LCL or DC. Our protocol instead utilizes APC within PBMC to present exogenously pulsed peptide pools from immunodominant viral antigens. This approach has previously been shown to be effective in generation of CMV, HAdV and EBV-specific CTL singly.<sup>81:184;191</sup> We have demonstrated for the first time that following stimulation

with peptide pools from multiple viral antigens, it is possible to select CTL with specificity against multiple viruses, this is likely to reflect enrichment for discrete populations of CMV, Adenovirus and EBV-specific CTL. Using tetramer staining, we detected enrichment of CD8<sup>+</sup> T-cells recognizing CMV and EBV epitopes following CD25 selection in 6 of 7 normal donors. ELISPOT assays demonstrated the simultaneous presence of bi- ( $n=2$ ) or trivirus ( $n=3$ ) specific cells in all evaluated donors, with a median 29-fold (6-168), 40-fold (1-247) and 16-fold (1-219) enrichment of cells secreting IFN- $\gamma$  in response to CMV pp65, adenovirus hexon and EBV LCL compared to unmanipulated PBMC from the same donors. Consistent with previous studies,<sup>180;182</sup> the magnitude of the response of CD25 selected CTL was highest for CMV, followed by EBV and then HAdV. Given the short stimulation period, we would not expect overgrowth of CTL with specificity for an individual virus, so that the differences in the frequencies of CTL specific for the 3 viruses in these assays are likely to reflect the different precursor frequencies for CMV, EBV and HAdV-specific CTL in donor blood. It is possible that the addition of epitopes to the EBV peptide pool could enhance the enrichment of EBV CTL - in our cohort, each donor could potentially recognize a median 6 of the 23 EBV epitopes. While tetramer-positive CD8<sup>+</sup> T-cells recognizing hexon were seen in only 1 evaluable donor, IFN- $\gamma$  responses were detected in 3 of 5 donors after CD25 selection. This is likely to reflect the fact that T-cell response to HAdV is mainly mediated by CD4<sup>+</sup> lymphocytes<sup>192</sup> and the immunodominant hexon epitopes are not identified for many HLA restrictions as well as the lower frequency of HAdV-specific CTL.

It should be noted that multi-virus specific CTL cultures were generated only from CMV-seropositive donors. Previous studies have demonstrated the difficulty of generating CTL from seronegative donors, as existing protocols expand memory rather than prime naïve T-cell responses. As 90% of adult donors have been infected by adenovirus and EBV, this is generally not an issue for these viruses. However, only 60 % of the population is seropositive for CMV, which may limit the applicability of our approach in patients with CMV seronegative donors.

The peptide pools used for stimulation of virus-specific CTL were designed to stimulate both CD4<sup>+</sup> and CD8<sup>+</sup> virus-specific T-cells. Previous studies suggest that virus-specific CD4<sup>+</sup> T helper cells are needed to maintain responses *in vivo*.<sup>193</sup> In this regard, the presence of high proportion of CD4<sup>+</sup> (mean 67%) T-cells in our CD25 selected population may improve the durability of antiviral T-cell responses following adoptive immunotherapy, as well as broadening their target specificity to include HLA Class II restricted antigens such EBNA-1 and hexon. As expected, the majority of CD25 selected CTL show a memory phenotype which may also favour sustained responses *in vivo*.

For safe adoptive transfer, virus-specific T-cells should have little alloreactivity. In our system, alloreactive T-cells should not be activated to express CD25 and selected CTL should therefore have reduced alloreactivity compared with unmanipulated PBMC. While our data from proliferation assays shows negligible proliferative responses of CD25-selected T-cells to 3<sup>rd</sup> party stimulators in all donors, this is complicated by the enrichment of Tregs in the CD25-selected fraction, which rendered our T-cells generally unresponsive to antigenic stimuli, so that it is difficult to be certain of the alloreactivity. However, recent data has shown that even when alloreactive T-cells are detectable *in vitro* in virus-specific CTL, this was not associated with the development of clinical GVHD when CTL were adoptively transferred post-SCT.<sup>194</sup> Further,

given that CD25-based selection of 450 ml blood draws gave a median yield of  $2.2 \times 10^7$  T-cells, equivalent to a dose of  $3 \times 10^5$ /kg for a 70kg recipient, and that even with unmanipulated donor lymphocyte infusions in the HLA matched unrelated donor setting, doses of  $10^6$  CD3<sup>+</sup>/kg rarely cause GVHD,<sup>195</sup> we believe that the likelihood of GVHD following adoptive immunotherapy with these doses of CD25-selected CTL is low. The presence of Tregs within our selected fraction may further reduce this risk.

Since CD25 is highly expressed on Tregs,<sup>196</sup> these are enriched by our selection methodology. Consistent with this, a significant proportion of CD25 enriched T-cells (median 21% of CD4<sup>+</sup> T-cells immediately after selection) showed a CD4<sup>+</sup> CD25<sup>+</sup> FoxP3<sup>+</sup> CD127<sup>-</sup> Treg phenotype. While flow cytometric distinction between Tregs and activated T-cells that transiently upregulate CD25 and FoxP3<sup>197</sup> is difficult and some down regulation of FoxP3 was indeed seen when cells were rested, a proportion of selected T-cells retained this Treg phenotype. More importantly, CD25 selected T-cells from all donors were able to effectively prevent the proliferation of autologous PBMC in response to allogeneic stimulators in suppression assays, demonstrating the presence of functional Tregs in CD25 enriched T-cells. Further studies are needed to determine if restimulation of CD25 enriched T-cells with viral antigens *in vitro* would enhance CTL responses at the expense of Tregs. The infusion of Tregs in murine models had a protective effect against the development of GVHD<sup>198;199</sup> and early clinical studies<sup>200;201</sup> provide support for such an approach. Potentially therefore, CD25 enriched CTL may have a beneficial effect in terms of GVHD. However, previous studies suggest high Treg : T-effector ratios are required for this effect<sup>199</sup> and it may be that the numbers of Tregs produced using our methodology are too small to confer significant clinical benefit.

One key issue is whether the presence of Tregs within the CD25 enriched fraction will influence the function of virus-specific CTL. Our data demonstrate that enriched CTL are able to secrete IFN- $\gamma$  in response to stimulation with viral antigens and lyse EBV infected target cells. The observed absence of proliferation in response to viral antigens may reflect the *in vitro* system used, since suppression by Tregs is contact dependent.<sup>202</sup> In the absence of such cell-cell contact when enriched cells are adoptively transferred *in vivo*, it is unlikely that infused Tregs will prevent proliferation of virus-specific CTL. In support of this, data from murine models suggest that the co-infusion of Tregs and conventional T-cells enhances rather than abrogates recovery of virus-specific immune reconstitution through prevention of GVHD.<sup>203</sup>

Our protocol is GMP compliant and scale-up experiments were performed under GMP conditions. Clinical grade PepTivator mixes for CMV pp65 and HAdV5 hexon are available (Miltenyi), while the EBV peptide mix has already been used in a clinical study.<sup>81</sup> Cultures were performed in serum-free medium and selection performed in a closed system using clinical grade CD25 reagent which is CE marked for clinical application. The selection methodology used (CliniMACS) is already in widespread clinical use, so that our approach could be broadly applicable in many transplant centers. Starting with 450 ml blood, we routinely generated enough CD25 enriched cells for adoptive transfer of  $10^7$ /m<sup>2</sup> multi-virus specific CTL, a dose similar to that used in previous clinical studies of immunotherapy with CTL generated by repetitive antigenic stimulation<sup>75;180;181</sup> and significantly higher than those previously achieved using IFN- $\gamma$  capture.<sup>80</sup>

Further, particularly in the presence of viral reactivation, infused T-cells are likely to expand significantly post-infusion.<sup>77:181</sup>

In conclusion, we have developed a rapid, simple methodology for the simultaneous selection of T-cells with multiple viral-specificities and Tregs in a single 3 day culture. Potentially this approach could be extended to other pathogens where immunodominant antigens have been identified. Because of the speed and simplicity of this methodology, this approach may significantly broaden the applicability of adoptive T-cell transfer to restore cellular immunity to viruses post-SCT. However, the clinical utility of this approach will require evaluation in well-designed clinical studies.

### **Funding and Disclosures**

All authors approved the final manuscript for publication. The authors reported no potential conflicts of interest.

## Supplementary data

Type	Short name	Amino acid sequence	Antigen	HLA restriction
Class I & II	11-amino acid overlapping	15-mer peptide pool	CMV- pp65	All
	covering complete sequence of protein			
Class I & II	11-amino acid overlapping	15-mer peptide pool	AdV5-hexon	All
	covering complete sequence of protein			
Class I	CLG	CLGGLLTMV	EBV- LMP2	A*0201
	GLC	GLCTLVAML	EBV- BMLF1	A*0201
	YVL	YVLDHLIVV	EBV- BRLF1	A*0201
	RLR	RLRAEAQVK	EBV- EBNA3A	A*0301
	RPP	RPPIFIRRL	EBV- EBNA3A	B*0702
	QPR	QPRAPIRPI	EBV- EBNA3C	B*0702
	QAK	QAKWRLQTL	EBV- EBNA3A	B*0801
	RAK	RAKFKQLL	EBV- BZLF1	B*0801
	IVT	IVTDFSVIK	EBV- EBNA3B	A*1101
	DEV	DEVEFLGHY	EBV- BMLF1	B*1801
	RYS	RYSIFFDYM	EBV- EBNA3A	A*2402
	TYS	TYSAGIVQI	EBV- EBNA3B	A*2402
	TYP	TYPVLEEMF	EBV- BRLF1	A*2402
	RRİY	RRİYDLIEL	EBV- EBNA3C	B*2702/04/05
	YPL	YPLHEQHGM	EBV- EBNA3A	B*3501
	EPL	EPLPQGQLTAY	EBV- BZLF1	B*3501
	IED	IEDPPFNSL	EBV- LMP2	B*4001
	KEH	KEHVIQNAF	EBV- EBNA3C	B*4402
	VEI	VEITPYKPTW	EBV- EBNA3B	B*44
Class II	PYYV	PYYVVDLSVRGM	EBV- BHRF1	DRB1*04
	FGQL	FGQLTPHTKAVYQPR	EBV- BLLF1	DRB1*13
	IPQC	IPQCRLTPLSRLPFG	EBV- EBNA1	DRB1*13/14
	TDAW	TDAWRFAMNYPRNPT	EBV- BNRF1	DRB1*15

**Table 3.S1.** Peptide pools used for activation of lymphocytes with specificity for Cytomegalovirus, Adenovirus and Epstein-Barr virus



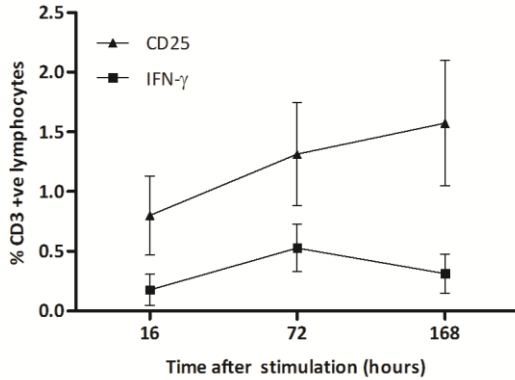


**Figure 3.S1.** Flow cytometric analysis of EBV-specific CD3<sup>+</sup> T cells after stimulation *in vitro* with EBV immunodominant peptides for 16, 72 and 168 hours. Percentage of IFN- $\gamma$  producing and CD25 expressing in total CD3<sup>+</sup> T cells in peripheral blood of 7 EBV-seropositive normal donors. The frequency of CD3<sup>+</sup>/CD25<sup>+</sup> or CD3<sup>+</sup>/IFN- $\gamma$  T cells is shown as the mean percentage (+SEM) after subtraction of IgG isotype and unstimulated controls. Squares show IFN- $\gamma$  secreting cells while triangles show CD25 positive cells.



# Chapter 4

## The effect of cidofovir on adenovirus plasma DNA levels in stem cell transplantation recipients without T cell reconstitution

Published in:  
Biology of Blood and Marrow Transplantation  
2015; 21: 293-299

Gertjan Lugthart  
Marloes A. Oomen  
Cornelia M. Jol-van der Zijde  
Lynne M. Ball  
Dorine Bresters  
Wouter J.W. Kollen  
Frans J. Smiers  
Clementien L. Vermont  
Robbert G.M. Bredius  
Marco W. Schilham  
Maarten J.D. van Tol *and*  
Arjan C. Lankester

## Abstract

**Background:** Cidofovir is frequently used to treat life-threatening human adenovirus (HAdV) infections in immunocompromised children after hematopoietic stem cell transplantation (HSCT). However, the anti-viral effect irrespective of T cell reconstitution remains unresolved.

**Methods:** Plasma HAdV DNA levels were monitored by real-time quantitative PCR during 42 cidofovir treatment episodes for HAdV viremia in 36 pediatric allogeneic HSCT recipients. HAdV load dynamics was related to T and NK cell reconstitution measured by flow cytometry.

**Results:** To evaluate the *in vivo* anti-adenoviral effect of cidofovir, we focused on 20 cidofovir treatment episodes lacking concurrent T cell reconstitution. During 2-10 weeks of follow-up in the absence of T cells, HAdV load reduction (n=7) or stabilization (n=8) were observed in 15/20 treatments. Although HAdV load reduction was always accompanied by NK cell expansion, HAdV load stabilization was measured in two children lacking both T and NK cell reconstitution. In cases with T cell reconstitution, rapid HAdV load reduction (n=14) or stabilization (n=6) was observed in 20/22 treatments.

**Conclusion:** In the absence of T cells, cidofovir treatment was associated with HAdV viremia control in the majority of cases. Although the contribution of NK cells cannot be excluded, cidofovir has the potential to mediate HAdV load stabilization in the time pending T cell reconstitution.

## Highlights

- Cidofovir is used to treat human adenovirus viremia in pediatric HSCT recipients
- Evaluation of the antiviral effect of cidofovir is biased by T cell reconstitution
- In the absence of T cells, cidofovir can mediate HAdV load stabilization
- NK cell expansion during HAdV load reduction in the absence of T cells

## Introduction

Human adenoviruses (HAdV) are non-enveloped double-stranded DNA viruses. Currently, more than 50 serotypes have been described. In healthy individuals, HAdV infections cause self-limiting infections such as conjunctivitis, upper respiratory tract-, urinary tract- or gastrointestinal infections.<sup>50</sup> In pediatric hematopoietic stem cell transplantation (HSCT) recipients, HAdV reactivations or primary infections can progress to viremia and disseminated disease. It is broadly accepted that T cells are essential for the protection from and clearance of HAdV viremia.<sup>38;204;205</sup> However, in the absence of T cell surveillance, the mortality of HAdV viremia is high because of progression to HAdV related multi-organ failure (HAdV/MOF).<sup>38;41;51;206-208</sup> The adoptive transfer of donor-derived adenovirus specific T cells is a promising treatment,<sup>205;209</sup> but is not available in all transplant centers. Therefore, pre-emptive pharmacological treatment is of great importance for the majority of patients with HAdV viremia. To this end, ribavirin and cidofovir have been explored. The evidence for a beneficial effect of ribavirin is limited to case reports and ribavirin could not prevent the progression of HAdV viremia in the absence of lymphocyte reconstitution.<sup>52</sup> Cidofovir (Vistide®), a monophosphate nucleotide analogue with *in vitro* anti-viral activity against different HAdV strains,<sup>210-213</sup> is a widely used anti-viral agent for HAdV infections post HSCT.

A number of studies have addressed the anti-adenoviral effect of cidofovir, but results are highly variable with treatment successes ranging from 24-98%.<sup>55-59;214;215</sup> The discrepancies in cidofovir effectiveness might be related to the fact that HAdV viremia and cidofovir treatment generally occur during the critical phase of lymphocyte reconstitution after HSCT.<sup>38;41;206;207</sup> When T cell reconstitution is not taken into account, this will result in a biased evaluation of the effect of cidofovir. An unbiased evaluation of the *in vivo* anti-adenoviral effect of cidofovir is required because the use of cidofovir is associated with considerable nephrotoxicity.<sup>53-56</sup>

In this study, we aimed to evaluate the *in vivo* anti-viral effect of cidofovir in patients with HAdV viremia after pediatric HSCT without the confounding effect of concomitant T cell reconstitution. Hereto, we monitored the change of plasma HAdV DNA levels during cidofovir treatment, focusing on cidofovir treatments in the absence of T cell reconstitution.

## Methods

### Ethics statement

Transplantations were performed according to European society for Blood and Marrow Transplantation (EBMT) guidelines. Peripheral blood samples were routinely obtained. Data were analyzed after approval by the institutional review board (protocol P01.028 and P02.099). Informed consent was provided by the patient and/or a parent or guardian.

### **Patients and cidofovir treatment**

Between January 2003 and December 2012, 321 children received 363 transplantations at the pediatric HSCT unit of the Leiden University Medical Center (LUMC). Thirty-nine HSCT recipients were treated with cidofovir for HAdV viremia. One patient was not evaluable as she died from pre-existent neurodegenerative disease within the first two weeks of treatment. From two other patients, no follow-up of the plasma HAdV DNA levels (HAdV load) was available, leaving 36 evaluable HSCT recipients. Six patients received two separate cidofovir treatment episodes for the same HAdV viremia and were analyzed twice. In total, 42 cidofovir treatment episodes were analyzed (Table 4.1).

In general, cidofovir treatment was initiated pre-emptively when the HAdV load was 3 log (1000) viral DNA copies/ml (c/ml) at two consecutive time points.<sup>41</sup> Reasons to stop treatment were: HAdV load reduction, HAdV load stabilization below <3 log c/ml, nephrotoxicity or treatment failure. Cidofovir (Vistide<sup>®</sup>, Gilead Sciences Inc., Foster City, CA, US) was administered intravenously thrice weekly at 1 mg/kg body weight.<sup>214</sup> Supportive care consisted of hyperhydration with intravenous saline (3L/m<sup>2</sup> body surface/24h) and oral probenecid (25 mg/kg) at -3, +1 and +8 hours from the start of cidofovir infusion.<sup>53</sup> Other anti-viral drugs were discontinued during cidofovir treatment. See supplemental methods and Table 4.S1 for a detailed description of patient inclusion and HSCT characteristics.

### **Monitoring of HAdV plasma DNA levels and lymphocyte reconstitution**

HAdV reactivations were routinely monitored through twice-weekly plasma screening for viral DNA by real time quantitative PCR as described previously.<sup>159</sup> The lower level of detection of this assay was 1.7 log viral DNA c/ml. Monitoring was initiated at day +3 post HSCT and continued until T cells reached 300 cells/  $\mu$ l of peripheral blood. To monitor immune reconstitution, peripheral blood white blood cell counts including full leukocyte differentiations were performed 2-3x/week. The lower level of detection of lymphocytes was 10-20 cells/ $\mu$ l. Flow cytometric analysis was performed weekly to quantify NK and T cell reconstitution as described in the supplemental methods and Table 4.S3. T cells were defined as CD3<sup>+</sup> cells in the CD45<sup>+</sup> CD33/CD235a/CD14<sup>-</sup> lymphocyte gate and NK cells were defined as CD3<sup>-</sup> CD56<sup>+</sup> cells in the lymphocyte gate.

### **Definitions of HAdV load dynamics and lymphocyte reconstitution during cidofovir treatment**

HAdV load dynamics was evaluated during cidofovir treatment. Reduction and increase were defined as a  $\geq 1$  log (tenfold) change of the HAdV load. Stabilization was defined as a <1 log change in HAdV load. Both reduction and stabilization of the HAdV load were regarded as viremia control. To discriminate between the (potential) effect of T cell reconstitution and cidofovir treatment on HAdV load dynamics, we applied the low threshold of 50 T cells/ $\mu$ l of peripheral blood.

We first analyzed HAdV load dynamics in 42 cidofovir treatments without (n=20) and with (n=22) T cell reconstitution in the first two weeks after treatment initiation. Subsequently, we

focused on the 20 cidofovir treatments in the absence of concomitant T cell reconstitution. In this group, HAdV load change was evaluated between treatment initiation and one week after the last dose of cidofovir. In cases with T cell reconstitution before the end of treatment (n=6), follow-up was stopped at 1 week before T cell numbers reached 50 cells/ $\mu$ l to exclude the confounding effect of T cells on the HAdV load.

## Statistical Analysis

Statistical analysis was performed using SPSS Statistics 20 (IBM SPSS Inc., Chicago, IL, US). GraphPad Prism 6.00 (GraphPad Software, San Diego, CA, US) was used to construct figures. Because data did not follow Gaussian distribution, the Mann-Whitney U test was used for the analysis of numerical parameters. Pearson's Chi-square tests were used for analysis of categorical parameters.

Patient characteristics (n=36)		n / median	% / range
Age (year)		4.5	0.5 - 18
HSCT indication	<i>Primary Immunodeficiency</i>	8	22%
	<i>Benign Hematological Disorder</i>	12	33%
	<i>Hematological Malignancy</i>	16	44%
Conditioning	<i>Reduced Intensity</i>	6	17%
	<i>Myeloablative</i>	30	83%
Donor Type	<i>Identical Related Donor</i>	2	6%
	<i>Other Related Donor</i>	7	19%
	<i>Matched Unrelated Donor</i>	27	75%
Graft Source	<i>Bone Marrow, T cell replete</i>	16	44%
	<i>Bone Marrow, T cell depleted</i>	1	3%
	<i>PBSC, T cell replete</i>	2	6%
	<i>PBSC, T cell depleted</i>	8	22%
	<i>Cord Blood</i>	9	25%
Serotherapy	<i>Anti-thymocyte globulin</i>	23	64%
	<i>Alemtuzumab</i>	13	36%
GvHD prophylaxis	<i>None</i>	4	11%
	<i>CsA</i>	3	8%
	<i>CsA + Methotrexate</i>	18	50%
	<i>CsA + Methylprednisolone</i>	9	25%
	<i>CsA + MMF</i>	2	6%
Acute Graft versus Host Disease $\geq$ grade II		5	14%
Cidofovir treatment	<i>One episode</i>	30	83%
	<i>Two episodes</i>	6	17%
First day plasma HAdV DNA level $>1.7 \log c/mL^1$		20	3 - 96
First day plasma HAdV DNA level $2x >3 \log c/mL^1$		28	8 - 117
First day of first cidofovir treatment episode <sup>1</sup>		29	7 - 121
Final outcome	<i>HAdV clearance</i>	27	75%
	<i>Death from HAdV / MOF</i>	6	17%
	<i>Death from other cause</i>	3	8%
Cidofovir treatment episodes (n=42)		n / median	range
Day start cidofovir <sup>1</sup>		31	7 - 214
Plasma HAdV DNA level at start ( $\log c / mL$ )		4.1	1.7 - 6.5
Treatment duration (days)		16	1 - 99

**Table 4.1. Patient and cidofovir treatment characteristics.**

Abbreviations: HAdV: human adenovirus, HSCT: hematopoietic stem cell transplantation, PBSC: peripheral blood stem cells, GvHD: graft-versus-host disease, CsA: Cyclosporin A, MMF: mycophenolate mofetil, HAdV/MOF: HAdV related multi-organ failure. 1: day post HSCT. Categorical data: number (percentage). Numerical data: median (range).

## Results

### Characteristics of cidofovir treated patients

The effect of cidofovir treatment on the HAdV load was evaluated in 36 HSCT recipients, of whom the characteristics are summarized in Tables 1 and S1. Six patients received a second cidofovir treatment episode (Figure 4.S1), resulting in 42 evaluable cidofovir treatments. Cidofovir treatment was initiated at a median of 31 (range 7-214) days after HSCT. At treatment initiation, the HAdV load was median 4.1 (range 1.7-6.5) log c/ml and median treatment duration was 16 (range 1-99) days. 40/42 cases received  $\geq 1$  week (3 doses) of cidofovir (Tables 1 and 2).

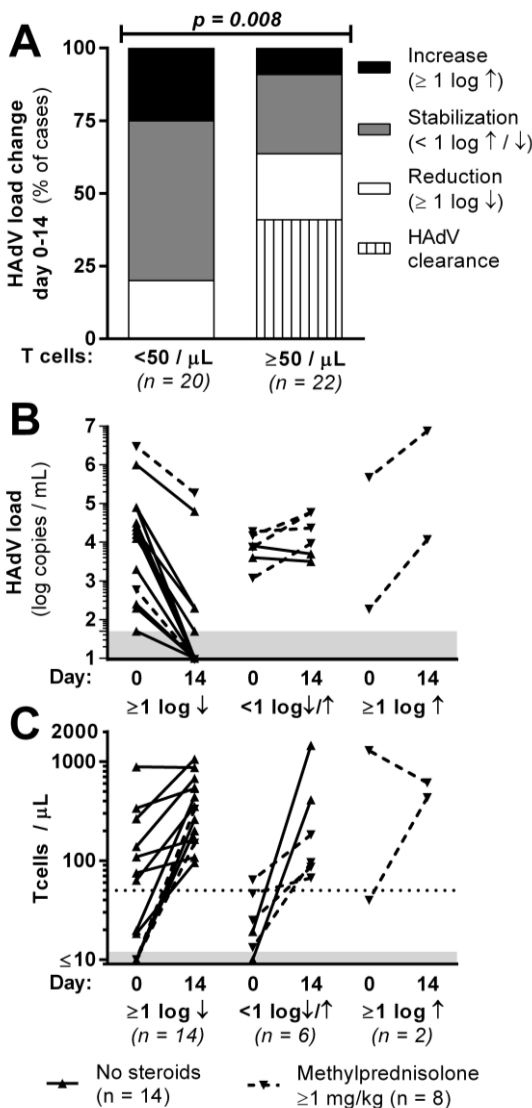


**Figure 4.1. HAdV load dynamics in relation to T cell reconstitution.**

**(A)** Change of plasma human adenovirus DNA levels (HAdV load) between the start of treatment (day 0) and day 14 of cidofovir treatment in cases with T cell numbers  $< 50$  cells/ $\mu\text{L}$  ( $n=20$ , left bar) and T cell numbers  $\geq 50$  cells/ $\mu\text{L}$  ( $n=22$ , right bar) within this time period. HAdV load change: clearance: dashed,  $\geq 1$  log reduction: white, stabilization: gray,  $\geq 1$  log increase: black.  $p$ -value: Pearson's Chi Square test.

**(B)** Change of HAdV load between day 0 and 14 in 22 cidofovir treatments with T cell numbers  $\geq 50$  cells/ $\mu\text{L}$ . Solid lines: cases without steroid treatment. Interrupted lines: methylprednisolone  $> 1$  mg/kg of body weight. Shaded area: HAdV load below limit of detection (1.7 log c/ml).

**(C)** Change of T cell numbers between day 0 and 14 in 22 cidofovir treatments with T cell reconstitution. Solid lines: cases without steroid treatment. Interrupted lines: methylprednisolone  $> 1$  mg/kg of body weight. Shaded area: T cells below limit of detection (10 cells/ $\mu\text{L}$ ).



### HAdV load dynamics in relation to T cell reconstitution

T cells have been demonstrated to play a crucial role in viral control and could form a major confounder in the analysis of the anti-viral effect of cidofovir. To test this hypothesis, we first divided the 42 cidofovir treatments in cases without ( $n=20$ ) and with ( $n=22$ ) T cell reconstitution in the first two weeks after treatment initiation (Table 4.2). The groups did not differ with respect to HSCT related parameters and HAdV viremia characteristics (Table 4.S2).

In 11/20 cidofovir treatments (55%) with T cell numbers below 50 cells/ $\mu\text{l}$ , plasma HAdV DNA levels were stable in the first two weeks after treatment initiation. The HAdV load increased  $\geq 1$  log c/ml in 5/20 treatments (25%) and HAdV load reduction –but no clearance– was measured in 4/20 treatments (20%) without T cell reconstitution (Figure 4.1A).

In contrast, in 14/22 cidofovir treatments (64%) with concomitant T cell reconstitution, HAdV load reduction or HAdV clearance was observed within two weeks after treatment initiation. The HAdV load was stable in 6/22 treatments (27%) with T cell reconstitution and increased  $\geq 1$  log in only 2/22 cases (9%), who simultaneously received high dose ( $>1\text{mg/kg}$  methylprednisolone) steroid treatment (Figure 4.1 B-C). Hence, it can be concluded that the evaluation of the antiviral effect of cidofovir treatment is strongly influenced by T cell reconstitution ( $p=0.008$ , Figure 4.1A).

### HAdV load dynamics in the absence of T cell reconstitution

To exclude the confounding effect of T cells, HAdV load dynamics was further analyzed in the 20 cidofovir treatments with  $<50$  T cells/ $\mu\text{l}$  of peripheral blood (Table 4.2 & Figure 4.2). In these cases, the evaluation period was extended –from 14 days used in the previous section– to the time frame between treatment initiation and one week after the last dose of cidofovir ( $n=14$ ) or 1 week before T cell numbers reached 50 cells/ $\mu\text{l}$  ( $n=6$ ).

A  $\geq 1$  log HAdV load reduction was observed in 7/20 treatments (35%) during a median 28 day evaluation period in the absence of T cells (Figure 4.2A). In 8/20 cidofovir treatments (40%), the HAdV load did not change significantly between the start and end of the evaluation period (median 18 days, Figure 4.2B). In the 5 remaining cases (25%), the HAdV load increased  $\geq 1$  log despite cidofovir treatment during median 21 days of follow up in the absence of T cells (Figure 4.2C).

### NK cell expansion during HAdV control in the absence of T cell reconstitution

In the majority of the cases without T cell reconstitution,  $\text{CD3}^- \text{CD56}^+$  NK cells were already present at the start of cidofovir treatment (Figure 4.2 D-F). Reduction of the HAdV load during cidofovir treatment coincided with a dynamic increase in NK cell numbers in all 7 cases (8-29 fold NK cell expansion, Figure 4.2D). In comparison, NK cell expansion was observed in 4/8 cidofovir treatments with HAdV load stabilization (Figure 4.2E) and 2/5 treatments with HAdV load increase (Figure 4.2F,  $p=0.05$ ).

### HAdV load stabilization in the absence of both T and NK cells

We finally analyzed the anti-viral effect of cidofovir on the HAdV load in HSCT recipients lacking both T- and NK cell reconstitution to exclude the possible contribution of NK cells to HAdV control as well. Two HSCT recipients fulfilled these criteria. In patient A (UPN 600.1a), no engraftment occurred and the HAdV viremia was stable during 3 weeks of cidofovir treatment in the absence of any lymphocytes (Figure 4.2 A, D, open diamonds & Figure 4.S1 D). The viremia was ultimately cleared after lymphocyte reconstitution following a re-transplantation. In patient B (UPN 545.1b), a graft rejection was treated with the lymphocyte depleting antibody alemtuzumab. The HAdV load was stable in the absence of lymphocytes over a 4 weeks period, after which HAdV dissemination occurred under cidofovir treatment (Figure 4.2 C, F, open diamonds & Figure 4.S1 B).

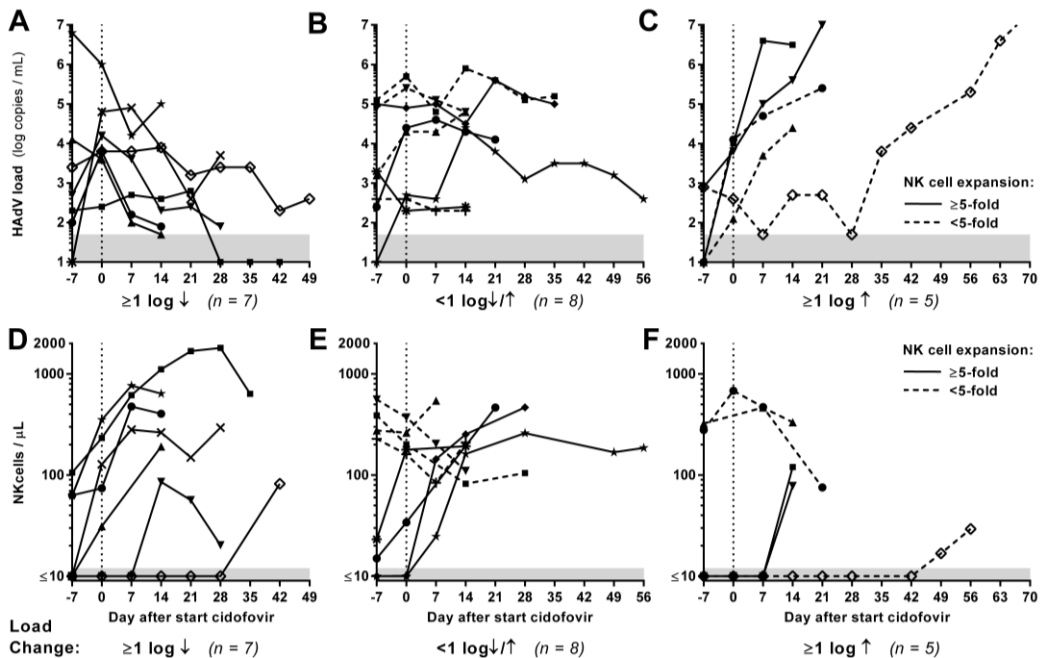


**Figure 4.2. HAdV control in the absence of T cells.**

**(A-C)** Plasma human Adenovirus (HAdV) DNA levels in 20 cidofovir treatments with T cell numbers  $< 50$  cells/ $\mu\text{L}$ . Follow-up was stopped at 1 week after the last dose of cidofovir or 1 week before T cell numbers reached 50 cells/ $\mu\text{L}$ . HAdV load change:  $\geq 1$  log reduction (A,  $n = 7$ ), stabilization (B,  $n = 8$ ) or  $\geq 1$  log increase (C,  $n = 5$ ). Solid lines: cases with  $\geq 5$  fold NK cell expansion, interrupted lines: cases without NK cell expansion. Vertical dotted line: start of treatment. Shaded area: HAdV load below limit of detection (1.7 log c/ml).

**(D-F)** Absolute numbers of NK cells in peripheral blood in cases with HAdV load reduction (D), stabilization (E) and increase (F). Solid lines: cases with  $\geq 5$  fold NK cell expansion, interrupted lines: cases without NK cell expansion. Identical symbols in corresponding figures represent individual cases. Vertical dotted line: start of treatment. Shaded area: NK cells below limit of detection (10 cells/ $\mu\text{L}$ ).

## Discussion

Here, we report a systematic analysis of the effect of cidofovir treatment on HAdV viremia after HSCT, using plasma viral DNA levels as an objective parameter while taking concomitant lymphocyte reconstitution into account. In line with our hypothesis, rapid HAdV load reduction and HAdV clearance during cidofovir treatment were associated with concurrent T cell reconstitution. In the absence of T cell reconstitution, the HAdV viremia was controlled in 75% of cidofovir treatments, which can be attributed to cidofovir although a role of NK cell reconstitution cannot be excluded. Of note, in 2 cases, HAdV load stabilization was observed during a >3 week cidofovir treatment in the absence of both NK and T cells.

Because of the strong correlation between T cell reconstitution and HAdV load reduction as reported earlier<sup>38;204;205</sup> and supported by our data, we focused our analysis on the 20 cidofovir treatment episodes in HSCT recipients lacking T cell reconstitution. In view of the often fatal outcome of a progressing HAdV viremia,<sup>51</sup> HAdV load reduction or stabilization can be regarded as a beneficial result. In line with the *in vitro* virostatic capacity of cidofovir,<sup>210-213</sup> control of the HAdV viremia was observed in 15 out of 20 cidofovir treatments in the absence of T cell reconstitution. However, reduction of the HAdV load (n=7) always coincided with a  $\geq 5$  fold increase of NK cell numbers in the peripheral blood. Consequently, the contribution of NK cell reconstitution to HAdV control in HSCT recipients without T cell reconstitution cannot be excluded. Usually, NK cells are the first lymphocytes to reach normal levels after HSCT.<sup>216;217</sup> Although the NK cell response to HAdV is not as well described as the NK cell mediated control of other viruses like influenza, cytomegalovirus and hepatitis C virus,<sup>218-220</sup> a limited number of studies reported NK cell activity against HAdV infected cells.<sup>221-223</sup> Our data further support a role for NK cells in the initial HAdV control in patients with a delayed T cell reconstitution. At the same time, NK cell expansion did not always coincide with HAdV load reduction and the presence of NK cells was no guarantee for HAdV load stabilization.

In many studies, final outcome of HAdV viremia is used as a primary endpoint of cidofovir effectiveness, and concomitant lymphocyte reconstitution is often ignored. This bears the risk to overestimate the *in vivo* anti-viral effect of cidofovir. Indeed, Walls *et al.* reported the clearance of HAdV viremia in 8 out of 9 pediatric HSCT recipients with HAdV loads >3 log c/ml in the absence of anti-viral therapy.<sup>224</sup> For this reason, an unbiased evaluation of the anti-viral capacity of cidofovir –and other pharmacological interventions– for human adenoviral infections after HSCT is only possible by monitoring HAdV load dynamics in patients that lack concomitant lymphocyte reconstitution. Only two patients in our cohort met this condition. In both cases, the HAdV viremia remained stable over a 3-4 weeks period. Consequently, cidofovir may also have contributed to the HAdV load stabilization observed in HSCT recipients lacking T cell reconstitution or with suppressed anti-viral T cell responses due to high dose systemic steroids.<sup>37;225;226</sup>

Of note, cidofovir treatment could not prevent the progression of HAdV viremia in 7/42 cidofovir treatments (17%), all in the absence of T cell reconstitution or during high dose steroid treatment. With respect to the cause of these treatment failures, no firm conclusions can be drawn. *In vitro* studies reported comparable cidofovir susceptibility between different HAdV species.<sup>210-213</sup> In our

UPN	HAdV viremia				CDV treatment				Lymphocyte reconstr.			HAdV load change <sup>7</sup>		Reason stop follow-up <sup>8</sup>	
	First day PCR <sup>1</sup>	Day PCR 2x > 3 log <sup>1</sup>	Load at start CDV <sup>2</sup>	Sero-type	Species	Treat-ment #	Day Start <sup>1</sup>	Dura-tion <sup>3</sup>	T cell <sup>4</sup>	NK cell <sup>5</sup>	Ster-oids <sup>6</sup>	Day 14 <sup>5</sup>	Last day follow-up <sup>3,8</sup>		
T cells >50 cells/ $\mu$ L 14 days after start cidofovir															
543.1a	14	19	5.9	31	A	1	28	9	-	+	-	↓	↓ (14)	Stop CDV	
549.1	19	30	3.8	2	C	1	30	7	-	+	-	↓	↓ (14)	Stop CDV	
555.1	8	23	3.6	31	A	1	28	7	-	+	-	↓	↓ (14)	Stop CDV	
808.1	12	23	4.2	?	?	1	23	21	-	+	-	↓	↓ (28)	Stop CDV	
600.1a	26	29	3.8	1	C	1	30	49	-	+	+	=	↓ (56)	Stop CDV	
616.1	13	20	4.4	3,31	B,C	1	17	27	-	+	+	=	↓ (28)	T cell $\geq$ 50	
721.1	39	-	2.4	?	?	1	44	37	-	+	+	=	↓ (42)	Stop CDV	
514.3	20	27	4.4	2	C	1	31	14	-	+	-	=	= (21)	Stop CDV	
543.1b	n.a.	n.a.	5.7	2,31	A,C	2	55	41	-	-	-	=	= (35)	T cell $\geq$ 50	
554.2	17	53	5.4	1	C	1	53	8	-	-	-	=	= (14)	Stop CDV	
560.1	27	48	4.9	5	C	1	48	42	-	+	+	=	= (35)	T cell $\geq$ 50	
625.2	43	-	2.3	1	C	1	59	9	-	+	-	=	= (14)	Stop CDV	
648.2	70	75	4.3	31	A	1	78	50	-	-	-	=	= (14)	T cell $\geq$ 50	
681.1a	24	34	2.9	?	?	1	40	7	-	-	-	=	= (14)	Stop CDV	
545.1b	n.a.	n.a.	2.6	5,31	A,C	2	39	64	-	-	+	=	↑ (70)	Stop CDV	
551.1	19	33	2.7	31	A	1	21	47	-	+	-	↑	= (56)	Stop CDV	
613.1	40	46	4.1	5	C	1	44	17	-	-	+	↑	↑ (21)	Stop CDV	
719.1	5	8	4.0	31	A	1	7	28	-	+	-	↑	↑ (14)	T cell $\geq$ 50	
799.1	25	39	2.1	31	A	1	28	40	-	-	-	↑	↑ (14)	T cell $\geq$ 50	
804.1	7	16	3.8	31	A	1	17	11	-	+	-	↑	↑ (21)	Stop CDV	
558.1	14	19	1.7	31	A	1	23	7	-	+	-	c	n.a.	T cell $\geq$ 50	
586.1	61	75	4.5	1	C	1	77	12	-	-	-	c	n.a.	T cell $\geq$ 50	
648.1	6	-	2.8	31	A	1	17	14	-	+	+	c	n.a.	T cell $\geq$ 50	
681.1b	n.a.	n.a.	2.3	?	?	2	95	3	-	-	-	c	n.a.	T cell $\geq$ 50	
697.1	5	23	4.3	?	?	1	21	12	-	-	-	c	n.a.	T cell $\geq$ 50	
732.1	10	20	4.4	?	?	1	19	1	-	+	-	c	n.a.	T cell $\geq$ 50	
787.1b	n.a.	n.a.	2.4	?	?	2	112	21	-	-	-	c	n.a.	T cell $\geq$ 50	
816.1	5	22	4.2	31	A	1	23	11	-	+	-	c	n.a.	T cell $\geq$ 50	
817.1	34	37	3.3	?	?	1	38	10	-	-	-	c	n.a.	T cell $\geq$ 50	
515.2	12	16	6.5	1,2	C	1	16	24	-	+	+	↓	↓ (n.a.)	T cell $\geq$ 50	
587.1	20	-	4.1	31	A	1	31	7	-	+	-	↑	n.a.	T cell $\geq$ 50	
594.1b	n.a.	n.a.	6.0	1	C	2	214	73	-	-	-	↓	↓ (n.a.)	T cell $\geq$ 50	
600.1b	n.a.	n.a.	4.9	1	C	2	100	10	-	-	-	↓	↓ (n.a.)	T cell $\geq$ 50	
823.1	20	23	4.9	?	?	1	22	12	-	+	-	↓	↓ (n.a.)	T cell $\geq$ 50	
515.1	65	72	4.3	2	C	1	79	48	-	-	+	=	n.a.	T cell $\geq$ 50	
545.1a	3	10	3.9	5	C	1	10	15	-	-	-	=	n.a.	T cell $\geq$ 50	
594.1a	21	28	3.9	1	C	1	32	80	-	+	+	=	n.a.	T cell $\geq$ 50	
597.1	5	12	4.2	31	A	1	8	99	-	-	+	=	n.a.	T cell $\geq$ 50	
686.2	87	101	3.6	2	C	1	107	15	-	+	-	=	n.a.	T cell $\geq$ 50	
787.1a	18	20	3.1	1	C	1	20	28	-	+	+	=	n.a.	T cell $\geq$ 50	
634.1	96	117	5.4	2	C	1	121	36	-	-	+	↑	n.a.	T cell $\geq$ 50	
671.1	52	66	2.3	1	C	1	48	70	-	-	+	↑	n.a.	T cell $\geq$ 50	
T cells >50 cells/ $\mu$ L 14 days after start cidofovir															

cohort, cidofovir treatment failures were observed both in patients with HAdV species A as well as species C. Whereas cidofovir resistant HAdV strains have been generated *in vitro*,<sup>227</sup> no resistance was reported in clinical HAdV isolates from cidofovir treated HSCT recipients.<sup>210-213</sup> Possibly, inter-patient variations in cidofovir pharmacokinetics may have contributed to failure of cidofovir treatment as well. In view of the nephrotoxicity of cidofovir,<sup>53-56</sup> the observed treatment failures emphasize the need for new and less toxic pharmacological interventions like brincidofovir (CMX001), the orally bioavailable lipid conjugate of cidofovir<sup>61</sup> as well as adoptive immunotherapy based interventions<sup>205;209</sup> for patients with a delayed T cell reconstitution. The sensitive PCR methods used for the virological monitoring post HSCT carry the risk of overtreatment which might lead to avoidable toxicity.<sup>224;228</sup> Longitudinal monitoring of lymphocyte reconstitution can identify patients with better odds on a favorable outcome of HAdV viremia. Indeed, the presence of even a low number of T cells ( $\geq 50$  cells/ $\mu$ l) in patients without steroid treatment was associated with a rapid HAdV load reduction. The frequent monitoring of T cell reconstitution can be a valuable tool to prevent the unnecessary installment or continuation of cidofovir treatment. A comparable approach has already been applied successfully in the management of cytomegalovirus and Epstein-Barr virus infections post HSCT.<sup>39;229</sup> Altogether, a subgroup of patients with HAdV viremia post HSCT might benefit from cidofovir treatment through a stabilization of the HAdV load pending lymphocyte reconstitution. Nevertheless, T cell reconstitution remains essential for viral clearance. For clinical decision making, the combined monitoring of plasma HAdV DNA levels and lymphocyte reconstitution provides an objective tool for the guidance of personalized antiviral treatment and to prevent the unnecessary exposure to cidofovir.

## Funding and Disclosures

GL was supported by a Leiden University Medical Center MD/PhD fellowship  
All authors declare that no potential conflicts of interest exist.

**Table 4.2 (previous page). Details of human adenovirus viremia, cidofovir treatment, lymphocyte reconstitution and HAdV load dynamics.**

Treatments are ordered based on T cell reconstitution and HAdV load change. Abbreviations: UPN: Unique Patient Number, decimal: 1st, 2nd or 3th HSCT, letter: 1st (a) or 2nd (b): cidofovir treatment episode. HAdV: Human Adenovirus, n.a.: not applicable, ? : not analyzed, CDV: cidofovir. <sup>1</sup>Days after hematopoietic stem cell transplantation (HSCT). <sup>2</sup>Plasma HAdV DNA levels in log copies/ml. <sup>3</sup>Days from start cidofovir treatment. <sup>4</sup>T cell numbers in peripheral blood  $\geq 50$  cells/ $\mu$ l within 14 days after treatment initiation. <sup>5</sup> $\geq 5$  fold expansion of NK cell number in peripheral blood. <sup>6</sup>Prednisone  $\geq 1$  mg/kg body weight during cidofovir treatment. <sup>7</sup>Reduction (↓) / Increase (↑): plasma HAdV DNA levels changed  $\geq 1$  log c/ml after initiation of cidofovir treatment. Stabilization (=):  $< 1$  log c/ml change of HAdV load. Clearance (c): plasma HAdV DNA levels below lower limit of detection at 2 consecutive time points. <sup>8</sup>Follow-up was stopped at 1 week after the last dose of cidofovir or 1 week before T cell numbers reached 50 cells/ $\mu$ l.



## Supplemental Data

### Supplemental Methods

#### Patient inclusion

During post-transplant follow up, HAdV DNA was detected in plasma at least once in 111 out of 363 transplantations (31%) and the HAdV load reached 3 log c/ml at two consecutive time points after 40 transplantations (11%, disseminated HAdV viremia). In general, cidofovir was initiated when the HAdV load reached 3 log c/ml at two consecutive time points.<sup>41</sup> Patients treated with cidofovir after two different HSCT procedures (n=2, UPN 515 and 648) were regarded as separate HSCT recipients. Of 40 patients with a disseminated HAdV viremia, five were not treated because of a palliative setting (n=3) or a stable HAdV load (n=2).

Thirty-two out of 35 cidofovir treated disseminated HAdV viremias were evaluable: one patient died of pre-existent neurodegenerative disease within the first two weeks of treatment and from two patients, no follow up of HAdV load was available. Additionally, in 4 patients, cidofovir was initiated for HAdV viremia with a HAdV load <3 log c/ml, adding up to 36 patients. Six patients received two separate cidofovir treatment episodes for the same HAdV viremia and were analyzed twice. Cidofovir treatment was discontinued for at least 2 weeks between two treatment episodes. In total, 42 cidofovir treatment episodes were analyzed (Table 4.2 and S1).

#### Flow cytometry

Peripheral blood mononuclear cells (PBMC) were separated using ficoll-isopaque density gradient centrifugation (LUMC Pharmacy, Leiden, NL), washed twice and resuspended in RPMI cell culture medium (PAA Laboratories, Pasching, AT), supplemented with Human Serum Albumin (HSA, 0.8 mg/ml, Sanquin, Amsterdam, NL) and penicillin/streptomycin (P/S, 100 U/ml and 100 µg/ml, Lonza, Verviers, BE). Red cell lysis buffer (LUMC Pharmacy) was added to the cells and after 10 minutes incubation at room temperature, PBMC were washed and resuspended in FACS buffer (Phosphate Buffered Saline (Braun, Melsungen, GE) containing 10 mg/ml Bovine Serum Albumin (Sigma-Aldrich, St. Louis, MO, US) and 3 mM Ethylenediaminetetraacetic Acid (Merck, Darmstadt, GE). Cells were stained for 30 minutes at 4°C with the antibodies listed in Table 4.S3 at their optimal concentration. Four-color flow cytometry was performed on a BD FACS Calibur II flow cytometer (Becton Dickinson Biosciences (BD), Franklin Lakes, NJ, US) and data were analyzed using BD Cellquest software.

Patient Characteristics			HSCT characteristics								
UPN	Age (year)	Sex	HSCT indication	Donor Type	Graft Source	Graft Manip.	Conditioning	Serotherapy	aGVHD prophylaxis	aGvHD	Cidofovir treatments
514.3	13.7	M	SAA	IRD	BM	-	RIC	Alemtuzumab	CSA/MTX	-	1
515.1	3.6	M	WAS	MUD	PBSC	TCD	RIC	Alemtuzumab	CSA	-	1
515.2	4.5	M	WAS	MUD	PBSC	-	RIC	Alemtuzumab	CSA/MTX	-	1
543.1	4.7	F	AML	MUD	PBSC	TCD	MA	Alemtuzumab	CSA/MTX	-	2
545.1	2.3	M	JMML	MUD	BM	-	MA	ATG	CSA/MTX	-	2
549.1	1.2	F	MDS	MUD	BM	TCD	MA	ATG	CSA	-	1
551.1	17.8	M	ALL	ORD	PBSC	TCD	MA	Alemtuzumab	-	-	1
554.2	10.6	F	ALL	MUD	BM	-	MA	ATG	CSA/MTX	-	1
555.1	0.5	M	SCID-OS	ORD	BM	-	RIC	Alemtuzumab	CSA/MTX	-	1
558.1	13.2	M	β-Thalass.	MUD	BM	-	MA	Alemtuzumab	CSA/MTX	-	1
560.1	7.6	M	FA	MUD	CB	-	MA	Alemtuzumab	CSA/Pred	-	1
586.1	15.1	M	AML	MUD	BM	-	MA	ATG	CSA/MTX	Grade II	1
587.1	13.2	F	LAD-1/var.	MUD	PBSC	-	RIC	Alemtuzumab	CSA/MMF	-	1
594.1	1.7	M	WAS	MUD	CB	-	MA	ATG	CSA/Pred	-	2
597.1	1.3	F	JMML	MUD	CB	-	MA	ATG	CSA/Pred	Grade III	1
600.1	6.3	F	AML	MUD	CB	-	MA	ATG	CSA/Pred	-	2
613.1	4.1	F	MDS	MUD	CB	-	MA	ATG	CSA/Pred	Grade III	1
616.1	3.4	M	β-Thalass.	ORD	PBSC	TCD	MA	Alemtuzumab	CSA	-	1
625.2	2.2	F	β-Thalass.	IRD	BM	-	MA	ATG	CSA/MTX	-	1
634.1	16.6	F	β-Thalass.	ORD	PBSC	TCD	MA	Alemtuzumab	CSA/MMF	-	1
648.1	1.9	M	HLH	MUD	CB	-	MA	ATG	CSA/Pred	-	1
648.2	2.4	M	HLH	ORD	PBSC	TCD	MA	ATG	-	-	1
671.1	10.2	F	CID	MUD	CB	-	MA	ATG	CSA/Pred	Grade III	1
681.1	3.5	F	β-Thalass.	MUD	BM	-	MA	ATG	CSA/MTX	-	2
686.2	7.3	M	AML	ORD	PBSC	TCD	MA	ATG	-	-	1
697.1	3.1	M	AML	MUD	BM	-	MA	ATG	CSA/MTX	-	1
719.1	2.1	M	ALL	MUD	BM	-	MA	ATG	CSA/MTX	-	1
721.1	4.4	M	SAA/DKC	MUD	CB	-	MA	ATG	CSA/Pred	-	1
732.1	3.9	M	β-Thalass.	MUD	BM	-	MA	ATG	CSA/MTX	Grade II	1
787.1	4.5	M	ALL	MUD	CB	-	MA	ATG	CSA/Pred	-	2
799.1	8.1	F	SAA	ORD	PBSC	TCD	MA	Alemtuzumab	-	-	1
804.1	1.1	M	β-Thalass.	MUD	BM	-	MA	ATG	CSA/MTX	-	1
808.1	17.8	M	MDS	MUD	BM	-	MA	Alemtuzumab	CSA/MTX	-	1
816.1	7.6	M	AML	MUD	BM	-	MA	ATG	CSA/MTX	-	1
817.1	14.7	M	AML	MUD	BM	-	MA	ATG	CSA/MTX	-	1
823.1	7.3	F	BMF	MUD	BM	-	RIC	ATG	CSA/MTX	-	1

**Table 4.S1. Patient characteristics**

Abbreviations: UPN: Unique Patient Number, decimal: 1st, 2nd or 3th transplantation M: Male, F: Female. ALL: Acute Lymphoid Leukemia, AML: Acute Myeloid Leukemia, β-Thalass.: β-Thalassemia major, BMF: Bone Marrow Failure, CID: Combined Immunodeficiency, DKC: Dyskeratosis Congenita, FA: Fanconi Anemia, HLH: Hemophagocytic Lymphohistiocytosis, JMML: Juvenile Myelomonocytic Leukemia, LAD-1/Var.: Leukocyte Adhesion Deficiency 1 / Variant, MDS: Myelodysplastic Syndrome, OS: Omenn Syndrome, SAA: Severe Aplastic Anemia, SCID: Severe Combined Immunodeficiency, WAS: Wiskott-Aldrich Syndrome. HSCT: Hematopoietic Stem Cell Transplantation, MUD: Matched Unrelated Donor, IRD: Identical Related Donor, ORD: Other Related Donor, BM: Bone marrow, CB: Cord blood, PBSC: Peripheral Blood Stem Cells, TCD: T cell depletion of the graft. RIC: Reduced Intensity Conditioning, MA: Myeloablative conditioning. ATG: Anti-Thymocyte Globulin, CSA: Cyclosporin A, MMF: Mycophenolate Mofetil, MTX: Methotrexate, Pred: Prednisone, aGvHD: acute Graft-versus-Host-Disease.



		T cells < 50 (n=20)		T cells ≥ 50 (n=22)		p-value
		n / median	% / range	n / median	% / range	
Age (year)		<b>4.3</b>	0.5 - 18	<b>4.5</b>	1.1 - 17	0.55
HSCT indication	Primary Immunodeficiency	<b>2</b>	10%	<b>7</b>	32%	0.18
	Benign Hematological Disorder	<b>8</b>	40%	<b>5</b>	23%	
	Hematological Malignancy	<b>10</b>	50%	<b>10</b>	46%	
Conditioning	Reduced Intensity	<b>2</b>	10%	<b>4</b>	18%	0.45
	Myeloablative	<b>18</b>	90%	<b>18</b>	82%	
Donor Type	Identical Related Donor	<b>2</b>	10%	<b>0</b>	0%	0.26
	Other Related Donor	<b>5</b>	25%	<b>2</b>	9%	
	Matched Unrelated Donor	<b>13</b>	65%	<b>20</b>	91%	
Graft Source	Bone Marrow, T cell replete	<b>9</b>	45%	<b>9</b>	41%	0.26
	Bone Marrow, T cell depleted	<b>1</b>	5%	<b>0</b>	0%	
	PBSC, T cell replete	<b>0</b>	0%	<b>2</b>	9%	
	PBSC, T cell depleted	<b>6</b>	30%	<b>3</b>	14%	
	Cord Blood	<b>4</b>	20%	<b>8</b>	36%	
Serotherapy	Anti-thymocyte globulin	<b>11</b>	55%	<b>17</b>	77%	0.13
	Alemtuzumab	<b>9</b>	45%	<b>5</b>	23%	
GvHD prophylaxis	None	<b>3</b>	15%	<b>1</b>	5%	0.33
	CyclosporinA	<b>2</b>	10%	<b>1</b>	5%	
	CyclosporinA + Methotrexate	<b>11</b>	55%	<b>10</b>	46%	
	CyclosporinA + Methylprednisolone	<b>4</b>	20%	<b>8</b>	36%	
	CyclosporinA + MMF	<b>0</b>	0%	<b>2</b>	9%	
Acute Graft versus Host Disease ≥ grade II		<b>1</b>	5%	<b>4</b>	18%	0.19
Cidofovir treatment	First episode	<b>18</b>	90%	<b>18</b>	82%	0.45
	Second episode	<b>2</b>	10%	<b>4</b>	18%	
First day HAAdV load >1.71 log c/mL <sup>1</sup> (n=36 1st episodes)		<b>20</b>	5 - 70	<b>19</b>	3 - 96	0.73
First day HAAdV load 2x>3 log c/mL <sup>1</sup> (n=36 1st episodes)		<b>30</b>	8 - 75	<b>23</b>	10 - 117	0.84
First day of first cidofovir treatment <sup>1</sup> (n=36 1st episodes)		<b>30</b>	7 - 78	<b>23</b>	8 - 121	0.61
Day start cidofovir <sup>1</sup>		<b>31</b>	7 - 78	<b>32</b>	8 - 214	0.71
HAAdV load at start (Log c / mL)		<b>3.9</b>	2.1 - 5.9	<b>4.2</b>	1.7 - 6.5	0.72
Peak HAAdV load in period day -7 to +14 from start treatment		<b>4.6</b>	2.7 - 6.8	<b>4.7</b>	2.4 - 6.9	0.68
Treatment duration (days)		<b>24</b>	7 - 64	<b>15</b>	1 - 99	0.78

**Table 4.S2. Patient characteristics of treatments with <50 and ≥ 50 T cells/ μl 14 days after start cidofovir**

Abbreviations: HAAdV: human adenovirus, HSCT: hematopoietic stem cell transplantation, PBSC: peripheral blood stem cells, GvHD: graft-versus-host disease, MMF: mycophenolate mofetil, HAAdV/MOF: HAAdV related multi-organ failure. HAAdV load: plasma HAAdV DNA level. <sup>1</sup>: day post HSCT. Categorical data: number (percentage). Numerical data: median (range). *p*-values: Pearson's Chi Square test (categorical data) or Mann-Whitney U test (numerical data) comparing the two groups.

Type	Antibody	Fluorochrome	Clone	Supplier
<i>Lymphocyte gate</i>	<b>CD45</b>	FITC	2D1	BD
	<b>CD14</b>	PE	MOP9	BD
	<b>CD33</b>	PE	P67.6	BD
	<b>CD235a</b>	PE	11E4B-7-6	BC
<i>Lymphocyte subsets</i>	<b>CD3</b>	PerCP-Cy5.5	SK7	BD
	<b>CD19</b>	APC	J4.119	BC
	<b>CD56</b>	APC	N901	BC

**Table 4.S3. Antibodies used for flowcytometry**

FITC: Fluorescein isothiocyanate, PE: phycoerythrin, PERCP: Peridinin chlorophyll, Cy: Cyanine, APC: Allophycocyanin, BD: Becton Dickinson Biosciences, Franklin Lakes, NJ, US, BC: Beckman Coulter, Brea, CA, US,

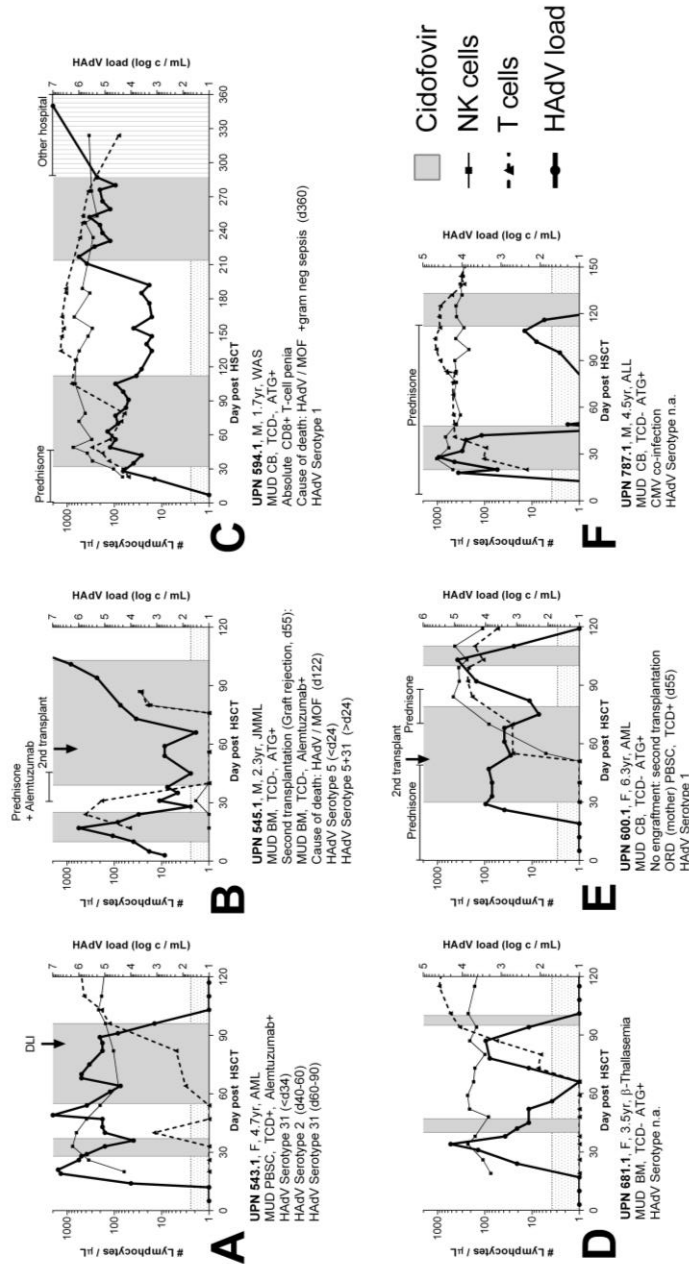


**Figure 4.S1. HAAdV load dynamics in 6 patients who received two cidofovir treatment episodes.**

Plasma human adenovirus DNA levels (HAAdV load, bold lines, right Y-axis) are plotted as a function of time post HSCT (days, X-axis). T cell numbers (interrupted lines) and NK cell numbers (solid lines) are plotted on the left Y-axis. Gray shaded area: Cidofovir treatment episodes. Abbreviations: UPN: Unique Patient Number, decimal: 1st, 2nd or 3th transplantation M: Male, F: Female. Yr: Year. ALL: Acute Lymphoid Leukemia, AML: Acute Myeloid Leukemia,  $\beta$ -Thalass.:  $\beta$ -Thalassemia major, JMML: Juvenile Myelomonocytic Leukemia, WAS: Wiskott-Aldrich Syndrome. MUD: Matched Unrelated Donor, BM: Bone marrow, CB: Cord blood, PBSC: Peripheral Blood Stem Cells, TCD: T cell depletion of the graft. ATG: Anti-Thymocyte Globulin, DLI: donor lymphocyte infusion. N.A.: not available.



# Chapter 5

## CD56<sup>dim</sup>CD16<sup>-</sup> NK cell phenotype can be induced by cryopreservation

Published in:

Blood

2015; 125: 1842-1843

Gertjan Lugthart

Monique M. van Ostaijen-ten Dam

Maarten J.D. van Tol

Arjan C. Lankester *and*

Marco W. Schilham

## **Abstract**

Early after hematopoietic stem cell transplantation, NK cells are temporary susceptible to cryopreservation-induced phenotypic changes. This emphasizes the importance to validate flowcytometric results with fresh PBMC samples to become aware of potential situation-specific cryopreservation-induced phenotypic changes.

*To the editor:*

Natural Killer (NK) cells can contribute to the control of different viruses.<sup>218;219</sup> Recently, Azzi and colleagues described the role of early-differentiated NK cells in Epstein-Barr virus driven infectious mononucleosis (IM).<sup>121</sup> Besides the conventional CD56<sup>bright</sup>CD16<sup>+/-</sup> and CD56<sup>dim</sup>CD16<sup>+</sup> NK cell populations, a phenotypically distinct CD56<sup>dim</sup>CD16<sup>-</sup> NK cell population was transiently observed during acute IM.

We have also observed this CD56<sup>dim</sup>CD16<sup>-</sup> NK cell phenotype in cryopreserved PBMC from hematopoietic stem cell transplantation (HSCT) recipients, especially early after transplantation. However, only the conventional CD56<sup>bright</sup>CD16<sup>+/-</sup> and CD56<sup>dim</sup>CD16<sup>+</sup> NK cells were detected in freshly analyzed PBMC, indicating that the CD56<sup>dim</sup>CD16<sup>-</sup> phenotype is induced by cryopreservation (Figure 5.1A).

Blood samples were obtained from 9 pediatric HSCT recipients and 4 healthy donors after written informed consent and approval by the institutional review board (protocol P02.099). PBMC were isolated using ficoll-isopaque separation within 6h after blood withdrawal and analyzed by flowcytometry. The remainder of cells was cryopreserved in liquid nitrogen, thawed and reanalyzed. NK cells were defined as CD19<sup>-</sup>CD3<sup>+</sup>CD7<sup>+</sup>CD56<sup>+/16<sup>+/-</sup></sup> cells within the live (DAPI) CD45<sup>+</sup> CD14<sup>-</sup>CD33<sup>-</sup>CD235a<sup>-</sup> lymphocyte gate.<sup>230</sup>

In fresh PBMC, CD56<sup>dim</sup>CD16<sup>-</sup> cells constituted <3% of NK cells, mainly caused by overspill from CD56<sup>bright</sup>CD16<sup>+/-</sup> or CD56<sup>dim</sup>CD16<sup>+</sup> NK cells.<sup>105;231</sup> In contrast, CD56<sup>dim</sup>CD16<sup>-</sup> cells represented a larger and distinct population in cryopreserved PBMC (Figure 5.1 A-B). These cells accounted for 17-36% of cryopreserved NK cells at 3 weeks after HSCT (fresh vs. cryopreserved:  $p < 0.001$ , paired t-test), rapidly decreasing in the weeks thereafter (Figure 5.1 C-D). This CD56<sup>dim</sup>CD16<sup>-</sup> NK cell population was identified with various monoclonal antibodies (CD56-clones N901/HCD56; CD16-clones 3G8/B73.1). Interestingly, the cryopreservation-induced CD56<sup>dim</sup>CD16<sup>-</sup> population was also enlarged when healthy donor blood was stored for 24h at room temperature before PBMC were isolated (Figure 5.1E), suggesting a relationship with the vitality of PBMC prior to cryopreservation.<sup>232;233</sup>

We hypothesized that the cryopreservation induced CD56<sup>dim</sup>CD16<sup>-</sup> NK cells originated from either CD56<sup>bright</sup>CD16<sup>+/-</sup> or CD56<sup>dim</sup>CD16<sup>+</sup> NK cells as a consequence of reduced CD56 or CD16 expression, respectively. At three weeks after HSCT, predominantly the largest CD56<sup>bright</sup>CD16<sup>+/-</sup> NK cell population was decreased after cryopreservation (mean 67 to 46% of NK cells,  $p = 0.002$ ), coinciding with the appearance of the CD56<sup>dim</sup>CD16<sup>-</sup> phenotype. One week later, both a reduction of CD56<sup>bright</sup>CD16<sup>+/-</sup> (45 to 36%,  $p = 0.01$ ) and CD56<sup>dim</sup>CD16<sup>+</sup> (54 to 41%,  $p = 0.01$ ) NK cells was observed. At one year after HSCT and in healthy donors, CD56<sup>dim</sup>CD16<sup>+</sup> NK cells formed the majority of NK cells and mainly this phenotype was reduced after cryopreservation (Figure 5.1 C-E). Thus, depending on time after HSCT, both CD56<sup>bright</sup>CD16<sup>+/-</sup> and CD56<sup>dim</sup>CD16<sup>+</sup> NK cells could contribute to the CD56<sup>bright</sup>CD16<sup>+/-</sup> phenotype.

A skewing towards the early-differentiated NKG2A<sup>+</sup>KIR<sup>-</sup> NK cell phenotype is observed early after HSCT as well as during acute IM<sup>121;126</sup>, raising the possibility that these cells might be particularly sensitive to cryopreservation. However, the presence of NKG2A<sup>+</sup>KIR<sup>-</sup> NK cells and occurrence of CD56<sup>dim</sup>CD16<sup>-</sup> NK cells showed different kinetics (Figure 5.1 F-G). In multivariate

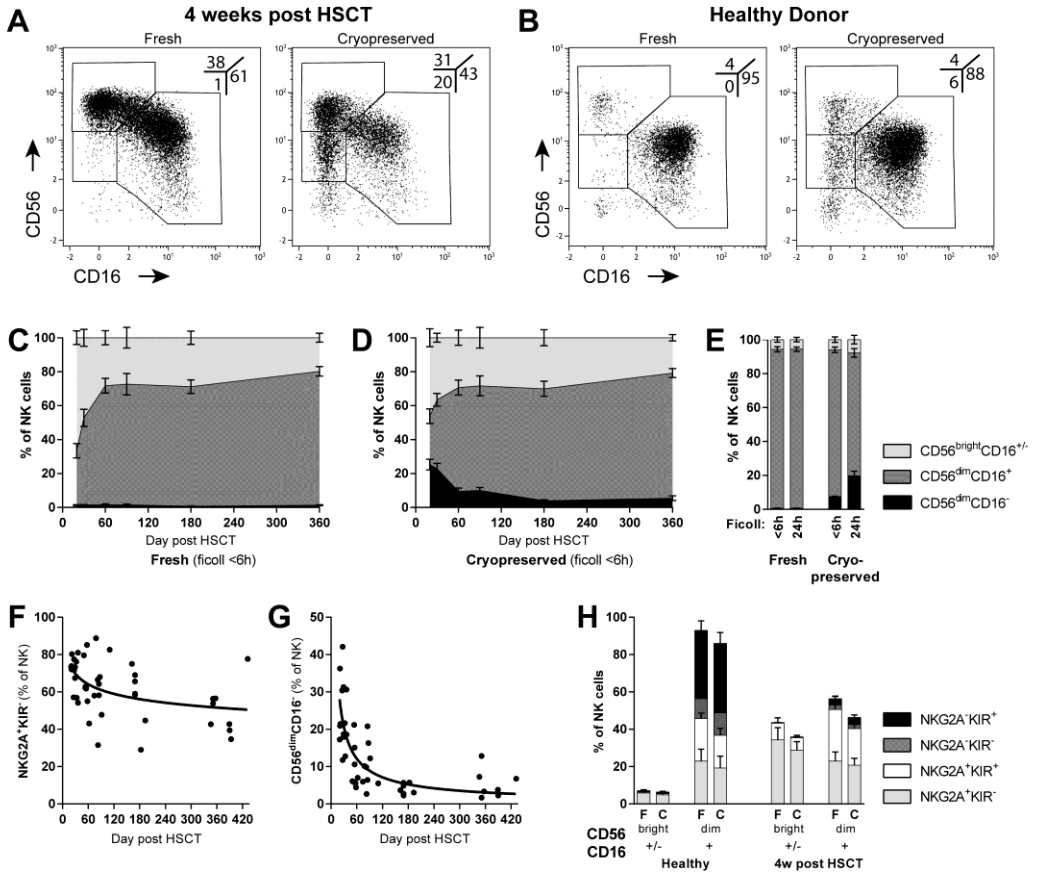


**Figure 5.1. CD56<sup>dim</sup>CD16<sup>-</sup> NK cell phenotype can be induced by cryopreservation.**

(A-B) Representative FACS plots of fresh and cryopreserved NK cells from hematopoietic stem cell transplantation (HSCT) recipients at 4 weeks after transplantation (A) and healthy donors (B). (C-D) Longitudinal NK cell reconstitution in 9 HSCT recipients based on the paired evaluation of fresh (C) and cryopreserved (D) PBMC. Shown is the contribution (mean  $\pm$  SEM) of CD56<sup>bright</sup>CD16<sup>+/-</sup> (light gray), CD56<sup>dim</sup>CD16<sup>+</sup> (dark gray) and CD56<sup>dim</sup>CD16<sup>-</sup> cells (black) to the NK cell compartment. (E) Evaluation of fresh (left) and cryopreserved (right) NK cells after direct (<6h) or delayed (24h) separation of PBMC from EDTA blood. Shown is the mean  $\pm$  SEM of 4 healthy donors. (F-G) Contribution of early-differentiated NKG2A<sup>+</sup>KIR<sup>-</sup> NK cells (F) and cryopreservation-induced CD56<sup>dim</sup>CD16<sup>-</sup> NK cells (G) to the total NK cell population, expressed as a function of time after HSCT. (H) Differentiation of NK cells based on the expression of NKG2A and KIRs on NK cells in fresh (F) and cryopreserved (C) PBMC. Shown is the percentage of NKG2A<sup>+</sup>KIR<sup>-</sup> (light gray), NKG2A<sup>+</sup>KIR<sup>+</sup> (white), NKG2A<sup>-</sup>KIR<sup>+</sup> (dark gray) and NKG2A<sup>-</sup>KIR<sup>-</sup> (black) NK cells divided over the CD56<sup>bright</sup>CD16<sup>+/-</sup> and CD56<sup>dim</sup>CD16<sup>+</sup> NK cell phenotypes. Bars represent mean  $\pm$  SEM of 4 healthy donors or 2 HSCT recipients at 4 weeks after transplantation.

analysis, the percentage of CD56<sup>dim</sup>CD16<sup>-</sup> cells was only correlated with time after HSCT and not to the percentage of NKG2A<sup>+</sup>KIR<sup>-</sup> cells ( $p < 0.0001$  vs.  $p = 0.35$ , linear regression on log-transformed data). Importantly, no significant differences were observed between the NKG2A/KIR phenotype of CD56<sup>dim</sup>CD16<sup>+</sup> and CD56<sup>bright</sup>CD16<sup>+/-</sup> NK cells when analyzed before and after cryopreservation (Figure 5.1H).



Altogether, NK cells are temporarily more sensitive to cryopreservation-induced phenotype changes in the first weeks after HSCT. This might relate to the CD56<sup>dim</sup>CD16<sup>-</sup> NK cell phenotype which was transiently observed during the acute phase of IM.<sup>121</sup> Both during acute IM and early after HSCT, CD56<sup>dim</sup>CD16<sup>-</sup> NK cells are observed under inflammatory conditions. This raises the possibility that cryopreservation-induced phenotypic changes are related to activation-associated cellular mechanisms.

Clinical situations like the absence of T cells after HSCT or viral infections provide unique opportunities to study human NK cell biology. It should be taken into account that under such circumstances, NK cells may be transiently susceptible to cryopreservation-induced phenotype changes. Since the CD56<sup>dim</sup>CD16<sup>-</sup> NK cells can originate from both conventional NK cell populations, we recommend to assess the cryopreservation-induced CD56<sup>dim</sup>CD16<sup>-</sup> NK cells separately to avoid phenotype-skewing of the conventional populations. Our data emphasize the importance to validate flowcytometric results with fresh PBMC samples to become aware of potential cryopreservation-induced phenotypic changes.

## Funding and Disclosures

This work was supported by the Dutch Cancer Society (grant UL-2011-5133). GL was supported by a Leiden University Medical Center MD/PhD fellowship.

## Gating strategy

FACS-data were acquired on a Becton Dickinson (BD) LSRII flow cytometer and analyzed using Beckman Coulter (BC) Kaluza software.

Gating strategy (Figure 5.1 A-E, G): Forward scatter vs. DAPI(*Sigma-Aldrich*): live → CD45<sup>+</sup>(FITC, *clone 2D1, BD*) vs. CD14(PE, *MOP9, BD*) & CD33(PE, *P67.6, BD*) & CD235a(PE, *KC16, BC*) → CD19(APC, *J4.119, BC*) → CD3(BrilliantViolet421, *UCHT1, BD*) vs. CD7<sup>+</sup>(Alexa700, *M-T701, BD*) → CD56(PE-Texas Red, *N901, BC*) vs. CD16(BV711, *3G8, BD*).

Gating strategy (Figure 5.1 F & H): Forward scatter vs DAPI(*Sigma-Aldrich*): live → CD14(APC, *MOP9, BD*) & CD19<sup>-</sup>(APC, *J4.119, BC*) → CD3(BrilliantViolet421, *UCHT1, BD*) vs. CD7<sup>+</sup>(Alexa700, *M-T701, BD*) → CD56(PE-Texas Red, *N901, BC*) vs. CD16(BV711, *3G8, BD*) → NKG2A (PE-Cy7, *Z199, BC*) vs. KIR (PE, combination of CD158e + a/h + i + b/j (*DX9, BD + EB6, BC + FES172, BC + GL183, BC*)).



# Chapter 6

## Expansion of cytotoxic CD56<sup>bright</sup> NK cells during T cell deficiency after allogeneic hematopoietic stem cell transplantation

Published in:

Journal of Allergy and Clinical Immunology

2017; 140: 1466-1469

Gertjan Lugthart

Marieke Goedhart

Merle M. van Leeuwen

Janine E. Melsen

Cornelia M. Jol-van der Zijde

Carly Vervat

Monique M. van Ostaijen-ten Dam

Anja M. Jansen-Hoogendijk

Maarten J.D. van Tol

Arjan C. Lankester *and*

Marco W. Schilham

## **Abstract**

We describe a compensatory expansion of activated cytotoxic CD56<sup>bright</sup> NK cells during T-cell deficiency after hematopoietic stem cell transplantation. This mimics the situation in severe inborn T-cell deficiencies and unmasks the functional and phenotypic versatility of NK cells.

To the editor:

Cytokine-producing, non-cytotoxic  $CD56^{\text{bright}}CD16^{\text{+/-}}$  ( $CD56^{\text{bright}}$ ) NK cells constitute a minor population of NK cells in blood of healthy individuals.<sup>87;95;97</sup> Both early after hematopoietic stem cell transplantation (HSCT) and in patients with severe inborn T-cell deficiencies, NK cells are skewed towards the  $CD56^{\text{bright}}$  NK cell phenotype.<sup>126;127;216;234</sup> These clinical situations are marked by the absence of T-cells. The role of NK cells in immunity may normally be overshadowed by the presence of T cells. Therefore, transient T-cell deficiency after HSCT provides an opportunity to unveil compensatory adaptations in the  $CD56^{\text{bright}}$  NK cell compartment.

We evaluated the reconstitution of T and NK cells in ninety-three pediatric acute leukemia patients who received an HSCT from a matched-unrelated donor (MUD) or HLA-identical related donor (IRD). See Supplemental Data for methods and cohort description. Delayed T-cell reconstitution was defined as  $<100$  T-cells/ $\mu\text{l}$  at four weeks after HSCT and occurred in 33 patients (35%). In patients with a delayed T-cell reconstitution,  $CD56^{\text{bright}}$  NK cells expanded to high numbers, reaching median 320 cells/ $\mu\text{l}$  (range 5-1255) at four weeks after HSCT. In contrast,

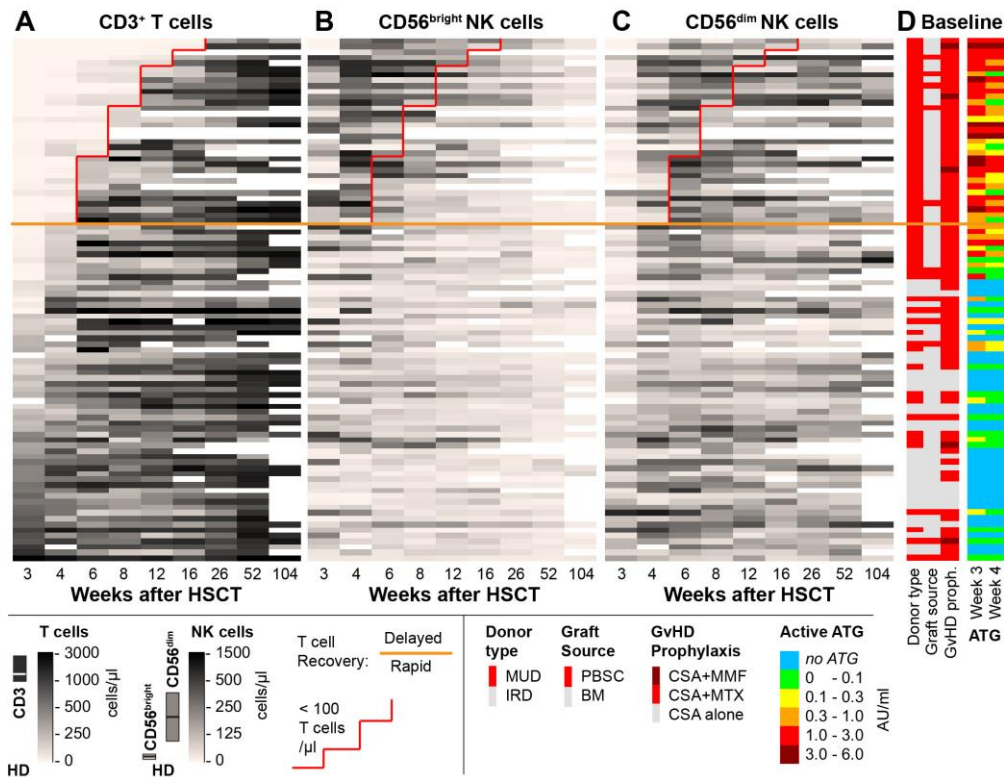


**Figure 6.1. Expansion of  $CD56^{\text{bright}}$  NK cells in patients with delayed T-cell reconstitution.**

(A-C) Reconstitution of T-cells (A),  $CD56^{\text{bright}}$  (B) and  $CD56^{\text{dim}}$  NK cells (C) in 93 HSCT recipients. Each row represents a patient. Patients were sorted by T-cell reconstitution. HD values are shown in legend.

(D) Side bars displaying donor type, graft source, graft versus host (GvHD) prophylaxis and active (T-cell binding) ATG concentration. Abbreviations: PBSC: peripheral blood stem cells, BM: bone marrow, CSA: cyclosporin A, MTX: methotrexate, MMF: mycophenolate mofetil, AU: arbitrary units.

this strong expansion of CD56<sup>bright</sup> NK cells was only observed in a minority of patients with a rapid T-cell reconstitution (Figure 6.1B and Figure 6.S1A). CD56<sup>bright</sup> NK cell numbers remained high until T-cell reconstitution occurred, as demonstrated by inverse log-linear correlation between T-cell numbers and CD56<sup>bright</sup> NK cell numbers at 4, 8, 12 and 16 weeks after HSCT (Figure 6.1A-B and Figure 6.S1B). The skewing towards CD56<sup>bright</sup> NK cells after HSCT is often used to support the hypothesis that CD56<sup>bright</sup> NK cells are the precursors of CD56<sup>dim</sup> NK cells. However, recovery of CD56<sup>dim</sup> NK cells after HSCT was independent of T-cell reconstitution (Figure 6.1C and Figure 6.S1A,C), arguing against a sequential reconstitution of CD56<sup>bright</sup> and CD56<sup>dim</sup> NK cells.

We compared patients with >300 CD56<sup>bright</sup> NK cells/ $\mu$ l in the first 3-6 weeks after HSCT (n=38) to those without CD56<sup>bright</sup> NK cell expansion (<300 CD56<sup>bright</sup> NK cells/ $\mu$ l, n=55) to study the correlation with various other HSCT parameters. In multivariate analysis, CD56<sup>bright</sup> NK cell expansion was only correlated with the use of anti-thymocyte globulin (ATG) serotherapy (overlapping with MUD donors,  $p < 0.001$ ) and the absence of T-cells at four weeks after transplantation ( $p = 0.002$ , Table 6.S1). Because ATG serotherapy leads to delayed T-cell reconstitution<sup>30,33</sup>, we conclude that delayed T-cell reconstitution represents the main determinant of the expansion of CD56<sup>bright</sup> NK cells.

Next, we measured the longitudinal expression of 34 chemokine-receptors, adhesion-molecules and NK cell markers on CD56<sup>bright</sup> NK cells from HSCT recipients (n=20) and healthy donors (HD, n=16). *t*-SNE analysis visualizing these phenotypic data revealed that CD56<sup>bright</sup> NK cells at 3-4 weeks after HSCT differed from CD56<sup>bright</sup> NK cells in steady state conditions (Figure 6.2A-B). Post-transplant CD56<sup>bright</sup> NK cells had a significantly increased expression of inflammatory chemokine-receptors (CCR2, CCR5 and CX3CR1) and the skin-specific cutaneous lymphocyte antigen (CLA, Figure 6.2B and Figure 6.S2). CLA and CX3CR1 were transiently expressed, while other receptors remained high for weeks (CCR5) or months (CCR2). This suggests specific regulation of individual chemokine-receptor expression rather than a general activation of NK cells. Interestingly, post-transplant CD56<sup>bright</sup> NK cells had a reduced expression of the chemokine-receptors CCR7 and CXCR3, indicating reduced homing to lymphoid organs (Figure 6.2B). Together, these data emphasize that post-transplant CD56<sup>bright</sup> NK cells have adopted the phenotype of effector cells.

Post-transplant CD56<sup>bright</sup> NK cells lacked the early differentiation markers CD127 and CD27. A proportion of these cells expressed KIRs and CD57, late differentiation markers normally only expressed by CD56<sup>dim</sup> NK cells. This suggests that post-transplant CD56<sup>bright</sup> NK cells are more differentiated than HD CD56<sup>bright</sup> NK cells, although the expression of these markers can also be affected by *in vitro* activation.<sup>97,127</sup>

Conventional CD56<sup>bright</sup> NK cells are abundant cytokine producers but do not express granzyme B at rest, requiring pre-activation to obtain cytolytic potential.<sup>87,95</sup> The IFN- $\gamma$  and TNF- $\alpha$  production and perforin expression of NK cells early after HSCT was comparable to healthy donors (Figure 6.2C and E3).<sup>126,127</sup> However, post-transplant CD56<sup>bright</sup> NK cells expressed granzyme B at rest (94 vs 15% (HD),  $p = 0.002$ , Figure 6.2D). Accordingly, they were cytotoxic without pre-activation. Their cytotoxicity was comparable to NK cells from three or more months after HSCT and healthy donors, both containing predominantly CD56<sup>dim</sup> NK cells (Figure 6.2E).

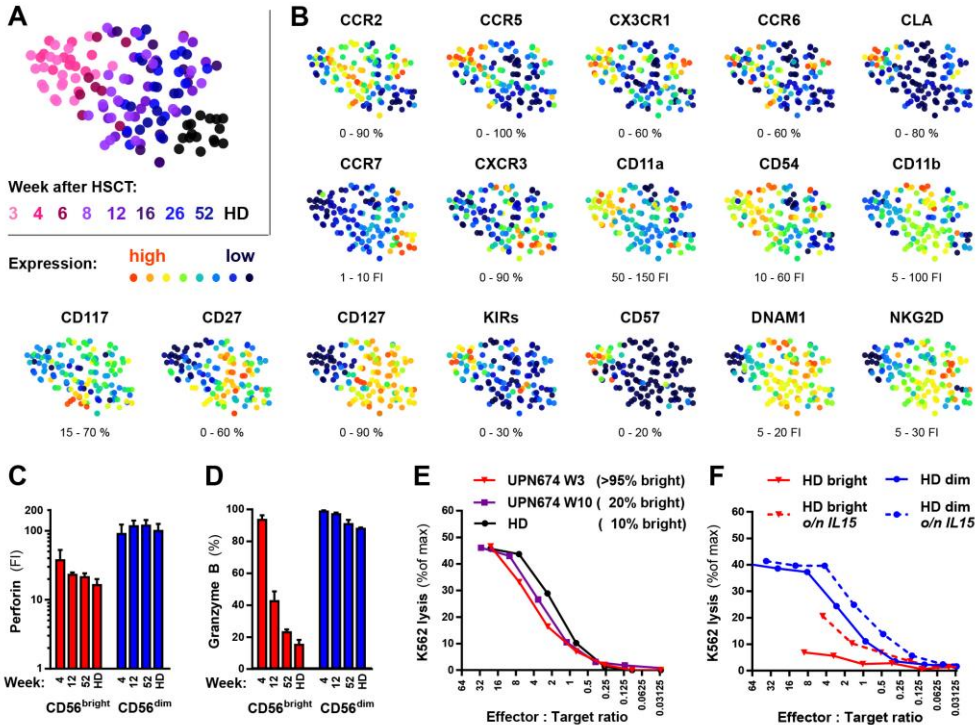


**Figure 6.2. Phenotype and function of CD56<sup>bright</sup> NK cells after HSCT**

(A-B) *t*-SNE analysis of the expression of 34 cell-surface markers on CD56<sup>bright</sup> NK cells in 134 samples from 20 HSCT recipients and 16 HD. Distance between dots indicates the difference in phenotype. Plots are colored by time after HSCT (A) and marker-expression (B). Range: percentage or fluorescence-intensity (FI). For gating strategy and non-depicted markers: see Supplemental Data.

(C-D) Intracellular expression of granzyme B and perforin in NK cells at 4, 12 and 52 weeks after HSCT (n=3) and HD (n=3). Bars: mean +/- SEM.

(E-F) Cytotoxicity of: (E) unmanipulated PBMC 3 and 10 weeks after HSCT and HD (Week 3: >95% CD56<sup>bright</sup>). (F) Resting and overnight IL15-activated FACS-purified HD NK cells. Representative graphs of three (E) and two (F) experiments.

In contrast, purified HD CD56<sup>bright</sup> NK cells were only cytotoxic after overnight activation with IL15 (Figure 6.2F). Together, the functional profile of post-transplant CD56<sup>bright</sup> NK cells corresponds with that of conventional, cytokine secreting CD56<sup>bright</sup> NK cells that have acquired cytolytic potential, most likely as result of *in vivo* activation.

Various studies have highlighted the inferior outcome of patients with a delayed T-cell reconstitution after ATG serotherapy.<sup>30;33</sup> In subgroup analysis, transplant-related mortality, leukemia-relapse and overall-survival were comparable between patients with rapid T-cell reconstitution (n=60) and patients with a delayed T-cell reconstitution but with CD56<sup>bright</sup> NK cell expansion (n=26, Table 6.S2). Only patients lacking both rapid T-cell reconstitution and CD56<sup>bright</sup> NK cells expansion (n=7) had a high mortality. This suggests that NK cells may be able to bridge the T-cell deficient period after HSCT.

The expansion of activated CD56<sup>bright</sup> NK cells with increased effector characteristics in the setting of T-cell deficiency could be elicited by infectious or non-infectious inflammatory triggers. In view of the role of NK cells in antiviral immunity, it is possible that the expansion of CD56<sup>bright</sup> NK cells is driven by viral infections which frequently occur in the T-cell deficient period after HSCT.

Our data are in line with the reported observations in patients with severe inborn or acquired T-cell deficiencies. In patients with RAG and ARTEMIS deficiencies, an increased proportion of NK cells had the CD56<sup>bright</sup> phenotype, and these cells degranulated strongly upon coculture with K562.<sup>235</sup> In HIV patients, an inverse correlation between CD4<sup>+</sup> T-cell numbers and CD56<sup>bright</sup> NK cells was observed. These cells also had a reduced expression of CCR7 and an increased expression of granzyme B.<sup>236</sup>

Together with the changes in the NK cell compartment in other T-cell deficient situations, our data demonstrate that CD56<sup>bright</sup> NK cells form a versatile cell population which can expand and acquire additional effector functions in the absence of T-cells. The reactive changes in the NK cell compartment may represent a compensatory response of NK cells to inflammatory or infectious triggers when T-cells are not present to exert their function. The setting of T-cell deficiency provides a unique opportunity to further study the biology of human NK cells and their role in human disease.

## Acknowledgements

The authors thank Prof. dr. F. Koning, dept. of immunohematology and blood transfusion, LUMC, Leiden, the Netherlands for critical reading of the manuscript

## Funding and Disclosures

Research was financially supported with a grant from the Dutch Cancer Society (#UL 2011-5133). GL was supported by a Leiden University Medical Center MD/PhD fellowship.



## Supplemental data

### Supplemental Methods

#### Patients, blood samples and ethics statement

Between 1-1-2005 and 31-12-2014, 99 pediatric acute lymphoblastic leukemia (ALL) or acute myeloid leukemia (AML) patients received a bone marrow (BM) or peripheral blood stem cell (PBSC) graft from an identical related (IRD) or matched unrelated donor (MUD) after myeloablative conditioning in the Leiden University Medical Center. Only patients who received anti-thymocyte globulin (ATG, Thymoglobulin, Genzyme, Cambridge, MA, USA) or no serotherapy were evaluated (n=94). Patients were only included after their first transplantation. One patient who died within one week after HSCT was excluded, resulting in a cohort of 93 patients. Patients received a graft from a matched-unrelated donor (MUD, n=60) or HLA-identical related donor (IRD, n=33). MUD transplantation was always combined with ATG serotherapy. 15 patients received a peripheral blood stem cell graft graft, the remaining 78 patients received a BM graft. The median age was 9.2 years (range 0.8-17.8).

All transplantations were performed according to national protocols and in line with the recommendations of the European group for Blood and Marrow Transplantation. Peripheral blood samples taken at 3, 4, 6, 8, 12, 16, 26, 52 and 104 weeks after HSCT were evaluated. Follow up ended earlier when leukemia relapsed (n=20) or the patient died (n=10). Blood samples were freshly analyzed. In addition, blood samples were cryopreserved and used for phenotypic and functional analyses with approval of the institutional review board (protocol P01.028). Informed consent was obtained from all patients and/or their parents or legal guardians.

#### Monitoring of immune reconstitution

To monitor immune reconstitution, peripheral blood white blood cell counts including full leukocyte differentiation were performed weekly. Freshly isolated peripheral blood mononuclear cells (PBMC) were analyzed by flow cytometry to determine the size of different lymphocyte populations and subsets. PBMC were separated from EDTA blood using ficoll-isopaque density gradient centrifugation (LUMC Pharmacy, Leiden, NL) and stained with antibodies as listed in Table 6.S3. Four-color flow cytometry was performed on a BD FACS Calibur II flow cytometer (Becton Dickinson Biosciences (BD), Franklin Lakes, NJ, US) and data were analyzed using BD Cellquest software. Lymphocytes were defined as CD45<sup>+</sup> CD33/CD235a/CD14<sup>-</sup> cells within the forward / sideward scatter lymphocyte gate. T cells and NK cells were defined as CD3<sup>+</sup> cells and CD3<sup>-</sup>CD56<sup>+</sup> cells in the lymphocyte population, respectively. In a separate tube, CD56<sup>bright</sup>CD16<sup>+/-</sup> and CD56<sup>dim</sup>CD16<sup>+</sup> NK cells were gated within the CD3<sup>-</sup>CD14<sup>-</sup> lymphocyte gate (Figure 6.S4 A-B).

## Multicolor flowcytometry

The expression of 42 cell surface markers (17 chemokine receptors, 10 adhesion molecules and 15 NK cell markers) was measured on CD56<sup>bright</sup> and CD56<sup>dim</sup> NK cells in a subgroup of 20 HSCT recipients and 16 healthy donors. For this, patients were selected that did not receive prednisolone. Cryopreserved PBMC were thawed and subjected to a three step staining procedure after 1h recovery at 37°C / 5% CO<sub>2</sub> in AIM-V medium (Life Technologies) with 10% fetal calf serum (FCS, GE Hyclone, Logan, UT, US). All antibodies used are listed in Table 6.S3. PBMC were first incubated with unconjugated antibodies, washed twice and stained with fluorochrome-labeled secondary antibodies. For the third step, PMNC were stained with directly labeled antibodies in the presence of normal mouse serum (5% (v/v), Seralab, London, UK). Prior to analysis, DAPI (25 ng/ml, Sigma-Aldrich) was added.

Data were acquired on a LSR II flow cytometer (Becton Dickinson (BD), Franklin Lakes, NJ, US) using FACS Diva Software (v6.1, BD). Data were acquired on different days, but with the same instrument settings. For each experiment, spectral overlap was compensated based on single stained cells. All samples from an individual patient were measured in a single experiment. The cell surface marker panel was validated for the use on cryopreserved cells by the comparison between fresh and cryopreserved PBMC from four healthy donors and two HSCT recipients at one month after HSCT. We excluded CD56<sup>dim</sup>CD16<sup>-</sup> NK cells from further phenotypic characterization as they constituted a separate population in cryopreserved but not in fresh PBMC.<sup>237</sup> Also, CD49b was excluded from further analysis because the expression of this marker was significantly reduced on cryopreserved cells (data not shown). The other markers could be measured reliably on cryopreserved NK cells.

The gating strategy is depicted in Figure 6.S4C. CD56<sup>bright</sup>CD16<sup>+/-</sup> and CD56<sup>dim</sup>CD16<sup>+</sup> NK cells were defined as living, non-doublet CD3<sup>-</sup>CD7<sup>+</sup> lymphocytes expressing CD56 and/or CD16. Flow cytometric data were analyzed using Kaluza software (v1.3, Beckman Coulter, Brea, CA, US). For each NK cell population, the expression of the cell surface markers was calculated as follows: for cell surface markers with a bimodal expression, the percentage of positive cells minus isotype control was calculated; for markers with a continuous expression, the ratio of geomean fluorescence intensity of marker and isotype control (FI) was calculated.

## t-SNE analysis of cell surface receptor expression data

We used *t*-distributed stochastic neighbor embedding (*t*-SNE) analysis to visualize the flowcytometry data.<sup>238;239</sup> The population expression profile of 34 cell surface markers on CD56<sup>bright</sup> NK cells from 134 blood samples of 20 patients and 16 healthy donors were combined in this *t*-SNE analysis. The following markers were included in the analysis: chemokine receptors CCR2, CCR5, CCR6, CCR7, CXCR1, CXCR2, CXCR3, CXCR4, CXCR6 and CX3CR1; adhesion molecules cutaneous lymphocyte antigen (CLA), Integrin  $\beta$ 7 (ITGB7), CD11a, CD11b, CD31, CD44, CD49d, CD54 and CD162; NK cell receptors CD27, CD57, CD69, CD94, CD117, CD127, NKp30, NKp44, NKp46, NKp80, NKG2A, NKG2C, NKG2D, DNAM1 and pan-KIR mix. CD56 and CD16 were not included in the *t*-SNE analysis as these markers were used for the population definition. The cell surface markers CCR1, CCR3, CCR4, CCR8, CCR9, CCR10,

CXCR5 and CD103 were not included in the *t*-SNE analysis because these receptors were neither expressed on CD56<sup>bright</sup> nor on CD56<sup>dim</sup> NK cells. For missing data, the average expression of the cell surface marker on the concerning NK cell subset at that time point was used.

Population expression data (percentage or FI) for each marker were normalized on a scale from 0-100, with each value expressed as a percentage of the range between the highest and the lowest value. Two-dimensional Barnes-Hut *t*-SNE analysis was performed.<sup>240;241</sup> Plots show all individual samples and are based on the *t*-SNE field parameters V1 and V2. Because of the random effect in *t*-SNE analysis, 20 runs of *t*-SNE were performed, all resulting in comparable plots. Afterwards, dots were colored to highlight different time-points (Figure 6.1A). The relative expression of individual cell surface markers was plotted in separate dot plots (Figure 6.1B). To reduce the visual impact of outliers to the color-coding display, the very low (<p2.3) and very high (>p97.7) values for each cell surface marker were replaced by the p2.3 and p97.7 value after the *t*-SNE analysis but before the construction of plots of individual cell surface marker expression.

### In vitro assessment of cytotoxicity and cytokine production

To assess the cytotoxic potential of post-transplant CD56<sup>bright</sup> NK cells, PBMC from 3 patients with >95% CD56<sup>bright</sup> NK cells at 1 month after HSCT were used in a chromium release assay and compared with PBMC from 3 months after HSCT (with CD56<sup>dim</sup> and CD56<sup>bright</sup> NK cells) and with healthy donor PBMC. After thawing, cells were rested overnight in AIM-V medium with 10% FCS in 96-well round bottom plates (Greiner Bio-One, Kremsmünster, Austria) and their cytotoxicity against K562 cells was evaluated in a 4h chromium release assay as previously described.<sup>242</sup> The cytotoxicity of unselected NK cells from PBMC was compared to the cytotoxicity of purified healthy donor CD56<sup>bright</sup> and CD56<sup>dim</sup> NK cells. For this, CD56<sup>bright</sup> and CD56<sup>dim</sup> NK cells were purified by fluorescence activated cell sorting (FACS) from freshly isolated healthy donor PBMC as described previously,<sup>243</sup> and rested overnight in the absence or presence of IL15 (10 ng/ml, Cellgenix, Freiburg, Germany).

Cytokine production of post-transplant CD56<sup>bright</sup> NK cells was evaluated in PBMC from three patients at 1, 3 and 12 months post HSCT and 2 healthy donors. 2-4x10<sup>5</sup> PBMC were cultured in AIM-V medium with 10% FCS for 16-18h. Cells were either unstimulated (medium) or stimulated with recombinant human IL12 (10 ng/ml, Peprotech, Rocky Hill, NJ, US), IL15 (10 ng/ml), IL18 (20 ng/ml, MBL International, Woborn, MA, US) or combinations of these monokines. BD golgistop (1:1500, BD) was added during the last 4h of culture. Cells were harvested, stained for cell surface markers, fixed and permeabilized and stained for intracellular interferon- $\gamma$  and tumor necrosis factor- $\alpha$  (IFN- $\gamma$  & TNF- $\alpha$ , Table 6.S3) in a paraformaldehyde/ saponin based intracellular staining protocol as previously described.<sup>244</sup>

### Measurement of active ATG concentrations

Patients receiving a stem cell graft from a MUD received ATG at a cumulative dose of 10 mg/kg body weight in 3-4 doses from day -5 to -1 pre-HSCT. Active ATG levels were routinely measured using quantitative flow cytometry assays as previously described.<sup>33</sup> Active ATG was

defined as the fraction of the product capable of binding to the HUT-78 T cell line. In short, HUT cells were incubated with fourfold dilutions of patient serum, washed and incubated with Alexa Fluor 647 (A647) labeled goat anti-rabbit IgG (Life Technologies, Carlsbad, CA, USA). Subsequently, cells were washed and the FI for A647 was measured by flow cytometry on a BD FACS Calibur II flow cytometer. To construct a reference curve, HUT cells were incubated in 25% pooled human serum supplemented with known amounts of ATG straight from the vial of the supplier. Active ATG was measured in arbitrary units (AU). Five mg/ml ATG was arbitrarily set at containing an active ATG concentration of 5000 AU/ml.<sup>33</sup>

### Data analysis and statistics

Data were analyzed and figures were constructed in R (version 3.3.2, 64 bit; R Foundation, Vienna, Austria) and GraphPad Prism (Version 7.02, GraphPad Software, San Diego, CA, US). Data were pre-processed using the R package dplyr<sup>245</sup> Barnes-Hut *t*-SNE analysis was performed using the R package Rtsne.<sup>240</sup> Heatmaps and dot plots were built using the R packages Heatmap3, ggplot2 and Rcolorbrewer.<sup>246-248</sup> Linear regression analysis on log-transformed data was used to evaluate the correlation between T- and NK cell numbers. Univariate associations between HSCT characteristics and the hyperexpansion of CD56<sup>bright</sup> NK cells after HSCT (>300 cells/  $\mu$ l) were evaluated using logistic regression analysis. The Firth penalized likelihood bias-reduction method was applied for categorical variables with complete data separation using the R package logistf.<sup>249</sup> Parameters with *p-values* <0.10 in univariate analysis were included in a multivariate logistic regression analysis using backward stepwise elimination. For subgroup analysis, chi-square test was used to compare the distribution of categorical parameters between all 4 groups and (combinations of) subgroups. Unpaired t tests on log-transformed data were used to compare cell numbers and cell surface marker expression on CD56<sup>bright</sup> NK cells between patient samples and/or healthy donors. *P-values* <0.01 were considered statistically significant. The Bonferroni-Holm method was used to correct for multiple comparisons.<sup>250</sup>

	CD56 <sup>bright</sup> NK cells >300 cells/ $\mu$ l (n=38)		CD56 <sup>bright</sup> NK cells <300 cells/ $\mu$ l (n=55)		<i>p</i> value	
	<i>N</i>	%	<i>N</i>	%	<i>Univariate</i> <sup>1</sup>	<i>Multivariate</i> <sup>2</sup>
<b>Baseline</b>						
Donor type <sup>3</sup> <b>MUD</b> (vs. IRD)	37	97.4%	23	41.8%	<0.001	NA <sup>3</sup>
Graft Source <b>PBSC</b> (vs. BM)	9	23.7%	6	10.9%	0.100	NS
GvHD Prophylaxis <sup>4</sup> <b>CSA+MTX</b>	35	92.1%	36	65.5%	0.001	NS <sup>4</sup>
<b>CSA alone</b>	0	0.0%	17	30.9%		
<b>CSA+MMF</b>	3	7.9%	2	3.6%		
Serotherapy <sup>3</sup> <b>ATG</b> (vs. none)	37	97.4%	23	41.8%	<0.001	<0.001
<100 T cells/ $\mu$ l at week 4	26	68.4%	7	12.7%	<0.001	0.002
	<b>Median</b>	<b>Range</b>	<b>Median</b>	<b>Range</b>		
ATG conc. at week 3 (AU/ml)	1.12	0 - 5.9	0.32	0 - 4.9	0.016	NS
ATG conc. at week 4 (AU/ml)	0.39	0 - 3.7	0.06	0 - 1.7	0.032	NS
Age (years)	7.7	0.8 - 17.7	10.7	0.8 - 17.8	0.042	NS
<b>Outcome</b>	<i>N</i>	%	<i>N</i>	%	<i>Univariate</i>	<i>Multivariate</i> <sup>5</sup>
CMV viremia ( $2x > 10^3$ copies/ml)	6	15.8%	8	14.5%	0.870	
EBV viremia ( $2x > 10^3$ copies/ml)	13	34.2%	6	10.9%	0.006	0.15
hAdV viremia ( $2x > 10^3$ copies/ml)	4	10.5%	4	7.3%	0.580	
Acute GvHD (grade II-IV)	6	15.8%	16	29.1%	0.140	0.64
Chronic GvHD (extended)	3	7.9%	6	10.9%	0.440	
Leukemia relapse	7	18.4%	14	25.5%	0.430	
Transplant related mortality	2	5.3%	5	9.1%	0.490	
One year survival	33	86.8%	44	80.0%	0.390	
Overall survival	26	73.7%	37	67.3%	0.510	

**Table 6.S1. Comparison of HSCT recipients with and without CD56<sup>bright</sup> NK cell hyperexpansion**

Baseline characteristics and outcome parameters of HSCT recipients with and without hyperexpansion of CD56<sup>bright</sup> NK cells (>300 cells/ $\mu$ l) within six weeks after HSCT. *p* values: <sup>1</sup>Univariate logistic regression analysis and <sup>2</sup>multivariate logistic regression analysis using backward stepwise elimination. <sup>3</sup>All MUD and none of the IRD graft recipients received ATG serotherapy. <sup>4</sup>The Firth penalized likelihood bias-reduction method was applied for categorical variables with complete data separation (CSA alone). <sup>5</sup>For outcome parameters, NK cell hyperexpansion was corrected for delayed T cell reconstitution in multivariate logistic regression analysis.

Abbreviations: MUD: matched unrelated donor, IRD: HLA identical related donor, PBSC: peripheral blood stem cells, BM: bone marrow, CSA: cyclosporin A, MTX: methotrexate, MMF: mycophenolate mofetil, ATG: anti-thymocyte globulin, AU: arbitrary units, CMV: cytomegalovirus, EBV: Epstein-Barr virus, hAdV: human adenovirus, NS: not significant.

**Table 6.S2. Subgroup analysis of outcome parameters**

Subgroup analysis of outcome parameters between HSCT recipients with a rapid (group I, II) and delayed (group III, IV) T cell reconstitution, with (group I, III) and without (group II, IV) CD56<sup>bright</sup> NK cell hyperexpansion. Rapid and delayed T cell reconstitution were defined as > or < 100 T cells /  $\mu$ l at 4 weeks after HSCT. Hyperexpansion of CD56<sup>bright</sup> NK cells was defined as >300 CD56<sup>bright</sup> NK cells /  $\mu$ l within six weeks after HSCT. Statistics: <sup>1</sup>chi square test comparing 4 groups and <sup>2</sup>chi square test comparing 2 groups. Abbreviations: CMV: cytomegalovirus, EBV: Epstein-Barr virus, hAdV: human adenovirus, GvHD: graft versus host disease.

Outcome	Group I T cells > 100/ $\mu$ l n = 12		Group II T cells < 100/ $\mu$ l at week 4 n = 48		Group III T cells < 100/ $\mu$ l n = 26		Group IV T cells < 300/ $\mu$ l n = 7		I vs. II vs. III vs. IV <sup>1</sup> p value <sup>1</sup>	III vs. (I+II) <sup>2</sup> T-NK+ vs. T+ p value <sup>2</sup>	IV vs. (I+II) <sup>2</sup> T-NK- vs. T+ p value <sup>2</sup>
	N	%	N	%	N	%	N	%			
CMV viremia ( $2x > 10^3$ copies/ml)	2	16.7%	7	14.6%	4	15.4%	1	14.3%	1.0	0.96	0.96
EBV viremia ( $2x > 10^3$ copies/ml)	3	25.0%	4	8.3%	10	38.5%	2	28.6%	<b>0.019</b>	<b>0.004</b>	0.22
hAdV viremia ( $2x > 10^3$ copies/ml)	1	8.3%	4	8.3%	3	11.5%	0	0.0%	0.83	0.64	0.43
Acute GvHD (grade II-IV)	3	25.0%	15	31.3%	3	11.5%	1	14.3%	0.26	0.067	0.38
Chronic GvHD (extended)	1	8.3%	6	12.5%	2	7.7%	0	0.0%	0.72	0.58	0.34
Leukemia relapse	1	8.3%	12	25.0%	6	23.1%	2	28.6%	0.73	0.89	0.77
Transplant related mortality	1	8.3%	3	6.3%	1	3.8%	2	28.6%	0.17	0.61	0.055
One year survival	11	91.7%	41	85.4%	22	85.6%	3	42.9%	<b>0.032</b>	0.80	<b>0.004</b>
Overall survival	9	75.0%	34	70.8%	19	73.1%	3	42.9%	0.43	0.89	0.12

**Table 6.S3 (next pages). Antibodies used for flow cytometry**

Staining was performed in a 96-well round-bottom plate with  $0.5-1.5 \times 10^6$  cells in 25  $\mu$ l per well for 30 min at 4°C in FACS buffer (Phosphate Buffered Saline (PBS, Braun, Melsungen, Germany) with bovine serum albumin (5 mg/ml, Sigma-Aldrich, St. Louis, MO, US) and sodium-azide (1 mg/ml, LUMC Pharmacy)) 1All four PE-conjugated  $\alpha$ -KIR antibodies were combined in a pan-KIR staining. CD: Cluster of differentiation. n/a: not applicable. m: mouse, r: rat. Fluorochromes: AF: Alexa Fluor, APC: Allophycocyanin, BV: Brilliant Violet, ECD: Energy Coupled Dye (=Phycoerythrin-Texas Red conjugate), FITC: Fluorescein isothiocyanate, PE: Phycoerythrin, PE-Cy5.5: Phycoerythrin-Cyanine5.5 conjugate, PE-Cy7: Phycoerythrin-Cyanine7 conjugate, PERCP-Cy5.5: Peridinin Chlorophyll-Cyanine5.5 conjugate, RD-1: Red Dye 1. Companies: AnceCell: AnceCell Corporation (Bayport, MN, USA), BC: Beckman Coulter (Brea, CA, USA), BD: Becton Dickinson Biosciences (San Jose, CA, USA), Biolegend: Biolegend (San Diego, CA, USA), DAKO: Dako Denmark, (Glostrup, Denmark), eBioscience: eBioscience (San Diego, CA, USA), Invitrogen: Invitrogen (Thermo Fisher Scientific, Waltham, MA, USA), Miltenyi: Miltenyi Biotec, (Bergisch Gladbach, Germany), R&D: R&D Systems (Minneapolis, MN, USA), Sanquin: Sanquin Reagents (Amsterdam, Netherlands), Southern: Southern Biotech (Birmingham, AL, USA).

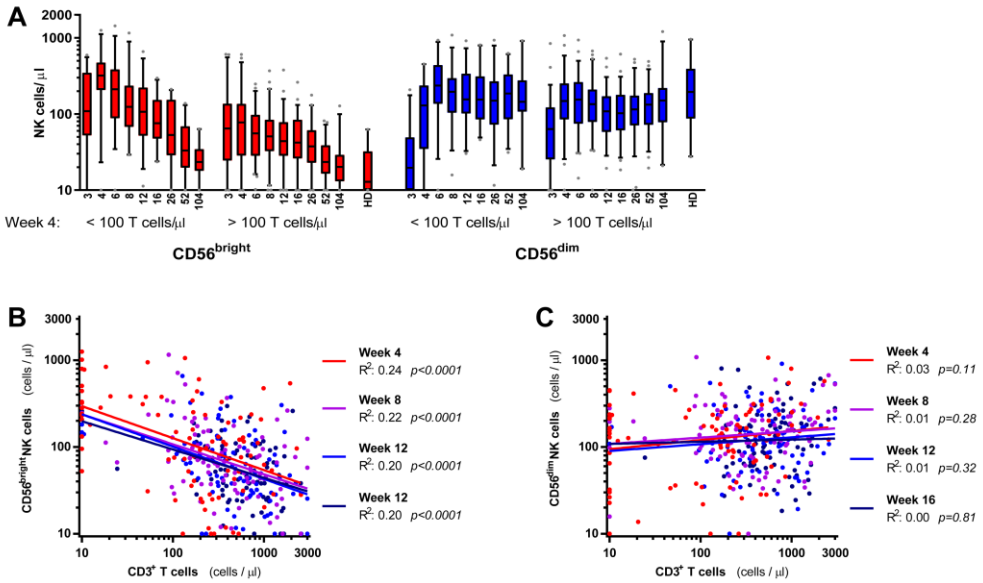
CD designation	Alternative name	Fluorochrome	Type	Clone	Company	Catalog#	Staining step
CD014	CD14	PE	m-IgG1	Mop9	BD	342408	Fresh Tube 1, Direct
CD033	SIGLEC3	PE	m-IgG1	P67.6	BD	345799	Fresh Tube 1, Direct
CD045	PTPRC	FITC	m-IgG1	2D1	BD	342408	Fresh Tube 1, Direct
CD056	NCAM1	APC	m-IgG1	N901	BC	IM2474	Fresh Tube 1, Direct
CD235a	GPA	PE	m-IgG1	11E4B-7-6	BC	A07792	Fresh Tube 1, Direct
CD003	CD3	PERCP-Cy5.5	m-IgG1	SK7	BD	340949	Fresh Tube 1+2, Direct
CD014	CD14	APC	m-IgG1	Mop9	BD	345787	Fresh Tube 2, Direct
CD016	FcγRIII	FITC	m-IgG1	3G8	BC	IM0814U	Fresh Tube 2, Direct
CD056	NCAM1	RD-1	m-IgG1	N901	BC	6603067	Fresh Tube 2, Direct
CD162	PSGL1	Unconjugated	m-IgG1	5D8-8-12	BC	IM2091	Primary
CD181	CXCR1	Unconjugated	m-IgG2a	42705	R&D	MAB330	Primary
CD182	CXCR2	Unconjugated	m-IgG2a	483112	R&D	MAB331	Primary
CD183	CXCR3	Unconjugated	m-IgG1	1C6	BD	557183	Primary
CD184	CXCR4	Unconjugated	m-IgG2b	44716	R&D	MAB172	Primary
CD185	CXCR5	Unconjugated	m-IgG2b	51505	R&D	MAB190	Primary
CD186	CXCR6	Unconjugated	m-IgG2b	56811	R&D	MAB699	Primary
CD191	CCR1	Unconjugated	m-IgG2b	53504	R&D	MAB145	Primary
CD192	CCR2	Unconjugated	m-IgG2b	48607	R&D	MAB150	Primary
CD194	CCR4	Unconjugated	m-IgG1	ID1	BD	551121	Primary
CD195	CCR5	Unconjugated	m-IgG2b	45531	R&D	MAB182	Primary
CD196	CCR6	Unconjugated	m-IgG2b	53103	R&D	MAB195	Primary
CD199	CCR9	Unconjugated	m-IgG2a	112509	R&D	MAB179	Primary
n/a	Isotype M-IgG1	Unconjugated	m-IgG1	11711	R&D	MAB002	Primary
n/a	Isotype M-IgG2a	Unconjugated	m-IgG2a	DAK-GO5	DAKO	X0943	Primary
n/a	Isotype m-IgG2b	Unconjugated	m-IgG2b	DAK-GO9	DAKO	X0944	Primary
n/a	Goat α m-IgG2b	AF488	polyclonal		Invitrogen	A21141	Secondary
n/a	Goat α m-IgG2b	AF647	polyclonal		Invitrogen	A21242	Secondary
n/a	Goat α m-IgG2b	PE	polyclonal		Southern	1092-09	Secondary
Secondary	Goat α M-IgG1	AF647	polyclonal		Invitrogen	A21240	Secondary
Secondary	Goat α M-IgG2a	AF647	polyclonal		Invitrogen	A21241	Secondary
CD003	CD3	BV510	m-IgG1	UCHT1	Biologend	300448	Direct, basis
CD007	GP40	Alexa700	m-IgG1	M-T701	BD	561603	Direct, basis
CD016	FcγRIII	BV711	m-IgG1	3G8	BD	563127	Direct, basis
CD056	NCAM1	ECD	m-IgG1	N901	BC	A82943	Direct, basis
CD011a	LFAI	FITC	m-IgG1	H111	BD	555383	Direct
CD011b	MAC1	FITC	m-IgM	1, B2	Sanquin	MI668	Direct
CD027	TNFRSF7	APC	m-IgG1	L128	BD	337169	Direct
CD031	PECAM1	PE	m-IgG1	WM59	BD	555446	Direct
CD044	HCAM	FITC	m-IgG1	J.173	BC	IM1219	Direct
CD049b	ITGA2	PE	m-IgG2a	I2F1	BD	555669	Direct
CD049d	ITGA4	PE	m-IgG2b	L25	BD	340296	Direct

Table 6.S3. Antibodies used for flow cytometry



CD designation	Alternative name	Fluorochrome	Type	Clone	Company	Catalog#	Staining step
CD054	ICAM1	PE	m-IgG1	HA58	BD	555511	Direct
CD057	B3GAT1	FITC	m-IgM	HNK1	BD	347393	Direct
CD069	EA-1	FITC	m-IgG1	L78	BD	347823	Direct
CD094	KLRD1	PE	m-IgG1	HP-3D9	BD	555889	Direct
CD103	ITGAE	FITC	m-IgG1	BER-ACT8	DAKO	F7138	Direct
CD117	c-kit	PE	m-IgG1	104D2	BD	332785	Direct
CD127	IL7R $\alpha$	FITC	m-IgG1	eBioRDR5	eBioscience	11-1278	Direct
CD158a/h <sup>1</sup>	KIR2DL1 DS1	PE <sup>1</sup>	m-IgG1	EB6	BC	A09778	Direct
CD158b/j <sup>1</sup>	KIR2DL2/3 DS2	PE <sup>1</sup>	m-IgG1	GL183	BC	IM2278U	Direct
CD158e <sup>1</sup>	KIR3DL1	PE <sup>1</sup>	m-IgG1	DX9	BD	555967	Direct
CD158f <sup>1</sup>	KIR2DS4	PE <sup>1</sup>	m-IgG1	FES172	BC	IM3337	Direct
CD159a	NKG2A	PE-Cy7	m-IgG2b	z199	BC	B10246	Direct
CD159c	NKG2C	APC	m-IgG1	134591	BC	B10246	Direct
CD183	CXCR3	AF647	m-IgG1	G025H7	R&D	FAB138A	Direct
CD193	CCR3	PE	r-IgG2a	61828	Biologend	353712	Direct
CD197	CCR7	FITC	m-IgG2a	150503	R&D	FAB155P	Direct
CD198	CCR8	APC	r-IgG2b	191704	R&D	FAB197F	Direct
n/a	CCR10	PE	r-IgG2a	314305	R&D	FAB1429A	Direct
n/a	CLA	APC	r-IgM	HECA-452	Milltenyi	FAB3478P	Direct
n/a	CX3CR1	PE	r-IgG2b	2A9-1	Biologend	130-098-573	Direct
CD226	DNAM1	FITC	m-IgG1	DX11	BD	341604	Direct
CD314	NKG2D	APC	m-IgG1	ID11	BD	559788	Direct
CD335	NKp46	PE	m-IgG1	BAB281	BC	558071	Direct
CD336	NKp44	PE	m-IgG1	Z231	BC	IM3711	Direct
CD337	NKp30	PE	m-IgG1	Z25	BC	IM3710	Direct
n/a	NKp80	APC	m-IgG1	5D12	BC	IM3709	Direct
n/a	ITGB7	APC	r-IgG2a	FIB504	Biologend	346708	Direct
n/a	Isotype m-IgG1	APC	m-IgG1	15H6	BC	551082	Direct
n/a	Isotype m-IgG1	FITC	m-IgG1	15H6	BC	731586	Direct
n/a	Isotype m-IgG1	PE	m-IgG1	X40	BC	731583	Direct
n/a	Isotype m-IgG2a	PE	m-IgG2a	X39	BD	345816	Direct
n/a	Isotype m-IgM	FITC	m-IgM	R4A3-22-12	BD	349053	Direct
n/a	Isotype R-IgG2a	APC	r-IgG2a	eBR2a	eBioscience	6602434	Direct
n/a	Isotype R-IgG2a	PE	r-IgG2a	54447	R&D	17-4321-71	Direct
n/a	Isotype R-IgM	APC	r-IgM	NIP/M-2	Southern	IC006P	Direct
n/a	Granzyme B	AF700	m-IgG1	GB11	BD	0120-11	Direct
n/a	Perforin	FITC	m-IgG2b	delta G9	Ancell	557971	Intracellular
n/a	Tumor Necrosis Factor $\alpha$	PE	m-IgG1	MAb11	BD	358-040	Intracellular
n/a	Interferon- $\gamma$	FITC	m-IgG1	4S.B3	BD	554513	Intracellular
n/a						554551	Intracellular

Table 6.S3. Antibodies used for flow cytometry (continued)



**Figure 6.S1. Correlation between T cell and NK cell reconstitution after HSCT.**

**(A)** Absolute cell numbers of CD56<sup>bright</sup> (red) and CD56<sup>dim</sup> (blue) NK cells at 3, 4, 6, 8, 12, 16, 26, 52 and 104 weeks after HSCT (n=93) and in healthy donors (n=16). Patients were divided in two groups based on T cell reconstitution < and > 100 cells/ $\mu$ l at 4 weeks after HSCT. Boxes: median and interquartile range, whiskers: 5-95 percentile, dots: outliers.

**(B-C)** Correlation of CD3+ T cell numbers with (A) CD56<sup>bright</sup> NK cell numbers and (B) CD56<sup>dim</sup> NK cell numbers at 4, 8, 12 and 16 weeks after hematopoietic stem cell transplantation (HSCT) in 93 patients. Statistics: Linear regression analysis on log-transformed data

**Figure 6.S2 (next pages). Cell surface marker expression on CD56<sup>bright</sup> and CD56<sup>dim</sup> NK cells.**

The expression of **(A)** chemokine receptors, **(B)** adhesion molecules and **(C)** NK cell receptors on CD56<sup>bright</sup> (red) and CD56<sup>dim</sup> (blue) NK cells at 3, 4, 6, 8, 12, 16, 26 and 52 weeks after HSCT (n=20) and healthy donors (HD, n=16). No expression of CCR1, CCR3, CCR4, CCR8, CCR9, CCR10, CXCR5 and CD103 was measured on NK cells (data not shown). Bars: mean +/- SEM, dots: individual patients. Expression: percentage of marker minus isotype control (%) or fluorescence intensity ratio of marker / isotype control (FI). Dotted line: normalized FI of isotype control. *p* values: Unpaired t test on log-transformed data. Comparison between healthy donor CD56<sup>bright</sup> NK cells and post-transplant CD56<sup>bright</sup> NK cells at week 4 (unless otherwise stated). *p* values are only shown when significant after Bonferroni-Holm correction for multiple comparisons. NS: not significant after Bonferroni-Holm correction.

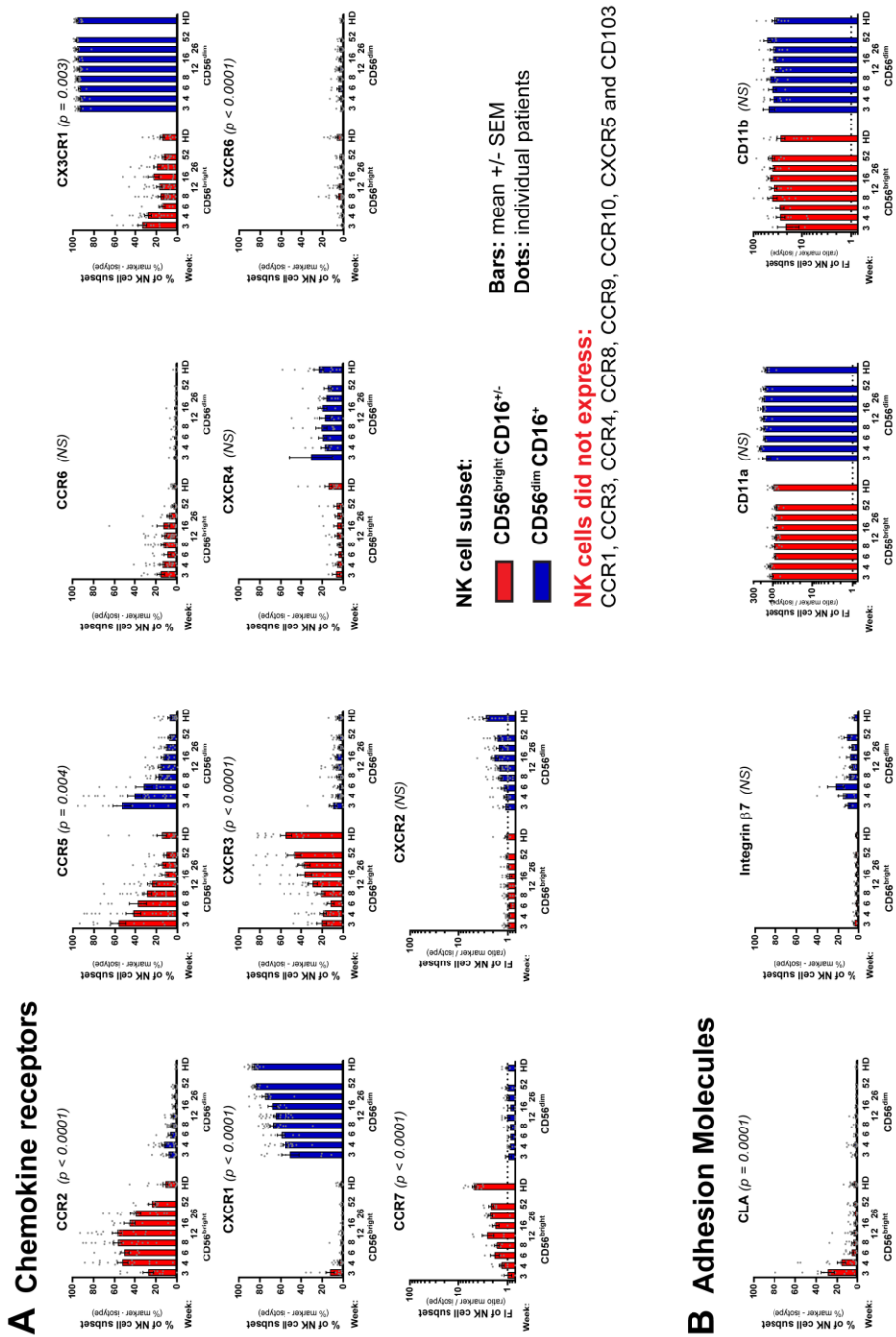


Figure 6.S2. Cell surface marker expression on CD56<sup>bright</sup> and CD56<sup>dim</sup> NK cells.

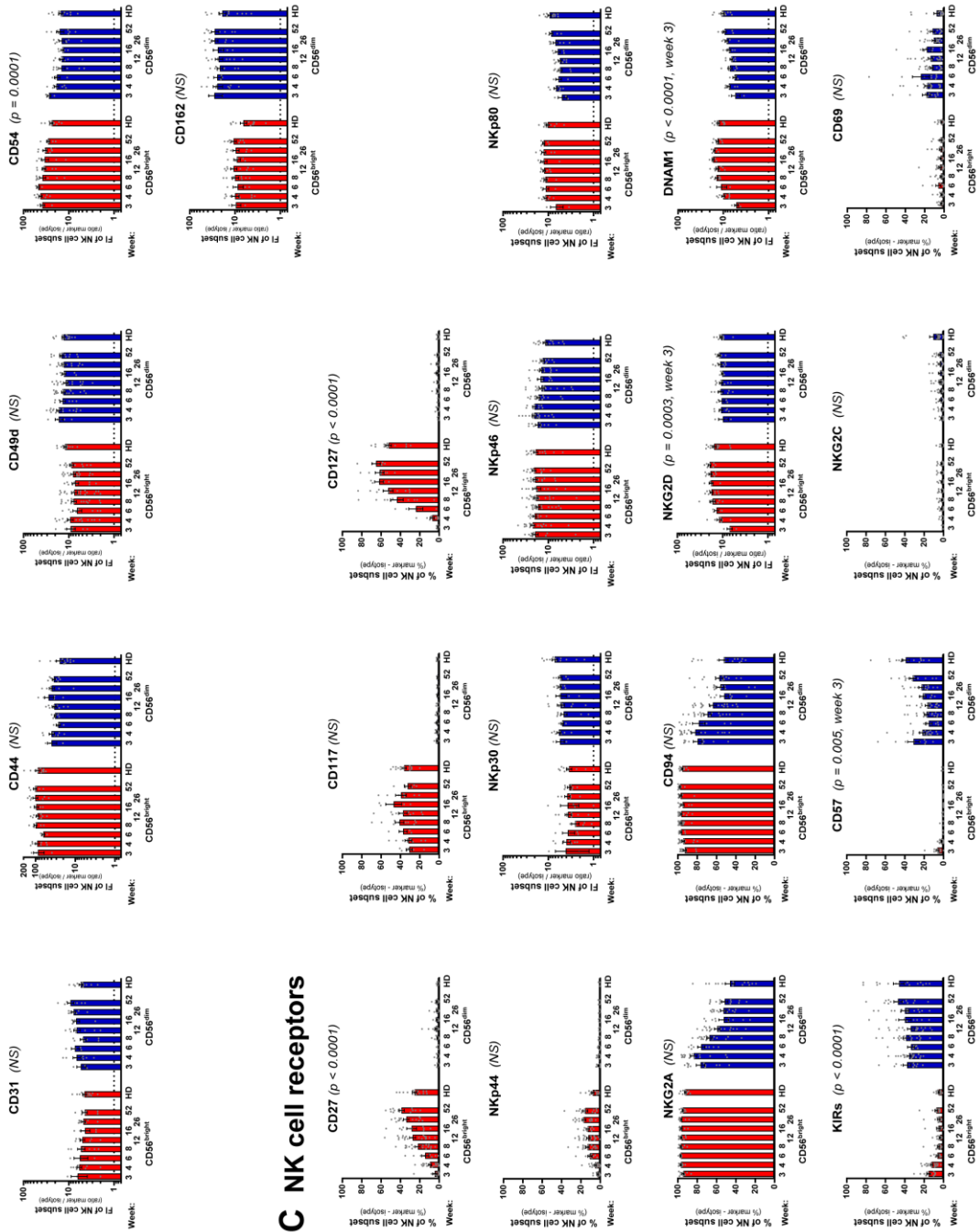
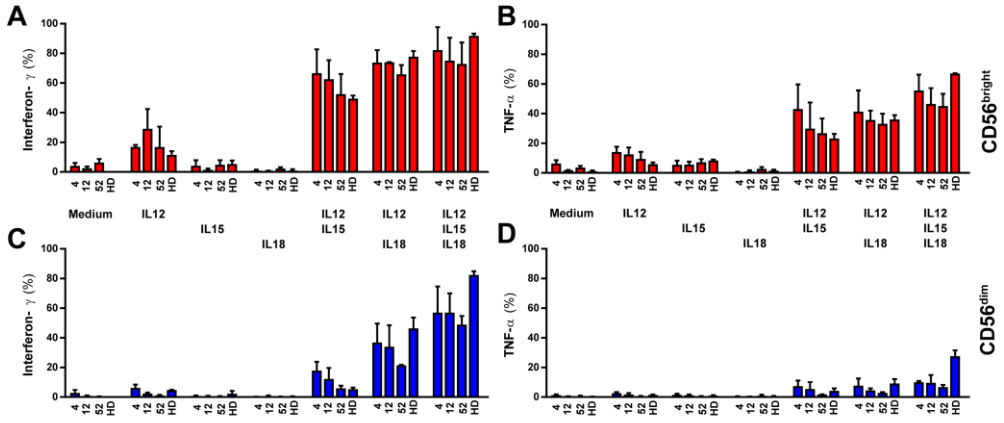
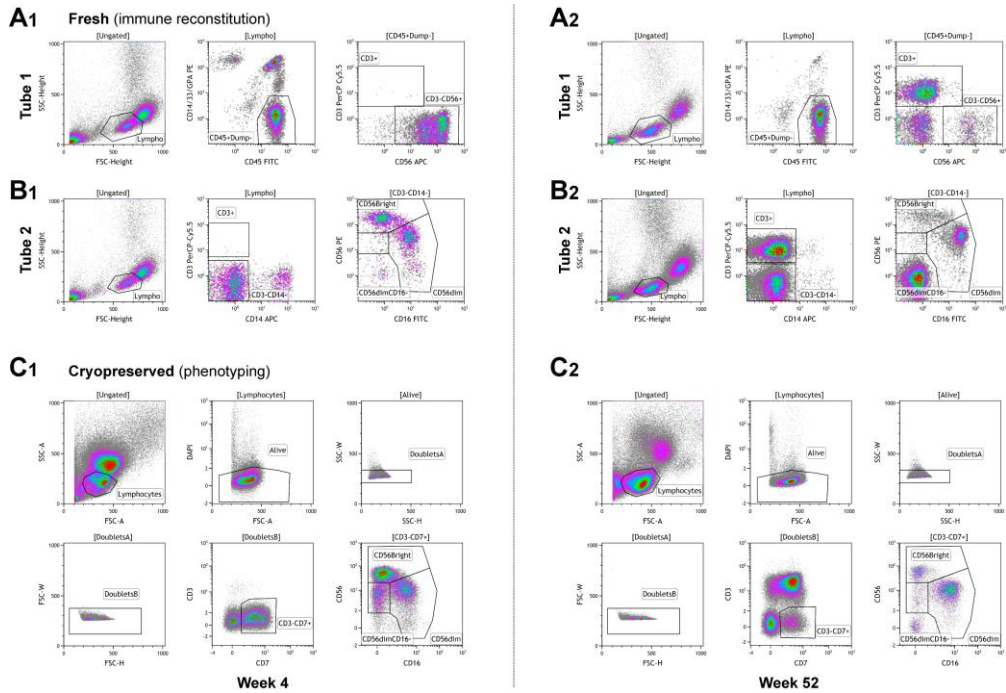


Figure 6.S2. Cell surface marker expression on CD56<sup>bright</sup> and CD56<sup>dim</sup> NK cells (continued).



**Figure 6.S3. Cytokine secretion of NK cells after HSCT.**

Intracellular expression of interferon- $\gamma$  (**A, C**) and TNF- $\alpha$  (**B, D**) in CD56<sup>bright</sup> (red, **A, B**) and CD56<sup>dim</sup> (blue, **C, D**) NK cells at 4, 12 and 52 weeks after HSCT (n=3) and healthy donors (n=2) cultured in absence or presence of (combinations of) IL12, IL15 or IL18. Bars: mean +/- SEM.



**Figure 6.S4. Gating strategy.**

The combination of flow cytometry on fresh PBMC, absolute leukocyte counts and full leukocyte differentiation was used to calculate absolute cell numbers of T cells, CD56<sup>bright</sup> and CD56<sup>dim</sup> NK cells. The expression of cell surface markers was evaluated on CD56<sup>bright</sup> and CD56<sup>dim</sup> NK cells using cryopreserved PBMC. An example of the gating strategy is shown for (A-B) fresh and (C) cryopreserved sample at four weeks (A1-C1) and one year after HSCT (A2-C2).

**(A)** In tube 1, lymphocytes were defined as CD45+ CD33/CD235a/CD14- within the forward / sideward scatter lymphocyte gate. T-cells and NK cells were defined as CD3+ cells and CD3-CD56+ cells in the lymphocyte population, respectively.

**(B)** In tube 2, CD56<sup>bright</sup>CD16<sup>+/-</sup> and CD56<sup>dim</sup>CD16<sup>+</sup> NK cells were gated within the CD3-CD14- lymphocyte gate.

**(C)** In cryopreserved samples, DAPI was used to exclude dead cells. CD56<sup>bright</sup>CD16<sup>+/-</sup> and CD56<sup>dim</sup>CD16<sup>+</sup> NK cells were defined as living, non-doublet CD3-CD7+ lymphocytes expressing CD56 and/or CD16. CD56<sup>dim</sup>CD16<sup>-</sup> NK cells were excluded as they represented a separate population in cryopreserved but not in fresh PBMC.





# Chapter 7

## Human lymphoid tissues harbor a distinct CD69<sup>+</sup>CXCR6<sup>+</sup> natural killer cell population

Published in:  
The Journal of Immunology  
2016; 197: 78-84

Gertjan Lugthart  
Janine E. Melsen  
Carly Vervat  
Monique M. van Ostaijen-ten Dam  
Willem E. Corver  
Dave L. Roelen  
Jeroen van Bergen  
Maarten J.D. van Tol  
Arjan C. Lankester *and*  
Marco W. Schilham

## Abstract

Knowledge on human NK cells is mainly based on conventional CD56<sup>bright</sup> and CD56<sup>dim</sup> NK cells from blood. However, most cellular immune interactions occur in lymphoid organs. Based on the co-expression of CD69 and CXCR6, we identified a major third NK cell subset in lymphoid tissues. This population represents 30-60% of NK cells in marrow, spleen and lymph node and is absent from blood. CD69<sup>+</sup>CXCR6<sup>+</sup> lymphoid tissue NK cells have an intermediate expression of CD56 and high expression of NKp46 and ICAM-1. In contrast to circulating NK cells, they have a bi-modal expression of the activating receptor DNAM-1. CD69<sup>+</sup>CXCR6<sup>+</sup> NK cells neither express the early markers c-kit and IL7R $\alpha$ , nor express *KIRs* or other late-differentiation markers. After cytokine stimulation, CD69<sup>+</sup>CXCR6<sup>+</sup> NK cells produce interferon- $\gamma$  at levels comparable to CD56<sup>dim</sup> NK cells. They constitutively express perforin, but require pre-activation to express granzyme B and exert cytotoxicity. After hematopoietic stem cell transplantation, CD69<sup>+</sup>CXCR6<sup>+</sup> lymphoid tissue NK cells do not exhibit the hyper-expansion as observed for both conventional NK cell populations.

CD69<sup>+</sup>CXCR6<sup>+</sup> NK cells constitute a separate NK cell population with a distinct phenotype and function. The identification of this NK cell population in lymphoid tissues provides tools to further evaluate the cellular interactions and role of NK cells in human immunity.

## Introduction

As effector lymphocytes of the innate immune system, natural killer cells contribute to the first line of immune defense through the lysis of virus-infected and malignant cells. Furthermore, NK cells play an important role in the initiation, enhancement and regulation of immune responses, directly through the secretion of cytokines and chemokines as well as via their interaction with other innate immune cells<sup>84;85;114;115;251-254</sup>.

Human NK cells are usually categorized in two main subsets: CD56<sup>bright</sup>CD16<sup>+/-</sup> (CD56<sup>bright</sup>) and CD56<sup>dim</sup>CD16<sup>+</sup> (CD56<sup>dim</sup>) NK cells<sup>95;254</sup>. CD56<sup>bright</sup> NK cells are considered to be the precursors of CD56<sup>dim</sup> NK cells and represent 5-15% of NK cells in blood<sup>97;100</sup>. CD56<sup>bright</sup> NK cells express low levels of c-kit (CD117) and typically express the inhibitory receptor CD94/NKG2A<sup>97;98;100</sup>. CD56<sup>dim</sup> NK cells lose the expression of NKG2A and acquire KIRs and CD57 as they continue to differentiate<sup>99</sup>. Both NK cell subsets produce IFN- $\gamma$  upon monokine stimulation<sup>101-103</sup>. CD56<sup>dim</sup> NK cells constitutively express high levels of perforin and granzyme B, resulting in efficient lysis of target cells without prior stimulation<sup>101</sup>. In contrast, CD56<sup>bright</sup> NK cells express perforin but require pre-activation to exert cytotoxicity<sup>95;100;254</sup>.

Most research on human NK cells is performed with circulating cells. However, the majority of NK cells is localized in lymphoid tissues<sup>255</sup>. Data obtained from murine experiments indicate lymphoid tissues as the primary site for cellular interactions of NK cells with other immune cells<sup>85;114;253</sup>. In humans, CD56<sup>bright</sup> NK cells are enriched in marrow and spleen, and comprise the vast majority of mature NK cells in lymph node<sup>90;107;108;256;257</sup>. Still, the mechanisms involved in the localization of human NK cells in lymphoid organs are largely unknown. Chemokine receptor expression patterns can provide information about human NK cell trafficking<sup>107;258</sup>. To investigate potential mechanisms of NK cell localization in lymphoid tissues, we compared the expression of chemokine receptors and adhesion molecules on circulating NK cells with NK cells in marrow, spleen and lymph node. Using this approach, we identified a major CD69<sup>+</sup>CXCR6<sup>+</sup> NK cell population in lymphoid tissues. This population of lymphoid tissue NK cells was not found in the circulation and had a distinct phenotype and function compared to conventional CD56<sup>bright</sup> and CD56<sup>dim</sup> NK cells.

## Material and Methods

### Tissues and ethics statement

With approval of the institutional review board (protocols P00.068 and P01.028), residual paired blood and bone marrow samples from 17 healthy bone marrow donors and 6 HSCT recipients were analyzed after informed consent was provided. In HSCT recipients, NK cell reconstitution was evaluated in marrow of pediatric acute leukemia patients who received an unmanipulated bone marrow (n=4) or peripheral blood stem cell (n=2) transplantation from a HLA-matched unrelated donor after myeloablative conditioning. MNC were isolated and samples were analyzed

immediately (9 HD) or after cryopreservation (8 HD, all HSCT). Small parts of splenic tissue from Dutch solid organ transplant donors (n=7) were obtained during explantation surgery as part of the standard diagnostic procedure for HLA-typing. In accordance with the Dutch law for organ donation, residual splenic tissue could be used for scientific research anonymously. Omental lymph nodes (n=3) were collected as leftover material from bariatric surgery and used anonymously in accordance with Dutch national ethical and professional guidelines (<http://www.federa.org>). Splenic tissues and lymph nodes were stored in University of Wisconsin solution at 4°C and processed within <12h after surgery. Tissues were dispersed through a 70 µm cell strainer, MNC were isolated and samples were analyzed immediately.

### Flow cytometry and cell sorting

For flow cytometry, MNC were subjected to a three step staining procedure. All antibodies used are listed in Table 7.S1. MNC were first incubated with unconjugated antibodies, washed twice and stained with fluorochrome-labeled secondary antibodies. For the third step, MNC were stained with directly labeled antibodies in FACS buffer containing 5% (v/v) mouse serum (Seralab, London, UK). Prior to analysis, DAPI (25 ng/ml, Sigma-Aldrich) was added. Data were acquired on a LSR II flow cytometer (Becton Dickinson (BD), Franklin Lakes, NJ, US) using FACS Diva Software (v6.1, BD). For FACS purification, NK cells were pre-enriched using the MACS untouched NK cell isolation kit (Miltenyi Biotec, Bergisch Gladbach, Germany) according to the manufacturers' instructions. Enriched NK cells were stained for cell surface markers (Table 7.S1). Based on the expression of CD56 and CD69, conventional CD56<sup>bright</sup> and CD56<sup>dim</sup> NK cells and lymphoid tissue NK cells were sorted on an ARIAIII cell sorter (BD).

### Gating strategy and data analysis

The gating strategy is depicted in Figure 7.S1A and Figure 7.1A-B. NK cells were defined as living CD45<sup>+</sup>CD19<sup>-</sup>CD3<sup>+</sup>CD7<sup>+</sup> lymphocytes expressing CD56 and/or CD16 but not high levels of CD117. Using this strategy, type 3 innate lymphoid cells or immature NK cells—mainly present in lymph node—were excluded<sup>91;259</sup>. CD69<sup>+</sup>CXCR6<sup>+</sup> lymphoid tissue NK cells were first selected by gating cells with the combined expression of CD69 and CXCR6. From the remaining NK cells, the conventional CD56<sup>bright</sup>CD16<sup>+/-</sup> and CD56<sup>dim</sup>CD16<sup>+</sup> NK cell subsets were defined based on the expression levels of CD56 and CD16. We excluded CD56<sup>dim</sup>CD16<sup>-</sup> NK cells from further phenotypic characterization as they formed a separate population in cryopreserved but not in fresh MNC<sup>237</sup>. Flow cytometric data were analyzed using Kaluza software (v1.3, Beckman Coulter, Brea, CA, US) and density plots were created with FACS Diva Software.

### In vitro stimulation and intracellular staining

MNC from paired blood and marrow (n=3) or spleen (n=3) were cultured in AIM-V (Life Technologies) with 10% fetal calf serum (GE Hyclone, Logan, UT, US) for 16-18h. Cells were either unstimulated (medium) or stimulated with recombinant human IL12 (10ng/ml, Peprotech, Rocky Hill, NJ, US), IL15 (10ng/ml, Cellgenix, Freiburg, Germany), IL18 (20ng/ml, MBL International, Woborn, MA, US) or combinations of these monokines. Brefeldin A (5µg/ml,

Sigma-Aldrich, IFN- $\gamma$  assay) or medium (perforin/granzyme B assay) was added during the last 4h of culture. MNC from marrow (n=4) were cultured overnight, followed by a 6h co-culture with K562 cells and/or IL12+IL18. BD golgistop (1:1500, BD) was added during the last 4h of culture. Cells were harvested and stained for cell surface markers, fixed and permeabilized using a paraformaldehyde/saponin based protocol as previously described<sup>244</sup> and stained for intracellular IFN- $\gamma$  or perforin and granzyme B (Table 7.S1). Since CD69 cannot be used as discriminative marker in activated NK cells, the combination of CD56, CD54 and CXCR6 was used to define lymphoid tissue NK cells after in vitro stimulation as alternative for CD69-CXCR6. The definition of ltNK cells based on CD56, CD54 and CXCR6 expression after short-term culture was validated by flow cytometry after in vitro stimulation of FACS purified NK cell populations (Figure 7.S2).

### Interferon- $\gamma$ , degranulation and chromium release assays

$1 \times 10^4$  FACS purified lymphoid tissue NK, CD56<sup>dim</sup> or CD56<sup>bright</sup> NK cells from marrow (n=3) were cultured in 96-well round bottom plates (Greiner Bio-One, Kremsmünster, Austria) for 18h in 100  $\mu$ l AIM-V with or without IL12, IL15 and IL18. Supernatant was harvested after 18h and the concentration of IFN- $\gamma$  was assessed using a Bio-Plex Luminex<sup>TM</sup> system assay (Bio-Rad, Veenendaal, The Netherlands) according to the manufacturers' instructions.

MNC from paired blood and marrow (n=6) or spleen (n=4) were cultured overnight in the absence or presence of IL15 (10ng/ml). The next day, CD107a FITC (BD) was added, followed by K562 cells (ratio 1:1) or culture medium. After one hour, BD golgistop was added and 4h later, cells were harvested and stained for cell surface markers (Table 7.S1). Again, the combination of CD56, CD54 and CXCR6 were used to define lymphoid tissue NK cells.

After FACS purification of NK cell subsets from marrow (n=2) or spleen (n=1), sufficient cell numbers to perform a chromium release assay were only obtained for lymphoid tissue NK and CD56<sup>dim</sup> NK cells. After overnight culture in the absence or presence of IL15 (10ng/ml), their cytotoxicity against K562 cells was evaluated in a 4h chromium release assay as previously described<sup>242</sup>.

### Statistics

For each cell surface marker, Z-scores were calculated using the average expression (percentage or geomean of fluorescence intensity) of each NK cell subset per tissue. A heat map was generated from the collective data by unsupervised hierarchical clustering using MultiExperimentViewer (v4.9) software<sup>260</sup>. Statistical tests were performed and graphs were built in GraphPad Prism software (v6.07, GraphPad, La Jolla, CA, US). Paired t tests were applied for the comparison of NK cell populations within the same tissue and between paired blood and marrow samples. Unpaired t tests were used to compare NK cell populations between different tissues. P values <0.05 were considered statistically significant. This threshold was adjusted using Bonferroni correction to correct for multiple testing of phenotypic markers.

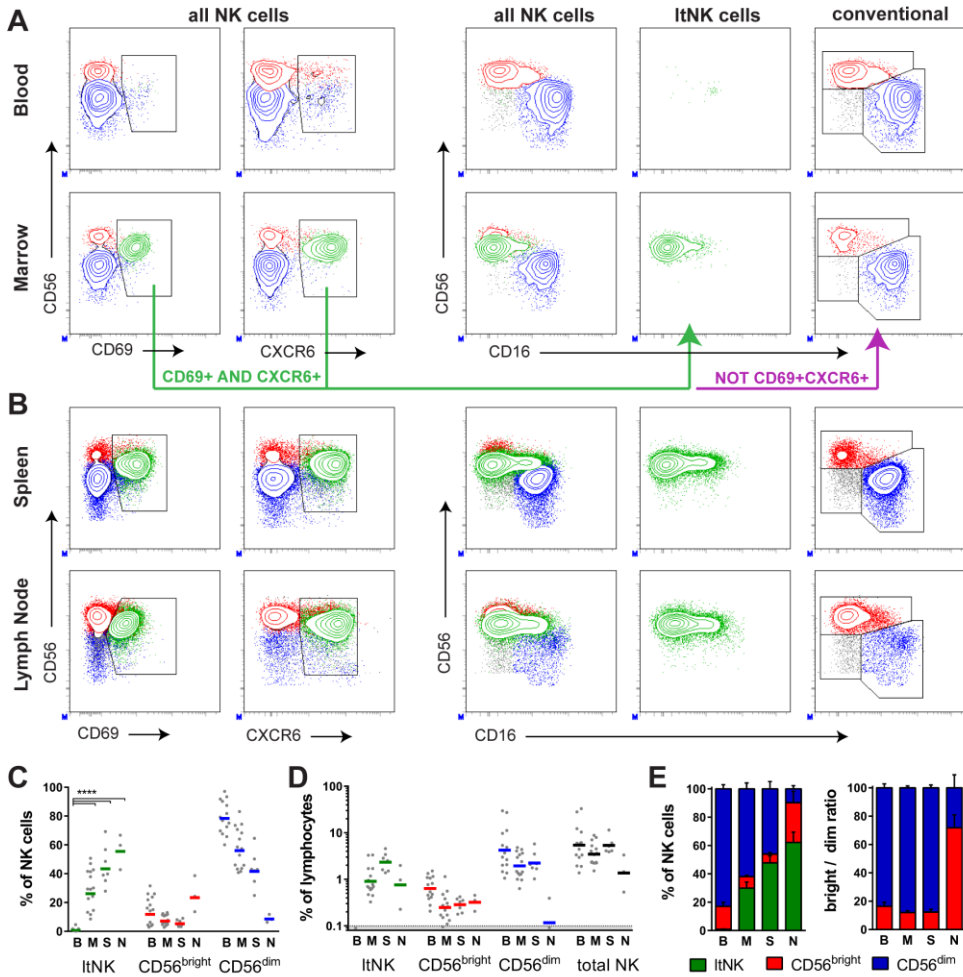


**Figure 7.1. Identification of lymphoid tissue NK cells.**

**(A-B)** Flow cytometric analysis of NK cells from blood, marrow, spleen and lymph node. NK cells were defined as living CD45<sup>+</sup>CD19<sup>-</sup>CD3<sup>+</sup>CD7<sup>+</sup> lymphocytes expressing CD56 and/or CD16, but not high levels of CD117 (see Methods for gating strategy). Within total NK cells, CD69<sup>+</sup>CXCR6<sup>+</sup> lymphoid tissue NK cells (ItNK, green) were first selected by gating cells with the combined expression of CD69 and CXCR6. From the remaining NK cells, the expression levels of CD56 and CD16 were used to define the conventional CD56<sup>bright</sup>CD16<sup>+/+</sup> (red) and CD56<sup>dim</sup>CD16<sup>+</sup> (blue) NK cell populations.

**(C-D)** Percentage of ItNK and conventional CD56<sup>bright</sup> and CD56<sup>dim</sup> NK cells in blood (B, n=17), marrow (M, n=17), spleen (S, n=7) and lymph node (N, n=3) expressed as **(C)** percentage of total NK cells and **(D)** percentage of total lymphocytes. Lines: geomean. Shaded area: below limit of detection. Statistics: paired t test (blood vs. marrow) or unpaired t test (other comparisons). \*\*\*\*: p-value <0.0001.

**(E)** Ratio of all NK cell subsets (left panel) and ratio between conventional CD56<sup>bright</sup> and CD56<sup>dim</sup> NK cells (right panel) in blood, marrow, spleen and lymph node. Bars: mean +/- SEM.

## Results

### Identification of CD69<sup>+</sup>CXCR6<sup>+</sup> lymphoid tissue NK cells

We evaluated human NK cells in blood and marrow to identify tissue specific expression patterns of chemokine receptors, adhesion molecules and NK cell receptors. A major NK cell population, identified by the combined expression of CD69 and CXCR6, was present in marrow in addition to the conventional CD56<sup>bright</sup> and CD56<sup>dim</sup> NK cell subsets (Figure 7.1A). The CD69<sup>+</sup>CXCR6<sup>+</sup> NK cell population was also observed in spleen and lymph node, but absent from blood (Figure 7.1A-B). Therefore, this population is further denoted as lymphoid tissue NK (LtNK) cells. In blood, single positive CXCR6<sup>+</sup> CD56<sup>bright</sup> (mean 12%) and CD56<sup>dim</sup> (mean 5%) NK cells were present, while very few circulating NK cells expressed CD69 (Figure 7.S1B).

CD69<sup>+</sup>CXCR6<sup>+</sup> lymphoid tissue NK cells represented 9-51% (mean 29%) of NK cells in marrow, 28-69% (mean 45%) of NK cells in spleen and 43-67% (mean 56%) of NK cells in lymph node (Figure 7.1C). The relative contribution of NK cells to the lymphocyte compartment varied between the investigated tissues. LtNK cells represented 0.9%, 2.3% and 0.8% (geomean) of lymphocytes in marrow, spleen and lymph node, respectively (Figure 7.1D).

Although CD56<sup>bright</sup> NK cells are considered to be enriched in lymphoid tissues, the ratio between conventional CD56<sup>bright</sup> and CD56<sup>dim</sup> NK cells in marrow and spleen turned out to be comparable to blood when LtNK cells were regarded as a separate population. In lymph node, however, CD56<sup>bright</sup> NK cells remained the predominant NK cell population when LtNK cells were analyzed separately (Figure 7.1E).

### Phenotype of lymphoid tissue NK cells

To further define the position of LtNK cells in NK cell development and differentiation, we evaluated their cell surface receptor expression profile in comparison to the conventional NK cell subsets (Figure 7.2A-B; Figure 7.S1B). For each NK cell subset, the expression profile of cell surface markers was similar in all tissues analyzed (Figure 7.2B; Figure 7.S1B). Compared to the conventional NK cells, LtNK cells expressed intermediate levels of CD56 and 4-43% (mean 18%) of LtNK cells expressed CD16. Besides CD69 and CXCR6, LtNK cells expressed high levels of the natural cytotoxicity receptor NKP46 and ICAM-1 (CD54). TNF receptor superfamily member CD27 was expressed by a large proportion (mean 66%) of LtNK cells and the chemokine receptor CCR5 was expressed by 18-71% (mean 37%) of LtNK cells (Figure 7.2; Figure 7.S1B).

Subsequently, we evaluated the expression of NK cell differentiation markers. In contrast to CD56<sup>bright</sup> NK cells, LtNK cells did not express the early differentiation markers c-kit (CD117) and IL7R $\alpha$  (CD127), distinguishing LtNK cells from immature NK cells and type 3 innate lymphoid cells (ILC)<sup>91,259</sup>. Furthermore, like CD56<sup>bright</sup> and CD56<sup>dim</sup> NK cells, LtNK cells expressed the transcription factor EOMES (data not shown). The inhibitory receptor NKG2A, which is lost during NK cell differentiation<sup>95,254</sup>, was expressed by a mean of 62% of LtNK cells, between the proportion of NKG2A<sup>+</sup> CD56<sup>bright</sup> and NKG2A<sup>+</sup> CD56<sup>dim</sup> NK cells (Figure 7.2; Figure 7.S1B). LtNK cells did not express CX3CR1, which is expressed by all CD56<sup>dim</sup> NK cells. Only a small proportion of LtNK cells expressed KIRs, KLRG1, CD57 and NKG2C (mean 5%, 4%, 0% and

2%, respectively, Figure 7.2; Figure 7.S1B). Together, these data indicate that ltNK cells have a mature phenotype but do not express markers acquired late in differentiation.

The activation markers NKp30 and NKG2D were uniformly expressed on all NK cell subsets. In contrast, ltNK cells expressed the activating receptor DNAM-1 in a bimodal fashion. Whereas DNAM-1 was expressed by all circulating NK cells, only 20-70% (mean 42%) of ltNK cells expressed DNAM-1 (Figure 7.2; Figure 7.S1B).

Next, we evaluated the expression of molecules associated with tissue localization of NK cells. LtNK cells did not express the adhesion molecule CD49a, distinguishing them from memory-like liver resident NK cells<sup>261</sup>. In contrast to tonsillar NK cells<sup>262,263</sup>, ltNK cells did not express the adhesion molecule CD103. Furthermore, the natural cytotoxicity receptor NKp44 was only expressed by a small minority of ltNK cells. Finally, the expression of chemokine receptor CXCR4 did not differ from the conventional NK cell subsets (Figure 7.2B; Figure 7.S1B). Together, based on these phenotypic criteria, ltNK cells represent a mature NK cell population which is uniform between the tissues and distinct from both conventional NK cell subsets.

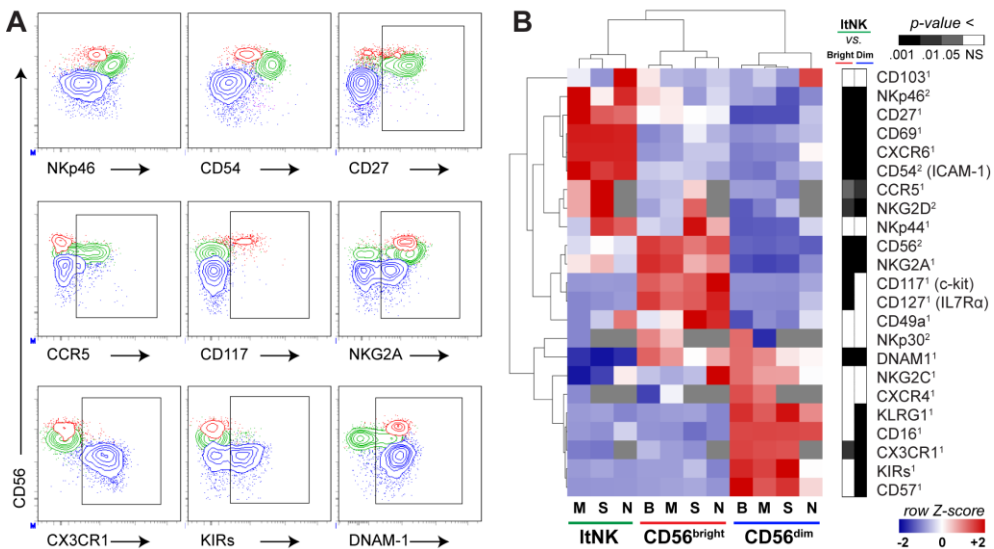


**Figure 7.2. Phenotype of NK cell subsets.**

**(A)** Selection of density plots showing cell surface marker expression on NK cells from marrow of a representative donor (HD17). Subsets: ltNK cells (green), CD56<sup>bright</sup> NK cells (red) and CD56<sup>dim</sup> NK cells (blue).

**(B)** Heat map generated from collective flow cytometry data by unsupervised hierarchical clustering. Z-scores were calculated using the average expression (<sup>1</sup>: percentage of subset or <sup>2</sup>: geomean of fluorescence intensity) of each cell surface marker on ltNK cells, CD56<sup>bright</sup> and CD56<sup>dim</sup> NK cells from blood (B, n=10-17), marrow (M, n=10-17), spleen (S, n=5-7) and lymph node (N, n=3). The side bar represents p-values of the comparison of ltNK cells with CD56<sup>bright</sup> (left) and CD56<sup>dim</sup> NK cells (right) from marrow. Statistics: paired t test. P-values <0.001 (black) remain statistically significant after Bonferroni correction for multiple testing. For gating strategy and bulk flow cytometry data: see Methods and Figure 7.S1B.



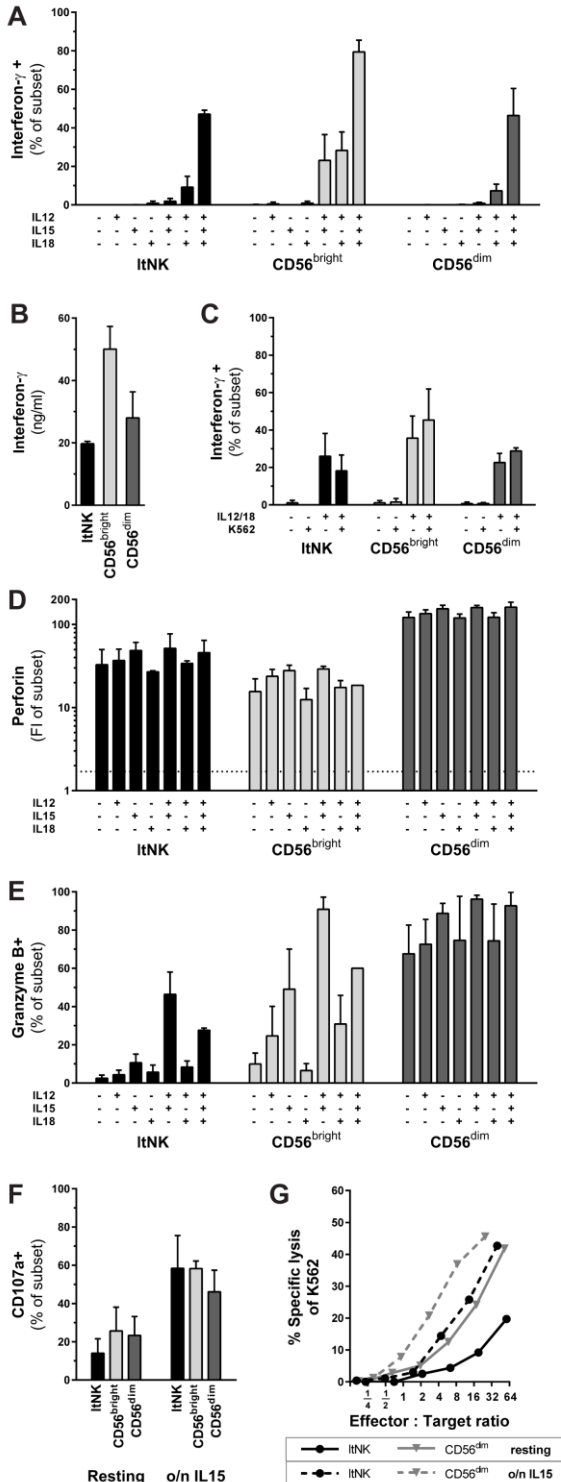


**Figure 7.3. Functional properties of NK cell subsets.**

(A, C) Intracellular expression of interferon- $\gamma$  of lymphoid tissue NK cells (ItNK), CD56<sup>bright</sup>CD16<sup>+</sup> NK cells and CD56<sup>dim</sup>CD16<sup>+</sup> NK cells. Mononuclear cells (MNC) from marrow (n=3) were cultured for 16-18h in absence or presence of (combinations of) IL12, IL15 or IL18. For (C), MNC from marrow (n=4) were cultured overnight, K562 cells and cytokines (IL12+IL18) were added for the last 6h of culture.

(B) Interferon- $\gamma$  production of FACS purified ItNK, CD56<sup>bright</sup> and CD56<sup>dim</sup> NK cells from marrow (n=3) upon 16-18h stimulation with IL12, IL15 and IL18. Shown is the interferon- $\gamma$  concentration in supernatant after subtraction of unstimulated cells.

(D-E) Intracellular expression of perforin and granzyme B of ItNK, CD56<sup>bright</sup> and CD56<sup>dim</sup> NK cells. MNC from marrow (n=3) were cultured for 16-18h in absence or presence of (combinations of) IL12, IL15 or IL18. FI: geomean of Fluorescence Intensity. Dotted line: FI of B cells (negative control).

(F) Degranulation of ItNK, CD56<sup>bright</sup> and CD56<sup>dim</sup> NK cells. Resting and overnight (o/n) IL15 activated MNC from marrow (n=6) were co-cultured with K562 cells for 4 hours. Shown is the percentage of CD107a<sup>+</sup> NK cells after subtraction of CD107a expression of NK cells cultured without K562 cells. Bars: mean +/- SD (A-F). See Figure 7.S3 for representative flow cytometry plots and Methods for gating strategy.

(G) Specific lysis of K562 cells in chromium release assay by resting (solid lines) and o/n IL15 activated (dashed lines) FACS purified ItNK cells (black, circles) and CD56<sup>dim</sup> NK cells (grey, triangles) from marrow. Representative graph of three experiments.

## Functional properties of lymphoid tissue NK cells

To determine the functional properties of ltNK cells, we compared their cytokine production and cytotoxicity with the conventional CD56<sup>bright</sup> and CD56<sup>dim</sup> NK cells. Results obtained with marrow derived NK cells are described here, but similar results were obtained with the NK cells from spleen and blood (Figure 7.S3).

After overnight stimulation with IL12+IL15, IL12+IL18 and IL12+IL15+IL18, respectively, a mean of 2%, 9% and 47% of ltNK cells produced IFN- $\gamma$ , which was comparable to the cytokine production of CD56<sup>dim</sup> NK cells. In contrast, 23%, 28% and 79% (mean) of the CD56<sup>bright</sup> NK cells produced IFN- $\gamma$  upon these stimuli (ltNK vs. CD56<sup>dim</sup> : NS, ltNK vs. CD56<sup>bright</sup> :  $p < 0.0001$ , Figure 7.3A and Figure 7.S3A). This was confirmed by an IFN- $\gamma$  secretion of 20, 50 and 28 ng/ml after IL12+IL15+IL18 stimulation of FACS purified ltNK, CD56<sup>bright</sup> and CD56<sup>dim</sup> NK cells (ltNK vs. CD56<sup>bright</sup> :  $p = 0.019$ , ltNK vs. CD56<sup>dim</sup> : NS, Figure 7.3B).

Co-culture of resting NK cells with K562 cells did not result in detectable intracellular IFN- $\gamma$  production. However, in the presence of IL12 and IL18, co-culture with K562 cells resulted in a (non-significant) increase in IFN- $\gamma$  production by CD56<sup>bright</sup> and CD56<sup>dim</sup> NK cells compared to cytokines alone. In contrast, IFN- $\gamma$  production of IL12+IL18 activated ltNK cells was not increased upon co-culture with K562 cells (Figure 7.3C).

To assess the cytolytic potential of ltNK cells, we first evaluated the expression of perforin and granzyme B. In resting state, ltNK cells expressed perforin at levels intermediate to CD56<sup>bright</sup> and CD56<sup>dim</sup> NK cells (ltNK vs. CD56<sup>bright</sup> :  $p < 0.01$ , ltNK vs. CD56<sup>dim</sup> :  $p < 0.0001$ , Figure 7.3D). In contrast to CD56<sup>dim</sup> NK cells, resting ltNK and CD56<sup>bright</sup> NK cells hardly expressed granzyme B (ltNK vs. CD56<sup>bright</sup> : NS, ltNK vs. CD56<sup>dim</sup> :  $p < 0.0001$ , Figure 7.3E). After overnight activation by IL12 and IL15, 46% (mean) of ltNK cells expressed granzyme B whereas the expression of granzyme B was upregulated in the majority of CD56<sup>bright</sup> NK cells (Figure 7.3D-E; Figure 7.S3B). Although with a slightly higher perforin and lower granzyme B expression, the cytolytic protein expression profile of ltNK was most comparable to CD56<sup>bright</sup> NK cells.

In CD107a based degranulation assays, a mean of 13% of resting ltNK cells externalized CD107a upon co-culture with K562 cells. Degranulation was increased to 60% after prior overnight IL15 activation. Both in rest and after pre-activation, the proportion of ltNK cells that externalized CD107a did not differ significantly from both CD56<sup>bright</sup> and CD56<sup>dim</sup> NK cells (Figure 7.3F; Figure 7.S3C).

Finally, we evaluated the lysis of K562 cells using FACS purified ltNK and CD56<sup>dim</sup> NK cells. Compared to CD56<sup>dim</sup> NK cells, ltNK cells had a low cytotoxicity in resting state. In line with the cytolytic protein expression profile and degranulation, their cytolytic capacity increased after overnight IL15 activation (Figure 7.3G). Altogether, ltNK cells produce IFN- $\gamma$  at levels comparable to CD56<sup>dim</sup> NK cells. In line with the functional properties of CD56<sup>bright</sup> NK cells, ltNK cells have a low natural cytotoxicity which is enhanced upon short-term activation.

## Reconstitution of lymphoid tissue NK cells after hematopoietic stem cell transplantation

Next, we evaluated the reconstitution of NK cell subsets in bone marrow after hematopoietic stem cell transplantation. Expressed as a percentage of NK cells, ItNK cells gradually increased towards healthy donor levels in the year after HSCT (Figure 7.4A). However, expressed semi-quantitatively as a percentage of lymphocytes, ItNK cells reached healthy donor levels at the third month after HSCT to remain stable thereafter (Figure 7.4B). This reconstitution profile differed significantly from the hyper-expansive reconstitution of conventional NK cells. The reconstitution of CD56<sup>bright</sup> and CD56<sup>dim</sup> NK cells in marrow mirrored their reconstitution in blood (data not shown and <sup>216,237</sup>). Conventional NK cells reached the highest levels at 1 month (CD56<sup>bright</sup>) and 3-6 months (CD56<sup>dim</sup>) after HSCT and gradually decreased to healthy donor levels at one year after HSCT. In conclusion, ItNK cells are not subjected to the hyper-expansion early after HSCT as observed for both conventional NK cell populations.

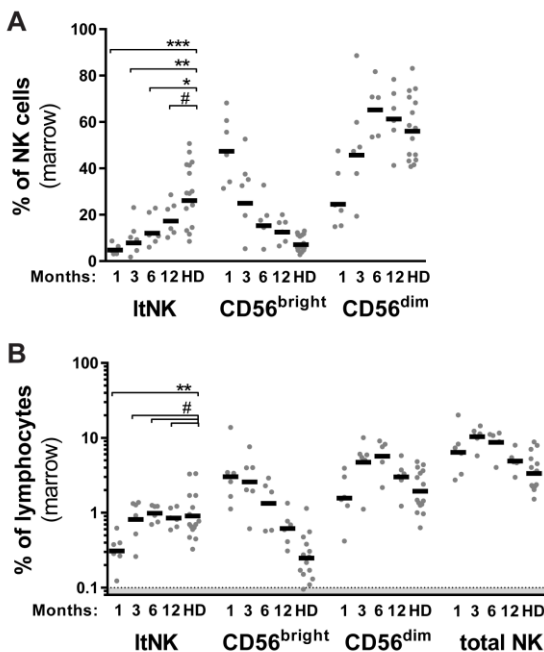


**Figure 7.4. Reconstitution of NK cell subsets in marrow after hematopoietic stem cell transplantation.**

Reconstitution of lymphoid tissue NK cells (ItNK) cells and conventional CD56<sup>bright</sup> and CD56<sup>dim</sup> NK cells in marrow at 1, 3, 6 and 12 months after pediatric allogeneic hematopoietic stem cell transplantation (HSCT), expressed as **(A)** percentage of total NK cells and **(B)** percentage of total lymphocytes. Lines: geometric mean. Shaded area: below limit of detection. Statistics: unpaired t test comparing the % of ItNK cells between HSCT recipients (n=6) and healthy donors (HD, n=17). For % of lymphocytes, data were log-transformed. #: p-value  $\geq 0.05$ , \*: p<0.05, \*\*: p<0.01, \*\*\*: p<0.001. See Methods for gating strategy.

## Discussion

Based on the co-expression of the tissue retention marker CD69 and chemokine receptor CXCR6, we identified a novel NK cell population in human lymphoid tissues (ItNK). With respect to their surface marker expression profile, these cells constitute a population which is distinct from the conventional CD56<sup>bright</sup> and CD56<sup>dim</sup> NK cell subsets. Functionally, ItNK cells share features with both CD56<sup>bright</sup> and CD56<sup>dim</sup> NK cells. In addition, ItNK cells have their own reconstitution kinetics after HSCT.

Lymphoid tissues are often considered to be enriched for CD56<sup>bright</sup> NK cells. However, this is only based on the expression pattern of CD56 and CD16<sup>90;107;108;256;257</sup>. Our data provide evidence that ItNK cells are not just a subpopulation of either of the conventional NK cell populations. The expression of the C-type lectin CD69 on ItNK cells is in line with their tissue residency. Although initially identified as an early lymphocyte activation marker<sup>264-266</sup>, CD69 has been recognized to play an important role in tissue retention<sup>267;268</sup>. In B- and T-cells, the expression of CD69 is inversely correlated with the expression of sphingosine-1-phosphate receptor 1, thereby inhibiting lymphocyte egress from tissues along the gradient of sphingosine-1-phosphate<sup>267;268</sup>.

The G-protein coupled chemokine receptor CXCR6 is often associated with liver resident lymphocytes<sup>269</sup>, but is also enriched on bone marrow resident CD69<sup>+</sup> memory T cells<sup>270</sup>. A recent report showed that the majority of CD56<sup>bright</sup> NK cells in human liver expresses CD69 or CXCR6<sup>271</sup>. Murine CXCR6<sup>+</sup>CD49a<sup>+</sup> liver resident NK cells display memory-like features; however, only few NK cells in human liver display the homologous CD49a<sup>+</sup>NKG2C<sup>+</sup>KIR<sup>+</sup> phenotype<sup>261;272;273</sup>. Similar to most liver NK cells, lymphoid tissue NK cells do not express CD49a, NKG2C or KIRs. As a consequence, it cannot be excluded that a population with a phenotype comparable to ItNK cells might also be present in human liver. Whether CXCR6 is associated with memory generation in human NK cells requires further investigation.

Strikingly, ItNK cells have a bimodal expression pattern of the activating NK cell receptor DNAM-1. DNAM-1 is involved in adhesion and immune synapse formation and has been shown to play an important role in the control of cytotoxicity<sup>274-277</sup>. A bimodal expression pattern of DNAM-1 on human NK cells has only been reported in bone marrow of myelodysplastic syndrome patients and in liver<sup>271;278</sup>. The high surface expression intensity of the activating NK cell receptor NKp46 on ItNK cells is in line with the description of NKp46<sup>bright</sup> NK cells in lymph node and spleen<sup>257</sup>. Moreover, an enrichment of CD27<sup>+</sup> NK cells was previously reported in human spleen<sup>279</sup>. Although these observations are likely to be a representation of the presence of ItNK cells in these organs, we are the first to use specific markers to discriminate the tissue resident NK cell population from conventional NK cells.

Like conventional NK cells, ItNK cells can be distinguished from helper-ILC1 through their expression of perforin and transcription factor EOMES, as well as from ILC2 and ILC3 by their lack of CD117 and CD127 expression<sup>89</sup>. Lymphoid tissue NK cells produced relatively low levels of IFN- $\gamma$ , similar to CD56<sup>dim</sup> NK cells and required prior stimulation to exert cytotoxicity. Together with the low expression of DNAM-1<sup>276;277</sup>, this gives the impression that ItNK cells may be a hypo-functional NK cell population. Possibly, these cells have an immunomodulatory function within the lymphoid tissues to bridge innate and adaptive immunity, rather than that they

exert one of the classical NK cell functions. In addition to their distinct phenotype and functional profile, the reconstitution pattern of ltNK cells after HSCT differs from that of the conventional NK cell subsets. Together, these arguments argue against the hypothesis that ltNK cells only represent a transient tissue equivalent of CD56<sup>bright</sup> or CD56<sup>dim</sup> cells trafficking through tissues. Our data do not allow for firm conclusions regarding the ontogeny of ltNK cells and their relation to the conventional NK cell populations. The lack of both very early (CD117, CD127) and late (CD57, KLRG1, NKG2C) NK cell receptors suggest that ltNK cells could represent a developmental intermediate between CD56<sup>bright</sup> and CD56<sup>dim</sup> NK cells. However, the distinct expression pattern of the markers NKp46, CD54 and DNAM-1 argues against this linear relationship. Alternatively, ltNK cells may constitute a separate tissue specific NK cell lineage, and develop independently from the circulating NK cells.

While knowledge on human NK cell biology is mainly derived from circulating CD56<sup>bright</sup> and CD56<sup>dim</sup> NK cells, lymphoid tissues contain the majority of human NK cells<sup>255</sup>. Importantly, our data indicate that lymphoid tissues are populated by a third distinct population of NK cells in addition to the conventional CD56<sup>bright</sup> and CD56<sup>dim</sup> NK cells. The identification of this specific lymphoid tissue resident NK cell population provides tools to further study cellular interactions of these NK cells in the lymphoid tissue microenvironment and their role in the regulation of immune responses.

## Acknowledgements

The authors thank G.M de Roo (LUMC department of Hematology) for his expert FACS sorting assistance, and Prof. Dr. H. Pircher (Universitätsklinikum Freiburg, Freiburg, Germany) for the kind gift of the  $\alpha$ -KLRG1 antibody 13F12F2.

## Funding and Disclosures

Research was financially supported with a grant from the Dutch Cancer Society (#UL 2011-5133). G.L. was supported by a Leiden University Medical Center MD/PhD fellowship

## Supplemental data

CD designation	Alternative name	Fluorochrome	Type	Clone	Company	Catalog#	Staining step
CD184	CXCR4	Unconjugated	m-IgG2b	44716	R&D	MAB172	Primary
CD186	CXCR6	Unconjugated	m-IgG2b	56811	R&D	MAB699	Primary
CD195	CCR5	Unconjugated	m-IgG2b	45531	R&D	MAB182	Primary
n/a	Isotype m-IgG2b	Unconjugated	m-IgG2b	DAK-GO9	DAKO	X0944	Primary
n/a	Goat $\alpha$ m-IgG2b	AF488	polyclonal		Invitrogen	A21141	Secondary
n/a	Goat $\alpha$ m-IgG2b	AF647	polyclonal		Invitrogen	A21242	Secondary
n/a	Goat $\alpha$ m-IgG2b	PE	polyclonal		Southern	1092-09	Secondary
CD003	CD3	BV421	m-IgG1	UCHT1	BD	562426	Direct
CD004	CD4	PE-Cy5.5	m-IgG1	13B8.2	BC	B16491	Direct
CD007	GP40	AF700	m-IgG1	M-T701	BD	561603	Direct
CD008	CD8	BV510	m-IgG1	SK1	BD	563919	Direct
CD014	CD14	PE	m-IgG1	M $\phi$ P9	BD	342408	Direct
CD014	CD14	PE-Cy7	mIgG2a	M5E2	BD	557742	Direct
CD016	Fc $\gamma$ RIII	BV711	m-IgG1	3G8	BD	563127	Direct
CD019	CD19	BV510	m-IgG1	SJ25C1	BD	562947	Direct
CD019	CD19	APC	m-IgG1	J3.119	BC	IM2470	Direct
CD020	MS4A1	PE-Cy7	m-IgG1	L27	BD	335828	Direct
CD027	TNFRSF7	APC	m-IgG1	L128	BD	337169	Direct
CD033	SIGLEC3	PE	m-IgG1	P67.6	BD	345799	Direct
CD045	PTPRC	PE-Cy5.5	m-IgG1	J33	BC	A54139	Direct
CD045	PTPRC	FITC	m-IgG1	2D1	BD	342408	Direct
CD049a	ITGA1	PE	m-IgG1	TS2/7	Biologend	328304	Direct
CD054	ICAM1	PE	m-IgG1	HA58	BD	555511	Direct
CD056	NCAM1	ECD	m-IgG1	N901	BC	A82943	Direct
CD056	NCAM1	ECD	m-IgG1	N901	BC	A82943	Direct
CD057	B3GAT1	FITC	m-IgM	HNK1	BD	347393	Direct
CD069	EA-1	FITC	m-IgG1	L78	BD	347823	Direct
CD069	EA-1	PE-Cy7	m-IgG1	L78	BD	347823	Direct
CD103	ITGAE	FITC	m-IgG1	BER-ACT8	DAKO	F7138	Direct
CD117	c-kit	PE	m-IgG1	104D2	BD	332785	Direct
CD127	IL7 $\alpha$	FITC	m-IgG1	eBioRDR5	eBioscience	11-1278	Direct
CD158a/h <sup>1</sup>	KIR2DL1 DS1	PE <sup>1</sup>	m-IgG1	EB6	BC	A09778	Direct
CD158b/j <sup>1</sup>	KIR2DL2/3 DS2	PE <sup>1</sup>	m-IgG1	GL183	BC	IM2278U	Direct
CD158e <sup>1</sup>	KIR3DL1	PE <sup>1</sup>	m-IgG1	DX9	BD	555967	Direct
CD158i <sup>1</sup>	KIR2DS4	PE <sup>1</sup>	m-IgG1	FES172	BC	IM3337	Direct
CD159a	NKG2A	PE	m-IgG2b	z199	BC	IM3291U	Direct
CD159c	NKG2C	APC	m-IgG1	134591	R&D	FAB138A	Direct
CD226	DNAM1	FITC	m-IgG1	DX11	BD	559788	Direct
CD235a	GPA	PE	m-IgG1	11E4B-7-6	BC	A07792	Direct
CD314	NKG2D	APC	m-IgG1	1D11	BD	558071	Direct
CD335	NKp46	PE	m-IgG1	BAB281	BC	IM3711	Direct
CD336	NKp44	PE	m-IgG1	Z231	BC	IM3710	Direct
n/a	KLRG1 <sup>2</sup>	AF488	m-IgG2a	13F12F2	n/a <sup>2</sup>	n/a <sup>2</sup>	Direct
n/a	CX3CR1	PE	r-IgG2b	2A9-1	Biologend	341604	Direct
n/a	Isotype m-IgG1	APC	m-IgG1	15H6	BC	731586	Direct
n/a	Isotype m-IgG1	FITC	m-IgG1	15H6	BC	731583	Direct
n/a	Isotype m-IgM	FITC	m-IgM	R4A3-22-12	BC	6602434	Direct
n/a	Isotype m-IgG1	PE	m-IgG1	X40	BD	345816	Direct
n/a	Isotype m-IgG2a	PE	m-IgG2a	X39	BD	349053	Direct
n/a	Granzyme B	AF700	m-IgG1	GB11	BD	557971	Intracellular
n/a	Interferon- $\gamma$	FITC	m-IgG1	4S.B3	BD	554551	Intracellular
n/a	Perforin	FITC	m-IgG2b	delta G9	Ancell	358-040	Intracellular
CD107a	LAMP1	FITC	m-IgG1	H4A3	BD	555800	In Culture

**Table 7.S1 (previous page). Antibodies used for flow cytometry.**

<sup>1</sup>All four PE-conjugated  $\alpha$ -KIR antibodies were combined in a pan-KIR staining.

<sup>2</sup> $\alpha$ -KLRG1 antibody was kindly provided by Prof. H. Pircher (Universitätsklinikum Freiburg, Freiburg, Germany)

CD: Cluster of differentiation. n/a: not applicable. m: mouse, r: rat.

*Fluorochromes:* AF: Alexa Fluor, APC: Allophycocyanin, BV: Brilliant Violet, ECD: Energy Coupled Dye (=Phycoerythrin-Texas Red conjugate), FITC: Fluorescein isothiocyanate, PE: Phycoerythrin, PE-Cy5.5: Phycoerythrin-Cyanine5.5 conjugate, PE-Cy7: Phycoerythrin-Cyanine7 conjugate.

*Companies:* AnceLL: AnceLL Corporation (Bayport, MN, USA), BC: Beckman Coulter (Brea, CA, USA), BD: Becton Dickinson Biosciences (San Jose, CA, USA), Biolegend: Biolegend (San Diego, CA, USA), DAKO: Dako Denmark, (Glostrup, Denmark), eBioscience: eBioscience (San Diego, CA, USA), Invitrogen: Invitrogen (Thermo Fisher Scientific, Waltham, MA, USA), R&D: R&D Systems (Minneapolis, MN, USA), Southern: Southern Biotech (Birmingham, AL, USA).

**Figure 7.S1 (next pages).****(A) Gating strategy for NK cells**

First, DAPI negative, non-doublet, CD45+CD19-CD3-CD7+ lymphocytes were selected (gate 1-6). Then, NK cells were defined as cells expressing CD56 and/or CD16 but not high levels of CD117 (gate 7-8). Using this strategy, type 3 innate lymphoid cells (ILC3) or immature NK cells (mainly present in lymph node, see ref 24 and 25) were excluded. Shown are density plots from marrow of a representative donor (HD17)

**(B) Flow cytometry data of cell surface marker expression.**

Left panels summarize the expression of surface markers on lymphoid tissue NK (ltNK, green) cells as well as conventional CD56<sup>bright</sup> (red) and CD56<sup>dim</sup> (blue) NK cells from blood (B, n=10-17, open bars), marrow (M, n=10-17, diagonally hatched bars), spleen (S, n=5-7, horizontally hatched bars) and lymph node (N, n=3, checkered bars). Expression: % positive (bimodal expression) or geomean of fluorescence intensity (FI, continuous expression). Bars: mean +/- SD. x: subset not present in blood, na: not assessed. Dashed line: isotype control FI.

In the right panels, a representative density plot displays the expression of each cell surface marker (X-axis) plotted against CD56 (Y-axis) on NK cells from marrow. Density plots are from healthy donor 16 (HD16), except for NKG2D (HD15), NKG2C (HD18), NKp30 (HD22), CXCR4 and CCR5 (HD6). See methods, Figure 7.S1A and Figure 7.1 for gating strategy.







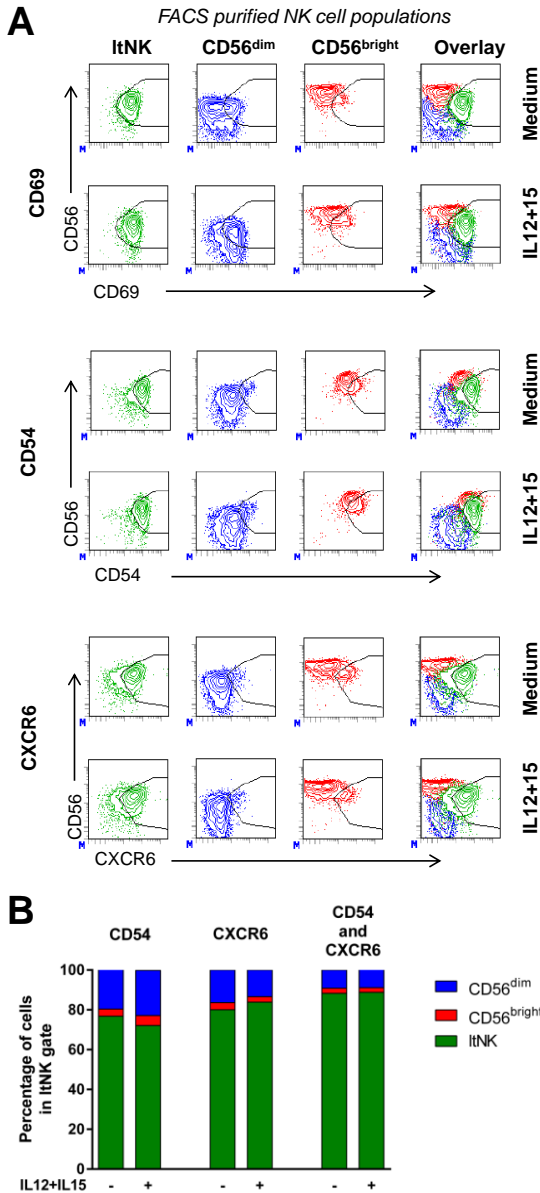


**Figure 7.S2. Validation of the use of CXCR6 and CD54 to identify ItNK cells after culture.**

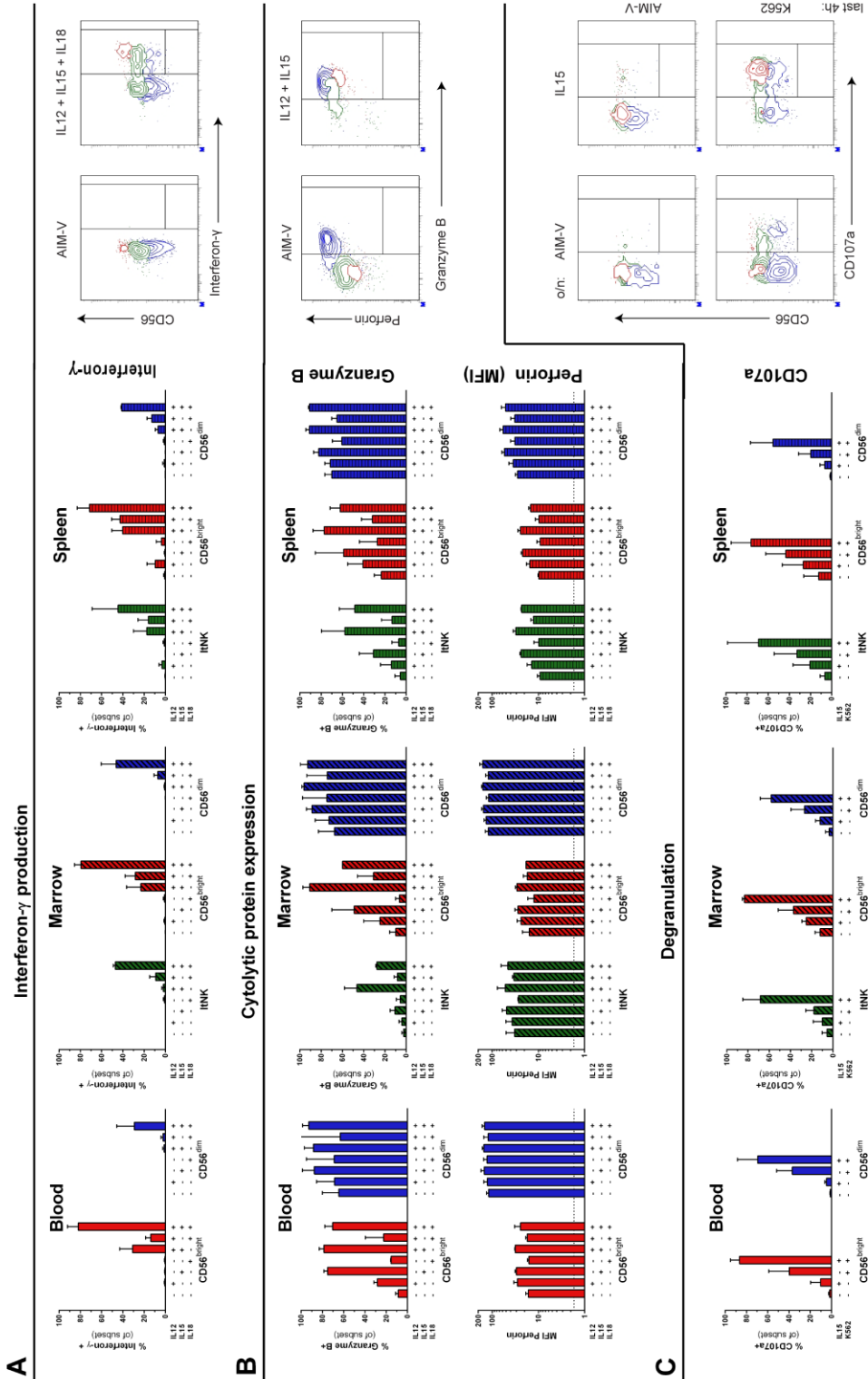
MACS-enriched NK cells from marrow were stained for cell surface markers and the three NK cell populations were FACS-sorted (see methods). Sorted NK cell populations were cultured for 18h with or without cytokines and stained for the expression of CD56 (PE-Cy5.5, BC), CD69 (PE-Cy7, BD), CD54 (PE, BD) and CXCR6.

(A) Individual density plots display the expression of CD69 (top), CD54 (middle) and CXCR6 (bottom) of FACS purified NK cell populations in rest (medium) or after activation (IL12+IL15). In the right column, composed overlay figures are shown. Gates are drawn as applied for the functional (intracellular staining) experiments.

(B) The percentage of contamination by CD56<sup>bright</sup> and CD56<sup>dim</sup> NK cells included within the lymphoid tissue NK cell (ItNK) gate if only CD54, only CXCR6 or a combination of CD54 and CXCR6 are used to define ItNK cells. Percentages were calculated from the original composition. The combined use of CD56, CD54 and CXCR6 to define ItNK cells results in 90% purity.

**Figure 7.S3 (next page). Functional properties of NK cell subsets from blood, marrow and spleen.**

Intracellular expression of (A) interferon- $\gamma$  and (B) perforin and granzyme B of NK cells from blood (n=3), marrow (n=3) and spleen (n=3) cultured for 16-18h in absence or presence of (combinations of) IL12, IL15 or IL18. Representative density plots display NK cells from marrow of HD6. (C) Degranulation (CD107a externalization) of resting and overnight (o/n) IL15 activated NK cells from blood (n=6), marrow (n=6) and spleen (n=4) cultured for 4h with or without K562 cells. Representative density plots display NK cells from marrow of HD7. Evaluated subsets: lymphoid tissue NK (ItNK) cells (green), CD56<sup>bright</sup>CD16<sup>+/-</sup> NK cells (red) and CD56<sup>dim</sup>CD16<sup>+/-</sup> NK cells (blue). Bars: mean  $\pm$  SD. See Methods for gating strategy.





# **Chapter 8**

## **Summary**

## Summary

**Chapter 1** provides the reader with basic background information regarding hematopoietic stem cell transplantation and viral complications after HSCT, as well as the clinical importance and immunologic background of the reconstitution of T cell and NK cell immunity after HSCT.

In the **first part** (Chapter 2-4) of this thesis, the focus is on the interaction between viral reactivation and T cell reconstitution.

In **Chapter 2**, we provide evidence that early and transient CMV reactivation leaves a long-lasting, dynamic and specific signature on the composition of the T cell compartment in pediatric HSCT recipients. We evaluated the composition of the cellular immune system in 131 HSCT recipients, of which 46 experienced a CMV reactivation in the first months after transplantation. One year after HSCT, patients that had encountered (and cleared) early CMV reactivation showed a marked relative as well as absolute expansion of the late differentiated CD8<sup>+</sup> EM and EMRA T cell populations, followed by a contraction in the second year after HSCT. This typical pattern was not seen in patients with early EBV or HAdV reactivation. CMV reactivation did not have a significant impact on CD4<sup>+</sup> T cells and NK cell numbers at one year after HSCT. Importantly, early CMV reactivation did not compromise the reconstitution of the naive and central memory compartments required for a balanced immune system with a broad specificity.

In **Chapter 3**, we describe the development of a clinical grade method to select virus-specific T cells for the restoration of T cell immunity against CMV, EBV and HAdV in one single procedure. Because not all virus-specific T cells produce interferon- $\gamma$  upon activation, we sought for alternatives for the interferon- $\gamma$  capture assay. For this, we compared the upregulation of various activation markers upon stimulation with viral peptide pools and identified CD25 as a good candidate. The proportion of T cells that upregulated CD25 expression was 3-7 times higher than the proportion of T cells producing IFN- $\gamma$ , indicating that a larger proportion of virus-specific T cells could be isolated using this approach. As CD25 is highly expressed on regulatory T cells (Treg), the cell-product generated using this approach was not only enriched for virus-specific cells and depleted of alloreactive cells, but was also capable of suppressing alloreactivity *in vitro*.

In **Chapter 4**, the effectiveness of pre-emptive cidofovir treatment for human adenovirus viremia was evaluated in 42 HAdV reactivations after HSCT. Rapid HAdV load reduction and HAdV clearance during cidofovir treatment were associated with concomitant T cell reconstitution (n=20). In the absence of T cell reconstitution (n=22), the HAdV viremia was controlled in 75% of cidofovir treatments. Reduction of the HAdV load in the absence of T cells always coincided with a  $\geq 5$ -fold increase of NK cell numbers in the peripheral blood. In only 2 out of 6 cases with an absence of both NK and T cells, HAdV load stabilization was observed during a >3 weeks period of cidofovir treatment. These data underscore the importance of T cell reconstitution to control adenovirus infections and the need for more effective antiviral drugs. In addition, these

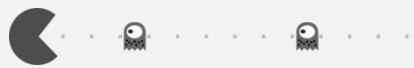
data are suggestive of a role for NK cells in the control of HAdV viremia when T cells are not present.

In the **second part** (Chapter 5-7) of this thesis, the focus is on NK cells.

**Chapter 5** addresses one of the restrictions of working with cryopreserved material. In freshly analyzed blood from healthy donors and HSCT recipients, the NK cell compartment consists of two subsets ( $CD56^{\text{bright}}CD16^{\text{+/-}}$  or  $CD56^{\text{dim}}CD16^{\text{+}}$ ). However, after cryopreservation of PBMC from HSCT recipients obtained in the first month after HSCT, a third NK cell subset appeared, which had a  $CD56^{\text{dim}}CD16^{\text{-}}$  phenotype. Because this artifact is only seen under specific conditions, these cells can be mistaken for an important and distinct NK cell population if flowcytometric results on biobanked material are not validated with freshly isolated PBMC.

In **Chapter 6**, the reconstitution of NK and T cells was evaluated in 93 pediatric allogeneic HSCT recipients treated for leukemia. Early after HSCT, an expansion of  $CD56^{\text{bright}}$  NK cells (>300 cells/ $\mu\text{l}$  blood) occurred in a subgroup of 38 patients characterized by a delayed T cell reconstitution. Post-transplant  $CD56^{\text{bright}}$  NK cells showed a high expression of inflammatory chemokine receptors and cutaneous lymphocyte antigen, but had a reduced expression of homeostatic chemokines. In contrast to healthy donor  $CD56^{\text{bright}}$  NK cells, post-transplant  $CD56^{\text{bright}}$  NK cells expressed granzyme B and were cytotoxic. Patients with  $CD56^{\text{bright}}$  NK cell expansion during delayed T cell reconstitution and patients with rapid T cell reconstitution had a similar clinical outcome. These data indicate that  $CD56^{\text{bright}}$  NK cells form a versatile cell population, which can expand and acquire additional effector functions when T cells are not present to exert their function.

In **Chapter 7**, we identified a novel NK cell population in human lymphoid tissues (ItNK) based on the co-expression of the tissue retention marker CD69 and the chemokine receptor CXCR6. This population represented 30-60% of NK cells in bone marrow (n=20), spleen (n=7) and lymph node (n=3), but was absent from peripheral blood. Their surface marker expression profile was distinct from the conventional  $CD56^{\text{bright}}$  and  $CD56^{\text{dim}}$  NK cell subsets. Functionally, ItNK cells produced interferon- $\gamma$  at levels comparable to  $CD56^{\text{dim}}$  NK cells. They constitutively expressed perforin, but like  $CD56^{\text{bright}}$  NK cells, they required pre-activation to express granzyme B and to exert cytotoxicity. After HSCT,  $CD69^{\text{+}}CXCR6^{\text{+}}$  lymphoid tissue NK cells showed a delayed reconstitution in comparison to conventional NK cell populations. The identification of this NK cell population in lymphoid tissues provides tools to further evaluate the cellular interactions and role of NK cells in human immunity.





# **Chapter 9**

## **General discussion and future perspectives**

In this chapter, the findings as described in this thesis and summarized in the previous chapter will be discussed in the context of the current literature and clinical perspective. First, the interaction of T cell reconstitution and viral infections after HSCT will be discussed. Then, pharmacological and adoptive immunotherapeutic interventions for the protection of viral infections in patients with a delayed T cell reconstitution will be addressed. Thirdly, the role of NK cells in patients lacking T cells will be reviewed. The fourth section of this chapter will focus on the novel lymphoid tissue NK cell population. Then, the possible relationship between the different human NK cell populations will be discussed. The concluding paragraph will summarize the main findings and implications of this thesis and provide perspectives for further research.

## 1 Interaction of viral infections and T cell reconstitution

Many studies have demonstrated the importance of the rapid reconstitution T cell immunity to achieve sustained control of viral reactivations after HSCT.<sup>37-39</sup> Eventually, T cell reconstitution occurs after every successful HSCT, but little is known about the influence of early viral infections on long term T cell reconstitution, which is addressed in Chapter 2.

The morbidity and mortality associated with herpesvirus infections after HSCT have dropped significantly in the last two decades as a result of the improved pre-emptive therapy. Still, the immunological impact of CMV infections remains an important subject of investigation. This attention is mainly driven by the relation between CMV reactivations and the reduced risk of acute myeloid leukemia (AML) relapse after HSCT.<sup>178;280</sup> Different mechanisms mediating this effect have been proposed. The first hypotheses are based on T cell responses: CMV-antigen presentation on CMV-infected AML blasts or cross reactivity between CMV antigens and tumor antigens both leading to leukemia-killing by (the abundantly present) CMV-specific CD8<sup>+</sup> T cells.<sup>178;281</sup> Alternatively, the anti-AML response can be mediated by NK cells as CMV infection leads to an increased expression of ligands for activating NK cell receptors on AML blasts, shifting the balance towards NK cell activation.<sup>129;282</sup>

The second reason for the persistent interest in CMV is the so-called “memory inflation”, initially observed in CMV seropositive elderly individuals.<sup>147;148</sup> Furthermore, CMV reactivations in solid organ transplant recipients receiving life-long immunosuppressive medication have been correlated to an accelerated and ongoing accumulation of late differentiated T-cells with a stable contribution of CMV-specific T cells.<sup>154;177</sup> This expansion of CMV-specific T cells is proposed to be induced by continuous or repetitive stimulation by (subclinical) CMV reactivations.<sup>283</sup> Memory inflation is associated with faster immunosenescence, increased systemic inflammation and a higher risk of cardiovascular disease.<sup>283</sup>

Investigation of the reconstitution of an immune system with an appropriate function and a broad repertoire after pediatric HSCT receives more attention nowadays as a consequence of the improved long term survival. After HSCT, CD8<sup>+</sup> T cell numbers continued to rise in the months following the clearance of CMV viremia. In the second year after HSCT, a regression of memory T cell numbers was observed (Chapter 2). These dynamics are comparable to the recently published observations of the impact of primary CMV infections in healthy children, as studied in the large Generation R study in Rotterdam.<sup>284;285</sup> Still, the magnitude of the T cell expansion was almost tenfold higher in HSCT recipients compared to healthy children (Chapter 2 and ref<sup>285</sup>). High viral loads are reached during CMV reactivation in the absence of T cell surveillance, resulting in latent infection of large numbers of cells. This strong antigenic stimulation in combination with the pro-inflammatory environment after HSCT could explain the difference between healthy children and HSCT recipients.<sup>143;164;165;286</sup>

In contrast to solid organ transplant recipients or elderly people, no memory inflation was observed after HSCT. Although the amplitude of the early T cell response was high after HSCT, the dynamics of this immune response mimics the normal immune response in healthy individuals, with a plateau phase followed by regression of CD8<sup>+</sup> T cell numbers. Also, CMV infection did not have a negative impact on thymic output, as the reconstitution of CD4<sup>+</sup> as well

as CD8<sup>+</sup> naïve T cells was not affected (Chapter 2). However, longer follow up is needed to evaluate whether disseminated CMV reactivations after HSCT can lead to premature memory inflation and related (immune) pathology in the decades after pediatric HSCT.

## 2 Bridging the time to T cell reconstitution

The chapters about viral complications and early immune reconstitution (Chapters 3, 4 and 6) focused on the time window between HSCT and the moment of T cell reconstitution. This period is of great clinical interest because patients are at risk for disseminating viral infections during this phase.<sup>37-39</sup> Because T cells are pivotal for the control of viral infections, most immunological and pharmacological interventions are aimed at accelerating T cell reconstitution or otherwise at bridging the time to T cell reconstitution.

### 2.1 Pharmacological intervention

For different reasons, HSCT recipients with HAdV infections are in a precarious situation. First, HAdV infections after HSCT form a typical pediatric problem, receiving relatively little attention from the general HSCT field. As a result, they do not benefit from research advances made in the adult HSCT setting. Also, in the pediatric population, antiviral drugs are prescribed off-label and large clinical trials needed for the development of novel antiviral agents are difficult to perform. In contrast to CMV and EBV, for which the use of pre-emptive therapy has greatly improved the outcome, the currently available antiviral drug cidofovir does not lead to adenoviral load reduction in the absence of lymphocyte reconstitution. At best, cidofovir resulted in temporal viral load stabilization (Chapter 4). Although this viral load stabilization can bridge the period until T cell reconstitution, in 17% of cases, HAdV viremia progressed despite cidofovir treatment. Additionally, cidofovir is highly nephrotoxic leading to both acute and chronic kidney injury after HSCT, limiting its use (G. Lugthart unpublished data and references<sup>53-56</sup>). In the next few years, the position of HSCT recipients with HAdV infections may improve as a result of the introduction of the novel drug brincidofovir. Brincidofovir is the orally bioavailable lipid conjugate of cidofovir and the first published data are promising, showing an increased effectiveness and a reduced toxicity profile.<sup>60,61</sup> The majority of HSCT recipients receiving brincidofovir as a treatment for HAdV infections had a rapid reduction of HAdV load during brincidofovir treatment.<sup>60,61</sup> Both studies did not report data on lymphocyte reconstitution during treatment, which is a major confounder in studies of drug efficacy. In the study by Hiwarkar *et al.*, brincidofovir was given as primary treatment, and reduction of HAdV load was observed independent of the time after HSCT, suggesting an effect which does not depend on the presence of lymphocytes.<sup>60</sup> Nevertheless, studies correlating HAdV loads with brincidofovir treatment in the absence of lymphocyte reconstitution are needed to confirm these promising data.

### 2.2 Adoptive transfer of virus-specific T cells

The administration of donor derived virus-specific T cells has been applied with promising results in the treatment of CMV and EBV reactivations after HSCT (reviewed in ref<sup>287</sup>). For HAdV,

success rates of virus-specific T cell therapy are more variable.<sup>288-290</sup> The generation of HAdV specific T cell products is complicated by the low frequency of HAdV-specific T cells in healthy donors, resulting in small doses of transferred virus specific T cells.<sup>288</sup> This was observed in Chapter 3 as well: despite enrichment, the frequency of HAdV specific T cells was low in the multi-virus specific T cell product.

A major limitation of virus-specific T cell therapy is the high level of viral dissemination and presence of HAdV-associated disease at the time of T cell infusion in the therapeutic setting. For this reason, infusion of T cells before progression to disease might be more successful. In Chapter 3, we developed a method to generate a product containing T cells specific for CMV, EBV and HAdV for prophylactic treatment. Whether the standard prophylactic administration of multivirus-specific T cells will become standard of care can be debated. Currently, the evidence for the pre-emptive use of virus-specific T cells is based on phase I studies. Three phase II randomized clinical trials (RCTs) with prophylactic administration of CMV-specific T cells after HSCT have been performed. All three studies finished three years ago. Results of one study were published and results of the second study were presented at the 2014 Annual Meeting of the American Society of Hematology, but have not been published yet. Results were comparable: although patients receiving prophylactic CMV-specific T cells had a lower severity of CMV reactivations and required less antiviral drugs, the incidence of CMV reactivations was not significantly reduced in the treatment arm.<sup>291;292</sup> Results of the third study have not been reported yet. At the moment, a multicenter RCT using multivirus-specific T cells is in preparation (TRACE, initiated by T. Feuchtinger, Tübingen, Germany).

The improvement of virus-specific T cell immunity is particularly needed in patients with an expected delay in T cell reconstitution. Importantly, delayed T cell reconstitution is strongly correlated with the exposure to serotherapy (Chapter 6 and refs<sup>30;33</sup>). If T cell depleting antibodies circulate in the HSCT recipient at the time of administration of the graft, these antibodies will also deplete the donor T cells infused with this graft. This is illustrated by the reduced success rate of HAdV-specific T cell therapy in patients who received serotherapy compared to patients without serotherapy.<sup>288</sup> Therefore, the concentration of circulating ATG or alemtuzumab should be monitored prior to infusion of the T cell product. By the time these antibodies are below the lympholytic level, T cell reconstitution will be eminent, reducing the need for adoptive T cell transfer. In the end, the personalized dosing of serotherapy will prevent overdosing of serotherapy, improve T cell reconstitution and reduce the need for virus-specific T cell therapy.

The number of patients that qualify to receive *prophylactic* multivirus-specific T cells to prevent one serious virus-infection after HSCT may turn out to be high (high number needed to treat). Still, a subgroup of HSCT recipients would in fact benefit from *targeted* adoptive T cell therapy. Identification of these patients will improve the effectiveness of adoptive immunotherapy. In Chapter 4 and 6, we identified subgroups of patients with a poor prognosis which lacked protective T- and NK cell reconstitution. This can be due to high concentrations of serotherapy or high dose steroid treatment because of the occurrence of acute GvHD. However, these patients will not benefit from adoptive immunotherapy as transferred T cells will be susceptible to immunosuppression by steroids or elimination by serotherapy. Other patients with a poor prognosis had graft failure or unexplained slow immune reconstitution. These patients often

require a retransplantation or stem cell boost, but it takes months before protective T cells recover from the newly infused stem cells. For these patients, adoptive transfer of virus-specific T cells should be applied in parallel with a stem cell boost to prevent further dissemination of viral infections.

### 3 Role for NK cells after HSCT

In healthy individuals, NK cell function may be overshadowed by the presence of T cells. We regarded the treatment induced T cell deficiency after HSCT as a model to study the potential of human NK cells in the absence of T cells.

#### 3.1 Interaction between viral infections and NK cell reconstitution

Various studies highlighted the inferior outcome of patients with a delayed T cell reconstitution after ATG serotherapy as part of the conditioning prior to HSCT.<sup>30,33</sup> In Chapter 6, we demonstrated that leukemia patients with delayed T cell reconstitution after ATG serotherapy together with an expansion of effector CD56<sup>bright</sup> NK cells did not have an inferior clinical outcome after HSCT compared to patients with rapid T cell reconstitution. In Chapter 4, a reduction of HAdV load was observed in the absence of T cells in patients with an expansion of (CD56<sup>bright</sup>) NK cells. Although it is impossible to discriminate between the relative contribution of cidofovir and NK cells, this suggests that HAdV infection elicits an NK cell expansion, and that an expansion of NK cells can lead to a reduction of the HAdV load. In Chapter 6, we observed a strong correlation between CD56<sup>bright</sup> NK cell expansion early after HSCT and the occurrence of EBV reactivations. Although this correlation was not statistically significant after multivariate correction for delayed T cell reconstitution, this (preliminary) observation can have immunological significance. As EBV seroprevalence is almost universal, the majority of HSCT recipients will experience a (subclinical) reactivation of EBV in the absence of T cell surveillance. Early after HSCT, NK cells are the only lymphocytes available to respond to viral triggers. Therefore, it is conceivable that EBV and HAdV infections contribute to the expansion of early differentiated NK cells after HSCT. For both viruses, NK cells alone were not able to control the infection. HAdV load reduction was mainly observed in the first weeks of the NK cell expansion. Still, the presence of high numbers of NK cells did not prevent from subsequent (secondary) HAdV dissemination (Chapter 4). Also, the peak of the viral load during EBV reactivations was observed in the weeks after the expansion of NK cells (G. Lugthart, unpublished data). In murine studies, depletion of NK cells was only associated with increased viral loads in the early phase of infection.<sup>116</sup> Our data support the hypothesis that NK cells play a role in the early immune response to viral infections, but are not able to clear these infections on their own. However, a direct relation between (control of) infection and NK cell expansion is hard to prove in HSCT recipients with many different infectious and inflammatory triggers.

In Chapter 6, we did not observe a correlation between CMV infections and the expansion of either CD56<sup>bright</sup> or CD56<sup>dim</sup> NK cells early after HSCT. The NK cell phenotype associated with

CMV infections, the late differentiated NKG2C<sup>+</sup> CD56<sup>dim</sup> NK cells, was not present during the early phase of CMV infection but expanded between 6 and 12 months after HSCT.<sup>129</sup> This expansion of late differentiated NK cells appears to be secondary and is reminiscent of the expansion of late differentiated CD8<sup>+</sup> T cells after CMV infections post HSCT (Chapter 2).<sup>129</sup> This marks a major difference with HAdV and EBV infections, where NK cells expand at the early phase of the infection. An extensive phenotyping of NK cells expanding during EBV and HAdV infections after HSCT can be used to identify “virus-specific” NK cell characteristics. In recent years, a number of studies have been published proposing that the NK cells responding during (primary) EBV infections have an early differentiated phenotype. An expansion of CD56<sup>bright</sup> and early differentiated NKG2A<sup>+</sup>KIR<sup>-</sup> CD56<sup>dim</sup> NK cells was observed in healthy individuals with primary EBV infections,<sup>120;121</sup> as well as after *in vitro* stimulation with EBV infected cells.<sup>293;294</sup> The distinct differentiation of NK cells associated with CMV and EBV infections is reminiscent of the differentiation of CMV and EBV specific CD8<sup>+</sup> T cells. Whereas CMV-specific CD8<sup>+</sup> memory T cells are characterized by a late differentiated CD27<sup>+/-</sup>CD28<sup>-</sup> EM and EMRA phenotype, EBV-specific T cells are mainly found in the early differentiated CD27<sup>+</sup>CD28<sup>+</sup> EM compartment.<sup>70</sup>

In a humanized NOD SCID gamma (NSG) mouse model, an expansion of NK cells was observed upon EBV infection, and depletion of NK cells resulted in higher viral loads and more severe disease.<sup>295</sup> Unfortunately, the study of human NK cell biology in this humanized NSG mouse model is complicated because of the lack of CD56 expression on NK cells.<sup>295;296</sup> *In vitro* experiments using activated, early differentiated NK cells from HSCT recipients can be used to investigate whether these cells have an increased potential against Epstein-Barr virus-transformed lymphoblastoid cell lines in comparison to healthy donor NK cells. Still, the complexity and combined problems of HSCT recipients make it hard to convincingly demonstrate virus driven NK cell responses. For this, immune monitoring during primary EBV infections in healthy individuals would be more suitable, yet this is hard to realize in view of practical and ethical considerations. In the follow-up of primary EBV infections, the first week of the immune response, during which NK cells might play a major role, will be missed. An alternative approach to increase the understanding of human NK cell immunity to EBV could be the simian lymphocryptovirus infection model in rhesus macaques.<sup>297;298</sup> This virus is very similar to the human EBV, whereas macaque NK cells are more comparable to human NK cells than commonly used murine NK cells.<sup>297;298</sup>

### 3.2 Compensatory adaptations of NK cells during T cell deficiency

The functional profile of post-transplant CD56<sup>bright</sup> NK cells corresponds with that of conventional, cytokine secreting CD56<sup>bright</sup> NK cells that have temporarily acquired cytolytic potential (Chapter 6). Other studies demonstrated a low cytotoxicity of post-transplant CD56<sup>bright</sup> NK cells, but in these studies the cells were subjected to prolonged *in vitro* culture before performing cytotoxicity assays or purified CD56<sup>bright</sup> cells acquired at three months after HSCT were investigated.<sup>136;216;299</sup> By that time, the granzyme B expression of CD56<sup>bright</sup> NK cells was already strongly reduced (Chapter 6).

CD56<sup>bright</sup> NK cells early after HSCT had an increased expression of receptors associated with migration towards inflamed tissues and skin, but were circulating in blood. The fact that these cells are circulating implies that the expression of chemokine receptors alone is not enough to retain these cells in tissues. We did not investigate whether CD56<sup>bright</sup> NK cells were further enriched in inflamed tissues or skin, which could improve the understanding of the data presented in Chapter 6. The chemokine receptor expression profile on circulating NK cells might be a reflection of the total circulating and non-circulating NK cell pool. Possibly, these cells are traveling towards tissues, or have just left the tissues. The circulating NK cells early after HSCT did not express CD69. Although CD69 was initially identified as an early lymphocyte activation marker,<sup>264-266</sup> CD69 has been increasingly recognized to play a role in tissue retention. This is mediated via the downregulation of sphingosine-1-phosphate receptor 1 (S1PR1), which is needed for cells to return to the blood stream.<sup>300;301</sup> Possibly, the inflammatory environment after HSCT results in the expression of chemokine receptors to increase their potential to rapidly access sites of inflammation. Once the cells enter their target tissue, the local expression of activating cytokines might engage CD69 expression to facilitate the retention in these tissues.

The expression of inflammatory chemokine receptors, combined with a strong IFN- $\gamma$  production and fully equipped cytotoxic machinery, enables CD56<sup>bright</sup> NK cells to respond rapidly in the early phase of viral infections after HSCT. Whether these cells expand in response to viruses, or as a result of general inflammation and cytokine storm remains to be elucidated. The strong expansion of CD56<sup>bright</sup> NK cells with acquired functional assets of CD56<sup>dim</sup> NK cells occurred in the presence of CD56<sup>dim</sup> NK cells. Why do cytotoxic CD56<sup>dim</sup> NK cells not expand themselves? Possibly, CD56<sup>bright</sup> NK cells are more sensitive to exogenous stimulation. This corresponds to the high proliferative capacity of *in vitro* activated healthy donor CD56<sup>bright</sup> NK cells compared to CD56<sup>dim</sup> cells.<sup>97</sup> Alternatively, *in vivo* activated CD56<sup>dim</sup> NK cells left the blood stream, or acquired a CD56<sup>bright</sup> phenotype, as has been reported for *in vitro* activated CD56<sup>dim</sup> NK cells.<sup>105</sup>

Our observations are in line with the limited reported observations in patients with severe inborn T cell deficiencies. In patients with RAG and ARTEMIS deficiencies, an increased proportion of NK cells had the CD56<sup>bright</sup> phenotype, and these cells displayed a high degranulation upon coculture with K562.<sup>235</sup> An increased proportion of CD56<sup>bright</sup> NK cells has been reported in patients with T cell receptor- $\gamma$ , - $\delta$  and - $\zeta$  deficiencies as well.<sup>302</sup> In a case report describing an X-linked SCID patient with the rare T-B+NK+ phenotype, an expansion of CD56<sup>bright</sup> NK cells was described.<sup>303</sup> In this patient, all skin infiltrating lymphocytes were CD56<sup>bright</sup> NK cells. This would match with the chemokine receptor expression profile observed after HSCT, with a temporarily increased expression of cutaneous lymphocyte antigen (CLA) on CD56<sup>bright</sup> NK cells. Finally, also in human immunodeficiency virus (HIV) infected patients with an acquired T cell deficiency, an inverse correlation was observed between CD4<sup>+</sup> T cell numbers and the proportion of NK cells with the CD56<sup>bright</sup> phenotype. Like post-transplant CD56<sup>bright</sup> NK cells, these cells had a reduced expression of CCR7 and an increased expression of granzyme B.<sup>236</sup> Together, these data demonstrate the flexibility of the human immune system and the potential of the minor CD56<sup>bright</sup> NK cell population in situations when T cells are not able to perform their task.



## 4 Identification of a lymphoid tissue resident NK cell subset

Most knowledge on the phenotype and function of NK cells is derived from cells present in blood. In the blood of healthy donors, CD56<sup>bright</sup> NK cells form a minor non-cytotoxic NK cell subset. In this thesis, we describe two situations in which CD56<sup>bright</sup> NK cells form a major cell subset with distinct phenotypic and functional properties. Using 12-color flowcytometry, we demonstrated that CD56<sup>bright</sup> NK cells expanding early after HSCT are distinct from CD56<sup>bright</sup> NK cell in steady state conditions (Chapter 6 and discussed in the previous section). Also, we discovered a third, phenotypically and functionally distinct NK cell population in lymphoid tissues (Chapter 7). A relative increase of CD56<sup>bright</sup>CD16<sup>+/-</sup> NK cells in lymphoid tissues has been discovered decades ago.<sup>108;216</sup> The use of CD56 and CD16 to discriminate the two main (CD56<sup>bright</sup> and CD56<sup>dim</sup>) NK cell populations originates from the era of 4-color flowcytometry. Many characteristics of circulating and easily available CD56<sup>bright</sup> NK cells have been extrapolated to draw conclusions about NK cell biology in tissues. Without the use of additional markers, this lymphoid tissue residing NK cell population (ItNK) could previously not be discriminated from conventional CD56<sup>bright</sup> and CD56<sup>dim</sup> NK cells. In future, the use of mass spectrometry (CyTOF®), measuring ~30 extracellular or intracellular proteins per cell, and single cell RNA sequencing, measuring the gene expression of ~10.000 genes will further increase this resolution.<sup>304;305</sup> Combined with advanced computerized data analysis, these new technologies will enable grouping and unveil relations between immune cell subsets without the investigator bias inevitably associated with the manual gating of cells which is currently applied.

### 4.1 Tissue retention and Mobility

Important mechanisms for tissue homing and retention are the engagement of chemokine receptors and adhesion molecules. ItNK cells have a distinct expression of chemokine receptors and adhesion molecules in comparison to circulating CD56<sup>bright</sup> NK cells from healthy individuals.<sup>306-308</sup> The discriminative cell surface markers used to identify ItNK cells are CD69 and the chemokine receptor CXCR6 (Chapter 7). Although CD69 was first identified as an activation marker, CD69 is now recognized to play an important role in tissue retention (see above).<sup>300;301</sup> Simultaneously with our discovery of CXCR6<sup>+</sup>(CCR5<sup>+</sup>) ItNK cells, a CXCR6<sup>+</sup>CCR5<sup>+</sup> human liver resident NK cell population was identified.<sup>261;271</sup> The chemokine receptors CXCR6 and CCR5 were also found to be expressed by murine liver resident NK cells and human lymphoid tissue, liver and lung resident T cells.<sup>269;270;273;309-312</sup> These observations support the hypothesis that these chemokine receptors are involved in tissue residency. Specialized tissue resident NK cells were first identified in the uterus.<sup>313-315</sup> Human uterine NK cells do not express CCR5, whereas their expression of CXCR6 has not been assessed. Instead, uterine NK cells uniformly express the adhesion molecule CD49a, while a proportion of uterine NK cells express CD103 as well.<sup>313-315</sup> These adhesion molecules are expressed by tissue resident NK cells in tonsil, T cells in lung and mucosa and mucosal innate lymphoid cells as well.<sup>262;311;316</sup> However, ItNK cells in bone marrow, spleen and lymph node, and the majority of human liver resident NK cells do not express these markers.<sup>261;271</sup> This suggests that mucosal and non-mucosal tissue resident lymphocytes apply a different mechanism of tissue retention. Interestingly,

(lymphoid) tissue-resident CD56<sup>bright</sup> NK cells lack the expression of CD62L (L-selectin) and CCR7, involved in recruitment of circulating lymphocytes to lymphoid tissues via high endothelial venules (HEVs).<sup>107;271;313</sup> Apparently, these receptors are not required for the retention of ltNK cells in lymphoid tissues. The uniform evaluation of chemokine receptor and adhesion molecule expression on NK cells from a broad range of human tissues could further improve the understanding of NK cell tissue residency and identify tissue specific characteristics.

## 4.2 Function and Interactions

Although ltNK cells appear to have a hypofunctional profile in resting state, they produce interferon- $\gamma$  and become cytotoxic after the appropriate *in vitro* stimulation (Chapter 7). In line with their specific tissue localization and phenotype, it is plausible that these cells have a local function that differs from the classical NK cell functions. Alternatively, they may form a reservoir of NK cells waiting for mobilization, which lose their tissue-retention and CD69<sup>+</sup>CXCR6<sup>+</sup> phenotype upon activation. In view of their similarities with liver resident NK cells, CD69<sup>+</sup>CXCR6<sup>+</sup> NK cells can be present in other tissues with an enrichment of CD56<sup>bright</sup> NK cells.<sup>106-108</sup> They can have a more general tissue-residing immune scavenger function protecting the local environment from invading pathogens. Uterine NK cells were shown to produce chemokines and angiogenic factors, suggesting a tissue-specific role in embryonic implantation.<sup>314;317;318</sup> Like other innate lymphoid cell types, NK cells in different tissues can have their own tissue specific function.<sup>88</sup> This can be addressed by the in parallel investigation of tissue resident NK cells from different tissues.

Murine liver (but not spleen) resident CXCR6<sup>+</sup>CD49a<sup>+</sup> NK cells have been shown to be involved in hapten- and virus specific memory NK cell responses.<sup>272;273</sup> In both mice and man, virus-specific T cells are enriched in the target-tissue of the respective virus (*e.g.* hepatitis virus in liver, EBV in bone marrow, influenza virus in lung).<sup>270;319-322</sup> Whether human tissue-resident NK cells play a role in such memory responses remains to be elucidated. We did not observe a difference between the size of the ltNK cell population in pediatric and adult bone marrow donors, arguing against the accumulation of an (antigen) experienced cell population (G. Lugthart, unpublished observation).

Based on the localization in lymphoid tissues, it is conceivable that ltNK cells play a role in the enhancement and polarization of adaptive immune responses.<sup>108;253</sup> Clues for the interactions of tissue resident NK cells with other cells may further be deduced from the nature of CXCL16, the exclusive ligand for CXCR6.<sup>323;324</sup> In contrast to most other chemokines, CXCL16 is expressed as a cell surface bound molecule which can be shed to function as a chemo-attractant. CXCL16 functions as a receptor for oxidized lipoprotein and bacteria, but has also been demonstrated to be involved in cellular interactions.<sup>325-328</sup> CXCL16 is expressed by both immune cells and other cells. For example, dendritic cells (DC) in T cell zones of the lymph node, liver sinusoids and –still unidentified– cells in the splenic red pulp express CXCL16. In concordance, NK cells have been shown to co-localize with DCs in T cell zones of lymph nodes and are mainly found in liver sinusoids and in red pulp of the spleen.<sup>108;256;257;271</sup> Fluorescence immunohistochemistry and confocal microscopy should be used to determine the exact tissue localization of ltNK cells and their interactions with the surrounding cells for a better understanding of their interactions and

possible function. In addition, gene expression data will unravel signaling pathways and transcription factors involved in tissue residency, as has been shown for tissue-resident T cells.<sup>311;329</sup> Furthermore, gene expression analysis can identify pathways involved in cellular processes to provide clues about their function and interactions.

It has been suggested that CXCR6-CXCL16 interactions play a role in the enhancement of immune-responses<sup>330;331</sup> Recently, it was shown that co-culture with CXCL16<sup>+</sup> activated dendritic cells stimulated CXCR6<sup>+</sup> murine NKT cells to produce IFN- $\gamma$ .<sup>332</sup> When this applies for NK cells, ItNK cells might play a role as a catalyst for the generation and polarization of CD4<sup>+</sup> Th1 immune responses and CD8<sup>+</sup> T cell responses in lymphoid organs. Based on the cellular interactions and gene expression data, targeted functional experiments can be designed to improve the understanding of the role of ItNK cells in human immune responses.

## 5 Relationship between different NK cell subsets

The skewing towards CD56<sup>bright</sup> NK cells after HSCT and the expression of the early differentiation markers CD27, CD117 and CD127 on CD56<sup>bright</sup> NK cells, but not CD56<sup>dim</sup> NK cells from healthy donor blood have led to the hypothesis that CD56<sup>bright</sup> NK cells are the precursors of CD56<sup>dim</sup> NK cells.<sup>91;216;299</sup> However, in Chapter 6, we show that the reconstitution of CD56<sup>dim</sup> NK cells after HSCT occurred independently of CD56<sup>bright</sup> NK cell- and T cell reconstitution. Furthermore, CD56<sup>bright</sup> NK cells early after HSCT did not have an immature, but rather an activated phenotype. This corresponds to the high proliferative capacity of *in vitro* activated healthy donor CD56<sup>bright</sup> NK cells compared to CD56<sup>dim</sup> cells.<sup>97</sup> Various studies reported the existence of phenotypic and functional intermediate stages in the progression from CD56<sup>bright</sup> to CD56<sup>dim</sup> NK cells in peripheral blood of healthy donors and patients after HSCT based on the expression of CD16, CD27 and CD117.<sup>100;126-128;279;333</sup> Notably, the increased expression of CD16 and reduced expression of CD117 and CD27 on CD56<sup>bright</sup> NK cells can be affected by cytokine-activation.<sup>100;126;127;279;334</sup> Therefore, the dynamics and phenotype of NK cell reconstitution in the inflammatory conditions early after HSCT might be more informative about the response of different NK cell subsets to *in vivo* stimulation rather than about their developmental (inter)relation.

The distinctive reconstitution profile of ItNK cells after HSCT (Chapter 7) indicates that these cells form a distinct subset with a limited expansion upon exogenous stimulation. Their recovery followed the reconstitution of CD56<sup>bright</sup> and CD56<sup>dim</sup> NK cells, arguing against a position as NK cell precursor-population or an intermediate between CD56<sup>bright</sup> and CD56<sup>dim</sup> NK cells. Another argument to reject the hypothesis that ItNK cells could be a precursor population, is the lack of expression of the early differentiation markers CD117 and CD127 on ItNK cells. It is unlikely that the lack of expression of these markers is caused by cellular activation, because the tissues in which ItNK cells were identified were harvested from a non-inflammatory environment in healthy donors.

The discovery of distinct tissue-resident CD56<sup>bright</sup> NK cell populations increases the number of possible relationships between the NK cell populations. Data from transcription factor-deficient mice suggested that circulating and tissue-resident NK cells are derived from different cell lineages.<sup>335</sup> However, the lack of CD56 expression on murine NK cells hampers the direct comparison to human NK cell populations. Transcriptome analysis comparing human uterine NK cells with both circulating CD56<sup>bright</sup> and CD56<sup>dim</sup> NK cells highlighted major differences in gene expression profile between the three NK cell populations.<sup>313</sup> Gene tracking data in rhesus macaques transplanted with lentiviral barcoded hematopoietic stem cells demonstrated that the lineage origin of the macaque NK cell homologues of CD56<sup>bright</sup> (CD56<sup>+</sup>CD16<sup>-</sup>) and CD56<sup>dim</sup> (CD56<sup>-</sup>CD16<sup>+</sup>) NK cells is different, suggesting that CD56<sup>dim</sup> NK cells do not develop from the CD56<sup>bright</sup> population.<sup>298</sup>

Rare patients with human NK cell deficiencies may provide clues about the developmental relationship between CD56<sup>bright</sup> and CD56<sup>dim</sup> NK cells as well. No mutations in transcription factors have been described as a putative cause of the lack of CD56<sup>dim</sup> NK cells while the CD56<sup>bright</sup> NK cells are spared. Patients with a partial minichromosome maintenance complex 4 (MCM4) deficiency, a molecule involved in proliferation, have reduced numbers of circulating CD56<sup>dim</sup> NK cells and normal numbers of CD56<sup>bright</sup> NK cells.<sup>336</sup> Mutations in the transcription factor gene *GATA2* result in the absence of CD56<sup>bright</sup> NK cells, while CD56<sup>dim</sup> NK cells are still present.<sup>337</sup> Together, these observations argue against the hypothesis that CD56<sup>dim</sup> NK cells are derived from CD56<sup>bright</sup> NK cells. The distinct phenotype and functional signature of ltNK cells supports the hypothesis that these NK cells develop locally, independently of the circulating NK cells. Nevertheless, additional studies are needed to shed new light on the developmental relationship between CD56<sup>bright</sup>, CD56<sup>dim</sup> and tissue-resident CD56<sup>bright</sup> NK cell populations and their precursors. Gene-expression data can be used to identify transcription factors that are preferentially expressed in one of the NK cell populations. The evaluation of ltNK cells in the bone marrow aspirations from patients with known defects of genes that play a role in the immune system could identify the impact of these genes on resident NK cells. Finally, life-span and relation of circulating and tissue resident NK cell subsets could be further studied by infusion of radioisotope labelled NK cell subsets in (humanized) animal models.

## 6 General conclusions

In this thesis, new insights in the complex and intertwined relationship between viral infections, T cells and natural killer cells after allogeneic HSCT in children are provided and discussed. Patients are at high risk of viral complication during the T cell deficient period early after HSCT. When viral infections occur, interventions to bridge the period until the recovery of antiviral T cell immunity are of great importance to improve the clinical outcome after HSCT. As a result of ongoing developments in the field, the perspective of some of the chapters may soon change. For example, the use of cidofovir for the treatment of HAdV infections may soon be history because of the introduction of the new (and promised to be better) drug brincidofovir. However, also brincidofovir should also be critically evaluated and related to HAdV load dynamics in the absence of lymphocyte recovery. The prophylactic use of adoptive T cell therapy for multiple viruses might never become the standard of care for pediatric HSCT recipients because of the improved understanding of the *in vivo* effectiveness and pharmacodynamics of serotherapy agents. These developments will result in personalized dosage schedules, reduction of over-dosage and a reduction of patients with a prolonged T cell deficiency after HSCT. Patients who lack T cell recovery in the absence of circulating serotherapy agents might benefit from targeted use of adoptive T cell therapy and should be identified. In addition to the importance of T cell reconstitution for the protection of viral reactivations, early CMV infections can explain the often observed severely skewed CD8<sup>+</sup> T cell memory compartment in the years after HSCT. However, we also showed that this is caused by an expansion of late differentiated T cells on top of an otherwise balanced immune system. Still, CMV reactivations after HSCT should be included in the late-effect evaluations of pediatric HSCT recipients reaching adulthood, to study its effect on (immune) pathology that might occur decades after HSCT.

Besides antiviral medication and the use of adoptive immunotherapy, NK cells may play a role in the protection against viruses when T cells are not available to perform their task. A strong expansion of CD56<sup>bright</sup> NK cells occurred in patients with a delayed T cell reconstitution, and these cells displayed functional and phenotypic adaptations. The correlation of specific viral infections with the expansion and function of distinct NK cell phenotypes after HSCT should be explored further, as the period of T cell deficiency after HSCT can be used as a model to improve the understanding of the role of NK cells in antiviral immunity. The identification of CD69 and CXCR6 to distinguish the distinct lymphoid tissue resident ItNK cell population from circulating cells enables the further characterization of the interactions of tissue-resident and circulating NK cells with other immune cells in lymphoid tissues. For example, gene expression analysis comparing tissue-resident and circulating NK cells can provide clues about the specific functions of tissue-resident NK cells, while immunohistochemistry and confocal microscopy may reveal the cellular interactions of tissue-resident NK cells. Importantly, both ItNK cells in lymphoid tissues and CD56<sup>bright</sup> NK cells early after HSCT have a distinct phenotype and function compared to conventional (CD56<sup>bright</sup>) NK cells. These data illustrate that human NK cell biology goes beyond the current models which are mainly based on circulating NK cells from healthy individuals. This invites for a re-assessment of the relationship between the different human NK cell populations and their role in human immunity.



# References

1. Copelan EA. Hematopoietic stem-cell transplantation. *N.Engl.J.Med.* 2006;354:1813-1826.
2. Gatti RA, Meuwissen HJ, Allen HD, Hong R, Good RA. Immunological reconstitution of sex-linked lymphopenic immunological deficiency. *Lancet* 1968;2:1366-1369.
3. De Koning J, van Bekkum DW, Dicke KA et al. Transplantation of bone-marrow cells and fetal thymus in an infant with lymphopenic immunological deficiency. *Lancet* 1969;1:1223-1227.
4. Juric MK, Ghimire S, Ogonek J et al. Milestones of Hematopoietic Stem Cell Transplantation - From First Human Studies to Current Developments. *Front Immunol.* 2016;7:470.
5. Passweg JR, Baldomero H, Bader P et al. Hematopoietic stem cell transplantation in Europe 2014: more than 40 000 transplants annually. *Bone Marrow Transplant* 2016;51:786-792.
6. Thomas ED, Buckner CD, Banaji M et al. One hundred patients with acute leukemia treated by chemotherapy, total body irradiation, and allogeneic marrow transplantation. *Blood* 1977;49:511-533.
7. Thomas ED, Storb R, Fefer A et al. Aplastic anaemia treated by marrow transplantation. *Lancet* 1972;1:284-289.
8. Lucarelli G, Isgro A, Sodani P, Gaziev J. Hematopoietic stem cell transplantation in thalassemia and sickle cell anemia. *Cold Spring Harb.Perspect.Med.* 2012;2:a011825.
9. Hansen JA, Clift RA, Thomas ED et al. Transplantation of marrow from an unrelated donor to a patient with acute leukemia. *N.Engl.J.Med.* 1980;303:565-567.
10. Beatty PG, Clift RA, Mickelson EM et al. Marrow transplantation from related donors other than HLA-identical siblings. *N.Engl.J.Med.* 1985;313:765-771.
11. Gluckman E, Broxmeyer HA, Auerbach AD et al. Hematopoietic reconstitution in a patient with Fanconi's anemia by means of umbilical-cord blood from an HLA-identical sibling. *N.Engl.J.Med.* 1989;321:1174-1178.
12. Reisner Y, Kapoor N, Kirkpatrick D et al. Transplantation for severe combined immunodeficiency with HLA-A,B,D,DR incompatible parental marrow cells fractionated by soybean agglutinin and sheep red blood cells. *Blood* 1983;61:341-348.
13. Russell NH, Hunter A, Rogers S, Hanley J, Anderson D. Peripheral blood stem cells as an alternative to marrow for allogeneic transplantation. *Lancet* 1993;341:1482.
14. Petersdorf EW. Risk assessment in haematopoietic stem cell transplantation: histocompatibility. *Best.Pract.Res.Clin.Haematol.* 2007;20:155-170.
15. Feng X, Hui KM, Younes HM, Brickner AG. Targeting minor histocompatibility antigens in graft versus tumor or graft versus leukemia responses. *Trends Immunol.* 2008;29:624-632.
16. Devergie A. Graft versus host disease. In: Apperley J, Carreras E, Gluckman E, Gratwohl A, Masszi T, eds. *Haematopoietic Stem Cell Transplantation*. Genova: Forum Service Editore; 2008:218-235.
17. Locatelli F, Lucarelli B, Merli P. Current and future approaches to treat graft failure after allogeneic hematopoietic stem cell transplantation. *Expert.Opin.Pharmacother.* 2014;15:23-36.
18. Klein J, Sato A. The HLA system. First of two parts. *N.Engl.J.Med.* 2000;343:702-709.
19. van Rood JJ, Oudshoorn M. Eleven million donors in Bone Marrow Donors Worldwide! Time for reassessment? *Bone Marrow Transplant* 2008;41:1-9.
20. Gragert L, Eapen M, Williams E et al. HLA match likelihoods for hematopoietic stem-cell grafts in the U.S. registry. *N.Engl.J.Med.* 2014;371:339-348.
21. World Marrow Donor Association. Bone Marrow Donors Worldwide. <https://www.bmdw.org> . 2017.
22. van Walraven SM, Brand A, Bakker JN et al. The increase of the global donor inventory is of limited benefit to patients of non-Northwestern European descent. *Haematologica* 2017;102:176-183.
23. Reisner Y, Hagin D, Martelli MF. Haploidentical hematopoietic transplantation: current status and future perspectives. *Blood* 2011;118:6006-6017.
24. Larghero J, Garcia J, Gluckman E. Sources and procurement of stem cells. In: Apperley J, Carreras E, Gluckman E, Gratwohl A, Masszi T, eds. *Haematopoietic Stem Cell Transplantation*. Genova: Forum Service Editore; 2008:112-127.
25. Ruggeri A, Paviglianiti A, Gluckman E, Rocha V. Impact of HLA in cord blood transplantation outcomes. *HLA.* 2016;87:413-421.
26. Anasetti C, Logan BR, Lee SJ et al. Peripheral-blood stem cells versus bone marrow from unrelated donors. *N.Engl.J.Med.* 2012;367:1487-1496.
27. Gratwohl A. Principles of conditioning. In: Apperley J, Carreras E, Gluckman E, Gratwohl A, Masszi T, eds. *Haematopoietic Stem Cell Transplantation*. Genova: Forum Service Editore; 2008:128-144.



28. ten Brink MH, Zwaveling J, Swen JJ et al. Personalized busulfan and treosulfan conditioning for pediatric stem cell transplantation: the role of pharmacogenetics and pharmacokinetics. *Drug Discov.Today* 2014;19:1572-1586.
29. Mohty M. Mechanisms of action of antithymocyte globulin: T-cell depletion and beyond. *Leukemia* 2007;21:1387-1394.
30. Admiraal R, van Kesteren C, Jol-van der Zijde CM et al. Association between anti-thymocyte globulin exposure and CD4+ immune reconstitution in paediatric haemopoietic cell transplantation: a multicentre, retrospective pharmacodynamic cohort analysis. *Lancet Haematol.* 2015;2:e194-e203.
31. Rebello P, Cwynarski K, Varughese M et al. Pharmacokinetics of CAMPATH-1H in BMT patients. *Cytotherapy.* 2001;3:261-267.
32. Waller EK, Langston AA, Lonial S et al. Pharmacokinetics and pharmacodynamics of anti-thymocyte globulin in recipients of partially HLA-matched blood hematopoietic progenitor cell transplantation. *Biol.Blood Marrow Transplant* 2003;9:460-471.
33. Willemsen L, Jol-van der Zijde CM, Admiraal R et al. Impact of serotherapy on immune reconstitution and survival outcomes after stem cell transplantations in children: thymoglobulin versus alemtuzumab. *Biol.Blood Marrow Transplant* 2015;21:473-482.
34. Storb R, Antin JH, Cutler C. Should methotrexate plus calcineurin inhibitors be considered standard of care for prophylaxis of acute graft-versus-host disease? *Biol.Blood Marrow Transplant* 2010;16:S18-S27.
35. Vossen JM, Guiot HF, Lankester AC et al. Complete suppression of the gut microbiome prevents acute graft-versus-host disease following allogeneic bone marrow transplantation. *PLoS.One.* 2014;9:e105706.
36. Mathewson ND, Jenq R, Mathew AV et al. Gut microbiome-derived metabolites modulate intestinal epithelial cell damage and mitigate graft-versus-host disease. *Nat.Immunol.* 2016;17:505-513.
37. Cwynarski K, Ainsworth J, Cobbold M et al. Direct visualization of cytomegalovirus-specific T-cell reconstitution after allogeneic stem cell transplantation. *Blood* 2001;97:1232-1240.
38. Heemskerk B, Lankester AC, van VT et al. Immune reconstitution and clearance of human adenovirus viremia in pediatric stem-cell recipients. *J.Infect.Dis.* 2005;191:520-530.
39. Annels NE, Kalpoe JS, Bredius RG et al. Management of Epstein-Barr virus (EBV) reactivation after allogeneic stem cell transplantation by simultaneous analysis of EBV DNA load and EBV-specific T cell reconstitution. *Clin.Infect.Dis.* 2006;42:1743-1748.
40. Ahmad N, Drew WL, Lagunoff M. Herpesviruses. In: Ryan KJ, Ray CJ, eds. *Sherris Medical Microbiology*. New York: McGraw-Hill Education, Inc; 2014:245-270.
41. van Tol MJ, Claas EC, Heemskerk B et al. Adenovirus infection in children after allogeneic stem cell transplantation: diagnosis, treatment and immunity. *Bone Marrow Transplant.* 2005;35:S73-S76.
42. Gottschalk S, Rooney CM, Heslop HE. Post-transplant lymphoproliferative disorders. *Annu.Rev.Med.* 2005;56:29-44.
43. Ljungman P, Hakki M, Boeckh M. Cytomegalovirus in hematopoietic stem cell transplant recipients. *Hematol.Oncol.Clin.North Am.* 2011;25:151-169.
44. Renaud C, Englund JA. Antiviral therapy of respiratory viruses in haematopoietic stem cell transplant recipients. *Antivir.Ther.* 2012;17:175-191.
45. Ljungman P. Molecular monitoring of viral infections after hematopoietic stem cell transplantation. *Int.J.Hematol.* 2010;91:596-601.
46. Boeckh M, Nichols WG. The impact of cytomegalovirus serostatus of donor and recipient before hematopoietic stem cell transplantation in the era of antiviral prophylaxis and preemptive therapy. *Blood* 2004;103:2003-2008.
47. Maffini E, Giaccone L, Festuccia M et al. Treatment of CMV infection after allogeneic hematopoietic stem cell transplantation. *Expert.Rev.Hematol.* 2016;9:585-596.
48. Boeckh M, Kim HW, Flowers ME, Meyers JD, Bowden RA. Long-term acyclovir for prevention of varicella zoster virus disease after allogeneic hematopoietic cell transplantation--a randomized double-blind placebo-controlled study. *Blood* 2006;107:1800-1805.
49. Verhoeven DH, Claas EC, Jol-van der Zijde CM et al. Reactivation of Human Herpes Virus-6 After Pediatric Stem Cell Transplantation: Risk Factors, Onset, Clinical Symptoms and Association With Severity of Acute Graft-Versus-Host Disease. *Pediatr.Infect.Dis.J.* 2015;34:1118-1127.
50. Lenaerts L, De CE, Naesens L. Clinical features and treatment of adenovirus infections. *Rev.Med.Virol.* 2008;18:357-374.

51. Schilham MW, Claas EC, van ZW et al. High levels of adenovirus DNA in serum correlate with fatal outcome of adenovirus infection in children after allogeneic stem-cell transplantation. *Clin.Infect.Dis.* 2002;35:526-532.
52. Lankester AC, Heemskerk B, Claas EC et al. Effect of ribavirin on the plasma viral DNA load in patients with disseminating adenovirus infection. *Clin.Infect.Dis.* 2004;38:1521-1525.
53. Lalezari JP, Drew WL, Glutzer E et al. (S)-1-[3-hydroxy-2-(phosphonylmethoxy)propyl]cytosine (cidofovir): results of a phase I/II study of a novel antiviral nucleotide analogue. *J.Infect.Dis.* 1995;171:788-796.
54. Vandercam B, Moreau M, Goffin E et al. Cidofovir-induced end-stage renal failure. *Clin.Infect.Dis.* 1999;29:948-949.
55. Bhadri VA, Lee-Horn L, Shaw PJ. Safety and tolerability of cidofovir in high-risk pediatric patients. *Transpl.Infect.Dis.* 2009;11:373-379.
56. Ljungman P, Ribaud P, Eyrich M et al. Cidofovir for adenovirus infections after allogeneic hematopoietic stem cell transplantation: a survey by the Infectious Diseases Working Party of the European Group for Blood and Marrow Transplantation. *Bone Marrow Transplant.* 2003;31:481-486.
57. Robin M, Marque-Juliet S, Scieux C et al. Disseminated adenovirus infections after allogeneic hematopoietic stem cell transplantation: incidence, risk factors and outcome. *Haematologica* 2007;92:1254-1257.
58. Symeonidis N, Jakubowski A, Pierre-Louis S et al. Invasive adenoviral infections in T-cell-depleted allogeneic hematopoietic stem cell transplantation: high mortality in the era of cidofovir. *Transpl.Infect.Dis.* 2007;9:108-113.
59. Yusuf U, Hale GA, Carr J et al. Cidofovir for the treatment of adenoviral infection in pediatric hematopoietic stem cell transplant patients. *Transplantation* 2006;81:1398-1404.
60. Hiwarkar P, Amroliya P, Sivaprakasam P et al. Brincidofovir is highly efficacious in controlling adenoviremia in pediatric recipients of hematopoietic cell transplant. *Blood* 2017;129:2033-2037.
61. Florescu DF, Pergam SA, Neely MN et al. Safety and efficacy of CMX001 as salvage therapy for severe adenovirus infections in immunocompromised patients. *Biol.Blood Marrow Transplant.* 2012;18:731-738.
62. Bosch M, Khan FM, Storek J. Immune reconstitution after hematopoietic cell transplantation. *Curr.Opin.Hematol.* 2012;19:324-335.
63. Khan FM, Sy S, Louie P et al. Nasal epithelial cells of donor origin after allogeneic hematopoietic cell transplantation are generated at a faster rate in the first 3 months compared with later posttransplantation. *Biol.Blood Marrow Transplant* 2010;16:1658-1664.
64. Naughton MA, Botto M, Carter MJ et al. Extrahepatic secreted complement C3 contributes to circulating C3 levels in humans. *J.Immunol.* 1996;156:3051-3056.
65. Alper CA, Johnson AM, Birtch AG, Moore FD. Human C'3: evidence for the liver as the primary site of synthesis. *Science* 1969;163:286-288.
66. Auffermann-Gretzinger S, Lossos IS, Vayntrub TA et al. Rapid establishment of dendritic cell chimerism in allogeneic hematopoietic cell transplant recipients. *Blood* 2002;99:1442-1448.
67. Andani R, Robertson I, Macdonald KP et al. Origin of Langerhans cells in normal skin and chronic GVHD after hematopoietic stem-cell transplantation. *Exp.Dermatol.* 2014;23:75-77.
68. Klein L, Kyewski B, Allen PM, Hogquist KA. Positive and negative selection of the T cell repertoire: what thymocytes see (and don't see). *Nat.Rev.Immunol.* 2014;14:377-391.
69. Becattini S, Latorre D, Mele F et al. T cell immunity. Functional heterogeneity of human memory CD4(+) T cell clones primed by pathogens or vaccines. *Science* 2015;347:400-406.
70. Appay V, van Lier RA, Sallusto F, Roederer M. Phenotype and function of human T lymphocyte subsets: consensus and issues. *Cytometry A* 2008;73:975-983.
71. Weinberg K, Blazar BR, Wagner JE et al. Factors affecting thymic function after allogeneic hematopoietic stem cell transplantation. *Blood* 2001;97:1458-1466.
72. Eefting M, von dem Borne PA, de Wreede LC et al. Intentional donor lymphocyte-induced limited acute graft-versus-host disease is essential for long-term survival of relapsed acute myeloid leukemia after allogeneic stem cell transplantation. *Haematologica* 2014;99:751-758.
73. van Bergen CA, van Luxemburg-Heijs SA, de Wreede LC et al. Selective graft-versus-leukemia depends on magnitude and diversity of the alloreactive T cell response. *J.Clin.Invest* 2017;127:517-529.
74. Einsele H, Roosnek E, Rufer N et al. Infusion of cytomegalovirus (CMV)-specific T cells for the treatment of CMV infection not responding to antiviral chemotherapy. *Blood* 2002;99:3916-3922.

75. Rooney CM, Smith CA, Ng CY et al. Infusion of cytotoxic T cells for the prevention and treatment of Epstein-Barr virus-induced lymphoma in allogeneic transplant recipients. *Blood* 1998;92:1549-1555.
76. Peggs KS, Verfuert S, Pizzey A et al. Adoptive cellular therapy for early cytomegalovirus infection after allogeneic stem-cell transplantation with virus-specific T-cell lines. *Lancet* 2003;362:1375-1377.
77. Cobbold M, Khan N, Pourghesari B et al. Adoptive transfer of cytomegalovirus-specific CTL to stem cell transplant patients after selection by HLA-peptide tetramers. *J.Exp.Med.* 2005;202:379-386.
78. Goepfert PA, Bansal A, Edwards BH et al. A significant number of human immunodeficiency virus epitope-specific cytotoxic T lymphocytes detected by tetramer binding do not produce gamma interferon. *J.Virol.* 2000;74:10249-10255.
79. De Rosa SC, Lu FX, Yu J et al. Vaccination in humans generates broad T cell cytokine responses. *J.Immunol.* 2004;173:5372-5380.
80. Feuchtinger T, Matthes-Martin S, Richard C et al. Safe adoptive transfer of virus-specific T-cell immunity for the treatment of systemic adenovirus infection after allogeneic stem cell transplantation. *Br.J.Haematol.* 2006;134:64-76.
81. Moosmann A, Bigalke I, Tischer J et al. Effective and long-term control of EBV PTLD after transfer of peptide-selected T cells. *Blood* 2010;115:2960-2970.
82. Mackinnon S, Thomson K, Verfuert S, Peggs K, Lowdell M. Adoptive cellular therapy for cytomegalovirus infection following allogeneic stem cell transplantation using virus-specific T cells. *Blood Cells Mol.Dis.* 2008;40:63-67.
83. Leen AM, Bollard CM, Mendizabal AM et al. Multicenter study of banked third-party virus-specific T cells to treat severe viral infections after hematopoietic stem cell transplantation. *Blood* 2013;121:5113-5123.
84. Krebs P, Barnes MJ, Lampe K et al. NK-cell-mediated killing of target cells triggers robust antigen-specific T-cell-mediated and humoral responses. *Blood* 2009;113:6593-6602.
85. Martin-Fontecha A, Thomsen LL, Brett S et al. Induced recruitment of NK cells to lymph nodes provides IFN-gamma for T(H)1 priming. *Nat.Immunol.* 2004;5:1260-1265.
86. Dokun AO, Kim S, Smith HR et al. Specific and nonspecific NK cell activation during virus infection. *Nat.Immunol.* 2001;2:951-956.
87. Vivier E, Raulot DH, Moretta A et al. Innate or adaptive immunity? The example of natural killer cells. *Science* 2011;331:44-49.
88. Artis D, Spits H. The biology of innate lymphoid cells. *Nature* 2015;517:293-301.
89. Serafini N, Vossenrich CA, Di Santo JP. Transcriptional regulation of innate lymphoid cell fate. *Nat.Rev.Immunol.* 2015;15:415-428.
90. Eissens DN, Spanholtz J, van der Meer A et al. Defining early human NK cell developmental stages in primary and secondary lymphoid tissues. *PLoS.One.* 2012;7:e30930.
91. Freud AG, Yu J, Caligiuri MA. Human natural killer cell development in secondary lymphoid tissues. *Semin.Immunol.* 2014;26:132-137.
92. Freud AG, Becknell B, Roychowdhury S et al. A human CD34(+) subset resides in lymph nodes and differentiates into CD56bright natural killer cells. *Immunity.* 2005;22:295-304.
93. Freud AG, Yokohama A, Becknell B et al. Evidence for discrete stages of human natural killer cell differentiation in vivo. *J.Exp.Med.* 2006;203:1033-1043.
94. Hughes T, Briercheck EL, Freud AG et al. The transcription Factor AHR prevents the differentiation of a stage 3 innate lymphoid cell subset to natural killer cells. *Cell Rep.* 2014;8:150-162.
95. Montaldo E, Del Zotto G., Della Chiesa M. et al. Human NK cell receptors/markers: a tool to analyze NK cell development, subsets and function. *Cytometry A* 2013;83:702-713.
96. Melsen JE, Lughart G, Lankester AC, Schilham MW. Human Circulating and Tissue-Resident CD56(bright) Natural Killer Cell Populations. *Front Immunol.* 2016;7:262.
97. Romagnani C, Juelke K, Falco M et al. CD56 bright CD16 - Killer Ig-Like Receptor - NK Cells display longer telomeres and acquire features of CD56 dim NK Cells upon activation. *J.Immunol.* 2007;178:4947-4955.
98. Matos ME, Schnier GS, Beecher MS et al. Expression of a functional c-kit receptor on a subset of natural killer cells. *J.Exp.Med.* 1993;178:1079-1084.
99. Bjorkstrom NK, Riese P, Heuts F et al. Expression patterns of NKG2A, KIR, and CD57 define a process of CD56dim NK-cell differentiation uncoupled from NK-cell education. *Blood* 2010;116:3853-3864.
100. Beziat V, Duffy D, Quoc SN et al. CD56brightCD16+ NK cells: a functional intermediate stage of NK cell differentiation. *J.Immunol.* 2011;186:6753-6761.

101. Fauriat C, Long EO, Ljunggren HG, Bryceson YT. Regulation of human NK-cell cytokine and chemokine production by target cell recognition. *Blood* 2010;115:2167-2176.
102. Anfossi N, Andre P, Guia S et al. Human NK cell education by inhibitory receptors for MHC class I. *Immunity*. 2006;25:331-342.
103. De Maria A., Bozzano F, Cantoni C, Moretta L. Revisiting human natural killer cell subset function revealed cytolytic CD56(dim)CD16+ NK cells as rapid producers of abundant IFN-gamma on activation. *Proc.Natl.Acad.Sci.U.S.A* 2011;108:728-732.
104. Cooper MA, Fehniger TA, Turner SC et al. Human natural killer cells: a unique innate immunoregulatory role for the CD56(bright) subset. *Blood* 2001;97:3146-3151.
105. Takahashi E, Kuranaga N, Satoh K et al. Induction of CD16+ CD56bright NK cells with antitumour cytotoxicity not only from CD16- CD56bright NK Cells but also from CD16- CD56dim NK cells. *Scand.J.Immunol.* 2007;65:126-138.
106. Westermann J, Pabst R. Distribution of lymphocyte subsets and natural killer cells in the human body. *Clin.Investig.* 1992;70:539-544.
107. Carrega P, Bonaccorsi I, Di Carlo E. et al. CD56(bright)perforin(low) noncytotoxic human NK cells are abundant in both healthy and neoplastic solid tissues and recirculate to secondary lymphoid organs via afferent lymph. *J.Immunol.* 2014;192:3805-3815.
108. Fehniger TA, Cooper MA, Nuovo GJ et al. CD56bright natural killer cells are present in human lymph nodes and are activated by T cell-derived IL-2: a potential new link between adaptive and innate immunity. *Blood* 2003;101:3052-3057.
109. Lanier LL. Up on the tightrope: natural killer cell activation and inhibition. *Nat.Immunol.* 2008;9:495-502.
110. Newman KC, Riley EM. Whatever turns you on: accessory-cell-dependent activation of NK cells by pathogens. *Nat.Rev.Immunol.* 2007;7:279-291.
111. Hoglund P, Brodin P. Current perspectives of natural killer cell education by MHC class I molecules. *Nat.Rev.Immunol.* 2010;10:724-734.
112. Cooley S, Xiao F, Pitt M et al. A subpopulation of human peripheral blood NK cells that lacks inhibitory receptors for self-MHC is developmentally immature. *Blood* 2007;110:578-586.
113. Parham P, Moffett A. Variable NK cell receptors and their MHC class I ligands in immunity, reproduction and human evolution. *Nat.Rev.Immunol.* 2013;13:133-144.
114. Pak-Wittel MA, Yang L, Sojka DK, Rivenbark JG, Yokoyama WM. Interferon-gamma mediates chemokine-dependent recruitment of natural killer cells during viral infection. *Proc.Natl.Acad.Sci.U.S.A* 2013;110:E50-E59.
115. Crome SQ, Lang PA, Lang KS, Ohashi PS. Natural killer cells regulate diverse T cell responses. *Trends Immunol.* 2013;34:342-349.
116. Bancroft GJ, Shellam GR, Chalmer JE. Genetic influences on the augmentation of natural killer (NK) cells during murine cytomegalovirus infection: correlation with patterns of resistance. *J.Immunol.* 1981;126:988-994.
117. Biron CA, Byron KS, Sullivan JL. Severe herpesvirus infections in an adolescent without natural killer cells. *N.Engl.J.Med.* 1989;320:1731-1735.
118. Orange JS. Natural killer cell deficiency. *J.Allergy Clin.Immunol.* 2013;132:515-525.
119. Della CM, Muccio L, Moretta A. CMV induces rapid NK cell maturation in HSCT recipients. *Immunol.Lett.* 2013;155:11-13.
120. Williams H, McAulay K, Macsween KF et al. The immune response to primary EBV infection: a role for natural killer cells. *Br.J.Haematol.* 2005;129:266-274.
121. Azzi T, Lunemann A, Murer A et al. Role for early-differentiated natural killer cells in infectious mononucleosis. *Blood* 2014;124:2533-2543.
122. Ruggeri L, Capanni M, Urbani E et al. Effectiveness of donor natural killer cell alloreactivity in mismatched hematopoietic transplants. *Science* 2002;295:2097-2100.
123. Miller JS, Soignier Y, Panoskaltis-Mortari A et al. Successful adoptive transfer and in vivo expansion of human haploidentical NK cells in patients with cancer. *Blood* 2005;105:3051-3057.
124. Locatelli F, Moretta F, Brescia L, Merli P. Natural killer cells in the treatment of high-risk acute leukaemia. *Semin.Immunol.* 2014;26:173-179.
125. Bosch M, Dhadda M, Hoegh-Petersen M et al. Immune reconstitution after anti-thymocyte globulin-conditioned hematopoietic cell transplantation. *Cytotherapy.* 2012;14:1258-1275.

126. Dulphy N, Haas P, Busson M et al. An unusual CD56(bright) CD16(low) NK cell subset dominates the early posttransplant period following HLA-matched hematopoietic stem cell transplantation. *J.Immunol.* 2008;181:2227-2237.
127. Vukicevic M, Chalandon Y, Helg C et al. CD56bright NK cells after hematopoietic stem cell transplantation are activated mature NK cells that expand in patients with low numbers of T cells. *Eur.J.Immunol.* 2010;40:3246-3254.
128. Silva A, Andrews DM, Brooks AG, Smyth MJ, Hayakawa Y. Application of CD27 as a marker for distinguishing human NK cell subsets. *Int.Immunol.* 2008;20:625-630.
129. Foley B, Cooley S, Verneris MR et al. Cytomegalovirus reactivation after allogeneic transplantation promotes a lasting increase in educated NKG2C+ natural killer cells with potent function. *Blood* 2011
130. Foley B, Cooley S, Verneris MR et al. NK cell education after allogeneic transplantation: dissociation between recovery of cytokine-producing and cytotoxic functions. *Blood* 2011;118:2784-2792.
131. Pical-Izard C, Crocchiolo R, Granjeaud S et al. Reconstitution of natural killer cells in HLA-matched HSCT after reduced-intensity conditioning: impact on clinical outcome. *Biol.Blood Marrow Transplant* 2015;21:429-439.
132. Simonetta F, Pradier A, Bosshard C et al. NK Cell Functional Impairment after Allogeneic Hematopoietic Stem Cell Transplantation Is Associated with Reduced Levels of T-bet and Eomesodermin. *J.Immunol.* 2015;195:4712-4720.
133. Bjorklund AT, Schaffer M, Fauriat C et al. NK cells expressing inhibitory KIR for non-self-ligands remain tolerant in HLA-matched sibling stem cell transplantation. *Blood* 2010;115:2686-2694.
134. Nguyen S, Kuentz M, Vernant JP et al. Involvement of mature donor T cells in the NK cell reconstitution after haploidentical hematopoietic stem-cell transplantation. *Leukemia* 2008;22:344-352.
135. Vago L, Forno B, Sormani MP et al. Temporal, quantitative, and functional characteristics of single-KIR-positive alloreactive natural killer cell recovery account for impaired graft-versus-leukemia activity after haploidentical hematopoietic stem cell transplantation. *Blood* 2008;112:3488-3499.
136. Nguyen S, Dhedin N, Vernant JP et al. NK-cell reconstitution after haploidentical hematopoietic stem-cell transplantations: immaturity of NK cells and inhibitory effect of NKG2A override GvL effect. *Blood* 2005;105:4135-4142.
137. Nguyen S, Beziat V, Dhedin N et al. HLA-E upregulation on IFN-gamma-activated AML blasts impairs CD94/NKG2A-dependent NK cytotoxicity after haplo-mismatched hematopoietic SCT. *Bone Marrow Transplant* 2009;43:693-699.
138. Ghasemzadeh M, Hosseini E, Schwarzer AP, Pourfathollah AA. NK cell maturation to CD56(dim) subset associated with high levels of NCRs overrides the inhibitory effect of NKG2A and recovers impaired NK cell cytotoxic potential after allogeneic hematopoietic stem cell transplantation. *Leuk.Res.* 2016;43:58-65.
139. Sinclair J. Human cytomegalovirus: Latency and reactivation in the myeloid lineage. *J.Clin.Virol.* 2008;41:180-185.
140. Hebart H, Einsele H. Clinical aspects of CMV infection after stem cell transplantation. *Hum.Immunol.* 2004;65:432-436.
141. Li CR, Greenberg PD, Gilbert MJ, Goodrich JM, Riddell SR. Recovery of HLA-restricted cytomegalovirus (CMV)-specific T-cell responses after allogeneic bone marrow transplant: correlation with CMV disease and effect of ganciclovir prophylaxis. *Blood* 1994;83:1971-1979.
142. Barron MA, Gao D, Springer KL et al. Relationship of reconstituted adaptive and innate cytomegalovirus (CMV)-specific immune responses with CMV viremia in hematopoietic stem cell transplant recipients. *Clin.Infect.Dis.* 2009;49:1777-1783.
143. Williams KM, Hakim FT, Gress RE. T cell immune reconstitution following lymphodepletion. *Semin.Immunol.* 2007;19:318-330.
144. Tchao NK, Turka LA. Lymphodepletion and homeostatic proliferation: implications for transplantation. *Am.J.Transplant.* 2012;12:1079-1090.
145. Romero P, Zippelius A, Kurth I et al. Four functionally distinct populations of human effector-memory CD8+ T lymphocytes. *J.Immunol.* 2007;178:4112-4119.
146. Appay V, Dunbar PR, Callan M et al. Memory CD8+ T cells vary in differentiation phenotype in different persistent virus infections. *Nat.Med.* 2002;8:379-385.
147. Gamadia LE, Rentenaar RJ, Baars PA et al. Differentiation of cytomegalovirus-specific CD8(+) T cells in healthy and immunosuppressed virus carriers. *Blood* 2001;98:754-761.
148. Looney RJ, Falsey A, Campbell D et al. Role of cytomegalovirus in the T cell changes seen in elderly individuals. *Clin.Immunol.* 1999;90:213-219.

149. Marchant A, Appay V, Van Der Sande M et al. Mature CD8(+) T lymphocyte response to viral infection during fetal life. *J.Clin.Invest* 2003;111:1747-1755.
150. Kuijpers TW, Vossen MT, Gent MR et al. Frequencies of circulating cytolytic, CD45RA+CD27-, CD8+ T lymphocytes depend on infection with CMV. *J.Immunol.* 2003;170:4342-4348.
151. Miles DJ, van der Sande M, Jeffries D et al. Cytomegalovirus infection in Gambian infants leads to profound CD8 T-cell differentiation. *J.Virol.* 2007;81:5766-5776.
152. Miles DJ, van der Sande M, Jeffries D et al. Maintenance of large subpopulations of differentiated CD8 T-cells two years after cytomegalovirus infection in Gambian infants. *PLoS.One.* 2008;3:e2905.
153. van de Berg PJ, van SA, ten Berge IJ, van Lier RA. A fingerprint left by cytomegalovirus infection in the human T cell compartment. *J.Clin.Virol.* 2008;41:213-217.
154. Cantisan S, Torre-Cisneros J, Lara R et al. Age-dependent association between low frequency of CD27/CD28 expression on pp65 CD8+ T cells and cytomegalovirus replication after transplantation. *Clin.Vaccine Immunol.* 2009;16:1429-1438.
155. Peggs KS, Verfuert S, Pizzey A et al. Reconstitution of T-cell repertoire after autologous stem cell transplantation: influence of CD34 selection and cytomegalovirus infection. *Biol.Blood Marrow Transplant.* 2003;9:198-205.
156. Luo XH, Huang XJ, Li D et al. Immune reconstitution to cytomegalovirus following partially matched-related donor transplantation: impact of in vivo T-cell depletion and granulocyte colony-stimulating factor-primed peripheral blood/bone marrow mixed grafts. *Transpl.Infect.Dis.* 2013;15:22-33.
157. Wursch AM, Gratama JW, Middeldorp JM et al. The effect of cytomegalovirus infection on T lymphocytes after allogeneic bone marrow transplantation. *Clin.Exp.Immunol.* 1985;62:278-287.
158. Niesters HG, van Esser J, Fries E et al. Development of a real-time quantitative assay for detection of Epstein-Barr virus. *J.Clin.Microbiol.* 2000;38:712-715.
159. Claas EC, Schilham MW, de Brouwer CS et al. Internally controlled real-time PCR monitoring of adenovirus DNA load in serum or plasma of transplant recipients. *J.Clin.Microbiol.* 2005;43:1738-1744.
160. Kalpoe JS, Kroes AC, de Jong MD et al. Validation of clinical application of cytomegalovirus plasma DNA load measurement and definition of treatment criteria by analysis of correlation to antigen detection. *J.Clin.Microbiol.* 2004;42:1498-1504.
161. Boeckh M, Ljungman P. How we treat cytomegalovirus in hematopoietic cell transplant recipients. *Blood* 2009;113:5711-5719.
162. Meijer E, Cornelissen JJ. Epstein-Barr virus-associated lymphoproliferative disease after allogeneic haematopoietic stem cell transplantation: molecular monitoring and early treatment of high-risk patients. *Curr.Opin.Hematol.* 2008;15:576-585.
163. van Tol MJ, Claas EC, Heemskerk B et al. Adenovirus infection in children after allogeneic stem cell transplantation: diagnosis, treatment and immunity. *Bone Marrow Transplant.* 2005;35 Suppl 1:S73-S76.
164. Shaulov A, Murali-Krishna K. CD8 T cell expansion and memory differentiation are facilitated by simultaneous and sustained exposure to antigenic and inflammatory milieu. *J.Immunol.* 2008;180:1131-1138.
165. Gamadia LE, van Leeuwen EM, Remmerswaal EB et al. The size and phenotype of virus-specific T cell populations is determined by repetitive antigenic stimulation and environmental cytokines. *J.Immunol.* 2004;172:6107-6114.
166. van Leeuwen EM, Koning JJ, Remmerswaal EB et al. Differential usage of cellular niches by cytomegalovirus versus EBV- and influenza virus-specific CD8+ T cells. *J.Immunol.* 2006;177:4998-5005.
167. Wherry EJ. T cell exhaustion. *Nat.Immunol.* 2011;12:492-499.
168. Cicin-Sain L, Sylwester AW, Hagen SI et al. Cytomegalovirus-specific T cell immunity is maintained in immunosenescent rhesus macaques. *J.Immunol.* 2011;187:1722-1732.
169. Day CL, Kaufmann DE, Kiepiela P et al. PD-1 expression on HIV-specific T cells is associated with T-cell exhaustion and disease progression. *Nature* 2006;443:350-354.
170. Hertoghs KM, Moerland PD, van SA et al. Molecular profiling of cytomegalovirus-induced human CD8+ T cell differentiation. *J.Clin.Invest* 2010;120:4077-4090.
171. Matloubian M, Concepcion RJ, Ahmed R. CD4+ T cells are required to sustain CD8+ cytotoxic T-cell responses during chronic viral infection. *J.Virol.* 1994;68:8056-8063.
172. Walter EA, Greenberg PD, Gilbert MJ et al. Reconstitution of cellular immunity against cytomegalovirus in recipients of allogeneic bone marrow by transfer of T-cell clones from the donor. *N.Engl.J.Med.* 1995;333:1038-1044.

173. van Leeuwen EM, Remmerswaal EB, Heemskerk MH, ten Berge IJ, van Lier RA. Strong selection of virus-specific cytotoxic CD4+ T-cell clones during primary human cytomegalovirus infection. *Blood* 2006;108:3121-3127.
174. Dechanet J, Merville P, Lim A et al. Implication of gammadelta T cells in the human immune response to cytomegalovirus. *J.Clin.Invest* 1999;103:1437-1449.
175. Lafarge X, Merville P, Cazin MC et al. Cytomegalovirus infection in transplant recipients resolves when circulating gammadelta T lymphocytes expand, suggesting a protective antiviral role. *J.Infect.Dis.* 2001;184:533-541.
176. Remmerswaal EB, Havenith SH, Idu MM et al. Human virus-specific effector-type T cells accumulate in blood but not in lymph nodes. *Blood* 2012;119:1702-1712.
177. Klarenbeek PL, Remmerswaal EB, ten Berge IJ et al. Deep sequencing of antiviral T-cell responses to HCMV and EBV in humans reveals a stable repertoire that is maintained for many years. *PLoS.Pathog.* 2012;8:e1002889.
178. Elmaagacli AH, Steckel NK, Koldehoff M et al. Early human cytomegalovirus replication after transplantation is associated with a decreased relapse risk: evidence for a putative virus-versus-leukemia effect in acute myeloid leukemia patients. *Blood* 2011;118:1402-1412.
179. Gustafsson A, Levitsky V, Zou JZ et al. Epstein-Barr virus (EBV) load in bone marrow transplant recipients at risk to develop posttransplant lymphoproliferative disease: prophylactic infusion of EBV-specific cytotoxic T cells. *Blood* 2000;95:807-814.
180. Leen AM, Myers GD, Sili U et al. Monoculture-derived T lymphocytes specific for multiple viruses expand and produce clinically relevant effects in immunocompromised individuals. *Nat.Med.* 2006;12:1160-1166.
181. Leen AM, Christin A, Myers GD et al. Cytotoxic T lymphocyte therapy with donor T cells prevents and treats adenovirus and Epstein-Barr virus infections after haploidentical and matched unrelated stem cell transplantation. *Blood* 2009;114:4283-4292.
182. Fujita Y, Leen AM, Sun J et al. Exploiting cytokine secretion to rapidly produce multivirus-specific T cells for adoptive immunotherapy. *J.Immunother.* 2008;31:665-674.
183. Gerdemann U, Christin AS, Vera JF et al. Nucleofection of DCs to generate Multivirus-specific T cells for prevention or treatment of viral infections in the immunocompromised host. *Mol.Ther.* 2009;17:1616-1625.
184. Zandvliet ML, Falkenburg JH, van LE et al. Combined CD8+ and CD4+ adenovirus hexon-specific T cells associated with viral clearance after stem cell transplantation as treatment for adenovirus infection. *Haematologica* 2010
185. Rickinson AB, Lee SP, Steven NM. Cytotoxic T lymphocyte responses to Epstein-Barr virus. *Curr.Opin.Immunol.* 1996;8:492-497.
186. Wills MR, Carmichael AJ, Mynard K et al. The human cytotoxic T-lymphocyte (CTL) response to cytomegalovirus is dominated by structural protein pp65: frequency, specificity, and T-cell receptor usage of pp65-specific CTL. *J.Virol.* 1996;70:7569-7579.
187. Zandvliet ML, van LE, Jedema I et al. Co-ordinated isolation of CD8(+) and CD4(+) T cells recognizing a broad repertoire of cytomegalovirus pp65 and IE1 epitopes for highly specific adoptive immunotherapy. *Cytotherapy.* 2010
188. Savoldo B, Cubbage ML, Durett AG et al. Generation of EBV-specific CD4+ cytotoxic T cells from virus naive individuals. *J.Immunol.* 2002;168:909-918.
189. Altman JD, Moss PA, Goulder PJ et al. Phenotypic analysis of antigen-specific T lymphocytes. *Science* 1996;274:94-96.
190. Karlsson H, Brewin J, Kinnon C, Veys P, Amrolia PJ. Generation of trispecific cytotoxic T cells recognizing cytomegalovirus, adenovirus, and Epstein-Barr virus: an approach for adoptive immunotherapy of multiple pathogens. *J.Immunother.* 2007;30:544-556.
191. Zandvliet ML, Falkenburg JH, Jedema I et al. Detailed analysis of IFN $\gamma$  response upon activation permits efficient isolation of cytomegalovirus-specific CD8+ T cells for adoptive immunotherapy. *J.Immunother.* 2009;32:513-523.
192. Flomenberg P, Piaskowski V, Truitt RL, Casper JT. Characterization of human proliferative T cell responses to adenovirus. *J.Infect.Dis.* 1995;171:1090-1096.
193. Walter EA, Greenberg PD, Gilbert MJ et al. Reconstitution of cellular immunity against cytomegalovirus in recipients of allogeneic bone marrow by transfer of T-cell clones from the donor. *N.Engl.J.Med.* 1995;333:1038-1044.

194. Melenhorst JJ, Leen AM, Bollard CM et al. Allogeneic virus-specific T cells with HLA alloreactivity do not produce GVHD in human subjects. *Blood* 2010
195. Dazzi F, Szydlo RM, Craddock C et al. Comparison of single-dose and escalating-dose regimens of donor lymphocyte infusion for relapse after allografting for chronic myeloid leukemia. *Blood* 2000;95:67-71.
196. Sakaguchi S. Naturally arising CD4+ regulatory t cells for immunologic self-tolerance and negative control of immune responses. *Annu.Rev.Immunol.* 2004;22:531-562.
197. Wang J, Ioan-Facsinay A, van der Voort EI, Huizinga TW, Toes RE. Transient expression of FOXP3 in human activated nonregulatory CD4+ T cells. *Eur.J.Immunol.* 2007;37:129-138.
198. Hoffmann P, Ermann J, Edinger M, Fathman CG, Strober S. Donor-type CD4(+)CD25(+) regulatory T cells suppress lethal acute graft-versus-host disease after allogeneic bone marrow transplantation. *J.Exp.Med.* 2002;196:389-399.
199. Taylor PA, Lees CJ, Blazar BR. The infusion of ex vivo activated and expanded CD4(+)CD25(+) immune regulatory cells inhibits graft-versus-host disease lethality. *Blood* 2002;99:3493-3499.
200. Brunstein CG, Miller JS, Cao Q et al. Infusion of ex vivo expanded T regulatory cells in adults transplanted with umbilical cord blood: safety profile and detection kinetics. *Blood* 2010
201. Di IM, Falzetti F, Carotti A et al. Tregs prevent GVHD and promote immune reconstitution in HLA-haploidentical transplantation. *Blood* 2011;117:3921-3928.
202. Thornton AM, Shevach EM. Suppressor effector function of CD4+CD25+ immunoregulatory T cells is antigen nonspecific. *J.Immunol.* 2000;164:183-190.
203. Nguyen VH, Shashidhar S, Chang DS et al. The impact of regulatory T cells on T-cell immunity following hematopoietic cell transplantation. *Blood* 2008;111:945-953.
204. Leen AM, Sili U, Vanin EF et al. Conserved CTL epitopes on the adenovirus hexon protein expand subgroup cross-reactive and subgroup-specific CD8+ T cells. *Blood* 2004;104:2432-2440.
205. Zandvliet ML, Falkenburg JH, van LE et al. Combined CD8+ and CD4+ adenovirus hexon-specific T cells associated with viral clearance after stem cell transplantation as treatment for adenovirus infection. *Haematologica* 2010;95:1943-1951.
206. Howard DS, Phillips II GL, Reece DE et al. Adenovirus infections in hematopoietic stem cell transplant recipients. *Clin.Infect.Dis.* 1999;29:1494-1501.
207. Chakrabarti S, Mautner V, Osman H et al. Adenovirus infections following allogeneic stem cell transplantation: incidence and outcome in relation to graft manipulation, immunosuppression, and immune recovery. *Blood* 2002;100:1619-1627.
208. Walls T, Shankar AG, Shingadia D. Adenovirus: an increasingly important pathogen in paediatric bone marrow transplant patients. *Lancet Infect.Dis.* 2003;3:79-86.
209. Feuchtinger T, Matthes-Martin S, Richard C et al. Safe adoptive transfer of virus-specific T-cell immunity for the treatment of systemic adenovirus infection after allogeneic stem cell transplantation. *Br.J.Haematol.* 2006;134:64-76.
210. Morfin F, Dupuis-Girod S, Frobert E et al. Differential susceptibility of adenovirus clinical isolates to cidofovir and ribavirin is not related to species alone. *Antivir.Ther.* 2009;14:55-61.
211. Naesens L, Lenaerts L, Andrei G et al. Antiadenovirus activities of several classes of nucleoside and nucleotide analogues. *Antimicrob.Agents Chemother.* 2005;49:1010-1016.
212. Morfin F, Dupuis-Girod S, Mundweiler S et al. In vitro susceptibility of adenovirus to antiviral drugs is species-dependent. *Antivir.Ther.* 2005;10:225-229.
213. Muller WJ, Levin MJ, Shin YK et al. Clinical and in vitro evaluation of cidofovir for treatment of adenovirus infection in pediatric hematopoietic stem cell transplant recipients. *Clin.Infect.Dis.* 2005;41:1812-1816.
214. Hoffman JA, Shah AJ, Ross LA, Kapoor N. Adenoviral infections and a prospective trial of cidofovir in pediatric hematopoietic stem cell transplantation. *Biol.Blood Marrow Transplant.* 2001;7:388-394.
215. Mynarek M, Ganzenmueller T, Mueller-Heine A et al. Patient, virus and treatment-related risk factors in pediatric adenovirus infection after stem cell transplantation: results of a routine monitoring program. *Biol.Blood Marrow Transplant.* 2013
216. Jacobs R, Stoll M, Stratmann G et al. CD16- CD56+ natural killer cells after bone marrow transplantation. *Blood* 1992;79:3239-3244.
217. Storek J, Dawson MA, Storer B et al. Immune reconstitution after allogeneic marrow transplantation compared with blood stem cell transplantation. *Blood* 2001;97:3380-3389.
218. Jost S, Altfeld M. Control of human viral infections by natural killer cells. *Annu.Rev.Immunol.* 2013;31:163-194.



219. Lanier LL. Evolutionary struggles between NK cells and viruses. *Nat.Rev.Immunol.* 2008;8:259-268.
220. Biron CA, Nguyen KB, Pien GC, Cousens LP, Salazar-Mather TP. Natural killer cells in antiviral defense: function and regulation by innate cytokines. *Annu.Rev.Immunol.* 1999;17:189-220.
221. Pahl JH, Verhoeven DH, Kwappenberg KM et al. Adenovirus type 35, but not type 5, stimulates NK cell activation via plasmacytoid dendritic cells and TLR9 signaling. *Mol.Immunol.* 2012;51:91-100.
222. Miller G, Lahrs S, Pillarisetty VG, Shah AB, DeMatteo RP. Adenovirus infection enhances dendritic cell immunostimulatory properties and induces natural killer and T-cell-mediated tumor protection. *Cancer Res.* 2002;62:5260-5266.
223. Routes JM. IFN increases class I MHC antigen expression on adenovirus-infected human cells without inducing resistance to natural killer cell killing. *J.Immunol.* 1992;149:2372-2377.
224. Walls T, Hawrami K, Ushiro-Lumb I et al. Adenovirus infection after pediatric bone marrow transplantation: is treatment always necessary? *Clin.Infect.Dis.* 2005;40:1244-1249.
225. La Rosa AM, Champlin RE, Mirza N et al. Adenovirus infections in adult recipients of blood and marrow transplants. *Clin.Infect.Dis.* 2001;32:871-876.
226. Ozdemir E, St John LS, Gillespie G et al. Cytomegalovirus reactivation following allogeneic stem cell transplantation is associated with the presence of dysfunctional antigen-specific CD8+ T cells. *Blood* 2002;100:3690-3697.
227. Gordon YJ, Aralullo-Cruz TP, Johnson YF, Romanowski EG, Kinchington PR. Isolation of human adenovirus type 5 variants resistant to the antiviral cidofovir. *Invest Ophthalmol.Vis.Sci.* 1996;37:2774-2778.
228. Ljungman P. Would monitoring CMV immune responses allow improved control of CMV in stem cell transplant patients. *J.Clin.Virol.* 2006;35:493-495.
229. Solano C, Benet I, Remigia MJ et al. Immunological monitoring for guidance of preemptive antiviral therapy for active cytomegalovirus infection in allogeneic stem-cell transplant recipients: a pilot experience. *Transplantation* 2011;92:e17-e20.
230. Hauser A, Schratlbauer K, Najdanovic D et al. Optimized quantification of lymphocyte subsets by use of CD7 and CD33. *Cytometry A* 2013;83:316-323.
231. Lutz CT, Karapetyan A, Al-Attar A et al. Human NK cells proliferate and die in vivo more rapidly than T cells in healthy young and elderly adults. *J.Immunol.* 2011;186:4590-4598.
232. Kaplan J, Nolan D, Reed A. Altered lymphocyte markers and blastogenic responses associated with 24 hour delay in processing of blood samples. *J.Immunol.Methods* 1982;50:187-191.
233. Olson WC, Smolkin ME, Farris EM et al. Shipping blood to a central laboratory in multicenter clinical trials: effect of ambient temperature on specimen temperature, and effects of temperature on mononuclear cell yield, viability and immunologic function. *J.Transl.Med.* 2011;9:26.
234. Dobbs K, Notarangelo LD. 2016 CIS Annual Meeting Abstract 4514: NK cells from patients with RAG and ARTEMIS deficiency have an immature phenotype and display increased degranulation capacity - implications for hematopoietic stem cell transplantation. *J.Clin.Immunol.* 2016;36:283-284.
235. Dobbs K, Tabellini G, Calzoni E et al. Natural Killer Cells from Patients with Recombinase-Activating Gene and Non-Homologous End Joining Gene Defects Comprise a Higher Frequency of CD56bright NKG2A+++ Cells, and Yet Display Increased Degranulation and Higher Perforin Content. *Front Immunol.* 2017;8:798.
236. Hong HS, Ahmad F, Eberhard JM et al. Loss of CCR7 expression on CD56(bright) NK cells is associated with a CD56(dim)CD16(+) NK cell-like phenotype and correlates with HIV viral load. *PLoS.One.* 2012;7:e44820.
237. Lugthart G, van Ostaijen-ten Dam MM, van Tol MJ, Lankester AC, Schilham MW. CD56(dim)CD16(-) NK cell phenotype can be induced by cryopreservation. *Blood* 2015;125:1842-1843.
238. van der Maaten LJ, Hinton GE. Visualizing High-Dimensional Data Using t-SNE. *Journal of Machine Learning Research* 2008;15:2579-2605.
239. van der Maaten LJ. Accelerating t-SNE using Tree-Based Algorithms. *Journal of Machine Learning Research* 2014;15:3221-3245.
240. Krijthe JH, van der Maaten LJ. Rtsne: T-Distributed Stochastic Neighbor Embedding using a Barnes-Hut Implementation. <https://CRAN.R-project.org/package=Rtsne> 2015;v0.11:
241. Bjorklund AK, Forke M, Picelli S et al. The heterogeneity of human CD127(+) innate lymphoid cells revealed by single-cell RNA sequencing. *Nat.Immunol.* 2016;17:451-460.
242. Pahl JH, Ruslan SE, Buddingh EP et al. Anti-EGFR antibody cetuximab enhances the cytolytic activity of natural killer cells toward osteosarcoma. *Clin.Cancer Res.* 2012;18:432-441.

243. Lugthart G, Melsen JE, Vervat C et al. Human Lymphoid Tissues Harbor a Distinct CD69+CXCR6+ NK Cell Population. *J.Immunol.* 2016;197:78-84.
244. Heemskerck B, van Vreeswijk T., Veltrop-Duits LA et al. Adenovirus-specific CD4+ T cell clones recognizing endogenous antigen inhibit viral replication in vitro through cognate interaction. *J.Immunol.* 2006;177:8851-8859.
245. Wickham H, Francois R. dplyr: A Grammar of Data Manipulation. <https://CRAN.R-project.org/package=dplyr> 2016;v0.5.0:
246. Zhao S, Guo Y, Sheng Q, Shyr Y. heatmap3: An Improved Heatmap Package. <https://CRAN.R-project.org/package=heatmap3> 2015;v1.1.1:
247. Wickham H, Chang W. ggplot2: Create Elegant Data Visualisations Using the Grammar of Graphics. <https://CRAN.R-project.org/package=ggplot2> 2016;v2.2.1:
248. Neuwirth E. RColorBrewer: ColorBrewer Palettes. <https://CRAN.R-project.org/package=RColorBrewer> 2014;v1.1-2:
249. Heinze G, Ploner M, Dunkler D, Southworth H. logistf: Firth's Bias-Reduced Logistic Regression. <https://CRAN.R-project.org/package=logistf> 2013;v1.22:
250. Holm S. A simple sequentially rejective multiple test procedure. *Scandinavian Journal of Statistics* 1979;6:65-70.
251. Scharton TM, Scott P. Natural killer cells are a source of interferon gamma that drives differentiation of CD4+ T cell subsets and induces early resistance to *Leishmania major* in mice. *J.Exp.Med.* 1993;178:567-577.
252. Gerosa F, Baldani-Guerra B, Nisii C et al. Reciprocal activating interaction between natural killer cells and dendritic cells. *J.Exp.Med.* 2002;195:327-333.
253. Askenase MH, Han SJ, Byrd AL et al. Bone-Marrow-Resident NK Cells Prime Monocytes for Regulatory Function during Infection. *Immunity.* 2015;42:1130-1142.
254. Vivier E, Raulet DH, Moretta A et al. Innate or adaptive immunity? The example of natural killer cells. *Science* 2011;331:44-49.
255. Westermann J, Pabst R. Distribution of lymphocyte subsets and natural killer cells in the human body. *Clin.Investig.* 1992;70:539-544.
256. Ferlazzo G, Pack M, Thomas D et al. Distinct roles of IL-12 and IL-15 in human natural killer cell activation by dendritic cells from secondary lymphoid organs. *Proc.Natl.Acad.Sci.U.S.A* 2004;101:16606-16611.
257. Tomasello E, Yessaad N, Gregoire E et al. Mapping of Nkp46(+) Cells in Healthy Human Lymphoid and Non-Lymphoid Tissues. *Front Immunol.* 2012;3:344.
258. Gregoire C, Chasson L, Luci C et al. The trafficking of natural killer cells. *Immunol.Rev.* 2007;220:169-182.
259. Hazenberg MD, Spits H. Human innate lymphoid cells. *Blood* 2014;124:700-709.
260. Saeed AI, Sharov V, White J et al. TM4: a free, open-source system for microarray data management and analysis. *Biotechniques* 2003;34:374-378.
261. Marquardt N, Beziat V, Nystrom S et al. Cutting edge: identification and characterization of human intrahepatic CD49a+ NK cells. *J.Immunol.* 2015;194:2467-2471.
262. Ferlazzo G, Thomas D, Lin SL et al. The abundant NK cells in human secondary lymphoid tissues require activation to express killer cell Ig-like receptors and become cytolytic. *J.Immunol.* 2004;172:1455-1462.
263. Cella M, Fuchs A, Vermi W et al. A human natural killer cell subset provides an innate source of IL-22 for mucosal immunity. *Nature* 2009;457:722-725.
264. Cosulich ME, Rubartelli A, Riso A, Cozzolino F, Bargellesi A. Functional characterization of an antigen involved in an early step of T-cell activation. *Proc.Natl.Acad.Sci.U.S.A* 1987;84:4205-4209.
265. Hara T, Jung LK, Bjorndahl JM, Fu SM. Human T cell activation. III. Rapid induction of a phosphorylated 28 kD/32 kD disulfide-linked early activation antigen (EA 1) by 12-*o*-tetradecanoyl phorbol-13-acetate, mitogens, and antigens. *J.Exp.Med.* 1986;164:1988-2005.
266. Lopez-Cabrera M, Santis AG, Fernandez-Ruiz E et al. Molecular cloning, expression, and chromosomal localization of the human earliest lymphocyte activation antigen AIM/CD69, a new member of the C-type animal lectin superfamily of signal-transmitting receptors. *J.Exp.Med.* 1993;178:537-547.
267. Cyster JG, Schwab SR. Sphingosine-1-phosphate and lymphocyte egress from lymphoid organs. *Annu.Rev.Immunol.* 2012;30:69-94.
268. Shioh LR, Rosen DB, Brdickova N et al. CD69 acts downstream of interferon-alpha/beta to inhibit S1P1 and lymphocyte egress from lymphoid organs. *Nature* 2006;440:540-544.

269. Geissmann F, Cameron TO, Sidobre S et al. Intravascular immune surveillance by CXCR6+ NKT cells patrolling liver sinusoids. *PLoS.Biol.* 2005;3:e113.
270. Palendira U, Chinn R, Raza W et al. Selective accumulation of virus-specific CD8+ T cells with unique homing phenotype within the human bone marrow. *Blood* 2008;112:3293-3302.
271. Hudspeth K, Donadon M, Cimino M et al. Human liver-resident CD56/CD16 NK cells are retained within hepatic sinusoids via the engagement of CCR5 and CXCR6 pathways. *J.Autoimmun.* 2015;66:40-50.
272. Peng H, Jiang X, Chen Y et al. Liver-resident NK cells confer adaptive immunity in skin-contact inflammation. *J.Clin.Invest* 2013;123:1444-1456.
273. Paust S, Gill HS, Wang BZ et al. Critical role for the chemokine receptor CXCR6 in NK cell-mediated antigen-specific memory of haptens and viruses. *Nat.Immunol.* 2010;11:1127-1135.
274. Shibuya A, Campbell D, Hannum C et al. DNAM-1, a novel adhesion molecule involved in the cytolytic function of T lymphocytes. *Immunity.* 1996;4:573-581.
275. Enqvist M, Ask EH, Forslund E et al. Coordinated expression of DNAM-1 and LFA-1 in educated NK cells. *J.Immunol.* 2015;194:4518-4527.
276. Martinet L, Ferrari de Andrade L., Guillerey C et al. DNAM-1 expression marks an alternative program of NK cell maturation. *Cell Rep.* 2015;11:85-97.
277. Zhang Z, Wu N, Lu Y et al. DNAM-1 controls NK cell activation via an ITT-like motif. *J.Exp.Med.* 2015;212:2165-2182.
278. Carlsten M, Baumann BC, Simonsson M et al. Reduced DNAM-1 expression on bone marrow NK cells associated with impaired killing of CD34+ blasts in myelodysplastic syndrome. *Leukemia* 2010;24:1607-1616.
279. Vossen MT, Matmati M, Hertoghs KM et al. CD27 defines phenotypically and functionally different human NK cell subsets. *J.Immunol.* 2008;180:3739-3745.
280. Jacobsen N, Lonnqvist B, Ringden O et al. Graft-versus-leukaemia activity associated with cytomegalovirus seropositive bone marrow donors but separated from graft-versus-host disease in allograft recipients with AML. *Eur.J.Haematol.* 1987;38:350-355.
281. Nachbaur D, Clausen J, Kircher B. Donor cytomegalovirus seropositivity and the risk of leukemic relapse after reduced-intensity transplants. *Eur.J.Haematol.* 2006;76:414-419.
282. Fletcher JM, Prentice HG, Grundy JE. Natural killer cell lysis of cytomegalovirus (CMV)-infected cells correlates with virally induced changes in cell surface lymphocyte function-associated antigen-3 (LFA-3) expression and not with the CMV-induced down-regulation of cell surface class I HLA. *J.Immunol.* 1998;161:2365-2374.
283. Solana R, Tarazona R, Aiello AE et al. CMV and Immunosenescence: from basics to clinics. *Immun.Ageing* 2012;9:23.
284. van den Heuvel D, Jansen MAE, Nasserinejad K et al. Effects of nongenetic factors on immune cell dynamics in early childhood: The Generation R Study. *J.Allergy Clin.Immunol.* 2017;139:1923-1934.
285. van den Heuvel D, Jansen MA, Dik WA et al. Cytomegalovirus- and Epstein-Barr Virus-Induced T-Cell Expansions in Young Children Do Not Impair Naive T-cell Populations or Vaccination Responses: The Generation R Study. *J.Infect.Dis.* 2016;213:233-242.
286. Gamadia LE, van Leeuwen EM, Remmerswaal EB et al. The size and phenotype of virus-specific T cell populations is determined by repetitive antigenic stimulation and environmental cytokines. *J.Immunol.* 2004;172:6107-6114.
287. Bollard CM, Heslop HE. T cells for viral infections after allogeneic hematopoietic stem cell transplant. *Blood* 2016;127:3331-3340.
288. Feucht J, Opherck K, Lang P et al. Adoptive T-cell therapy with hexon-specific Th1 cells as a treatment of refractory adenovirus infection after HSCT. *Blood* 2015;125:1986-1994.
289. Creidy R, Moshous D, Touzot F et al. Specific T cells for the treatment of cytomegalovirus and/or adenovirus in the context of hematopoietic stem cell transplantation. *J.Allergy Clin.Immunol.* 2016;138:920-924.
290. Qasim W, Gilmour K, Zhan H et al. Interferon-gamma capture T cell therapy for persistent Adenoviraemia following allogeneic haematopoietic stem cell transplantation. *Br.J.Haematol.* 2013;161:449-452.
291. Peggs KS, Tholouli E, Chakraverty E et al. CMV~IMPACT: Results of a Randomized Controlled Trial of Immuno-Prophylactic Adoptive Cellular Therapy following Sibling Donor Allogeneic HSCT. *Blood* 20141109.

292. Blyth E, Clancy L, Simms R et al. Donor-derived CMV-specific T cells reduce the requirement for CMV-directed pharmacotherapy after allogeneic stem cell transplantation. *Blood* 2013;121:3745-3758.
293. Hatton O, Strauss-Albee DM, Zhao NQ et al. NKG2A-Expressing Natural Killer Cells Dominate the Response to Autologous Lymphoblastoid Cells Infected with Epstein-Barr Virus. *Front Immunol.* 2016;7:607.
294. Djaoud Z, Guethlein LA, Horowitz A et al. Two alternate strategies for innate immunity to Epstein-Barr virus: One using NK cells and the other NK cells and gammadelta T cells. *J.Exp.Med.* 2017
295. Chijioko O, Muller A, Feederle R et al. Human natural killer cells prevent infectious mononucleosis features by targeting lytic Epstein-Barr virus infection. *Cell Rep.* 2013;5:1489-1498.
296. Strowig T, Chijioko O, Carrega P et al. Human NK cells of mice with reconstituted human immune system components require preactivation to acquire functional competence. *Blood* 2010;116:4158-4167.
297. Carville A, Mansfield KG. Comparative pathobiology of macaque lymphocryptoviruses. *Comp Med.* 2008;58:57-67.
298. Wu C, Li B, Lu R et al. Clonal tracking of rhesus macaque hematopoiesis highlights a distinct lineage origin for natural killer cells. *Cell Stem Cell* 2014;14:486-499.
299. Ullah MA, Hill GR, Tey SK. Functional Reconstitution of Natural Killer Cells in Allogeneic Hematopoietic Stem Cell Transplantation. *Front Immunol.* 2016;7:144.
300. Mackay LK, Braun A, Macleod BL et al. Cutting edge: CD69 interference with sphingosine-1-phosphate receptor function regulates peripheral T cell retention. *J.Immunol.* 2015;194:2059-2063.
301. Shiow LR, Rosen DB, Brdickova N et al. CD69 acts downstream of interferon-alpha/beta to inhibit S1P1 and lymphocyte egress from lymphoid organs. *Nature* 2006;440:540-544.
302. Vales-Gomez M, Estes G, Aydogmus C et al. Natural killer cell hyporesponsiveness and impaired development in a CD247-deficient patient. *J.Allergy Clin.Immunol.* 2016;137:942-945.
303. Shibata F, Toma T, Wada T et al. Skin infiltration of CD56(bright) CD16(-) natural killer cells in a case of X-SCID with Omenn syndrome-like manifestations. *Eur.J.Haematol.* 2007;79:81-85.
304. Bendall SC, Simonds EF, Qiu P et al. Single-cell mass cytometry of differential immune and drug responses across a human hematopoietic continuum. *Science* 2011;332:687-696.
305. Buettner F, Natarajan KN, Casale FP et al. Computational analysis of cell-to-cell heterogeneity in single-cell RNA-sequencing data reveals hidden subpopulations of cells. *Nat.Biotechnol.* 2015;33:155-160.
306. Inngjerdigen M, Damaj B, Maghazachi AA. Expression and regulation of chemokine receptors in human natural killer cells. *Blood* 2001;97:367-375.
307. Campbell JJ, Qin S, Unutmaz D et al. Unique subpopulations of CD56+ NK and NK-T peripheral blood lymphocytes identified by chemokine receptor expression repertoire. *J.Immunol.* 2001;166:6477-6482.
308. Berahovich RD, Lai NL, Wei Z, Lanier LL, Schall TJ. Evidence for NK cell subsets based on chemokine receptor expression. *J.Immunol.* 2006;177:7833-7840.
309. Heydtmann M, Lalor PF, Eksteen JA et al. CXC chemokine ligand 16 promotes integrin-mediated adhesion of liver-infiltrating lymphocytes to cholangiocytes and hepatocytes within the inflamed human liver. *J.Immunol.* 2005;174:1055-1062.
310. Germanov E, Veinotte L, Cullen R et al. Critical role for the chemokine receptor CXCR6 in homeostasis and activation of CD1d-restricted NKT cells. *J.Immunol.* 2008;181:81-91.
311. Hombrink P, Helbig C, Backer RA et al. Programs for the persistence, vigilance and control of human CD8+ lung-resident memory T cells. *Nat.Immunol.* 2016;17:1467-1478.
312. Morgan AJ, Guillen C, Symon FA et al. CXCR6 identifies a putative population of retained human lung T cells characterised by co-expression of activation markers. *Immunobiology* 2008;213:599-608.
313. Koopman LA, Kopcow HD, Rybalov B et al. Human decidual natural killer cells are a unique NK cell subset with immunomodulatory potential. *J.Exp.Med.* 2003;198:1201-1212.
314. Manaster I, Mizrahi S, Goldman-Wohl D et al. Endometrial NK cells are special immature cells that await pregnancy. *J.Immunol.* 2008;181:1869-1876.
315. Montaldo E, Vacca P, Chiossone L et al. Unique Eomes(+) NK Cell Subsets Are Present in Uterus and Decidua During Early Pregnancy. *Front Immunol.* 2015;6:646.
316. Fuchs A, Vermi W, Lee JS et al. Intraepithelial type 1 innate lymphoid cells are a unique subset of IL-12- and IL-15-responsive IFN-gamma-producing cells. *Immunity.* 2013;38:769-781.
317. Hanna J, Goldman-Wohl D, Hamani Y et al. Decidual NK cells regulate key developmental processes at the human fetal-maternal interface. *Nat.Med.* 2006;12:1065-1074.

318. Vacca P, Pietra G, Falco M et al. Analysis of natural killer cells isolated from human decidua: Evidence that 2B4 (CD244) functions as an inhibitory receptor and blocks NK-cell function. *Blood* 2006;108:4078-4085.
319. Woon HG, Braun A, Li J et al. Compartmentalization of Total and Virus-Specific Tissue-Resident Memory CD8+ T Cells in Human Lymphoid Organs. *PLoS.Pathog.* 2016;12:e1005799.
320. Pallett LJ, Davies J, Colbeck EJ et al. IL-2high tissue-resident T cells in the human liver: Sentinels for hepatotropic infection. *J.Exp.Med.* 2017;214:1567-1580.
321. Purwar R, Campbell J, Murphy G et al. Resident memory T cells (T(RM)) are abundant in human lung: diversity, function, and antigen specificity. *PLoS.One.* 2011;6:e16245.
322. Posavad CM, Zhao L, Dong L et al. Enrichment of herpes simplex virus type 2 (HSV-2) reactive mucosal T cells in the human female genital tract. *Mucosal.Immunol.* 2017
323. Wilbanks A, Zondlo SC, Murphy K et al. Expression cloning of the STRL33/BONZO/TYMSTR ligand reveals elements of CC, CXC, and CX3C chemokines. *J.Immunol.* 2001;166:5145-5154.
324. Matloubian M, David A, Engel S, Ryan JE, Cyster JG. A transmembrane CXC chemokine is a ligand for HIV-coreceptor Bonzo. *Nat.Immunol.* 2000;1:298-304.
325. Gough PJ, Garton KJ, Wille PT et al. A disintegrin and metalloproteinase 10-mediated cleavage and shedding regulates the cell surface expression of CXC chemokine ligand 16. *J.Immunol.* 2004;172:3678-3685.
326. van d, V, Verweij V, de Witte TM et al. An alternatively spliced CXCL16 isoform expressed by dendritic cells is a secreted chemoattractant for CXCR6+ cells. *J.Leukoc.Biol.* 2010;87:1029-1039.
327. Shimaoka T, Nakayama T, Kume N et al. Cutting edge: SR-PSOX/CXC chemokine ligand 16 mediates bacterial phagocytosis by APCs through its chemokine domain. *J.Immunol.* 2003;171:1647-1651.
328. Shimaoka T, Nakayama T, Fukumoto N et al. Cell surface-anchored SR-PSOX/CXC chemokine ligand 16 mediates firm adhesion of CXC chemokine receptor 6-expressing cells. *J.Leukoc.Biol.* 2004;75:267-274.
329. Mackay LK, Minnich M, Kragten NA et al. Hobit and Blimp1 instruct a universal transcriptional program of tissue residency in lymphocytes. *Science* 2016;352:459-463.
330. Tabata S, Kadowaki N, Kitawaki T et al. Distribution and kinetics of SR-PSOX/CXCL16 and CXCR6 expression on human dendritic cell subsets and CD4+ T cells. *J.Leukoc.Biol.* 2005;77:777-786.
331. Fahy OL, Townley SL, McColl SR. CXCL16 regulates cell-mediated immunity to Salmonella enterica serovar Enteritidis via promotion of gamma interferon production. *Infect.Immun.* 2006;74:6885-6894.
332. Veinotte L, Gebremeskel S, Johnston B. CXCL16-positive dendritic cells enhance invariant natural killer T cell-dependent IFN $\gamma$  production and tumor control. *Oncoimmunology.* 2016;5:e1160979.
333. Yu J, Mao HC, Wei M et al. CD94 surface density identifies a functional intermediary between the CD56bright and CD56dim human NK-cell subsets. *Blood* 2010;115:274-281.
334. Romagnani C, Juelke K, Falco M et al. CD56bright CD16 - Killer Ig-Like Receptor - NK Cells Display Longer Telomeres and Acquire Features of CD56 dim NK Cells upon Activation. *J.Immunol.* 2007;178:4947-4955.
335. Sojka DK, Plougastel-Douglas B, Yang L et al. Tissue-resident natural killer (NK) cells are cell lineages distinct from thymic and conventional splenic NK cells. *Elife.* 2014;3:e01659.
336. Gineau L, Cognet C, Kara N et al. Partial MCM4 deficiency in patients with growth retardation, adrenal insufficiency, and natural killer cell deficiency. *J.Clin.Invest* 2012;122:821-832.
337. Mace EM, Hsu AP, Monaco-Shawver L et al. Mutations in GATA2 cause human NK cell deficiency with specific loss of the CD56(bright) subset. *Blood* 2013;121:2669-2677.



## **Dutch summary / Nederlandse samenvatting**





## Samenvatting

### Introductie

Hematopoïetische (bloedvormende) stamcellen zijn te vinden in het beenmerg en vormen een levenslange bron van rode bloedcellen, bloedplaatjes en witte bloedcellen. Het vervangen van de zieke stamcellen van een patiënt door de gezonde stamcellen van een donor staat bekend onder de term allogene hematopoïetische stamceltransplantatie, (HSCT), en wordt toegepast als behandeling van levensbedreigende of invaliderende, veelal aangeboren ziekten van het bloed- of afweersysteem, zoals ernstige afweerstoringen en ziektes van de rode bloedcellen (hemoglobinopathieën). Ook wordt deze therapie toegepast om het hematopoïetische systeem van patiënten met bloed- en lymfeklierkanker te herstellen na zeer intensieve chemotherapie en/of bestraling.

Bij een HSCT worden eerst de stamcellen en witte bloedcellen van de patiënt vernietigd met chemotherapie of bestraling, waardoor er ruimte in het beenmerg ontstaat voor de stamcellen van de donor. Om te voorkomen dat de stamcellen van de donor worden afgestoten door het afweersysteem van de patiënt, wordt ook het afweersysteem van de patiënt uitgeschakeld voorafgaande aan de stamceltransplantatie. Het is belangrijk dat de witte bloedgroep van de donor en patiënt zo veel mogelijk overeenkomen. Dit is nodig om de zogenaamde “aanvalziekte”, graft-versus-host disease, te voorkomen. Bij graft-versus-host disease vallen de witte bloedcellen van de donor de gezonde weefsels van de patiënt aan, wat bijvoorbeeld kan leiden tot ernstige diarree, huidproblemen of benauwdheid.

Na de stamceltransplantatie groeit er vanuit de stamcellen van de donor een compleet nieuw afweersysteem. Het volledig herstel van dit afweersysteem (immuun reconstitutie) kost ongeveer een jaar. Met name in de eerste maanden zijn patiënten vatbaar voor infecties. Daardoor kunnen virussen die bij gezonde mensen weinig klachten veroorzaken voor deze patiënten tot levensbedreigende ziekte leiden. Om de kans op graft-versus-host disease te verkleinen, krijgt de patiënt rondom de transplantatie afweer-onderdrukkende medicijnen. Deze medicijnen remmen niet alleen de graft-versus-host disease veroorzakende (allo-reactieve) afweercellen, maar ook de cellen die nodig zijn om infecties te bestrijden. Hierdoor is het extreem belangrijk om niet te veel, maar ook niet te weinig afweer-onderdrukkende medicijnen te gebruiken rondom de transplantatie.

Voor het schrijven van dit proefschrift werd de relatie tussen virale infecties en het herstel van het afweersysteem onderzocht. In het bijzonder werd het herstel van T-cellen en Natural Killer (NK)-cellen bestudeerd. T-cellen zijn cellen van het aangeleerde afweersysteem die een onmisbare rol hebben in de specifieke afweer tegen infecties. T-cellen doen dit onder andere door virus-geïnfekteerde cellen te doden en een goed gecoördineerde afweerreactie te organiseren. NK-cellen zijn cellen van het aangeboren afweersysteem die met name in de vroege fase van een infectie kunnen bijdragen aan het gevecht tegen een virusinfectie. Dit doen NK-cellen door het doden van virus-geïnfekteerde cellen, maar recent is steeds meer duidelijk geworden dat NK-cellen door middel van de productie van signaalstoffen ook een rol spelen in het activeren en aansturen van andere afweercellen. Echter de precieze rol van NK-cellen in gezondheid en ziekte is nog steeds niet helemaal duidelijk. In bloed van gezonde donoren circuleren twee subpopulaties van NK-

cellen die te onderscheiden zijn door de mate van expressie van het celmembraan eiwit CD56: CD56<sup>bright</sup> en CD56<sup>dim</sup> NK-cellen. De CD56<sup>bright</sup> NK-cellen vormen 10% van de NK-cellen, produceren vooral signaalstoffen en hebben in rust een lage cytotoxiciteit (cel-dodende capaciteit). CD56<sup>bright</sup> NK-cellen worden gezien als voorlopers van CD56<sup>dim</sup> NK-cellen, die van nature een sterke cytotoxiciteit hebben.

Het herstel van het afweersysteem is een belangrijke voorspeller voor een goede uitkomst van patiënten met virale infecties na HSCT. Een beter begrip van de interactie tussen verschillende spelers van het afweersysteem na transplantatie kan leiden tot mogelijkheden om het herstel van het afweersysteem na een stamceltransplantatie te beïnvloeden en complicaties te verminderen.

## Onderzoeksresultaten

In het **eerste deel** van dit proefschrift (Hoofdstuk 2-4) ligt de nadruk op de interactie tussen virusinfecties en het herstel van de afweer door T-cellen.

In **Hoofdstuk 2** wordt beschreven dat een reactivatie van het cytomegalovirus (CMV) kort na HSCT een langdurige, dynamische en specifieke afdruk achterlaat op het T-cel-compartiment. We bekeken de samenstelling van het cellulaire afweersysteem op 1 en 2 jaar na HSCT in 131 kinderen die een stamceltransplantatie kregen vanwege leukemie. 46 van de 131 kinderen kregen een CMV-activatie binnen de eerste 3 maanden na HSCT. Patiënten die kort na HSCT een CMV-activatie kregen, reageerden met een expansie van CD8<sup>+</sup> T-cellen, en zelfs een jaar later was er nog steeds sprake van een uitgesproken toename van laat gedifferentieerde CD8<sup>+</sup> geheugen-T-cellen (EM en EMRA). Deze expansie werd gevolgd door een regressie in het tweede jaar na transplantatie. Dit patroon werd niet gezien na vroege Epstein-Barr virus- (EBV) en adenovirus-infecties. CMV-activatie had geen significante invloed op CD4<sup>+</sup> T-cel- en NK-cel aantallen één jaar na HSCT. Tevens werd het herstel van naïeve T-cellen, die nodig zijn voor een gebalanceerd en gezond afweersysteem, niet negatief beïnvloed door vroege CMV-activaties na HSCT.

In **Hoofdstuk 3** beschrijven we de ontwikkeling van een klinisch toepasbare methode om in één procedure virus-specifieke T-cellen gericht tegen CMV, EBV en adenovirus uit het bloed van een gezonde donor te selecteren. Deze virus-specifieke cellen kunnen worden gebruikt om de T-cel-immuniteit tegen deze virussen te herstellen na HSCT zonder de kans op graft-versus-host disease te vergroten. Voor deze experimentele behandeling wordt momenteel vooral een interferon- $\gamma$  capture assay gebruikt. Echter, niet alle virus-specifieke cellen produceren interferon- $\gamma$  na activatie. Daarom zochten wij naar alternatieven voor het interferon- $\gamma$  capture assay. Hiervoor vergeleken wij de expressie van verschillende activatiemarkers op T-cellen na stimulatie met virale peptide pools. Op deze manier identificeerden we CD25 als een goede kandidaat. Het percentage van de T-cellen dat CD25 tot expressie bracht na stimulatie was 3-7 maal hoger dan het percentage T-cellen dat interferon- $\gamma$  produceerde. Dit geeft aan dat een groter deel van de virus-specifieke cellen kan worden gedetecteerd -en vervolgens geselecteerd- met deze methode. Omdat CD25 ook tot expressie komt op regulatoire T-cellen (Treg), bevat het cel-product dat op

deze manier wordt geproduceerd ook regulatoire T-cellen. Hierdoor is dit cel-product niet alleen verrijkt voor virus-specifieke cellen en daarmee vrij van allereactieve cellen (cellen die graft-versus-host disease veroorzaken), maar onderdrukken de CD25-geselecteerde cellen in de laboratoriumsetting ook allereactieve cellen.

In **Hoofdstuk 4** werd de effectiviteit van preëemptieve behandeling met het medicijn cidofovir tegen adenovirus-infecties na HSCT bestudeerd. Preëemptieve behandeling is een speciale vorm van preventieve behandeling en wordt toegepast bij medicijnen met veel bijwerkingen: behandeling wordt dan pas gestart wanneer het virus gedetecteerd wordt in het bloed, maar vóórdat het virus klachten geeft. Er werden 42 episodes van adenovirus-reactivatie in 36 patiënten bestudeerd. Een snelle daling van de adenovirus virale load (hoeveelheid virus-DNA per ml bloed) tijdens de cidofovir-behandeling was geassocieerd met een gelijktijdig herstel van T-cellen (n=20) en waarschijnlijk waren de T-cellen verantwoordelijk voor de snelle daling van het virus. In de afwezigheid van T-cellen (n=22) steeg de virale load in driekwart van de gevallen niet door tijdens cidofovir-behandeling. De vraag is echter of dit alleen door cidofovir kwam: een daling van de virale load in de afwezigheid van T-cellen werd alleen gezien bij patiënten die tegelijkertijd een expansie van NK-cellen had. In slechts 2 van de 6 patiënten waarbij geen T-, maar ook geen NK-cellen aanwezig waren, bleef de adenovirus virale load stabiel gedurende tenminste 3 weken cidofovir-therapie. In de andere 4 patiënten steeg de virale load door ondanks cidofovir-therapie. Deze resultaten ondersteunen het belang van T-cel-herstel voor de bescherming tegen ziekte en sterfte door adenovirus-infecties na HSCT. Ook geven deze resultaten aan dat er nieuwe, effectievere medicijnen nodig zijn. Ten derde suggereren deze resultaten dat NK-cellen een rol kunnen spelen in de bescherming tegen adenovirus-infecties in de periode dat T-cellen niet aanwezig zijn.

In het **tweede deel** van dit proefschrift ligt de nadruk op NK-cellen.

In **Hoofdstuk 5** wordt één van de beperkingen van het onderzoek doen met ingevroren en ontdooide witte bloedcellen besproken. In vers bloed bestaat het NK-cel-compartiment uit twee subpopulaties (CD56<sup>bright</sup>CD16<sup>+/-</sup> en CD56<sup>dim</sup>CD16<sup>+</sup>). Echter, bij de beoordeling van ingevroren en ontdooide witte bloedcellen van patiënten in de eerste maand na HSCT werd een derde subpopulatie gezien met een CD56<sup>dim</sup>CD16<sup>-</sup> fenotype. Deze cellen waren niet aanwezig in vers bloed dat direct na afname bij de patiënt werd geanalyseerd. Omdat dit artefact alleen werd gezien onder specifieke omstandigheden kort na HSCT zouden deze cellen abusievelijk kunnen worden aangezien voor een relevante nieuwe NK-cel-subpopulatie. Dit onderstreept het belang van het valideren van onderzoeksresultaten gebaseerd op ontdooide witte bloedcellen uit de biobank met vers geïsoleerde witte bloedcellen.

In **Hoofdstuk 6** werd het herstel van de T- en NK-cel-immuniteit geëvalueerd in 93 kinderen die een allogene HSCT kregen vanwege leukemie. Gemiddeld duurt het 4 tot 8 weken totdat de eerste T-cellen na een stamceltransplantatie terugkomen, terwijl NK-cellen al na 3 weken herstellen. Dit

biedt de mogelijkheid om naar de rol van NK-cellen te kijken in de (tijdelijke) afwezigheid van T-cellen.

Kort na de transplantatie werd een expansie van CD56<sup>bright</sup> NK-cellen (>300 cellen/ $\mu$ l bloed) gezien in een subgroep van 38 patiënten. Bij al deze 38 patiënten duurde het meer dan zes weken voordat T-cellen terugkwamen, terwijl de expansie van deze normaal kleine CD56<sup>bright</sup> NK-cel-populatie niet werd gezien in patiënten bij wie de T-cellen binnen vier weken na transplantatie terug kwamen. Deze cellen CD56<sup>bright</sup> NK-cellen kort na HSCT hadden een hoge expressie van chemokine-receptoren die een rol spelen bij de migratie van afweercellen naar ontstekingsreacties en van het molecuul cutaneous lymphocyte antigen dat betrokken is bij de migratie van cellen naar de huid. In tegenstelling tot CD56<sup>bright</sup> NK-cellen van gezonde donoren waren CD56<sup>bright</sup> NK-cellen kort na transplantatie wel cytotoxisch. Deze resultaten tonen aan dat CD56<sup>bright</sup> NK-cellen afhankelijk van de omstandigheden verschillende functionele eigenschappen kunnen hebben. Wanneer er geen T-cellen zijn, kunnen CD56<sup>bright</sup> NK-cellen snel expanderen. Ook krijgen zij in deze omstandigheden functionele capaciteiten die zij normaal niet hebben. Patiënten met een expansie van CD56<sup>bright</sup> NK-cellen ten tijde van een vertraagd T-cel-herstel hadden een klinische uitkomst vergelijkbaar met die van patiënten met een snel T-cel-herstel. Dit suggereert dat CD56<sup>bright</sup> NK-cellen kunnen compenseren voor de afwezige T-cellen.

In **Hoofdstuk 7** beschrijven wij de ontdekking van een nieuwe NK-cel-populatie in humane lymfoïde organen. Deze ‘lymphoid tissue NK-cellen’ (ltNK) werden geïdentificeerd door hun gelijktijdige expressie van de weefselretentie-marker CD69 en de chemokine-receptor CXCR6. Deze populatie vormde 30-60% van de NK-cellen in beenmerg (n=20), milt (n=7) en lymfklier (n=3) maar was niet detecteerbaar in perifere bloed. ltNK-cellen hebben een uniek expressiepatroon van oppervlaktemarkers in vergelijking met CD56<sup>bright</sup> en CD56<sup>dim</sup> NK-cellen in bloed. Deze ltNK-cellen hadden een interferon- $\gamma$  (signaalstof) productie die vergelijkbaar was met die van CD56<sup>dim</sup> NK-cellen. Hun cytotoxiciteit was meer vergelijkbaar met CD56<sup>bright</sup> NK-cellen aangezien zij activatie nodig hadden om cytotoxisch te worden. Na HSCT hadden CD69<sup>+</sup>CXCR6<sup>+</sup> lymphoid tissue NK-cellen een vertraagd herstel in vergelijking met CD56<sup>bright</sup> en CD56<sup>dim</sup> NK-cellen. De identificatie van deze NK-cel-populatie in lymfoïde organen biedt mogelijkheden om de interacties met andere afweercellen en de rol van NK-cellen in de werking van het menselijk afweersysteem verder te onderzoeken.

## Discussie en Conclusie

In dit proefschrift worden nieuwe inzichten in de complexe en ineengevlochten relatie tussen virale infecties, T-cellen en Natural Killer (NK) cellen na allogene hematopoïetische stamceltransplantatie in kinderen beschreven.

In de periode waarin T-cellen (nog) niet hersteld zijn na HSCT, hebben patiënten een groot risico op complicaties door virusinfecties. Wanneer een patiënt getroffen wordt door zo'n virusinfectie, is het van het grootst belang om de periode tot het moment dat T-cellen weer herstellen zo goed mogelijk te overbruggen. Door voortschrijdende ontwikkelingen in het vakgebied zou het kunnen dat een aantal van de hoofdstukken in dit proefschrift over een aantal jaar in een ander perspectief

komen te staan. Bijvoorbeeld zou het kunnen dat het gebruik van het medicijn cidofovir binnenkort niet meer gebruikt wordt, omdat er een nieuw middel (brincidofovir) op de markt geïntroduceerd wordt dat in de eerste onderzoeken veel effectiever lijkt te zijn. Echter, ook dat nieuwe medicijn zal op een kritische manier moeten worden geëvalueerd, en de werkzaamheid zal op dezelfde manier als cidofovir moeten worden gerelateerd aan het herstel van het afweersysteem. Het preventief toedienen van virus-specifieke T-cellen tegen verschillende virussen zal waarschijnlijk niet de standaard worden voor alle kinderen die een HSCT ondergaan. Dit komt doordat steeds minder kinderen een vertraagd T-cel-herstel zullen hebben door gepersonaliseerde dosering van chemotherapie en afweer-onderdrukkende medicijnen. Optimaal T cel herstel voor iedereen is echter een illusie. Er zullen dus patiënten blijven die zeer gebaat zijn bij virus-specifieke T-cel-therapie. Het blijft daarom van belang deze patiënten zo goed en zo vroeg mogelijk te identificeren zodat zij optimaal kunnen profiteren van deze vorm van behandeling.

Waar het belang van het herstel van T-cel-immuniteit voor de bescherming tegen virusinfecties kort na HSCT klip en klaar is, hebben wij laten zien dat de interactie tussen T-cellen en virussen verder gaat. Heel hoge aantallen CD8<sup>+</sup> T-cellen die regelmatig gezien worden in de jaren na HSCT kunnen worden verklaard door vroege CMV-infecties. Wij lieten echter ook zien dat dit komt door een expansie van laat gedifferentieerde geheugencellen bovenop een verder normaal en gebalanceerd afweersysteem. In hoeverre de vroege CMV infecties en de afweer-reactie hiertegen van invloed zijn op lange termijn immuun-pathologie is nog onopgehelderd en moet nog wel bestudeerd worden in studies naar de late effecten van HSCT voor (inmiddels volwassen geworden) kinderen.

Naast antivirale medicatie en adoptieve immunotherapie kunnen NK-cellen een rol spelen in de bescherming tegen virusinfecties wanneer T-cellen niet aanwezig zijn om hun taak te volbrengen. Wij zagen een sterke expansie van CD56<sup>bright</sup> NK-cellen in patiënten met een vertraagd T-cel-herstel na HSCT. Deze cellen waren fenotypisch en functioneel anders dan CD56<sup>bright</sup> NK-cellen in gezonde donoren. Een verdere verkenning van de relatie tussen de expansie van deze CD56<sup>bright</sup> NK-cellen en het optreden van specifieke virusinfecties is echter noodzakelijk. Op deze manier zou de T-cel-deficiënte periode na HSCT als model kunnen worden gebruikt om de rol van NK-cellen in antivirale immuniteit verder te onderzoeken. De identificatie van de markers CD69 en CXCR6 om een unieke NK-cel-populatie in lymfoïde organen te onderscheiden van circulerende NK-cellen, maakt het mogelijk om de interacties van weefsel-residente NK-cellen met andere immuuncellen verder te onderzoeken. Genexpressie-analyse zou een hint kunnen geven over de specifieke functie van weefsel-residente NK-cellen. Daarnaast kunnen met immunohistochemie en confocal microscopie de fysieke interactie van NK-cellen met andere afweercellen worden onderzocht.

In vergelijking met “gewone” NK-cellen in het bloed van gezonde donoren, hebben weefsel-residente NK-cellen en CD56<sup>bright</sup> NK-cellen kort na HSCT een uniek fenotype en een unieke functie. Dit illustreert dat de humane NK-cel-biologie veel complexer is dan de huidige modellen die gebaseerd zijn op NK-cellen uit het bloed van gezonde donoren laten zien. Daarom is een herevaluatie nodig van de relatie tussen verschillende humane NK-cel-populaties en hun rol in het menselijk afweersysteem.



## List of publications

## List of publications

Amir AL, van der Steen DM, van Loenen MM, Hagedoorn RS, de Boer R, Kester MD, de Ru AH, **Lugthart GJ**, van KC, Hiemstra PS, Jedema I, Griffioen M, van Veelen PA, Falkenburg JH, Heemskerk MH. PRAME-specific Allo-HLA-restricted T cells with potent antitumor reactivity useful for therapeutic T-cell receptor gene transfer. *Clin.Cancer Res.* 2011;17:5615-5625.

**Lugthart G**, Albon SJ, Ricciardelli I, Kester MG, Meij P, Lankester AC, Amrolia PJ. Simultaneous generation of multivirus-specific and regulatory T cells for adoptive immunotherapy. *J.Immunother.* 2012;35:42-53.

Albon SJ, Mancao C, Gilmour K, White G, Ricciardelli I, Brewin J, **Lugthart G**, Wallace R, Amrolia PJ. Optimization of methodology for production of CD25/CD71 allodepleted donor T cells for clinical use. *Cytotherapy.* 2013;15:109-121.

Ricciardelli I, Brewin J, **Lugthart G**, Albon SJ, Pule M, Amrolia PJ. Rapid generation of EBV-specific cytotoxic T lymphocytes resistant to calcineurin inhibitors for adoptive immunotherapy. *Am.J.Transplant* 2013;13:3244-3252.

**Lugthart G**, van Ostaijen-ten Dam MM, Jol-van der Zijde CM, van Holten TC, Kester MG, Heemskerk MH, Bredius RG, van Tol MJ, Lankester AC. Early cytomegalovirus reactivation leaves a specific and dynamic imprint on the reconstituting T cell compartment long-term after hematopoietic stem cell transplantation. *Biol.Blood Marrow Transplant* 2014;20:655-661.

**Lugthart G**, Oomen MA, Jol-van der Zijde CM, Ball LM, Bresters D, Kollen WJ, Smiers FJ, Vermont CL, Bredius RG, Schilham MW, van Tol MJ, Lankester AC. The Effect of Cidofovir on Adenovirus Plasma DNA Levels in Stem Cell Transplantation Recipients without T Cell Reconstitution. *Biol.Blood Marrow Transplant.* 2015;21:293-299.

**Lugthart G**, van Ostaijen-ten Dam MM, van Tol MJ, Lankester AC, Schilham MW. CD56(dim)CD16(-) NK cell phenotype can be induced by cryopreservation. *Blood* 2015;125:1842-1843.



**Lugthart G**, Melsen JE, Vervat C, van Ostaijen-ten Dam MM, Corver WE, Roelen DL, van Bergen J, van Tol MJ, Lankester AC, Schilham MW. Human Lymphoid Tissues Harbor a Distinct CD69+CXCR6+ NK Cell Population. *J.Immunol.* 2016;197:78-84.

Melsen JE, **Lugthart G**, Lankester AC, Schilham MW. Human Circulating and Tissue-Resident CD56(bright) Natural Killer Cell Populations. *Front Immunol.* 2016;7:262.

**Lugthart G**, Goedhart M, van Leeuwen MM, Melsen JE, Jol-van der Zijde CM, Vervat C, van Ostaijen-ten Dam MM, Jansen-Hoogendijk AM, van Tol MJD, Lankester AC, Schilham MW. Expansion of cytotoxic CD56bright natural killer cells during T-cell deficiency after allogeneic hematopoietic stem cell transplantation. *J.Allergy Clin.Immunol.* 2017;140:1466-1469.



# Curriculum Vitae



## Curriculum Vitae

Gerrit (Gertjan) Lugthart was born on May 2<sup>nd</sup> 1987 in Gorinchem. He grew up in the village of Harmelen. He attended secondary school at the Driestar College in Gouda, where he graduated cum laude in 2005. He continued his education by studying Medicine at the University of Leiden. In 2006, he joined an international student exchange program to study Pathology, Immunology and Microbiology at the Karolinska Institutet in Stockholm. In 2007, he was awarded a Leiden University Medical Center (LUMC) Excellent Student award, which gave him the possibility to start his first research project. He performed this project between 2007 and 2009 at the LUMC department of Hematology under supervision of dr. W.A.F. Marijt and dr. M.H.M. Heemskerk. Supported by personal grants from the Dutch Cancer Society, Scholten-Cordes Fund and Hendrik Muller Fund, he interrupted his medical training during the academic year of 2009/2010 for a research project at the University College London Institute of Child Health and Great Ormond Street Hospital in London, under supervision of prof. P.J. Amrolia. In 2012, he graduated cum laude from medical school. That year, he was also awarded an LUMC MD/PhD scholarship. With this financial support, he started his PhD research at the LUMC department of Pediatrics. His work, under supervision of dr. M.W. Schilham, dr. M.J.D. van Tol and Prof. A.C. Lankester was awarded with American Society of Hematology Abstract Achievement Awards in 2013 and 2015. In February 2016 he started his residency in paediatrics in the Juliana Children's Hospital in The Hague under supervision of dr. F. Brus and dr. G.J.A. Driessen. In November 2017, he continued his clinical work at the LUMC Willem-Alexander Children's Hospital under supervision of dr. R.G.M. Bredius. Gertjan is married to Anne-Marije Lugthart-Staat and is has a daughter, Lize.



## **Acknowledgements / Dankwoord**





## Acknowledgements / Dankwoord

Prof. A.C. Lankester, beste Arjan. Bedankt voor je aanstekelijke enthousiasme, je weet discussies altijd weer terug te brengen tot de kern. Dank voor de tijd die je vrijmaakte voor het aanscherpen van mijn manuscripten, waardoor die op het scherpst van de snede konden worden gepubliceerd.

Dr. M.W. Schilham, beste Marco. Dank voor je ruime beschikbaarheid voor diepgaande discussies over net verschenen artikelen of mijn nieuwste resultaten. Dank voor integriteit en kritische houding die maakten dat het overtuigen van reviewers weinig moeite kostte.

Dr. M.J.D. van Tol, beste Maarten. Dank voor je inhoudelijke bijdrage aan mijn artikelen en werkbesprekingen. Dank voor je oog voor detail: elke jota en tittel in dit proefschrift heb jij gezien en elke figuur onder de loep genomen.

Mijn collega's van het KJC ImmLab wil ik danken voor de hulp en gezelligheid. Monique van Ostajen, dank voor je expertise en technische adviezen. Els Jol, dank voor je enthousiasme, adviezen en geduld. Carly Vervat en Anja Jansen, dank voor jullie hulp bij het uitvoeren van mega-experimenten. Eline Steenwijk, dank voor je hulp bij het opzetten van de IHC kleuringen en Astrid van Halteren, bedankt voor je kritische en enthousiaste meedenken.

Wetenschapsstage studenten Marieke Goedhart, Merle van Leeuwen, Marloes Oomen en Janine Melsen wil ik bedanken voor hun inzet. Janine, het is super dat jij verder gaat waar het voor mij ophield, het is een eer om betrokken te mogen blijven bij jouw werk.

Collega's van de Hematologie, in het bijzonder Erik Marijt en Mirjam Heemskerk, dank voor jullie begeleiding in mijn eerste stappen in het laboratorium en in de wetenschap. Wim Corver en Guido de Roo, bedankt voor jullie technische ondersteuning met de LSR and Aria.

Prof. P.J. Amrolia, dear Persis, thanks for the great opportunity to work and learn in your lab. Sarah Albon, Jennifer Brewin, and Ida Ricciardelli, thank you for your help and the fun. Jonathan Barnes, Rory Paget-Wilkes and Edmund Sutton, thanks for the good time at Adelina Grove.

Atze de Vries en Geert Minderhoud, bedankt voor jullie inmiddels lange vriendschap. Ik vind het mooi dat jullie vandaag naast mij staan.

Stafleden, arts-assistenten en verpleegkundigen in het Juliana Kinderziekenhuis en LUMC wil ik bedanken voor de goede en leerzame tijd. Frank Brus en Gertjan Driessen, bedankt voor het bieden van de mogelijkheid om dit proefschrift parttime te kunnen afronden.

(Schoon)familie en vrienden, dank voor jullie interesse, maar nog meer voor de momenten dat jullie juist níet naar mijn proefschrift vroegen. Pa en ma, dank voor jullie liefde en steun. Lize, jouw lach geeft mij telkens nieuwe energie. Anne-Marije, zonder jou had ik dit proefschrift nooit kunnen afmaken. Ook voor jou was het niet altijd makkelijk. Dank je wel voor je ondersteuning, begrip en geduld!

